

File ID 455237
Filename Thesis

SOURCE (OR PART OF THE FOLLOWING SOURCE):

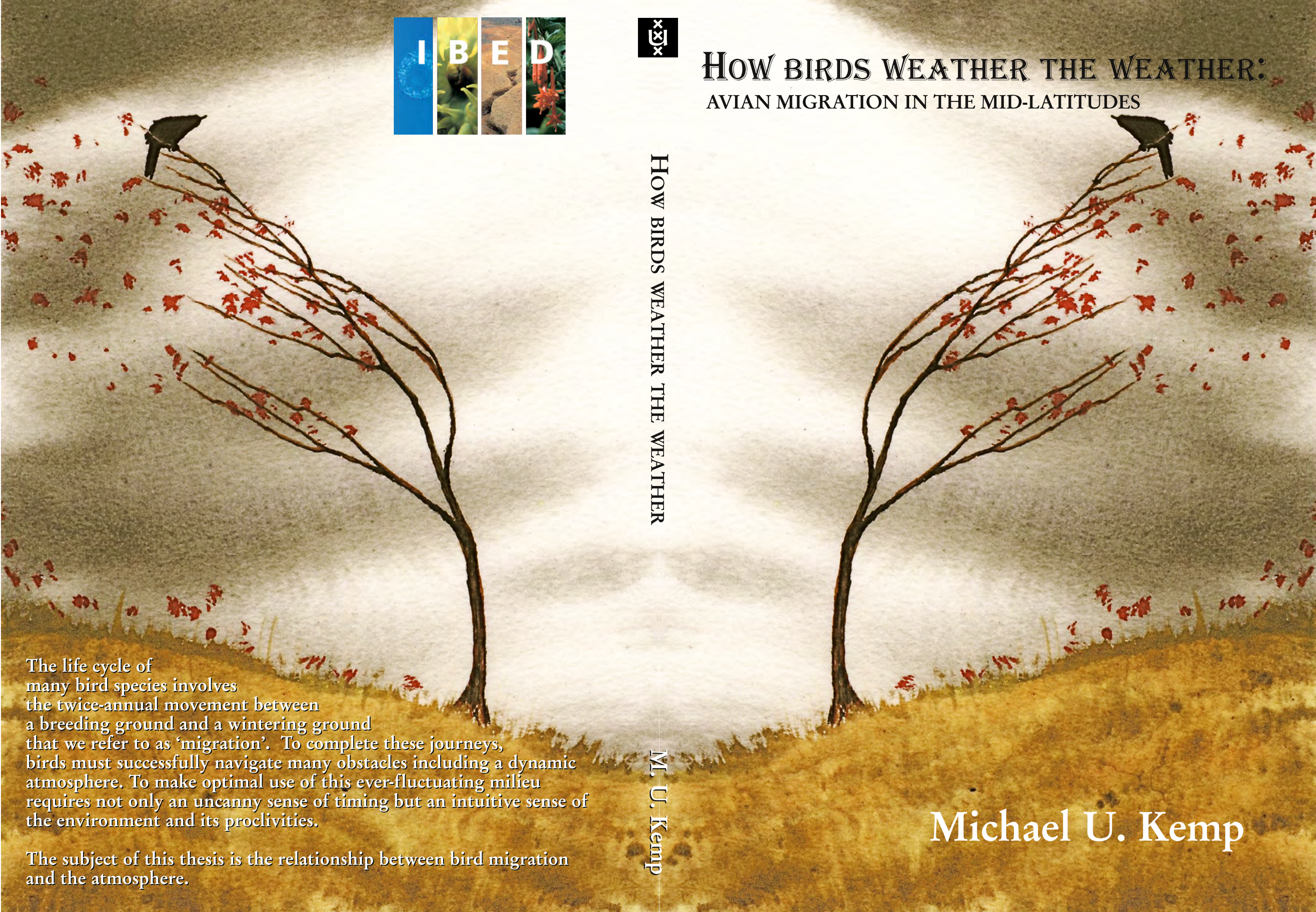
Type Dissertation
Title How birds weather the weather: avian migration in the mid-latitudes
Author M.U. Kemp
Faculty Faculty of Science
Year 2012
Pages viii, 207
ISBN 978-94-91407-06-2

FULL BIBLIOGRAPHIC DETAILS:

[*http://dare.uva.nl/record/421932*](http://dare.uva.nl/record/421932)

Copyright

It is not permitted to download or to forward/distribute the text or part of it without the consent of the author(s) and/or copyright holder(s), other than for strictly personal, individual use.



I B E D

x~~g~~x

HOW BIRDS WEATHER THE WEATHER:

AVIAN MIGRATION IN THE MID-LATITUDES

HOW BIRDS WEATHER THE WEATHER

M. U. Kemp

The life cycle of many bird species involves the twice-annual movement between a breeding ground and a wintering ground that we refer to as 'migration'. To complete these journeys, birds must successfully navigate many obstacles including a dynamic atmosphere. To make optimal use of this ever-fluctuating milieu requires not only an uncanny sense of timing but an intuitive sense of the environment and its proclivities.

The subject of this thesis is the relationship between bird migration and the atmosphere.

Michael U. Kemp

How birds weather the weather:

AVIAN MIGRATION IN THE MID-LATITUDES

This PhD project was carried out in the Computational Geo-Ecology group of the Institute for Biodiversity and Ecosystem Dynamics of the University of Amsterdam. The work was supported financially by the European Space Agency and the Ministry of Defence of the Netherlands.

This thesis is available for download from
<http://dare.uva.nl/record/421932>

Cover illustration: “Bird vs. Wind” by David Hayward
<http://www.nakedpastor.com/>

Printed by: Gildeprint Drukkerijen

ISBN: 978-94-91407-06-2

How birds weather the weather:

AVIAN MIGRATION IN THE MID-LATITUDES

ACADEMISCH PROEFSCHRIFT

ter verkrijging van de graad van doctor
aan de Universiteit van Amsterdam
op gezag van de Rector Magnificus
prof. dr. D. C. van den Boom

ten overstaan van een door het college voor promoties ingestelde
commissie, in het openbaar te verdedigen in de Agnietenkapel
op donderdag 18 oktober 2012, te 10.00 uur

door

Michael Ulric Kemp

geboren te Knoxville, TN, Verenigde Staten van Amerika

Promotiecommissie

Promotor: Prof. dr. ir. W. BOUTEN

Co-promotors: Dr. J.Z. SHAMOUN-BARANES
Dr. E.E. van LOON

Overige Leden: Prof. dr. A.A.M. HOLTSLAG
Prof. dr. J. HUISMAN
Dr. F. LIECHTI
Prof. dr. S.B.J. MENKEN
Prof. dr. T. PIERSMA
Prof. dr. W.P. de VOOGT

Faculteit der Natuurwetenschappen, Wiskunde en Informatica

Contents

Contents	iv
List of figures	vi
List of tables	vii
1 Introduction	1
1.1 Birds and migration	1
1.2 Navigation	3
1.3 Individual weather effects	4
1.3.1 Wind	4
1.3.2 Temperature	6
1.3.3 Humidity	6
1.3.4 Precipitation	7
1.3.5 Atmospheric pressure	7
1.4 Atmospheric data	8
1.5 Radar	10
1.6 Efficient analysis	12
1.7 Synopsis	13
2 RNCEP: global weather and climate data at your fingertips	15
2.1 Summary	15
2.2 Introduction	16
2.3 NCEP data	17
2.4 R scripts	17

2.5	Data over an area	19
2.5.1	Gather	19
2.5.2	Restrict	19
2.5.3	Aggregate	19
2.6	Data interpolated	20
2.7	Data visualized	22
2.8	Conclusion	22
3	Quantifying flow-assistance and implications for movement research	25
3.1	Abstract	25
3.2	Introduction	26
3.3	Flow-assistance	27
3.3.1	Full drift	28
3.3.2	Complete compensation	31
3.3.3	Partial compensation	32
3.3.4	Other strategies	33
3.4	Methods	33
3.4.1	Sensitivity analysis	33
3.4.2	Simulating trajectories	34
3.5	Results	36
3.5.1	Sensitivity analysis	36
3.5.2	Simulating trajectories	38
3.6	Discussion	38
3.6.1	Compensation	40
3.6.2	Preferred direction	43
3.6.3	Speed	44
3.6.4	Range	45
3.7	Conclusion	46
4	Can wind help explain seasonal differences in avian migration speed?	49
4.1	Abstract	49
4.2	Introduction	50
4.3	Data	51
4.3.1	Wind data	51
4.3.2	Radar data	52
4.4	Methods	52
4.4.1	Wind profit analysis	53
4.4.2	Flight analysis	53
4.5	Results	55

4.5.1	Wind conditions	55
4.5.2	Flight speed	57
4.6	Discussion	58
5	The influence of weather on altitude selection by nocturnal migrants in mid-latitudes	61
5.1	Abstract	61
5.2	Introduction	62
5.3	Materials and methods	65
5.3.1	Radar data	65
5.3.2	Meteorological data	67
5.3.3	Wind and altitude	71
5.3.4	GAM analysis	72
5.4	Results	73
5.4.1	Weather	73
5.4.2	Wind and altitude	76
5.4.3	GAM analysis	79
5.5	Discussion	82
5.6	Conclusion	86
6	Predicting migration intensity at multiple sites using operational weather radar	89
6.1	Introduction	89
6.2	Materials	91
6.2.1	Radar data	91
6.2.2	Predictor variables	92
6.3	Methods	95
6.3.1	Model development	96
6.3.2	Models for one location applied to the other	98
6.4	Results	98
6.4.1	Migratory dynamics and predictor variables	98
6.4.2	Baseline intensity	99
6.4.3	Autocorrelation	99
6.4.4	Model performance	105
6.5	Discussion	111
6.5.1	Model development	111
6.5.2	Flight safety	116
6.6	Conclusion	118

7 General discussion and synthesis	121
7.1 Weather or climate?	121
7.2 Optimal migration	123
7.3 Robust decision-making	124
7.4 Assessing drift	125
7.5 Quantifying model performance	129
7.6 Migration research	132
Bibliography	154
Summary	155
Samenvatting	161
Acknowledgments	167
Appendix A: Explicit descriptions of flow-assistance equations	171
Appendix B: FLAT model description	181
Appendix C: Wind maps and wind summaries for Europe	185
Appendix D: Results of simulation model predicting avian altitude distributions	199
Appendix E: Results of GAM model predicting avian altitude distributions	203

List of Figures

2.1	RNCEP area flowchart	18
2.2	RNCEP point flowchart	21
3.1	Flow-assistance	30
3.2	Flow-assistance difference	37
3.3	Flow-assistance sensitivity	39
3.4	Flow-assistance trajectories	42
4.1	W. Europe migration map	51
4.2	Spring wind summary plot	55
4.3	Autumn wind summary plot	57
5.1	De Bilt radar	66
5.2	Altitude distributions of bird density	68
5.3	Spring weather conditions	75
5.4	Autumn weather conditions	77
5.5	Altitude of best wind support vs. altitude of most birds	78
5.6	Wind support and bird density correlations	78
5.7	GAM results	81
6.1	Map of radar, HIRLAM, and NCEP locations	91
6.2	Time series: De Bilt and Den Helder	102
6.3	Tracks and headings	102
6.4	De Bilt: baseline intensity	103
6.5	Den Helder: baseline intensity	104
6.6	Autocorrelation in bird density	107

6.7	De Bilt: performance of models	108
6.8	Den Helder: performance of models	109
6.9	De Bilt: predicted vs. measured	111
6.10	Den Helder: predicted vs. measured	113
6.11	Weighted and unweighted predictions	118

List of Tables

3.1	Flow-assistance equations	29
3.2	Flow-assistance trajectories	43
4.1	Seasonal wind profit summary	57
4.2	Seasonal flight speeds	58
5.1	Variables to predict altitude	74
5.2	GAM variable selection	80
5.3	Best GAM models	80
6.1	Variables to predict migration intensity	97

Introduction

1.1 Birds and migration

Historical evidence suggests that birds have captured the imagination of humans for a very long time. Perhaps the earliest evidence of this is a 30,000 year-old avian figurine carved from mammoth ivory that was found in the Hohle Fels cave of modern-day Germany (Conard, 2003). Since then, bird feathers have adorned religious and ceremonial artifacts and attire, and feathers, feet, blood, etc. often play a central role in ceremonial customs and rituals. From isolated island tribes to the raucous celebration of Brazil's carnival, these customs persist today. Bird-related imagery pervades our literature and art, from holy books to Shakespeare to political propaganda. In fact, specific birds have come to symbolize particular ideas: doves reflect peace; eagles suggest strength; owls invoke wisdom; swans denote beauty; storks are associated with birth and ravens with death.

It is really no wonder birds have captured our imagination so. They inhabit a realm of the earth that for most of our history was unavailable to us; they take to the air in flight. In so doing, they liberate themselves from the potential confines of geographical barriers that would otherwise restrict their habitat. They are thus able to travel often great distances to avail themselves of the most beneficial habitat for different life stage events: e.g. breeding, fledging, molting. During summer, migratory birds travel to higher latitudes in order to breed where long days produce bountiful food resources. Due to the often harsh winters associated with these latitudes, local competition for resources is reduced and can even be restricted to those organisms able to make the migratory trek each year. Their chicks having had the benefit of their first weeks spent in high latitude summer, these birds then make their way back

to the warmer climes of lower latitudes as summer days shorten and winter approaches. Clearly there are benefits of being so mobile; nonetheless, this lifestyle brings a set of unique hazards known only to migrants.

The migratory journey itself is fraught with potential dangers, and birds must successfully navigate through changing landscapes and environments. In the middle latitudes, through which migratory birds commonly pass, violent storms are often associated with the transition between summer and winter. Yet even during times of more serene weather, there is the potential for dehydration and/or emaciation. Birds may be blown off course, potentially over areas where rest and food are unavailable such as the open ocean. Presuming that a bird is able to complete its migratory journey, there is still the potential of arriving at the breeding location too early to find there is no food yet available or arriving too late and being unable to secure a mate or having too little time to fledge young. Nonetheless, an almost unfathomable number of migratory individuals of a dazzling array of species make these migratory journeys twice each year.

At times of peak migration intensity, airspace over large areas of Western Europe become saturated by a multitude of different bird species, at different elevations, leaving from different points of departure, and bound for different destinations. These birds are complex biological beings each making their own decisions in a dynamic world. Nonetheless, many of these decisions are markedly similar across quite large groups. Certain strategies, which are generally more successful than others, are perpetuated by natural selection. Thus, birds that make “good” decisions survive to migrate and produce offspring who are then more likely to make a similar decision when confronted with similar circumstances. It is due to this that we see the flight strategies of so many birds, even across species, converging at similar times and locations.

Research suggests that certain environmental cues trigger related responses among many bird species. The length of the day, in conjunction with an internal clock or biorhythm, has been suggested as a driver of migratory restlessness (Gwinner and Helm, 2003; Gwinner, 2003). While this circannual rhythm can explain seasonal variability in migratory activity, there can be large variation in the intensity of migration from day-to-day even during the peak of migration season (Richardson, 1978). This day-to-day variability is believed to be a result of birds choosing to migrate during times with preferential weather conditions, and the altitudes at which birds fly during migration is also believed to be influenced by meteorological conditions. Wind direction and speed, precipitation, humidity, cloud cover, surface pressure and the types and relative positions of frontal boundaries have all been suggested to influence migration to varying degrees (Richardson, 1978; Erni et al., 2002b; van Belle et al., 2007;

Yaukey and Powell, 2008). However, the specific weather variables that trigger particular responses in birds are difficult to pin down. For instance, we find statistical relationships between particular atmospheric properties and the intensity of migration, allowing us to model different aspects of migration; however, weather variables are known to be strongly correlated in time and space making causal effects rather difficult to discern even with advanced statistical techniques (Pyle et al., 1993). Richardson (1978) makes a distinction between ‘ultimate’ and ‘proximate’ factors influencing migration. He suggests that certain atmospheric variables have direct (i.e. ‘ultimate’) selective influence on the evolution of migration by way of their impact on survivability, whereas ‘proximate’ variables are those that birds use to make migratory decisions and can be ultimate factors as well or serve as proxies for (possibly difficult to detect) ultimate factors.

1.2 Navigation and orientation

In order to successfully and consistently complete migratory journeys, birds must have some mechanism(s) by which they orient (i.e. determine direction) and navigate (i.e. chart a course to a remote goal) (Able, 2001). While it has long been suggested that birds exhibit an endogenous migratory direction, guiding even inexperienced migrants in seasonally-appropriate directions, the mechanism by which birds discern this direction has been more elusive. Current theory suggests that birds may possess two magneto-detection senses used for orientation: one composed of magnetite in the beak and one composed of light-sensing cryptochromes in the eyes (Wiltschko and Wiltschko, 2005). A recent study has even identified a group of cells in pigeons’ brains that respond to the direction and strength of the Earth’s magnetic field (Wu and Dickman, 2012). Birds are also believed to use celestial visual cues to discern direction (Emlen, 1967), and some have suggested olfactory cues may be used in navigation as well (Wallraff, 2004).

In order to assess the amount of displacement from their preferred direction of movement, birds are believed to use visual cues to determine drift (Richardson, 1990b). Alerstam (1979) suggests that if birds do assess drift in this way, they may be able to fully compensate using fixed objects on the ground; however, if a bird attempts to fully compensate for displacement using objects that are themselves somewhat displaced by the wind (such as waves in the sea or clouds in the sky), the bird will actually incur drift equivalent to the speed at which the reference object is displaced. Sound has also been theorized as a potential supplementary indicator of drift for migrating birds (Griffin and Hopkins, 1974); however, no specific evidence of this has been

found.

It is unlikely that (particularly experienced) birds conduct migratory journeys using an endogenous direction alone. It is argued that along with various “compasses” to discern direction, birds develop a mental map of their environment through experience to assist in navigation (Able, 2001) and that they use visual landmarks and geomagnetic “signposts” to help discern their location (Åkesson and Hedenström, 2007; Wiltschko and Wiltschko, 2005).

1.3 Individual weather effects

A great deal of theoretical and empirical research has gone into understanding the influence of particular atmospheric components on different aspects of bird migration and physiology. Here we will outline the current state of knowledge with regard to these individual weather effects, particularly with regards to nocturnal migrants engaged in flapping flight but with some consideration of other types of migrants as well.

1.3.1 Wind

Wind condition is considered one of the more influential atmospheric components on bird migration (Alerstam, 1979; Liechti, 2006). Wind speeds are of the same order of magnitude as bird airspeeds, so it is easy to understand how the speed and direction of the wind can have a large impact on the efficiency of migration.

Wind is believed to be of primary influence on the departure decisions of migrants (Richardson, 1990a; Erni et al., 2002b). While some early research suggested contrariwise, it is rather well established that most birds prefer to initiate migration with tailwinds (i.e. winds supporting movement in seasonally appropriate directions) than headwinds (i.e. winds opposing movement in seasonally appropriate directions) (Richardson, 1978). Beyond this broad generalization, however, there remains some ambiguity. For instance, some research suggests that birds avoid initiating migration in high-speed winds (Schaub et al., 2004; Richardson, 1990a). This may be particularly true of diurnal soaring migrants that rely on thermal uplift to gain altitude and reduce the energetic costs of migration, since high wind speeds can disrupt thermal development; however, considering wind speed in isolation of wind direction ignores the fact that these two components are linked such that the influence of each on migration is dependent on the value of the other (see Chapter 3). Consider, as well, that if a bird has one preferred direction of movement, there are many more directions into which the wind could blow that are unsupportive than directions that are supportive, making increasing wind speed more

often undesirable. Nonetheless, it is possible that birds prefer lower speed winds regardless of direction, since a bird may be more quickly and dramatically blown off course by higher speed winds if the direction of those winds shifts. Regardless, some migration takes place in almost all wind conditions, and persistent wind patterns along particular migration routes – in combination with an individual’s fuel reserves and the refueling opportunities of a particular location – can affect the optimality of departing under particular wind conditions (Alerstam and Lindström, 1990; Weber et al., 1998; Weber and Hedenström, 2000; Erni et al., 2002a).

Once in flight, wind directly influences the groundspeed and track direction (i.e. direction of movement relative to the Earth) of individual migrants. Therefore, wind condition influences the optimality of a bird selecting a particular airspeed, route, and altitude (Alerstam, 1979; Liechti, 2006). To optimally utilize their fuel reserves, for example, birds are expected to reduce their airspeed in tailwinds and increase their airspeed in head- and side winds (Liechti, 1995). Radar observations of migrants in different wind conditions have tended to support these expectations; however, Shamoun-Baranes et al. (2007) have raised concerns over the legitimacy of the approach used in many of these studies. It is often assumed that birds should select flight altitudes that maximize wind support such that they minimize the time and energy required for migration. While many previous studies have suggested this to be the case (e.g. Schmaljohann et al., 2009; Liechti et al., 2000; Bruderer et al., 1995b), we have found that a more appropriate phrasing is that birds select altitudes to avoid prohibitive winds and that lower altitudes are generally preferred (see Chapter 5).

Coupled with inherent variability in individual preferences (e.g. differences in the preferred direction of migration) and priorities (e.g. soaring migrants needing to utilize thermal uplift), variation in flight behavior and individual responses to wind likely arise from variability in the navigational capacities of different species (or even different age groups of the same species), since a bird’s ability to identify its own location and the location of its goal has some bearing on the optimal strategy for dealing with winds (Alerstam, 1979). A bird that knows the explicit location of its final goal, for example, can continually reorient itself toward that final goal, always choosing the most direct route to its final destination. A bird following an endogenous direction, however, has to base all wind compensation decisions around the more immediate goal of maintaining that endogenous direction. Knowledge (or lack thereof) that birds may have of persistent wind patterns along the migration route can also affect the optimal strategy for dealing with winds (Alerstam, 1979). For instance, if a bird can assume that side winds will be evenly distributed from both sides

of its preferred direction over the course of the migration route, compensation for side wind displacement may not be beneficial. Similarly, the frequency of beneficial winds in an area affects optimal departure decisions (Weber and Hedenström, 2000), so knowledge of this frequency may influence a bird's tolerance for accepting suboptimal winds.

1.3.2 Temperature

Migrants are generally found to initiate migration during cooler temperatures in autumn and warmer temperatures in spring (Richardson, 1990a). Clearly, cooler temperatures in autumn and warmer temperatures in spring indicate the approach of winter and summer, respectively, and birds may have developed an increased urge to migrate in response to these conditions. In both cases, however, these variations in temperature are often associated with wind conditions that are supportive of migratory movement for the particular season: winds from lower latitudes support movement toward the poles and usher in warmer temperatures, while winds from higher latitudes support movement toward the equator and bring cooler temperatures. It is possible, therefore, that relationships observed between migration intensity and temperature could be a coincidental result of the more direct relationship between migration intensity and supportive wind conditions. During flight, both very high (see Schmaljohann, 2008, and references therein) and very low temperatures (Klaassen, 1996) likely hamper migratory efficiency (at least through their impacts on the rate at which a bird loses endogenous water), and there is potentially some optimal range of temperatures within which birds operate most efficiently. While very low temperatures are associated with higher rates of energy expenditure in birds at rest (Wikelski et al., 2003), it remains unclear if this persists in birds during flight – particularly since migrants employing flapping flight likely produce excess heat that is better dissipated in cooler temperatures.

1.3.3 Humidity

As with temperature, humidity is also correlated with other atmospheric variables and indicative of synoptic conditions. Thus, correlations found between migration intensity and (changes in) humidity may be coincidental. Alternatively, humidity may represent one of the ‘proximate factors’ suggested by Richardson (1978).

Several theoretical studies suggest that the flight range of migrating birds may be severely limited by dehydration (Carmi et al., 1992; Klaassen, 1995, 1996). Thus, birds should prefer conditions of higher humidity. Nonetheless,

Schmaljohann et al. (2009) specifically tested whether birds migrating through the Sahara Desert selected altitudes that minimized energy expenditure (i.e. selection based on wind condition) or altitudes that minimized the rate of water-loss (i.e. selection based on humidity) and found that birds primarily selected altitudes that minimized energy expenditure. Elkins (2004) suggests that high humidity may be troublesome in combination with freezing temperatures, which could lead to the accumulation of ice on plumage; however birds have been observed flying at altitudes with temperatures well below freezing even when the atmosphere was very humid such that the formation of ice crystals was to be expected (Bruderer, 1971).

1.3.4 Precipitation

It is generally accepted that birds prefer to avoid migrating during precipitation events (Erni et al., 2002b; Richardson, 1990a), and precipitation is suggested to depress migratory altitudes (Bruderer, 1971). Any precipitation is likely to inhibit visibility, making navigation and the avoidance of obstacles more difficult. Liquid precipitation has the potential to saturate a bird making it heavier (and thus less efficient in flight) and also making it more difficult for the bird to regulate its internal body temperature. Solid precipitation such as hail has the obvious potential to inflict bodily damage if a bird is struck, and there are reported cases of large numbers of birds being killed by hail (Gates, 1933; Smith and Webster, 1955; Stout and Cornwell, 1976). As well, precipitation (and the often associated cloud cover) tend to cool the surface of the Earth during the day, which suppresses the development of thermals supportive of soaring migration.

1.3.5 Atmospheric pressure

While a correlation between (changes in) atmospheric pressure at the surface of the Earth and migratory activity is found (particularly in autumn) in statistical analyses of the timing of bird migration in relation to weather (Richardson, 1990a), it seems unlikely that changes in surface pressure over time directly influence migratory efficiency to a significant degree. Rather, atmospheric pressure at the surface and its changes over time are determined by one's position relative to high and low pressure systems, which is indicative of synoptic level conditions and therefore the states of many atmospheric variables that likely do influence migratory efficiency such as wind speed and direction, temperature, and precipitation. Thus, atmospheric pressure at the surface may also represent one of the 'proximate factors' that birds use to determine the overall suitability of the atmosphere for migration.

Pressure varies much more dramatically with altitude than it does at the Earth's surface, however, and decreasing atmospheric pressure with altitude can have a significant impact on a bird's flight efficiency (Pennycuick, 2008). Changes in pressure affect the lift-to-drag ratio of a flying bird. As pressure decreases, it becomes easier for a bird to move forward because parasitic drag decreases, but at the same time it becomes more difficult for the bird to maintain altitude because induced drag decreases. The trade-off between the two is such that birds are generally able to make more efficient progress at higher altitude (i.e. lower pressure); however, the act of climbing requires energy (Hedenström and Alerstam, 1992) that could otherwise be used to make forward progress, so a bird's flight must be sufficiently long to make up for the cost of climbing.

Atmospheric pressure is also directly related to oxygen partial pressure; as pressure decreases with altitude, so too does available oxygen. Birds have physiological adaptations resulting in a more efficient exchange of oxygen from the pulmonary to the circulatory system than mammals. For example, house sparrows (*Passer domesticus*) in a hypobaric chamber simulating atmospheric pressure at 6 km altitude were observed to be normally active, whereas white mice (*Mus musculus*) in equivalent conditions were described as 'moribund' and 'comatose' (Tucker, 1968). These sparrows even extracted a higher percentage of oxygen from the air entering their lungs at (simulated) 6 km than they did at sea level. It is argued, however, that because the birds have to increase pulmonary ventilation (i.e. take in more air) at higher altitude in order to extract sufficient amounts of oxygen, their rate of water-loss increases, which is expected to impose limitations on the bird's flight range (Carmi et al., 1992).

1.4 Atmospheric data

Atmospheric data of various types, obtained using a range of methods, are available in many different formats. The largest differences are perhaps between data that are measured using various instrumentation and data that are generated as output from models. Even this distinction, however, can be quite blurred. Atmospheric variables that are difficult to measure directly are often estimated using models describing their relationship with variables that are easier to measure. A variable as common as atmospheric humidity, for example, is rarely measured directly but rather estimated from calibrated relationships between it and variables easier to measure such as temperature, electrical resistance/capacitance, thermal conductivity, or absorption of particular bands of the electromagnetic spectrum (Foken and Nappo, 2008). As

well, measurements of various atmospheric variables are often used first to calibrate atmospheric models and then to validate (and even update) modeled output (see e.g. Kalnay et al., 1996). Conversely, modeling techniques are often used to fill gaps between and identify and correct errors in atmospheric measurements (see e.g. Hijmans et al., 2005).

In the following chapters, we make use of a variety of atmospheric variables obtained almost exclusively from gridded atmospheric models. Specifically, we utilize data from the National Centers for Environmental Prediction (NCEP) / National Centers for Atmospheric Research (NCAR) Reanalysis I data set (Kalnay et al., 1996), the NCEP / Department of Energy (DOE) Reanalysis II dataset (Kanamitsu et al., 2002), the analysis product of the European Centre for Medium-Range Weather Forecasts (ECMWF Persson, 2011) deterministic model, and the High-Resolution Limited Area Model (HIRLAM Cats and Wolters, 1996; Undén et al., 2002). The ECMWF and two NCEP data sets combine state-of-the-art analysis/forecast atmospheric models with data assimilation systems to produce high-quality gridded global datasets in a consistent manner over extensive time periods. They reflect a situation in which models and measurements are combined in order to maximize the full potential of each. The resolution of these global data sets can be somewhat coarse for some applications, however, which is why we have also utilized the HIRLAM data set. HIRLAM uses initial boundary conditions from a courser-scale global model, such as ECMWF, and similarly combines analysis/forecast atmospheric models with a data assimilation system to downscale these atmospheric data to a higher spatiotemporal resolution over a reduced spatiotemporal extent.

While in-situ and remote-sensing based atmospheric products, i.e. data obtained from various measurement devices, were also available and appropriate for many of our analyses, our use of gridded-atmospheric data has specific advantages. In particular, use of these data sets ensures that the methods we apply are reproducible and exportable. Researchers in other locations are not dependent on the availability of measured data in their area to conduct our analyses, and the results of their analyses should be directly comparable to our own due to similar input data. As well, because the atmospheric models we use incorporate forecasting systems, the relationships we uncover between bird migration and atmospheric dynamics, and the models we develop to describe these relationships, can be applied toward the prediction of future migratory conditions.

1.5 Radar as a tool in bird migration studies

Radar utilizes radio waves, electromagnetic radiation with a range of wavelengths between 1 mm and 100 km, and radar measurements are obtained from a two-stage system composed of a transmitter or antenna to project electromagnetic energy and a receiver or dish to capture any of the electromagnetic energy that is reflected or scattered by a distant object. From the time delay between the transmission of the radar signal and the return of the radar echo, the distance of the remote object can be determined. As well, due to the Doppler effect, any shift in frequency between the transmitted and received radio waves indicates the motion of the object relative to the receiver; a shift toward higher frequencies indicates an object moving toward the receiver, while a shift toward lower frequencies indicates an object moving away from the receiver. Water containing some impurities (e.g. salt), scatters radar signals quite strongly, so biological targets such as birds, whose lean body mass is often composed of more than 50% water (Ellis and Jr., 1991) containing electrolytes, can produce quite strong radar echoes.

Eastwood (1967) recounts when birds were first regularly detected by radar in the 1940's, when higher-power S-band radars came into use. Initially unrecognized by radar operators as birds, these 'spurious' echoes were dubbed 'angels', and they understandably caused trouble for operators interested in monitoring aircraft. Realizing the potential of radar technology in ornithological study, researchers in England, Switzerland, and the United States during the post World War II era began independently to build a body of research confirming that birds could be measured with radar. Since that time, radar has become the primary tool to study the migratory flight behavior of birds in relation to the environment (Bruderer, 1997).

The application of radar methods in bird migration studies revolutionized the field through the middle of the 20th century and showed us, among other things, the sheer amount of migration that occurs outside of our range of vision, particularly during the night. Radar continues to be an invaluable tool in the study of avian migration, allowing us to accurately quantify what we would otherwise be unable to see. It provides a platform for making high-resolution, standardized measurements at different times and places of the location, speed, direction, and wing-beat frequency of migratory individuals as well as the size and altitude distribution of migratory populations.

Often radar systems are set up for a particular purpose, and this usually means that some feature of the radar is exploited at the expense of another feature. A radar system, for instance, that is meant to measure the speed, direction, and even wing beat frequency of individual migrants may only be able to sample a small portion of the migrants in a passing population. Al-

ternatively, a system that measures the speed and direction of all individuals in a passing population, and gives detailed information on the intensity of migration, may lack in altitude resolution, while a system with high altitude resolution may be unable to resolve the behavior of each individual migrant. Thus researchers must utilize the strengths of a particular radar system and also realize its limitations. Potentially, data from multiple radar systems can be combined in analyses such that the strengths of each system are exploited. Regardless, radar technologies continue to improve and we may ultimately be able to discern both individual and population level dynamics with high lateral, altitudinal, and temporal resolution in a single radar system. A particularly exciting potential exists through the use of Doppler weather radar. Recently, algorithms have been developed to automatically extract bird migration information from operational weather radar (Dokter et al., 2011), creating the potential to revolutionize the study of bird migration once again. One particularly beneficial aspect of this development is that large geographical areas are already covered by networks of existing weather radar. Networks such as these allow for continuous continental-scale analyses able to consider variation in migratory behavior between areas far-removed from one another.

In the analyses herein, we make use of data obtained from Medium-Power military tracking radar (MPR) and Doppler weather radar. The MPR is a 10 cm wavelength S-band radar used operationally by the Royal Netherlands Air Force (RNLAf) to monitor the airspace over the Netherlands and track aircraft for military purposes. The MPR was equipped with the ROBIN4 (Radar Observation of Bird Intensities) software, developed by TNO Defense, Security, and Safety, to discriminate birds from other objects like aircraft and precipitation. Speed and direction can be discerned and measured by the MPR for individual birds at distances greater than 50 km and for flocks of birds at distances greater than 100 km. The MPR also provides information on the intensity of migration; however, the altitude resolution of this radar system is rather poor. The weather radars used in these analyses are 5 cm wavelength C-band Doppler radar used operationally by the Royal Netherlands Meteorological Institute (KNMI) to monitor atmospheric phenomena such as precipitation and wind condition. The algorithm developed by Dokter et al. (2011) allowed for the automated extraction of bird movement data from these weather radars, which were validated in a field campaign using a 3 cm X-band dedicated bird-detection radar of the type ‘Superfledermaus’ (Bruderer et al., 1995a). Migration intensity, along with the speed and direction of passing populations, is measured by these weather radars and summarized over the entire radar volume at discrete altitude intervals of 200 m thickness. Tracks of individual migrants are not calculated from these weather-radar data, however,

and the geographical extent of these radar measurements is much smaller than that of the MPR. Neither of the radar systems used in these analyses provides information on species composition, and both suffer from the well-known shortcoming of the use of radar in ornithology which is that birds in the lowest altitude layers are often missed due to interference from ground clutter.

1.6 The importance of tools and methods for efficient analysis

There are a great many seasonal and environmental factors influencing migration, and the particular influence of many of these factors can depend on the state of other factors. As well, there are a great many methods by which to quantify migratory activity. While this thesis focuses on radar methods, data from counting and ringing campaigns as well as various tracking devices, which continue to become lighter, smaller, and more accurate and energy efficient, provide a wealth of information that can quickly overwhelm. Equivalently, environmental data sets exist at increasingly higher spatial and temporal resolution, and, particularly concerning tracking devices, the spatial domain that must be considered is not known *a priori* and can be quite extensive.

Because of this, large amounts of data must be managed and organized and the efficiency with which this is done determines the overall effectiveness of migration research. Consider a researcher interested in birds' reaction to wind. This researcher spends time to manually collect relevant wind data and merge them with his or her bird data only to discover that the wind data retrieved describes wind conditions at an undesired altitude. The researcher must then start over and manually retrieve the wind data once again, being sure (again) that each mouse-click and key-stroke is correct. This same researcher, after obtaining wind data for the correct altitude, finds some significant results and shares these results with some colleagues in other locations who have similar sets of bird data. Before these new researchers can perform the same analysis, they must each retrieve wind data yet again for their particular location – which buttons did the first researcher click again? Now consider an alternative. Instead of manually retrieving their wind data, the original researcher integrated the retrieval of wind data into their analysis, likely through the use of a scripting language (e.g. R, Python, or Perl). Further, the original researcher designed the data retrieval portion of their analysis in a robust and flexible way such that adjusting the altitude and/or location from which the wind data were obtained required only that a few parameters be modified. While the first iteration of data retrieval is likely to be more time consuming

using this approach, this extra time is regained in spades by significantly reducing the time needed to retrieve the data for modifications and extensions to the analysis.

Analyses performed in this way are also explicitly reproducible. Along with the manuscript describing their results, researchers can provide unambiguous descriptions of their analyses in the form of a ‘script’. In doing so, any issues arising from data handling and processing are captured and traceable. Research conducted following this paradigm has one further advantage in that these scripts are effectively tools that can be used by others. Rather than each researcher needing to develop an equivalent tool, tools that are effective can naturally propagate through the scientific community. Through the use of open-source scripting languages, extensions, modifications, and improvements can be continually incorporated. Because of the benefits of research carried out in this way, we have developed a tool in the open-source R language (described in Chapter 2) that allows researchers to quickly and easily incorporate weather and climate data in their analyses.

The efficiency and effectiveness of bird migration studies is also determined in large part by the flexibility of the tools and methods used to visualize data during the exploratory phase of analyses. Interactive research environments, which allow for the rapid merging and visualization of many types of data, can minimize potential bottlenecks associated with suboptimal visualization. In light of the benefits of such a research environment, we have developed the Virtual Lab for Bird Migration Modeling (VL-BMM) combining a high-performance computing environment, multiple high-resolution monitors with variable modes of input, and high-speed access to relevant databases. As well as maximizing individual research potential, the VL-BMM facilitates collaboration as experts with different backgrounds (e.g. ornithology, meteorology, statistics) can interactively explore and discuss data and formulate and test ideas quickly and efficiently. The VL-BMM is also portable, making it useful for demonstrations, community outreach programs, and discussions with members of industry (e.g. aviation, military, and wind-energy production) who can benefit from products (e.g. forecast models) arising from bird migration studies.

1.7 Synopsis

The chapters herein span a range of topics centering around the relationship between birds and weather. We begin with two chapters describing tools, concepts, and methods meant to facilitate and guide analyses of bird migration in relation to weather. In Chapter 2, we introduce the RNCEP package

of functions to assist with the incorporation of atmospheric data in ecological studies. In Chapter 3, we discuss different methods of quantifying wind support for animals moving in flows. These methods require making specific behavioral assumptions, which we have incorporated into a dynamic simulation model built on functions contained in the RNCEP package. We then move on to two chapters exploring some specific influences of weather on migratory dynamics. In Chapters 4, we consider how persistent wind patterns, in relation to the direction of migratory flight, can influence migration speed, specifically affecting differences in migration speed between spring and autumn. In Chapter 5, we consider atmospheric factors that may influence the altitudes birds choose during migration. We attempt to determine the specific influence of these factors and the priority birds give each. Lastly in Chapter 6, we consider a practical application of bird migration studies in the context of flight safety. This chapter is quite different from the rest, as it is not concerned specifically with which atmospheric factors influence migration and how. Rather, we outline a method in this chapter to develop predictive models of migration intensity with the aim of providing accurate predictions rather than biological insight.

2

RNCEP: global weather and climate data at your fingertips

Kemp, M.U., van Loon, E.E., Shamoun-Baranes, J., & Bouten, W. (2012) Methods in Ecology and Evolution *3*:65-70

2.1 Summary

1. Atmospheric conditions strongly influence ecological systems, and tools that simplify the access and processing of atmospheric data can greatly facilitate ecological research.
2. We have developed RNCEP, a package of functions in the open-source R language, to access, organize and visualize freely available atmospheric data from two long-term high-quality data sets with global coverage.
3. These functions retrieve data, via the Internet, for either a desired spatiotemporal extent or interpolated to a point in space and time. The package also contains functions to temporally aggregate data, producing user-defined variables, and to visualize these data on a map.
4. By making access to atmospheric data and integration with biological data easier and more flexible, we hope to facilitate and encourage the exploration of relationships between biological systems and atmospheric conditions.

2.2 Introduction

Atmospheric conditions at different scales in space and time strongly influence a wide range of biological processes: from short-term atmospheric conditions, especially in the lowest troposphere (Stull, 1988), described collectively as weather, to longer-term average conditions (i.e. climate). For instance, the sex of some reptilian species' offspring is temperature-dependent (Janzen, 1994); humidity influences the rate of dehydration and therefore the level of activity in most amphibians (Shoemaker and Nagy, 1977); low temperatures and storms can influence avian reproduction (Wingfield, 1984); and atmospheric conditions are drivers of migration and long-distance transport in numerous taxa (Drake and Farrow, 1988; Dingle, 1996; Nathan, 2005; Newton, 2008). Recent trends in atmospheric conditions, for example rising temperatures and oscillations in pressure systems (e.g. North Atlantic Oscillation), have profound effects on marine and terrestrial ecosystems (e.g. Hughes, 2000; Ottersen et al., 2001; Walther et al., 2002; Parmesan, 2006). The connection between climate and biology cannot be overstated, as a species' ability to inhabit a particular geographic range is largely determined by the area's climate (MacArthur, 1972; Guisan and Zimmermann, 2000; Tarroso and Rebelo, 2010). Within the past century, climate change has influenced the geographical ranges and abundance of numerous species (Parmesan and Yohe, 2003; Root et al., 2003), in some cases leading to population and species extinctions (Pounds et al., 1999; Parmesan, 2006).

Clearly, this intimate relationship between short- and long-term atmospheric conditions and biological systems demonstrates the need to incorporate atmospheric data in ecological studies. A large amount of atmospheric data, stored in diverse formats, can be accessed through various Internet portals (Shamoun-Baranes et al., 2010); however, not all data are freely available. The National Centers for Environmental Prediction (NCEP)/National Center for Atmospheric Research (NCAR) Reanalysis data set (Kalnay et al., 1996), hereafter called R-1, and NCEP/Department of Energy (DOE) Reanalysis II data set (Kanamitsu et al., 2002), hereafter called R-2, are high-quality, well-documented, freely-available data sets with global coverage of numerous atmospheric variables. In recent years, these NCEP data sets have been increasingly used in ecological research including studies of phenology (e.g. Chmielewski and Rötzer, 2002; Cook et al., 2005), land cover and atmospheric interaction (e.g. Lawton et al., 2001; Marengo et al., 2008), and bird migration (e.g. Shamoun-Baranes et al., 2010, and references therein). NCEP data can be accessed via ftp where users can download a full year of data, a web service where users can select a temporally and spatially continuous subset of data, or queried directly from the Internet using the Open-source Project for a

network Data Access Protocol (OPenDAP Sgouros, 2004). In all cases, NCEP data are stored in the netCDF data format (a well-documented binary format for storing array-oriented scientific data; Rew et al., 2010) and the user needs to extract the data using specially developed software tools.

To facilitate the extraction, organization, aggregation and visualization of NCEP R-1 and R-2 data, we have developed the RNCEP package of functions in the R language for statistical computing and graphics (R Development Core Team, 2010). R is a freely available open-source computing environment that is highly extendable and can be run on multiple platforms. R is extensively used in ecological research with tools tailored to the ecological community (e.g. Calenge, 2006; Kneib and Petzoldt, 2007). This chapter describes the functionality of the RNCEP package.

2.3 The NCEP data sets

The NCEP/NCAR R-1 and NCEP/DOE R-2 are freely available state-of-the-art gridded reanalysis data sets with global coverage of many relevant atmospheric variables spanning 1957 to present and 1979 to present, respectively. Data for many variables are available at 17 pressure levels ranging from 1000 to 10 mb. Other variables describe conditions either at or near the surface. These data have a spatial resolution of $2.5^\circ \times 2.5^\circ$ and a temporal resolution of 6 h (00, 06, 12, 18 h UTC). Still other variables in these data sets are given on a global T62 Gaussian grid with 192 equally spaced longitudinal and 94 variably spaced latitudinal grid points, also in 6 h intervals.

2.4 The R scripts

Source code and binary distributions of the RNCEP package, with associated help files, are available via the CRAN repository (<http://www.cran.r-project.org/>) and can be installed on most systems by entering

```
install.packages('RNCEP', dependencies=TRUE)
```

 into an R command prompt. Installed in this way, help files may be called using standard R syntax (e.g. `?RNCEP`), and dependent packages are installed automatically. RNCEP depends on the R packages `abind` (Plate and Heiberger, 2004), `fields` (Furrer et al., 2010), `fossil` (Vavrek, 2011), `maps` (Becker et al., 2010), `tcltk` and `tgp` (Gramacy and Taddy, 2010); each is freely available via the CRAN repository.

We have designed several functions that can be used to facilitate common tasks when working with atmospheric data. These tasks are described in more detail in the following text and presented in schematic workflows (Figures 2.1 and 2.2).

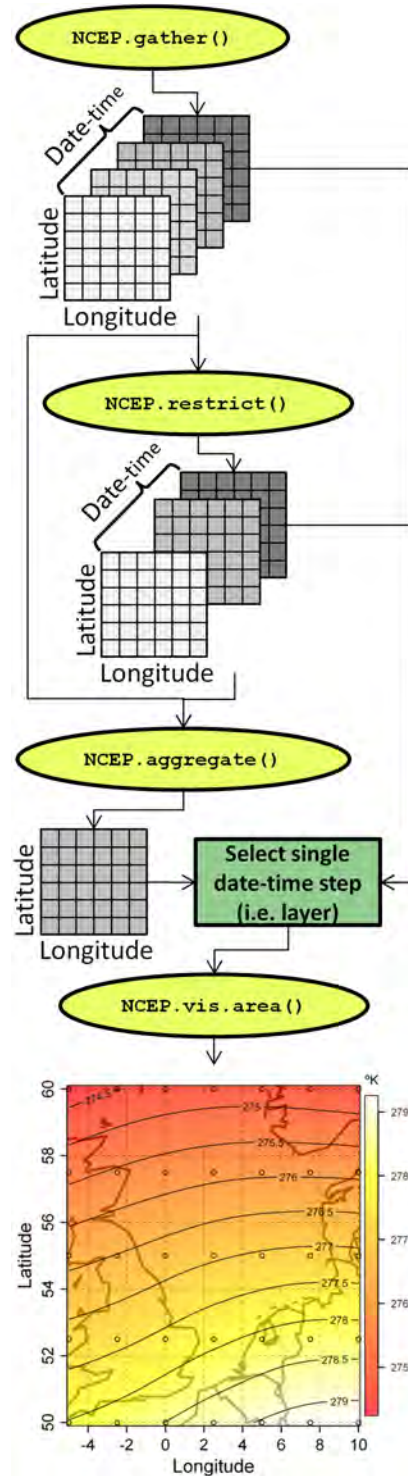


Figure 2.1: This flowchart illustrates a workflow to retrieve and organize data from the R-1 or R-2 dataset for a specified spatiotemporal extent using the RNCEP package. In the workflow, yellow ovals indicate functions in the RNCEP package. `NCEP.gather()` obtains data for a desired spatiotemporal extent. These data are arranged in a three-dimensional array comprising latitude, longitude, and date-time. Any undesired date-times can be removed from the array using `NCEP.restrict()`. `NCEP.aggregate()` temporally aggregates the data array to calculate user-defined summary statistics. `NCEP.vis.area()` visualizes a single date-time (or aggregated date-time) at any point in this process. We show a filled contour plot of mean temperature (K) at 1800 UTC from the 850 mb pressure level from 1 October to 15 October 1970-2000. At any stage, these data may be exported in various formats including those readable by third-party GIS software.

Utilizing R's extensive facilities, one can perform GIS and statistical operations on any retrieved atmospheric data from within R or data may be exported in a variety of formats, ranging from R's internal format to formats that can be imported into third-party GIS software (see the RNCEP help files).

2.5 R functions to retrieve and organize reanalysis data from a specified spatiotemporal extent

2.5.1 Task 1 – Gather NCEP data

The `NCEP.gather()` function retrieves data from the R-1 or R-2 data set, utilizing the OPeNDAP method of data access, for a given spatiotemporal range. Users must specify (i) the variable of interest, (ii) the level (i.e. pressure level, surface or T62 Gaussian grid) from which the variable is to be obtained, (iii) the desired spatial range, (iv) the desired month and year ranges and (v) whether data should come from the R-1 or R-2 data set. With these parameters specified, `NCEP.gather()` returns to the R environment a three-dimensional array containing the specified variable over the desired spatiotemporal range. For example, the user can extract air temperature at the 850 mb pressure level from the R-1 data set for October, 1970-2000, 50°N-60°N, 5°W-10°E (Figure 2.1).

2.5.2 Task 2 – Restrict NCEP data

The structure of the NCEP data sets makes it difficult to download an interrupted time series of data per year. For example, one cannot easily obtain data for only 1200 UTC every day for a specific month. The function `NCEP.restrict()` can be used to remove unwanted temporal intervals from the data imported into R in Task 1 using `NCEP.gather()`. Using `NCEP.restrict()`, one can remove data for a specified year, month, day, hour or any combination of the four. For the example in Figure 2.1, this function is used to restrict the temperature data to 1800 UTC and 1-15 October.

2.5.3 Task 3 – Aggregate NCEP data

Once an array of atmospheric data has been obtained, and the time series restricted, derived variables may be calculated by temporally aggregating or summarizing the array, for example by calculating a mean, percentage of occurrence or an accumulation. For instance, one could calculate mean maximum temperature to explain Malaria epidemics (Githeko and Ndegwa, 2001), the

frequency of tailwind assistance for migrating birds to explain the timing of spring arrival (Sinelschikova et al., 2007), or seasonal temperature accumulation (i.e. degree days) to explain variability in plant phenology Wang (1960). The `NCEP.aggregate()` function is applied to perform these temporal aggregations. It summarizes data at each grid point and returns a new array with the same spatial dimensions as the input array. The user specifies the function to apply (either an internal R-function such as ‘mean’, ‘max’ or ‘sum’ or a function created by the user) and whether or not to aggregate each temporal component: year, month, day and hour. While data returned by `NCEP.gather()` and `NCEP.restrict()` are technically weather data as they describe atmospheric conditions at relatively short temporal intervals, `NCEP.aggregate()` can be used to derive climate data by averaging the atmospheric data over a sufficiently long period. In the example in Figure 2.1, mean temperature at 1800 UTC from 1 to 15 October 1997-2000 is calculated.

2.6 R functions to interpolate reanalysis data to specified points in space and time

The function `NCEP.interp()` interpolates variables from the R-1 or R-2 data set to specified locations in space and time (see Figure 2.2 for a workflow of this procedure). The user must specify the atmospheric variable, level (again, pressure level, surface, or T62 Gaussian grid) from which the variable should be obtained, and spatial and temporal location to which the variable should be interpolated. Further optional arguments include parameters to control interpolation. `NCEP.interp()` will accept vectors as arguments and can, therefore, easily be applied to all of the points in an ecological data set with a single command. Thus, users could calculate the temperature and wind conditions at each location along the entire migratory route of an individually tracked animal (e.g. Shamoun-Baranes et al., 2003a, 2010, and references therein).

`NCEP.interp()` queries the NCEP data base, utilizing OPeNDAP via the Internet, obtaining data from the eight grid points surrounding the desired location in space and time. If the method of interpolation is given as ‘linear’, the function performs trilinear interpolation in latitude, longitude and time. Alternatively, if the method of interpolation is ‘IDW’, the function performs inverse distance weighting (Shepard, 1968) in space followed by linear interpolation in time. The user can turn off interpolation in space or time or both, in which case `NCEP.interp()` performs ‘nearest-neighbor’ interpolation returning the value of the closest grid point in space or time or both, respectively. Spatial interpolation is always performed assuming a spherical grid rather than a planar surface. To indicate the precision of an interpolated

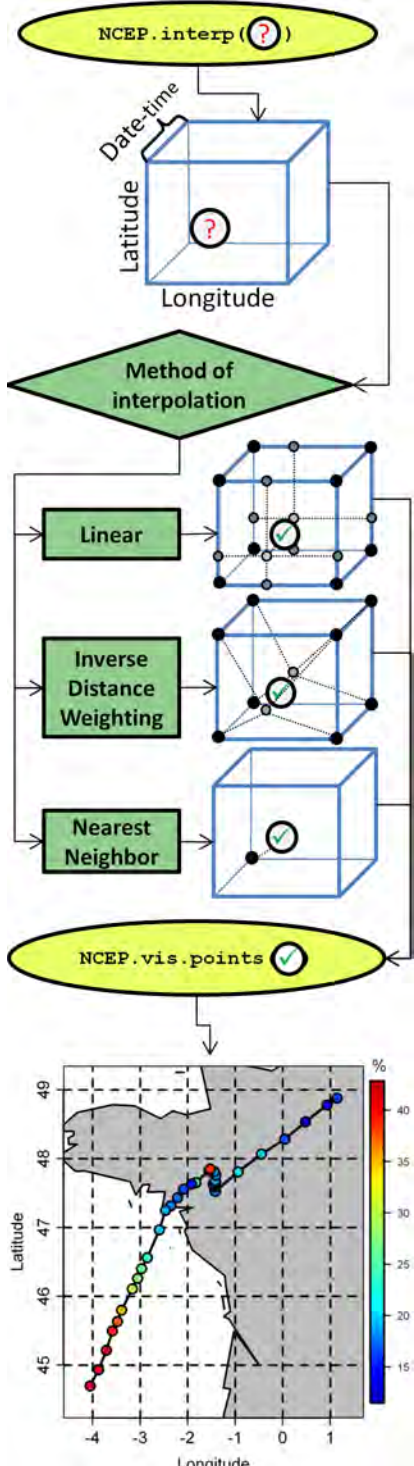


Figure 2.2: This flowchart illustrates a workflow to interpolate weather data from the R-1 or R-2 dataset to specified points in space and time using the RNCEP package. In the workflow, yellow ovals indicate functions in the RNCEP package. `NCEP.interp()` retrieves the eight data points in the R-1 or R-2 dataset surrounding the desired point in space and time. In the flowchart, a question-mark indicates a point in space and time to which interpolation will be performed. The cube indicates the eight grid points in the R-1 or R-2 dataset surrounding the desired point in space and time. The function `interpolate()` interpolates the data from the surrounding grid points using the specified method of interpolation. The question-mark becomes a check-mark after interpolation: the value is now known. `NCEP.vis.points()` visualizes interpolated data in their proper location on a map using color to indicate their value. Here, we see a migrating lesser black-backed gull (*Larus fuscus* Linnaeus, 1758) traveling from northeast to southwest. Its location, recorded by a mounted GPS tracking device, is shown between 17 and 19 September 2008 (median measurement interval: 21 min). The color of the points indicates the linearly-interpolated percentage of total cloud cover. The gull delayed crossing the Bay of Biscay for over 24 h, likely due to inclement weather suggested by the increased cloud cover.

result, `NCEP.interp()` calculates the standard deviation of the values used to perform the interpolation. Thus, precision is described in the same units as the interpolated output, with smaller values indicating less variability among the predictor points. Some variables in these data sets (e.g. cloud cover) should not be temporally interpolated as they describe conditions over an interval of time rather than at a specific point. For these variables, `NCEP.interp()` will not perform interpolation in time and instead automatically retrieves data describing the interval within which the specified date-time falls.

2.7 R functions to visualize reanalysis data

Regardless of whether data are obtained over a spatiotemporal extent or interpolated to a point in space and time, it is often desirable to visualize these data on a map.

`NCEP.vis.area()` produces a contour plot of a single date-time (or single aggregated date-time) from a data-array (Figure 2.1). Specifying only the input data-array and date-time to visualize, the user can quickly obtain a representative map. The map's spatial dimensions, for instance, are automatically set according to the spatial range of the input data-array. The user can also manually configure each aspect of the map.

`NCEP.vis.points()` produces a map indicating the value of a variable interpolated to point locations as obtained using `NCEP.interp()` (Figure 2.2). The color of each point indicates the interpolated value. The user only needs to specify the location of each point and the value of the variable at that point to produce a representative map, yet all aspects of the map are configurable.

2.8 Conclusion

RNCEP is intended to streamline access to and organization of atmospheric data from two freely available high-quality gridded data sets with global coverage. Although other tools exist to extract and visualize these data, e.g. GrADS (Doty et al., 1995) and IDV (Murray et al., 2003), the RNCEP package integrates those functions that are particularly useful for an ecologist: data download, format conversion, subset, aggregation, interpolation and visualization. The package enables rapid adjustment of the spatial and temporal ranges obtained, translating logical user input into the necessary commands in OPeNDAP and returns data in an easily interpretable, unpacked format. Further, RNCEP does not require that any data be stored locally, nor must any particular data base connection be maintained. With only an Internet connection, data may be obtained on-demand, explored, manipulated, integrated

into R statistical analyses and either saved in various formats or discarded. In the future, other gridded data sets (e.g. the NCEP Global Ocean Data Assimilation System) that are available online in a stable format may be accessed using the approach of the RNCEP package. In this way, many functions in the RNCEP package may be applied directly to these new data sets.

Ecology is inherently a multidisciplinary field at the interface between various Earth systems. As such, tools to integrate data from the different systems, enabling efficient and versatile research, are an important aspect of an e-science environment (Hey and Trefethen, 2005). We hope RNCEP will facilitate and encourage the incorporation of atmospheric data into ecological research and promote the exploration of relationships between biological systems and atmospheric conditions. To cite RNCEP or acknowledge its use, cite this article as follows, substituting the version of the package that you used for ‘R package version 1.0.1’:

Kemp, M. U., van Loon, E. E., Shamoun-Baranes, J., and Bouten, W. (2011). RNCEP: global weather and climate data at your fingertips. *Methods in Ecology and Evolution*, 3: 65-70. doi: 10.1111/j.2041-210X.2011.00138.x (R package version 1.0.1).

Acknowledgments

NCEP R-1 and NCEP R-2 data were provided by the NOAA/OAR/ESRL PSD, Boulder, Colorado, USA, from their website at <http://www.esrl.noaa.gov/psd>. R-2 data were produced with the support of the U.S. National Weather Service and U.S. Department of Energy. Please acknowledge the use of NCEP data in any documents or publications. Our studies are facilitated by the BiG Grid infrastructure for e-Science (<http://www.bigggrid.nl>), Flysafe2 and the Dutch National Authority for Data concerning Nature (GaN; <http://www.gegevensautoriteitnatuur.nl>). The authors thank the associate editor of *Methods in Ecology and Evolution* and two anonymous reviewers for constructive comments on an earlier draft of the manuscript.

3

Quantifying flow-assistance and implications for movement research

Kemp, M.U., Shamoun-Baranes, J., van Loon, E.E., McLaren, J., Dokter, A.M., & Bouten, W. (2012) Journal of Theoretical Biology **308**:56-67

3.1 Abstract

The impact that flows of air and water have on organisms moving through these environments has received a great deal of attention in theoretical and empirical studies. There are many behavioral strategies animals can adopt to interact with these flows, and by assuming one of these strategies a researcher can quantify the instantaneous assistance an animal derives from a particular flow. Calculating flow-assistance in this way can provide an elegant simplification of a multivariate problem to a univariate one and has many potential uses; however, the resultant flow-assistance values are inseparably linked to the specific behavioral strategy assumed. We expect that flow-assistance may differ considerably depending upon the behavioral strategy assumed and the accuracy of the assumptions associated with that strategy. Further, we expect that the magnitude of these differences may depend on the specific flow conditions. We describe equations to quantify flow-assistance of increasing complexity (i.e. more assumptions), focusing on the behavioral strategies assumed by each. We illustrate differences in suggested flow-assistance between these equations and calculate the sensitivity of each equation to uncertainty in its particular assumptions for a range of theoretical flow conditions. We then simulate trajectories that occur if an animal behaves according to the assumptions inherent in these equations. We find large differences in flow-assistance between the equations, particularly with increasing lateral flow and

increasingly supportive axial flow. We find that the behavioral strategy assumed is generally more influential on the perception of flow-assistance than a small amount of uncertainty in the specification of an animal's speed (i.e. $< 5 \text{ ms}^{-1}$) or preferred direction of movement (i.e. $< 10^\circ$). Using simulated trajectories, we show how differences between flow-assistance equations can accumulate over time and distance. The appropriateness and potential biases of an equation to quantify flow-assistance, and the behavioral assumptions the equation implies, must be considered in the context of the system being studied, particularly when interpreting results. Thus, we offer this framework for researchers to evaluate the suitability of a particular flow-assistance equation and assess the implications of its use.

3.2 Introduction

Flows of wind and water are some of the most important environmental factors affecting the movement of volant (i.e. flying; e.g. Chapman et al., 2010; Drake and Farrow, 1988; Kunz et al., 2008; Liechti, 2006; Richardson, 1990*b*) and natant (i.e. swimming; e.g. Cotté et al., 2007; Gaspar et al., 2006; Gibson, 2003; Luschi et al., 2003) organisms, respectively. There are several different behavioral strategies, recently reviewed by Chapman et al. (2011), that animals can adopt to make their way through these flows. By assuming a particular behavioral strategy, it is possible to simplify the potential effect of the two components of a flow (e.g. its speed and direction) into a single variable that reflects the support or resistance an animal experiences from the flow, allowing for quantitative comparisons between flow-conditions. Researchers of bird migration, for instance, frequently calculate such a variable (often termed “wind profit” or “wind effect”) to study e.g. flight altitudes (Bruderer et al., 1995*b*), flight speeds (Piersma and Jukema, 1990), flight range (Liechti and Bruderer, 1998), migration intensity (van Belle et al., 2007) and stopover behavior (Åkesson and Hedenström, 2000) in relation to wind conditions (see also Shamoun-Baranes et al., 2007, and references therein). Regardless of the species and the fluid through which it moves, however, correctly quantifying flow-assistance can improve our understanding of often complex biological movement processes including those involved in disease transmission (Sedda et al., 2012). Furthermore, this quantification is likely to become increasingly feasible as tracking devices become smaller (Bridge et al., 2011; Wikelski et al., 2007); animal-borne tracking systems (e.g. Wilson et al., 2008) and dedicated radar systems for animals as small as insects (Chapman et al., 2010) allow for consideration of both the relative motion and body orientation of individuals; and oceanographic (e.g. Rio and Hernandez, 2004) and atmospheric (e.g.

Undén et al., 2002) data sets improve in resolution and accuracy.

As mentioned, the categorization and/or quantification of flow-assistance necessitate explicit and sometimes implicit assumptions of an animal's behavior in relation to the flow. We suspect that a researcher's perception of flow-assistance, and therefore the results of analyses using a flow-assistance variable, may be quite different depending on the behavior assumed and the flow conditions that are encountered. Further, we suspect that the resultant flow-assistance values may be sensitive to uncertainty in these assumed behaviors and that the degree of this sensitivity may also depend on the particular flow conditions. The main goals of this chapter are to provide 1) a reference for potential equations to quantify flow-assistance that explicitly describes each equation's components and assumptions, 2) a comparison of the flow-assistance suggested by these equations for a range of flow conditions, 3) a quantification of the sensitivity of these equations to uncertainty in their respective assumptions, and 4) a methodology to simulate the trajectories that result from the behavior described by each equation. In so doing, we provide a framework for researchers to assess the appropriateness and implications of applying a particular method of flow-assistance quantification to their study system. While many examples provided throughout this chapter are related to birds, the concepts are relevant for any animal moving through air or water.

We begin with an overview of different methods and equations to quantify flow-assistance, starting with those that require the fewest assumptions and progressing through more complex techniques requiring an increasing number of assumptions. Thereafter, we quantify the difference in flow-assistance suggested by these methods and calculate the sensitivity of the associated equations to uncertainty in their respective assumptions. Finally, we model flight trajectories over a given time period using different transport models to explore the potential divergence between these methods over time and distance due to their various behavioral rules.

3.3 Flow-assistance

In this section, we discuss different methods and equations to calculate flow-assistance. Unless otherwise stated, speeds and flow-assistance values are considered in ms^{-1} and directions are considered in degrees from north (with positive angles clockwise). When we introduce a flow-assistance equation, we will give it a name (e.g. "EQ^{Tailwind}") and use that name throughout this chapter. Table 3.1 gives the formula for each equation, and Figure 3.1 contains graphical representations of the flow-assistance values resulting from each equation for a range of theoretical flow conditions (speeds from 0-20 ms^{-1} and

directions from 0-360°). These flow-conditions correspond to Beaufort scale 0-8 or calm through gale force wind conditions in the atmosphere. More complete assessments of these methods and equations, including formal definitions, graphical depictions, and lists of components and assumptions, are located in Appendix A.

Chapman et al. (2011) identify eight unique behavioral strategies that organisms can apply to move in a flow and give examples of animals that are thought to apply each strategy. Two of these strategies suggest that the animal travels in the direction of the flow, either actively (i.e. by applying its own forward motion in the direction of the flow) or passively. According to either of these downstream transport strategies, flow-assistance is equal to flow-speed irrespective of flow direction ($\text{EQ}^{\text{FlowSpeed}}$; Figure 3.1; Table 3.1). Another of these strategies suggests that the animal actively moves against the flow (i.e. upstream transport), suggesting presumably that the slower the flow the better the flow-assistance ($\text{EQ}^{\text{NegFlowSpeed}}$; Figure 3.1; Table 3.1).

The remaining five strategies identified by Chapman et al. (2011) assume that an animal has a preferred direction of movement (pdm) (also called a “goal direction” or “endogenous direction”) that is independent of the direction of the flow. These strategies differ primarily with respect to how deviations from the pdm are handled, and they fall into three general categories: full drift, complete compensation, and partial compensation.

3.3.1 Full drift

Following a strategy of full drift, an animal applies all of its forward motion in its pdm and makes no attempt to compensate for any lateral displacement from this pdm caused by the flow conditions. In the simplest case, flow-assistance under a full drift strategy could be defined in binary terms: the flow gives assistance in the pdm or it does not ($\text{EQ}^{\text{Binary}}$; Figure 3.1; Table 3.1). Because $\text{EQ}^{\text{Binary}}$ produces a nominal, or at best ordinal, description of flow-assistance, we do not consider it in the quantitative analyses of this study. Increasing only slightly in complexity, we can define flow-assistance as the magnitude of the component of the flow along the pdm ($\text{EQ}^{\text{Tailwind}}$; Figure 3.1; Table 3.1), thereby ignoring any component of the flow that is perpendicular or lateral to the pdm. $\text{EQ}^{\text{Tailwind}}$ is probably the most prolific method used to describe flow-assistance and is the *de facto* method being applied anytime an author refers to a tail- or headwind component (e.g. Åkesson et al., 2002; Alerstam et al., 2011; Bruderer et al., 1995b; Richardson, 1978; Shamoun-Baranes et al., 2007).

Table 3.1: Equations introduced in this chapter to quantify flow-assistance. The abbreviated name of each equation (defined in sections 3.3-3.3.3) is given in the left column, and the accompanying formula for each equation is given in the right column. In these equations, flow-assistance (FA) is determined according to the speed of the flow (y) and, depending on the equation, attributes describing an animal's behavior or capabilities: i.e. its speed relative to the Earth (x), speed relative to the Earth in still conditions (x_s), speed relative to the flow (z), and/or proportion of compensation (f) for the component of the flow perpendicular to their preferred direction of movement. All speeds are given in the same units, typically ms^{-1} . The variable θ describes the angular difference between the direction into which the flow is moving and the animal's preferred direction of movement. More detailed definitions of these equations are given in Appendix A.

Name	Formula
$\text{EQ}^{\text{FlowSpeed}}$	$FA = y$
$\text{EQ}^{\text{NegFlowSpeed}}$	$FA = -1y$
$\text{EQ}^{\text{Binary}}$	$FA = \begin{cases} 0, & y \cos \theta \leq 0 \\ 1, & y \cos \theta > 0 \end{cases}$
$\text{EQ}^{\text{Tailwind}}$	$FA = y \cos \theta$
$\text{EQ}^{\text{Airspeed}}$	$FA = y \cos \theta + \sqrt{z^2 - (y \sin \theta)^2} - z$
$\text{EQ}^{\text{Groundspeed}}$	$FA = x - \sqrt{x^2 + y^2 - 2xy \cos \theta}$
$\text{EQ}^{\text{C.Groundspeed}}$	$FA = \begin{cases} x - \sqrt{x^2 + y^2 - 2xy \cos \theta}, & y \cos \theta \leq x \\ y \cos \theta - y \sin \theta , & y \cos \theta > x \end{cases}$
$\text{EQ}^{\text{M.Groundspeed}}$	$FA = (x_s + y \cos \theta) - \sqrt{(x_s + y \cos \theta)^2 + y^2 - 2(x_s + y \cos \theta) \cdot y \cos \theta}$
$\text{EQ}^{\text{PartialSpeed}}$	$FA = y \cos \theta + \sqrt{z^2 - (f \cdot y \sin \theta)^2} - z$

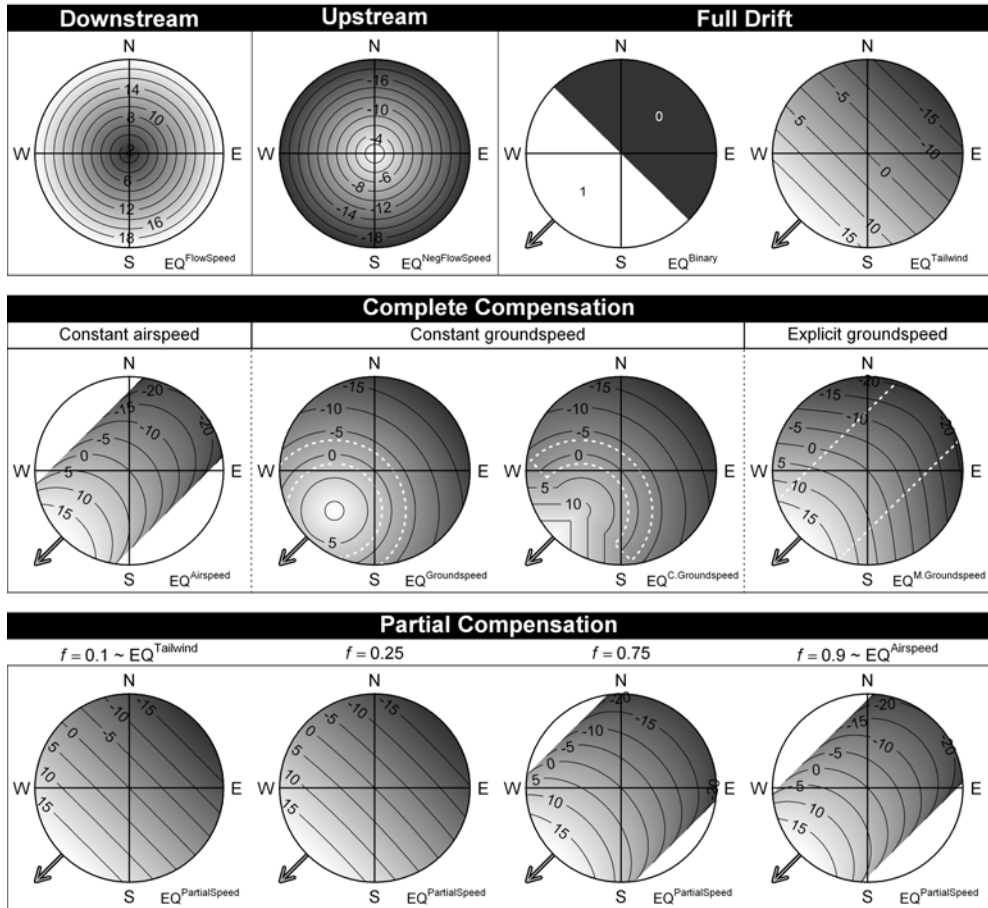


Figure 3.1: Contour plots of flow-assistance for a range of theoretical flow conditions resulting from different behavioral strategies to move in a flow. Solid vertical lines separate the behavioral strategies (downstream transport, upstream transport, full drift, complete compensation, and partial compensation; see sections 3.3-3.3.3 for details of each) and a dashed vertical line separates equations for the same strategy with different assumptions. The abbreviated name for each equation (given in sections 3.3-3.3.3) is shown at each plot's lower right corner. The area within each circular plot indicates particular combinations of flow direction and speed, i.e. direction in the plot indicates flow direction and the distance from the center indicates flow-speed with the edges corresponding to flow-speeds of 20 ms^{-1} . Continued on next page...

Figure 3.1 (continued): The contoured surface within these plots indicates the flow-assistance suggested by the equation for specific combinations of flow-speed and direction, with lighter colors indicating greater flow-assistance. A flow-assistance value of 10, for instance, indicates that, due only to the flow conditions, an animal is moved at 10 ms^{-1} toward its goal, whereas a flow-assistance of -10 indicates that an animal is moved at 10 ms^{-1} away from its goal. For equations in which an animal's speed relative to the flow varies, dashed white contour lines delineate the domain of the flow conditions in which the animal's speed relative to the flow will be between 10 and 15 ms^{-1} . Wherever appropriate, a preferred direction of movement (pdm) of 225° was assumed and is indicated by a large arrow in the southwest corner of each plot. If an equation required an assumed speed of any kind, it was set to 12 ms^{-1} . For the partial compensation equation, we show the resultant flow-assistance values produced by four different settings of the variable f , which describes the proportion of compensation ($f = 0$ is full drift; $f = 1$ is complete compensation).

3.3.2 Complete compensation

A strategy of complete compensation assumes that an animal compensates for all lateral displacement from its pdm caused by the flow conditions. To compensate for displacement, an animal must change its heading and, perhaps more importantly, its speed relative to the fixed Earth (i.e. its “groundspeed”) or its speed relative to the flow – which we will call its “airspeed” for simplicity and for comparison with literature related to flight. Note however that “swim speed”, used to describe an animal’s speed relative to the surrounding water (e.g. Castro-Santos, 2005; Prange, 1976; Sakai et al., 2011), can be considered an equivalent term in this context. When quantifying flow-assistance, it is critically important to understand whether, according to a particular equation, an animal is assumed to adjust its groundspeed or airspeed.

To calculate the influence of wind on the flight time of birds, Piersma and Jukema (1990) formulated an equation that assumes an animal has a fixed airspeed and adjusts its heading (and therefore groundspeed) to maintain its pdm ($\text{EQ}^{\text{Airspeed}}$; Figure 3.1; Table 3.1). With a fixed airspeed, there are always flow conditions in which an animal cannot maintain its pdm – specifically, this occurs when the strength of the lateral component of the flow exceeds the animal’s fixed airspeed. Under these conditions, $\text{EQ}^{\text{Airspeed}}$ produces no real solution. This conforms to the definition of complete compensation given by Chapman et al. (2011), which suggests that, even if an animal intends to completely compensate, any resultant deviation from the pdm negates a strategy of complete compensation.

To explore the effects of wind on migration intensity in central Europe, Erni et al. (2002b) defined a complete-compensation flow-assistance equation which assumes that, in order to maintain its pdm, an animal maintains a constant

groundspeed by adjusting its heading and airspeed ($\text{EQ}^{\text{Groundspeed}}$; Figure 3.1; Table 3.1). As a result of these assumptions, 1) the airspeed required of the animal has no upper limit and 2) flow-assistance has a maximum value that occurs when the animal has zero airspeed (i.e. when the flow is in the pdm at the preferred groundspeed). Thus even if the flow is precisely along the animal's pdm, flow-assistance degrades from optimum if the flow-speed is faster than the animal's constant groundspeed.

To partly address the issue of degrading flow-assistance under potentially more supportive flow conditions, Erni et al. (2005) applied a clause to $\text{EQ}^{\text{Groundspeed}}$. The resulting equation ($\text{EQ}^{\text{C.Groundspeed}}$; Figure 3.1; Table 3.1) retains the assumption of a constant groundspeed except for conditions in which the speed of the flow along the pdm exceeds that groundspeed. Under those conditions, $\text{EQ}^{\text{C.Groundspeed}}$ defines flow-assistance as the component of the flow along the pdm minus the absolute value of any component of the flow perpendicular to the pdm; however, the animal's reaction to these conditions (e.g. its ground- or airspeed and compensation for displacement) is ambiguous.

In this study, we introduce an additional full-compensation flow-assistance equation in which all flow conditions may be quantified, flow-assistance does not degrade from optimum under presumably more supportive flow conditions, and animal behavior is unambiguous for all flow-conditions. This new equation ($\text{EQ}^{\text{M.Groundspeed}}$; Figure 3.1; Table 3.1) is equivalent to $\text{EQ}^{\text{Groundspeed}}$ in still conditions and requires specification of the groundspeed an animal will exhibit in still conditions; however, contrary to $\text{EQ}^{\text{Groundspeed}}$, $\text{EQ}^{\text{M.Groundspeed}}$ does not assume that the animal's groundspeed will remain the same in all flow conditions. Rather, the groundspeed the animal exhibits in still conditions is modified by adding the component of the flow along the pdm. If the strength of the component of the flow along the pdm increases (or decreases), the animal's groundspeed increases (or decreases) equivalently. The animal then maintains that modified groundspeed by adjusting its airspeed and heading. Thus, similar to $\text{EQ}^{\text{Groundspeed}}$ and $\text{EQ}^{\text{C.Groundspeed}}$, the airspeed required of the animal according to $\text{EQ}^{\text{M.Groundspeed}}$ will fluctuate and has no upper-limit. For equations assuming variable airspeed, Figure 3.1 illustrates the domain of flow-conditions in which an animal's airspeed is between 10 and 15 ms^{-1} , which is reasonable for a passerine (Bloch and Bruderer, 1982; Bruderer and Boldt, 2001).

3.3.3 Partial compensation

The methods introduced so far assume that animals either completely compensate for displacement from their pdm or are fully drifted by any lateral component of the flow. The myriad of potential strategies between these ex-

tremes, generally referred to as strategies of “partial compensation” or “partial drift”, describe a situation in which an animal is drifted somewhat away from its pdm but not as far away as it would be drifted under a full drift strategy. To reduce lateral displacement from its pdm caused by the flow conditions, an animal may alter its heading or airspeed – adjusting either of which independently resulting in a concomitant change in the animal’s groundspeed – or a combination of the two.

One method to quantify flow assistance for a partial compensation strategy is to assume that an animal has a fixed airspeed and compensates for a specified proportion of the lateral component of the flow ($\text{EQ}^{\text{PartialSpeed}}$; Figure 3.1; Table 3.1) by adjusting its heading and therefore groundspeed. $\text{EQ}^{\text{PartialSpeed}}$ contains a parameter (f) describing the proportion of the lateral component of the flow for which the animal will compensate. Of particular appeal is that this equation can encompass not only strategies of partial compensation but also strategies of full drift and complete compensation depending on the value of f – setting f to zero reduces $\text{EQ}^{\text{PartialSpeed}}$ to $\text{EQ}^{\text{Tailwind}}$ (i.e. the animal is fully drifted), while setting f to one reduces $\text{EQ}^{\text{PartialSpeed}}$ to $\text{EQ}^{\text{Airspeed}}$ (i.e. the animal completely compensates). As with $\text{EQ}^{\text{Airspeed}}$, $\text{EQ}^{\text{PartialSpeed}}$ can also produce no real solution in some flow conditions. This occurs when, given its fixed airspeed, an animal cannot compensate for the specified proportion of the lateral component of the flow.

3.3.4 Other strategies

Thus far, we have discussed six of the eight behavioral strategies outlined by Chapman et al. (2011), but we have neglected mention of “compass-biased downstream orientation” and “over-compensation”. In the context of quantifying flow-assistance, compass-biased downstream orientation is indistinguishable from a strategy of partial compensation and could therefore be represented by an equation such as $\text{EQ}^{\text{PartialSpeed}}$. Over-compensation, however, describes a situation in which an animal has a (local or immediate) pdm that clearly differs from the pdm assumed by the researcher. Thus in the context of quantifying flow-assistance, the concept of over-compensation is not so much a unique behavioral strategy as an alternative specification of the pdm.

3.4 Methods

3.4.1 Sensitivity analysis

Considering the different behavioral assumptions inherent in these flow-assistance equations, we performed sensitivity analyses to determine whether (and to

what degree) perceived flow-assistance depended upon 1) the equation applied and 2) uncertainty in each equation's assumptions.

We first calculated the absolute difference in flow-assistance between the equations for a range of theoretical flow conditions (speeds from $0\text{-}20\text{ ms}^{-1}$ and directions from $0\text{-}360^\circ$) and show the results graphically. Further, we calculated the average of the flow-assistance values suggested by each equation over the same range of theoretical flow conditions to serve as a measure of the relative “optimism” of the flow-assistance equation – more optimistic equations therefore suggest larger estimates of flow-assistance on average than less optimistic equations. We assumed a speed (ground- or air- depending on the equation) of 12 ms^{-1} , which is representative of the airspeeds calculated for many migrating passerine species (Bloch and Bruderer, 1982; Bruderer and Boldt, 2001), and a pdm of 225° . When considering $\text{EQ}^{\text{PartialSpeed}}$, we set f (i.e. the proportion of compensation) to 0.5.

We then determined the sensitivity of each equation to uncertainty in its particular assumptions for a range of theoretical flow conditions (speeds from $0\text{-}20\text{ ms}^{-1}$ and directions from $0\text{-}360^\circ$) and show these differences graphically. For each equation that assumes a pdm, we calculated the difference in flow-assistance that resulted from a change in the pdm of 1° , 10° , and 30° (i.e. by comparing a pdm of 225° with pdms of 226° , 235° , and 255°). For each equation that assumes a ground- or airspeed, we calculated the difference in flow-assistance that resulted from a change in the assumed speed of 1, 2, and 5 ms^{-1} (i.e. by comparing a speed of 10 ms^{-1} with speeds of 11, 12, and 15 ms^{-1}). For $\text{EQ}^{\text{PartialSpeed}}$, we calculated the difference in flow-assistance that resulted from a change in f of 0.1, 0.25, and 0.5 (i.e. by comparing f set to 0.1 with f set to 0.2, 0.35, and 0.6). When not being tested, we set the pdm to 225° , any speed-related assumption to 12 ms^{-1} , and f to 0.5. We also performed an analytical assessment of the sensitivity of each equation to uncertainty in its various assumptions by calculating the partial derivative of the equation with respect to each assumption. These analytical results can be found in Appendix A.

3.4.2 Simulating trajectories

We expected that the suitability of a particular flow-assistance equation would depend upon not only the assumptions applied, but also on the study system including the actual conditions encountered. Further, we expected that the consequences of applying a particular equation may accumulate over time and distance. Thus, we developed a dynamic model for movement of individuals in a fluid medium, incorporating the concepts of a pdm and constraints on air- and groundspeed as specified by the flow-assistance equations. This “FFlow-

Assistance Trajectory model” (hereafter FLAT model) is described in detail in Appendix B and has been implemented in the open-source R language (R Development Core Team, 2010). The FLAT model can simulate the trajectory that an animal would exhibit in the real world if it acted according to the behavioral rules of a particular equation.

The FLAT model is an extension of the RNCEP package described in Chapter 2. The trajectory simulator function developed for this study, `NCEP.flight()`, makes use of the `NCEP.interp()` function to interpolate atmospheric data from the National Centers for Environmental Prediction (NCEP)/Department of Energy (DOE) Reanalysis II dataset (Kanamitsu et al., 2002) to any time and location.

We simulated the flight of a nocturnal passerine departing at sunset from the southern tip of Norway (58°N 7°E) intent on arriving at a particular goal location (54°N 0.161°W) on the coast of the U.K. For every night in October from 1980-2010, we simulated a trajectory if the equation being tested suggested positive flow-assistance at the time of take-off. We assumed that this simulated bird was able to fly for 13 hours with a pdm of 225° . We assumed a speed (ground- or air- depending on the equation) of 12 ms^{-1} , and we used wind conditions at the 925 mb pressure level. We considered whether or not a bird arrived within 50 km of its goal location (i.e. 54°N 0.161°W) as a primary measure of its success. We considered whether or not the bird arrived at the coast of the U.K. as a secondary measure of its success. We ended a night’s simulation as soon as the primary measure of success was achieved but otherwise allowed the simulation to run the full 13 hours. If at some point during a simulation the bird could not perform the actions specified by the flow-assistance equation (e.g. with $\text{EQ}^{\text{Airspeed}}$ the bird could not fully compensate with its fixed airspeed), the simulation for that night ended and the bird made no further progress. Otherwise, we placed no restrictions on the bird (e.g. with $\text{EQ}^{\text{Groundspeed}}$ we did not place an upper limit the bird’s airspeed); however, for equations that assumed variable airspeed (i.e. $\text{EQ}^{\text{Groundspeed}}$ and $\text{EQ}^{\text{M.Groundspeed}}$), we also reported measures of performance that resulted if we ended the simulations when the airspeed required of the bird was outside an acceptable range, which we defined as being between 10 and 15 ms^{-1} . We recorded the bird’s location and its (ground- and air-) speed as well as the flow conditions after each hour of the simulation.

Note that $\text{EQ}^{\text{C.Groundspeed}}$ does not specify the behavior of the animal for all flow conditions, so we did not consider that equation in these simulations. Further, $\text{EQ}^{\text{NegFlowSpeed}}$ does not produce positive flow-assistance values, so we initiated take-off for that equation only on nights when flow-speed was less than the bird’s assumed airspeed (i.e. 12 ms^{-1}).

From these simulated trajectories, we considered differences between the flow-assistance equations with regards to 1) the proportion of nights that take-off was initiated 2) the average distance to the goal at the end of the simulation, 3) the proportion of nights with a successful arrival according to our primary criteria (i.e. arrival within 50 km of the goal location), and 4) the proportion of nights with successful arrival according to our secondary criteria (i.e. arrival at the U.K. coast). We also visualized the resultant trajectories on a map.

3.5 Results

3.5.1 Sensitivity analysis

The difference in flow-assistance between each equation for a range of theoretical flow conditions is visualized in Figure 3.2. In general, these equations differ most with increasingly supportive axial flow and increasing lateral flow. The equations agree most often with prohibitive axial flow, and most equations agree completely with prohibitive flows containing no lateral component. Figure 3.2 also indicates the average flow-assistance resulting from each equation for the range of flow conditions we tested. These averages suggest that the less compensation assumed by an equation the more optimistic are its estimates of flow-assistance. We note, however, that these averages (particularly those of $\text{EQ}^{\text{PartialSpeed}}$, $\text{EQ}^{\text{Airspeed}}$, $\text{EQ}^{\text{M.Groundspeed}}$, $\text{EQ}^{\text{Groundspeed}}$, and $\text{EQ}^{\text{C.Groundspeed}}$) are dependent on the ground- or airspeed assumed and the range of flow-speeds that are considered.

The sensitivity of each individual equation to uncertainty in its particular assumptions is visualized in Figure 3.3. Clearly, larger errors in any given assumption produce larger differences in suggested flow-assistance. Interestingly, shifting the pdm produces a line of zero difference for flows along the axis between the two directions; however, differences tend to increase with increasing lateral flow and increasingly supportive axial flow that is not along this line of zero difference. For the ranges of uncertainty we tested, equations were more sensitive to the pdm than to airspeed, groundspeed, or f . Nevertheless, differences in flow-assistance from minor uncertainty in a particular assumption (i.e. $< 10^\circ$ for the pdm, $< 5 \text{ ms}^{-1}$ for the ground- or airspeed) are generally smaller than differences in flow-assistance between the equations themselves (cf. Figure 3.3). For any given flow conditions, the partial derivative equations in Appendix A allow for the explicit calculation of the sensitivity of a particular equation to a particular assumption.

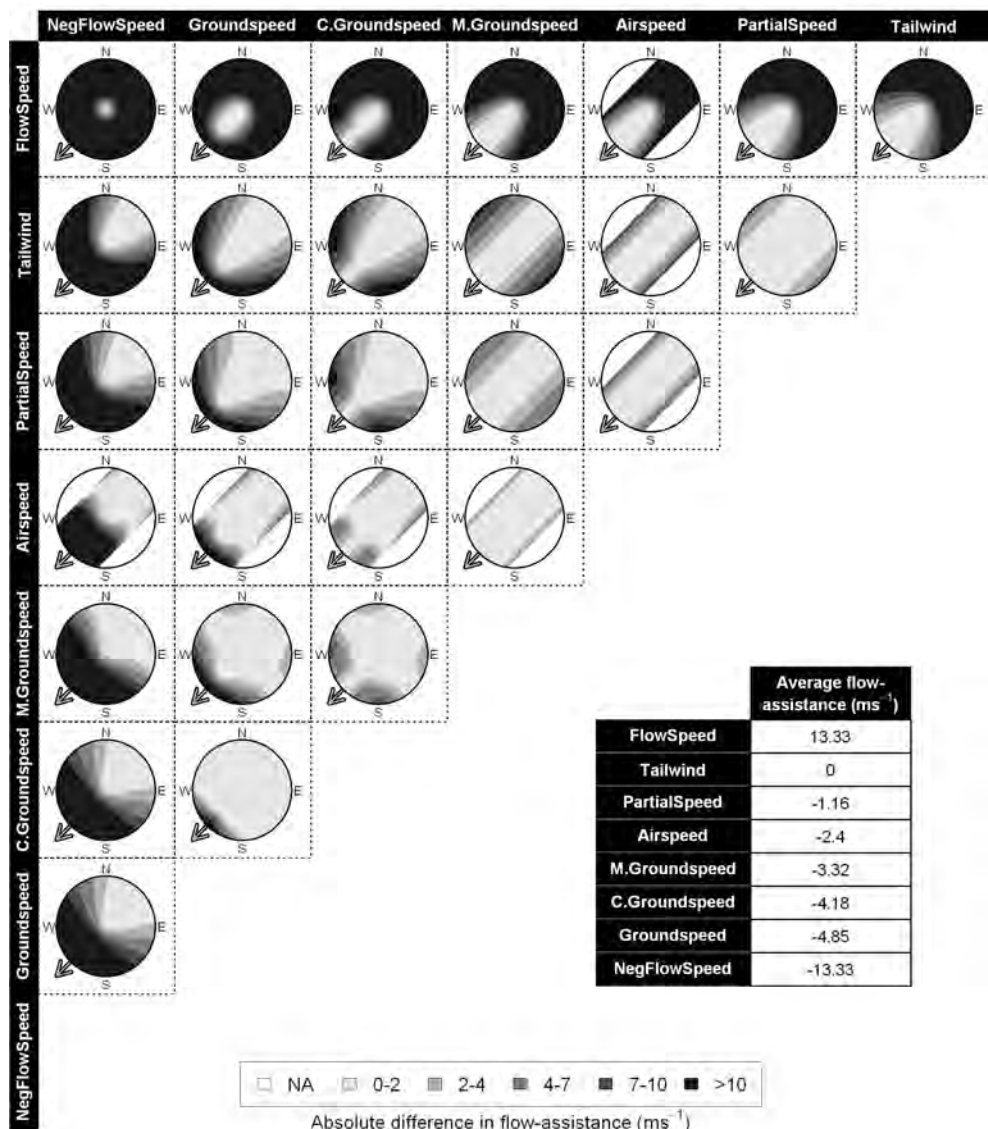


Figure 3.2: This figure contains 1) a main table with contour plots indicating the absolute difference in flow-assistance between different flow-assistance equations for a range of theoretical flow conditions and 2) a sub-table with the average flow-assistance suggested by each equation in ms^{-1} . In both tables, the equations are listed from top to bottom by decreasing average flow-assistance for the range of flow conditions we tested. Continued on next page...

Figure 3.2 (continued): In the main table, the contoured surface within the plots indicates the absolute difference (ms^{-1}) in flow-assistance between the equation in the row name and the equation in the column name, with darker shades of gray indicating greater difference; a key is given at the bottom of the figure illustrating the ranges encompassed by each shade of gray. Areas of the contoured surface in white have no real solution. Location within each circular plot indicates a particular combination of flow direction and speed, i.e. direction in each plot indicates flow direction and the distance from the center indicates flow-speed with the edges corresponding to flow-speeds of 20 ms^{-1} . Wherever appropriate, a preferred direction of movement (pdm) of 225° was assumed and is indicated by the large arrow in the southwest corner of each plot. If an equation required an assumed speed of any kind, it was set to 12 ms^{-1} . For $\text{EQ}^{\text{PartialSpeed}}$, we set f , i.e. the proportion of compensation, to 0.5.

3.5.2 Simulating trajectories

The trajectories that resulted from our simulation are shown graphically in Figure 3.4 and summary information for these trajectories is given in Table 3.2. Generally speaking, more optimistic equations (i.e. equations assuming less compensation and producing higher estimates of flow-assistance) are associated with a higher percentage of nights with take-off; however, these equations also resulted in larger distances to the goal location at the end of the simulation and a lower chance of successful arrival. We note that, had we run the simulation for 14 rather than 13 hours, $\text{EQ}^{\text{Groundspeed}}$ would have a 100% success rate for both the primary and secondary measures. Furthermore, recall that we allowed negative flow-assistance values at take-off for $\text{EQ}^{\text{NegFlowSpeed}}$. Had we not, the number of nights with take-off for that equation would have been zero. Based on the current simulation parameters and wind conditions, $\text{EQ}^{\text{M.Groundspeed}}$ resulted in the highest proportion of successful arrivals and the highest absolute number of successful arrivals according to either of our measures of success; however, when restrictions were placed on airspeed, the performance of equations assuming variable airspeed (i.e. $\text{EQ}^{\text{Groundspeed}}$ and $\text{EQ}^{\text{M.Groundspeed}}$) worsened considerably.

3.6 Discussion

Calculating flow-assistance is a useful way to evaluate the complex and non-linear effects of the two components of a flow (e.g. its speed and direction) on aspects of animal movement in static or dynamic models. In particular, calculating flow-assistance facilitates quantitative comparisons between different flow-conditions. We have shown that different definitions of flow-assistance are linked to different behavioral rules and, depending on the behavioral rules as-

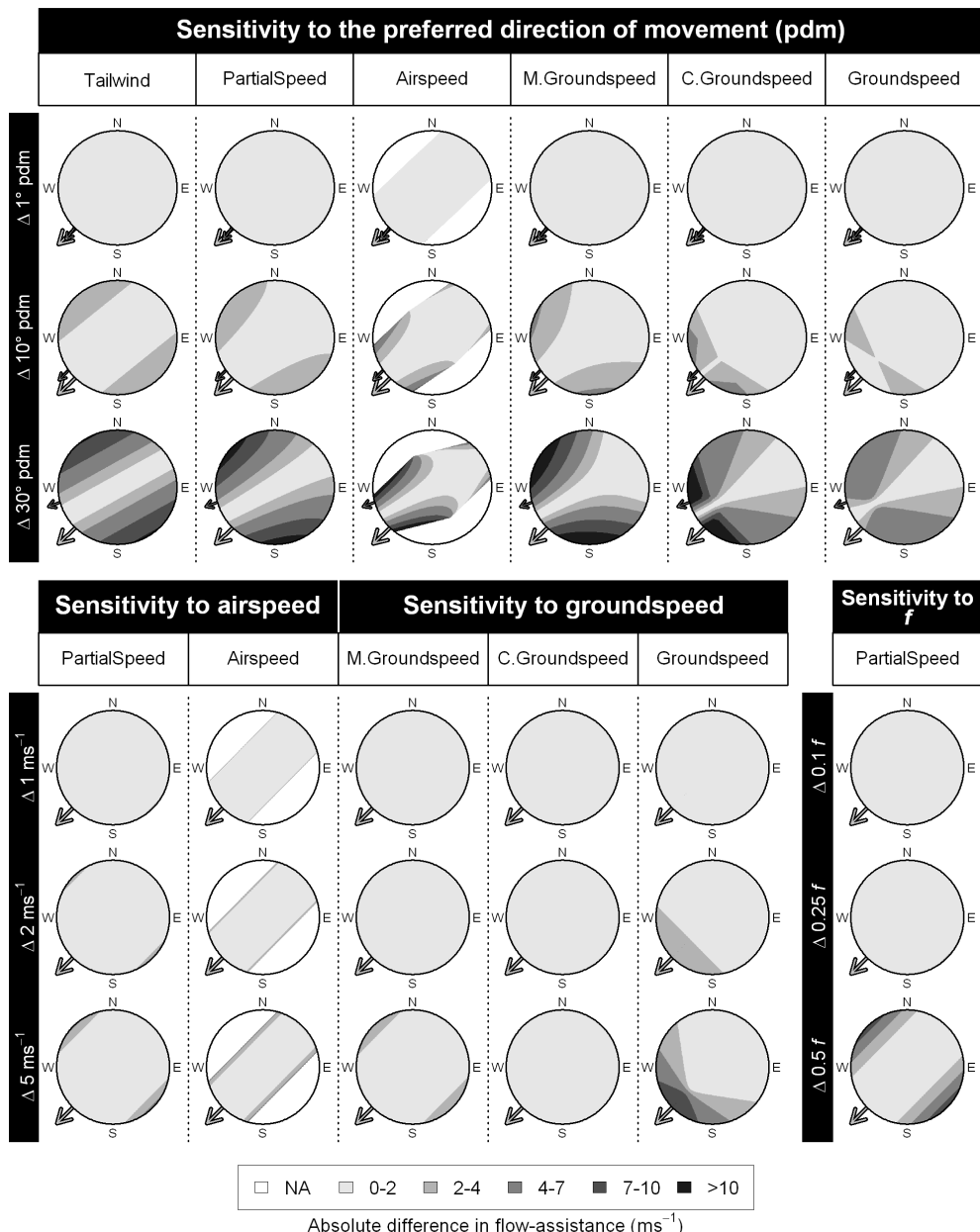


Figure 3.3: Contour plots indicating the absolute difference in flow-assistance, for a range of flow conditions, produced by uncertainty in an equation's assumptions. Continued on next page...

Figure 3.3 (continued): The assumption being tested is indicated in the major column header (cells shaded black), and the equation for which that assumption is being tested is indicated in the minor column header (cells shaded white). Within each group, equations are presented from left to right by decreasing average flow-assistance for the range of flow conditions we tested (see Figure 3.2). Row names indicate the amount of difference (i.e. uncertainty) in a given assumption. The contoured surface within these plots indicates the absolute difference in flow-assistance produced by the specified change in the specified assumption, with darker colors indicating greater difference; a key is given at the bottom of the figure illustrating the ranges encompassed by each shade of gray. Areas of the contoured surface in white have no real solution. Location within each circular plot indicates a particular combination of flow direction and speed, i.e. direction in the plot indicates flow direction and the distance from the center indicates flow-speed with the edges corresponding to flow-speeds of 20 ms^{-1} . When not being tested, the preferred direction of movement (pdm) was set to 225° (indicated by a large arrow in the southwest corner of each plot), any assumed speed was set to 12 ms^{-1} , and f (i.e. the proportion of compensation in $\text{EQ}_{\text{PartialSpeed}}$) was set to 0.5. When testing the effects of uncertainty in the pdm, the alternative pdm is indicated by a smaller arrow in the west-southwest of the plot.

sumed, the perception of flow-assistance can be quite different for the same flow conditions. These differences can shape our impression of the efficiency and/or success of an animal's movement through a flow. Ultimately, whether or not particular flow conditions are considered supportive at all is dependent on the equation applied. Thus, results derived through the use of a flow-assistance equation must be interpreted in the context of the behavior assumed by that equation, and we expand upon this point in sections 3.6.1-3.6.4.

3.6.1 Compensation and flow-assistance

The flow-assistance equations presented in this study describe varying degrees of compensation for lateral displacement, which can affect the flow-assistance an animal experiences for given flow conditions. Extreme examples of compensation for lateral displacement are represented by $\text{EQ}^{\text{FlowSpeed}}$ and $\text{EQ}^{\text{NegFlowSpeed}}$: the former describing a strategy of “ultimate drift” and producing the largest (i.e. most optimistic) estimates of flow-assistance and the latter a strategy of “ultimate compensation” and the smallest (i.e. most pessimistic) estimates of flow-assistance. What is highlighted by these extremes is that for any given flow conditions, more compensation results in lower flow-assistance values. In other words, an equation that assumes more compensation will never produce a larger estimate of flow-assistance than an equation that assumes less compensation, since compensation reduces flow-

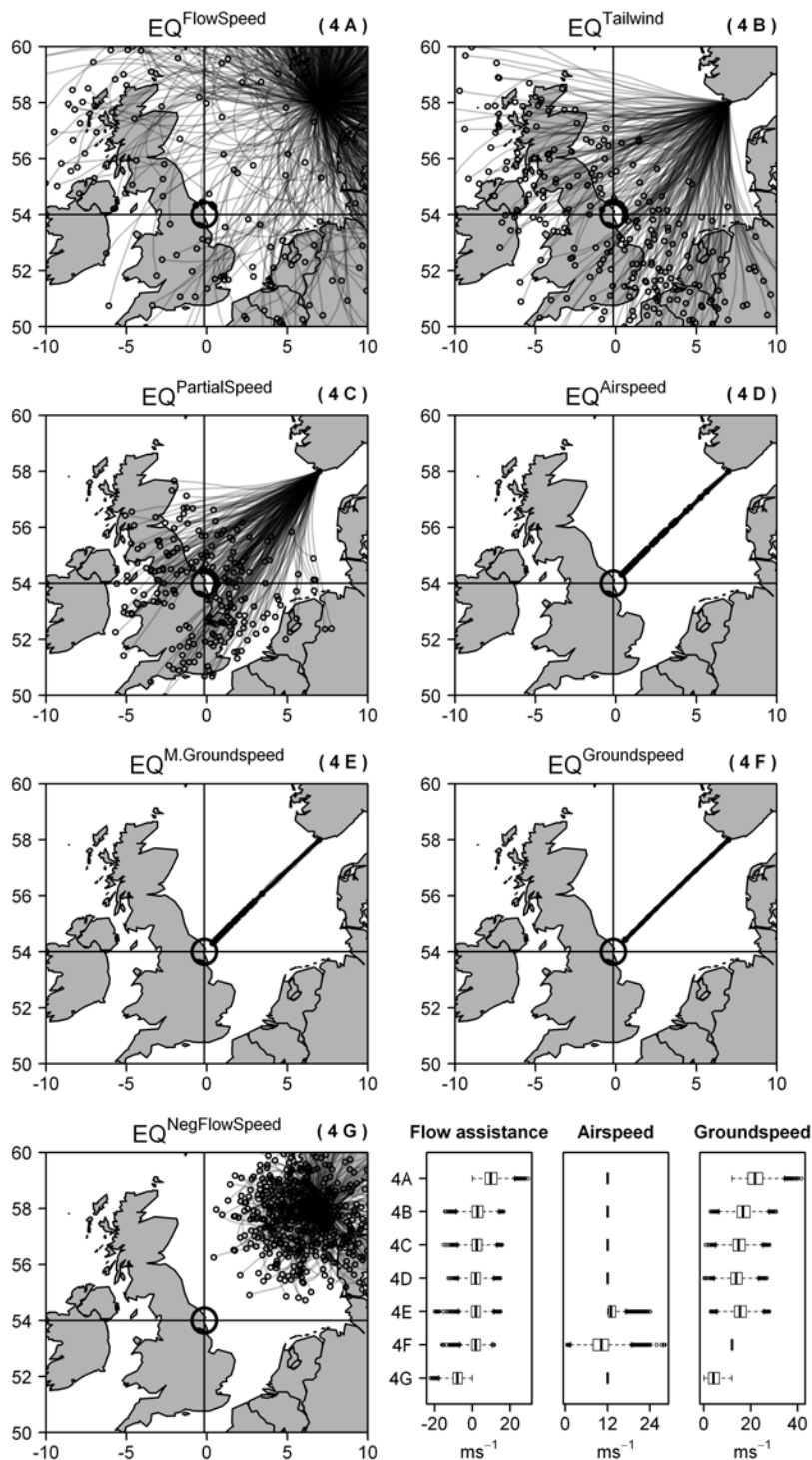


Figure 3.4 (previous page): Plots of the trajectories that resulted from our simulation and box-plots indicating distributions flow-assistance, air-, and groundspeeds. For each flow-assistance equation that specifies behavior, we simulated a nocturnal passerine – behaving according to the assumptions of the equation – leaving the southern tip of Norway (58°N 7°E) every night in October at sunset from 1980-2010 with a pdm of 225° intent on arriving at 54°N 0.161°W on the coast of the U.K. (indicated by the cross-hairs). See section 3.4.2 for more details. For each simulated trajectory, the path taken by the bird is indicated by a gray line and the bird’s ending location is indicated by an open circle. Each plot showing the trajectories for a given flow-assistance equation is given an abbreviated name (e.g. “4A”). These abbreviated names indicate the ordering of the equations by decreasing average flow-assistance for the range of flow-speeds we tested (see Figure 3.2). The box-plots use these abbreviated names to refer to the associated plot and, therefore, flow-assistance equation. These box-plots indicate the distributions of flow assistance encountered and the air- and groundspeeds exhibited during the simulation for each flow-assistance equation. Boxes in these box-plots indicate the upper and lower quartiles and median, “whiskers” indicate values < 1.5 times the inter-quartile range beyond the quartiles, and points indicate outliers.

assistance while drifting away from the pdm does not. Thus, the amount of compensation specified by an equation implicitly defines, for the system being studied, the importance of lateral displacement from the pdm; $\text{EQ}^{\text{Tailwind}}$, which assumes no compensation for displacement from the pdm, implies that drifting away from the pdm is of no consequence, while the complete compensation strategy underlying $\text{EQ}^{\text{Airspeed}}$ implies that it is necessary that the animal maintains its pdm.

It is possible that an animal switch between compensation strategies. For instance, an animal could completely compensate when the lateral flow component is small and begin to partially compensate or even fully drift as the lateral flow component increases. Alternatively, an animal could exhibit a full drift strategy up to some threshold of lateral displacement and only begin to (partially) compensate thereafter (McLaren et al., 2012). Klaassen et al. (2011) suggest that the degree of compensation by migrating raptors can vary dramatically by geographical region and also in relation to the flow conditions encountered. Thus for a given species, displacement from the pdm may be more or less important in different locations, and displacement to one side of the pdm may be more or less important than displacement to the other side. Conversely, Horton et al. (2011) observed migrating humpback whales completely compensating for displacement from their pdm through variable ocean currents for distances of 200 km or more.

Table 3.2: A summary of the trajectories simulated for each flow-assistance equation is given. Included are the percentage of nights during October 1980-2010 that take-off was initiated (i.e. flow-assistance was positive, except considering $\text{EQ}^{\text{NegFlowSpeed}}$, see section 3.4.2), the average distance (km) to the goal location ($54^{\circ}\text{N } 0.161^{\circ}\text{W}$) at the end of the simulations, the percentage of nights with take-off that resulted in a successful arrival according to our primary criteria (i.e. < 50 km from the goal location), and the proportion of nights with take-off that resulted in a successful arrival according to our secondary criteria (arrival at the U.K. coast). Values in parentheses indicate, for equations assuming variable airspeed, results that occurred when airspeeds were restricted to between 10 and 15 ms^{-1} . The equations are listed from top to bottom by decreasing optimism (i.e. decreasing average flow-assistance for the range of flow conditions we tested).

Equation	Nights with take-off (% of 961)	Average distance to goal (km)	Primary successful arrival (%)	Secondary successful arrival(%)
$\text{EQ}^{\text{FlowSpeed}}$	100	1296	1	6
$\text{EQ}^{\text{Tailwind}}$	29	364	8	51
$\text{EQ}^{\text{PartialSpeed}}$	26	207	17	60
$\text{EQ}^{\text{Airspeed}}$	18	100	63	63
$\text{EQ}^{\text{M.Groundspeed}}$	20 (17)	67 (132)	82 (61)	82 (61)
$\text{EQ}^{\text{Groundspeed}}$	18 (8)	68 (316)	0 (0)	0 (0)
$\text{EQ}^{\text{NegFlowSpeed}}$	66	623	0	0

3.6.2 The preferred direction of movement

A fundamental assumption of most of the equations in this chapter is that an animal has a pdm that is known. In fact, the pdm can be the most difficult variable to ascertain in these equations. While the dynamics of a flow and the groundspeed of an individual animal can be measured directly, and the airspeed of the animal then derived, it can be difficult to measure the pdm of a free-moving animal, particularly at smaller scales. There are some instances when researchers can presume a pdm with a high degree of certainty, for instance when flow-speeds are negligible or when an animal is nearby and returning to a known location such as its nest. Often, however, the pdm must be estimated from observed behavior, for example using ori-

tation cages (Åkesson and Sandberg, 1994; Emlen and Emlen, 1966) or radar (Chapman et al., 2010; Liechti et al., 2012). Regardless, this estimation can be problematic. Nievergelt et al. (1999) suggest that differences in pdm can occur between caged and free-moving animals, and Green and Alerstam (2002) show how non-random distributions of flow conditions may bias estimations of drift (and implicitly estimations of the pdm) in migrating birds. Importantly, we have found that small errors in the pdm (i.e. $< 10^\circ$) are generally less influential on the perception of flow-assistance than the overall behavioral strategy assumed.

While we retained a static pdm in our trajectory simulation, it is perfectly legitimate to assume that an animal adjusts its pdm at different spatial and temporal scales. For instance, hatchling loggerhead (*Caretta caretta*) and green turtles (*Chelonia mydas*) orient offshore, often against approaching waves (Lohmann and Lohmann, 1992; Salmon and Lohmann, 1989), in an initial “frenzied” swim to reach deeper water where they then make use of favorable ocean currents for dispersal (Hays et al., 2010; Salmon and Wyneken, 1987). Avian research also suggests that the pdm may not be consistent along the entire migratory journey (Fortin et al., 1999; Liechti et al., 2012; Thorup and Rabøl, 2001), and local adjustments to the pdm are especially likely in species avoiding a barrier or obstacle (e.g. Alerstam, 2001) or making use of thermal and/or orographic uplift (Brandes and Ombalski, 2004; Leshem and YomTov, 1996). To address this variability, Mandel et al. (2008) explored an elegant method of determining the pdm at local scales through the use of an autoregressive moving average of previous movement.

Depending on the level of knowledge an animal has of its own location in relation to the location of its end goal, the animal could alter its pdm at intervals along its journey to compensate for previous displacement (see e.g. Richardson, 1990b). In so doing, the animal could apply a full drift or partial compensation behavioral strategy and still arrive at a very specific goal location, and Alerstam (1979) explored the optimality of such behavior for different flow conditions. The FLAT model presented in this study can simulate this type of behavior allowing a researcher to consider flow-assistance according to a dynamic pdm that automatically adjusts toward a specified goal location.

3.6.3 Ground- and airspeed

Many of the equations discussed in this chapter require an assumed travel speed, given as either a ground- or airspeed. While we have shown that a small degree of uncertainty in these assumed speeds is less influential on the perception of flow-assistance than the equation applied, it is important for

a researcher to know which speeds vary and which speeds are held constant according to the assumptions of a particular equation.

For instance, with $\text{EQ}^{\text{Groundspeed}}$ an animal's groundspeed is presumed constant and, to completely compensate for drift, heading and airspeed are altered and are not constrained. The trajectories produced by $\text{EQ}^{\text{Groundspeed}}$ in our simulations exhibit airspeeds ranging from 0.6 to 28.2 ms^{-1} (Figure 3.4), which exceed both the upper and lower range of realistic and observed airspeeds for passerines (Bruderer and Boldt, 2001; Pennycuick, 2008). Thus, the assumptions underlying $\text{EQ}^{\text{Groundspeed}}$ – as well as those underlying $\text{EQ}^{\text{M.Groundspeed}}$ – may be inappropriate to apply in a simulation because of the potentially unrealistic airspeeds required to maintain full compensation. As we have seen, restricting the airspeeds allowed by these equations can considerably influence the results of analyses (see Table 3.2). $\text{EQ}^{\text{Groundspeed}}$ is a legitimate measure of flow-assistance, however, since any airspeed required of the animal decreases flow-assistance, and unrealistic airspeeds inevitably lead to poor flow-assistance values. Furthermore, $\text{EQ}^{\text{Groundspeed}}$ may be of particular use in some instances as it is the only equation we discussed that can reflect a situation in which an animal is assumed to dislike flows above a certain speed, even in a desirable direction.

3.6.4 Range estimation

Some of these equations have been used in an effort to incorporate flow effects into models to estimate the distance an animal can travel with a given amount of energy (Alerstam and Lindström, 1990). In a simple case, Weber et al. (1998) and Weber and Hedenström (2000), using $\text{EQ}^{\text{Binary}}$, expanded their modeled bird's flight range by 20% under supportive conditions (i.e. "good" winds) but left it unchanged under prohibitive conditions (i.e. "bad" winds). Others have used the quantitative measure of flow-assistance from $\text{EQ}^{\text{Tailwind}}$ (e.g. Delingat et al., 2008; Liechti and Bruderer, 1998) to modify flight range.

When incorporating flow-assistance into models to estimate swim or flight range, that range will be larger with flow-assistance equations that allow drift from the pdm than with equations that do not. Therefore when applying an equation that implicitly allows or ignores drift (e.g. $\text{EQ}^{\text{PartialSpeed}}$ or $\text{EQ}^{\text{Tailwind}}$), a researcher must be comfortable making one of the following two assumptions: 1) the animals under consideration will be drifted by whatever lateral flow is present (or remaining after partial compensation), but the displacement due to this drift is unimportant, or 2) the animal will compensate for whatever lateral flow is present (or remaining), but the energy required to do so is unimportant. Delingat et al. (2008), for instance, presumed the latter, stating that the birds in their study were not engaged in a full drift

strategy but rather that “the effects due to wind drift compensation... will be small in comparison with the overall range estimates.” Alternatively, the first assumption may be satisfied if, for the area or trajectory being studied, lateral flows are minimal enough or equally distributed across both sides of the pdm such that the resulting drift does not force the animal outside the bounds of its geographical goal. Our trajectory simulation showed that by allowing drift an animal may be unable to arrive at a specific goal location. Consider that only 8% of the trajectories simulated according to EQ^{Tailwind} resulted in a successful arrival according to our primary criteria (i.e. within 50 km of the goal location; Figure 3.4 and Table 3.2). However, this rate of success increases dramatically to 51% if the bird needs only to reach the U.K. mainland (Figure 3.4 and Table 3.2). Therefore, a flow-assistance equation that allows drift may overinflate estimates of an animal’s potential range if the system in question requires the animal to arrive at a very specific location and does not allow the animal to adjust its pdm during the journey. The FLAT model can be used to examine this possibility explicitly and determine if, for a particular system and behavior, an animal would be drifted outside the bounds of its goal location.

3.7 Conclusion

While a great deal of the literature cited and analyses performed in this chapter are avian-related, the concepts generally apply to all organisms traveling through a fluid environment. EQ^{FlowSpeed} can even be applied when considering objects such as seeds and pollen that have no means of self-propulsion or drift passively with the flow (Nathan et al., 2005). Nonetheless, the particulars of each system deserve consideration as there remain important differences relevant to the quantification of flow-assistance between animals and their mediums of travel: e.g. in contrast to a flying animal, a swimming animal may not need to maintain a minimum speed relative to the flow in order to stay afloat.

Quantifying flow-assistance according to a particular method implies certain behavioral rules. These behavioral rules, which govern an animal’s reaction to a flow or determine the relative importance of the flow, reflect an animal’s desired goals. These goals may be evaluated in intervals from seconds to seasons, or even lifetimes and likely fluctuate depending on factors such as life history stage (e.g. Luschi et al., 2003; Thorup et al., 2003), available energy (see e.g. Schmaljohann and Naef-Daenzer, 2011, and references therein), time of the season (Ellegren, 1993; James et al., 2005; Karlsson et al., 2012), distance to their desired goal (Karlsson et al., 2012; Liechti, 1995), and the

specific flow conditions in an area (Brodersen et al., 2008; Gaspar et al., 2006; Weber et al., 1998). A flow-assistance equation should therefore stipulate behavioral rules that reflect these goals, and the results of analyses must then be interpreted within the context of that behavior. Alternatively when the goals of an animal are uncertain, determining which flow-assistance equation best reproduces observed actions can be informative of an animal's behavior and desires. $\text{EQ}^{\text{PartialSpeed}}$ may be particularly attractive in this context as it can be varied by tuning one parameter controlling the degree of compensation.

In this chapter, we have outlined a framework to assess the appropriateness and implications of applying various methods to quantify flow-assistance. As demonstrated in this study, flow-assistance equations (and implicitly their assumptions) can be incorporated in a dynamic simulation model to study the specific implications of assuming a particular behavioral strategy, which can be quite informative when exploring the potential integration of flow-assistance in movement research.

Acknowledgments

We would like to thank Hans van Gasteren for discussion and comments on an earlier version of this manuscript and the IBED writers' club for their valuable critiques and suggestions. NCEP Reanalysis data provided by the NOAA/OAR/ESRL PSD, Boulder, Colorado, USA, from their Web site at <http://www.esrl.noaa.gov/psd/>. Our migration studies are facilitated by the NLeSC (<http://www.esciencecenter.com/>) and BiG Grid (<http://www.bigggrid.nl>) infrastructures for e-Science.

4

Can wind help explain seasonal differences in avian migration speed?

Kemp, M.U., Shamoun-Baranes, J., van Gasteren, H., Bouten, W. & van Loon, E.E. (2010) Journal of Avian Biology **41**:672-677

4.1 Abstract

A bird's groundspeed is influenced by the wind conditions it encounters. Wind conditions, although variable, are not entirely random. Instead, wind exhibits persistent spatial and temporal dynamics described by the general circulation of the atmosphere. As such, in certain geographical areas wind's assistance (or hindrance) on migratory flight is also persistent, being dependent upon the bird's migratory direction in relation to prevailing wind conditions. We propose that, considering the western migration route of nocturnal migrants through Europe, winds should be more supportive in spring than in autumn. Thus, we expect faster groundspeeds, contributing to faster overall migration speeds, in spring. To test whether winds were more supportive in spring than autumn, we quantified monthly wind conditions within western Europe relative to the seasonal direction of migration using 30 years (1978-2008) of wind data from the NCEP/NCAR Reanalysis dataset. We found that supporting winds were significantly more frequent for spring migration compared to autumn and up to twice as frequent at higher altitudes. We then analyzed three years (2006-2008) of nocturnal migratory groundspeeds measured with radar in the Netherlands which confirmed faster groundspeeds in spring than autumn. This seasonal difference in groundspeed suggests a 16.9% increase in migration speed from autumn to spring. These results stress the importance of considering the specific wind conditions experienced by birds when interpret-

ing migration speed. We provide a simple methodological approach enabling researchers to quantify regional wind conditions for any geographic area and time period of interest.

4.2 Introduction

It is suggested that passerine migration speed is faster in spring than autumn (Berthold, 2001; Newton, 2008). This asymmetry is thought to be driven by 1) evolutionary pressures on migrants (males in particular) to arrive early at the breeding grounds and establish themselves in prime territory (Kokko, 1999), 2) inexperienced juveniles driving down a population's migration speed in autumn (Berthold, 2001; Newton, 2008), and 3) seasonal differences in fuel deposition rate (see Bauchinger and Klaassen, 2005). Empirical evidence of faster total migration speeds in spring than autumn, however, is limited (Fransson, 1995; Yohannes et al., 2009). Though the theoretical driving mechanisms for this seasonal difference in migration speed should hold outside of the Palearctic-Afrotropic system, a recent study on the eastern Siberian stonechat *Saxicola torquata maura* (an inner-Asian migrant) found no significant difference in migration speed between spring and autumn (Raess, 2008). Even within the Palearctic system, Liechti and Bruderer (1995) found that ground-speeds during nocturnal migration over Israel were faster in autumn than in spring due to prevailing wind conditions. It seems likely, then, that other factors may contribute to seasonal (as well as geographic) variation in migration speed (Jenni and Schaub, 2003).

Migration speed (V_{migr}), as described by Hedenstrom and Alerstam (1998), is determined by three critical components (Equation 4.1): the bird's ground-speed (V_b), its rate of fuel accumulation (P_{dep}), and rate of energy consumption during flight (P_{flight}).

$$V_{migr} = \frac{V_b \cdot P_{dep}}{P_{dep} + P_{flight}} \quad (4.1)$$

In still-air conditions, V_{migr} is more strongly dependent on variation in P_{dep} than V_b because of the relationship between V_b and P_{flight} (Alerstam, 2003). Wind, however, can alter V_b without any adjustment in P_{flight} . Furthermore, a bird optimizing either energy or time is expected to reduce its airspeed, and hence P_{flight} , in tailwinds and, conversely, increase both in headwinds (Hedenstrom and Alerstam, 1995).

In light of wind's impacts on V_{migr} , it is important to note that wind conditions, while variable, exhibit persistent dynamics described by the general circulation of the atmosphere (Rohli and Vega, 2007). It follows, that winds in

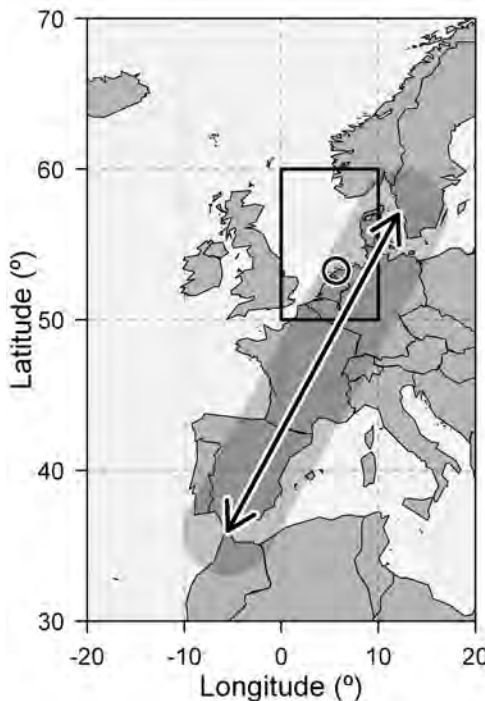


Figure 4.1: Map of western Europe indicating a generalized migration route and direction of migration for autumn (SW) and spring (NE). The radar measurement location in the Netherlands is circled.

certain geographical areas are consistently more (or less) beneficial to migration depending on the preferred direction of migratory movement in relation to prevailing wind conditions (Gauthreaux et al., 2005).

We propose that wind conditions encountered during migration through western Europe (Figure 4.2) are more supportive in spring than autumn. We therefore examine the wind conditions along this route and quantify them in relation to the seasonal direction of migration. Where wind conditions in spring are more beneficial than in autumn, we expect birds to exhibit faster groundspeeds (leading to faster migration speeds) in spring than autumn. We test this assumption using radar measurements of groundspeed during nocturnal migration over the Netherlands.

4.3 Data

4.3.1 Wind data

Gridded wind data from the 850 mb pressure level were obtained from the National Center for Environmental Prediction (NCEP)/National Center for Atmospheric Research (NCAR) Reanalysis dataset (Kalnay et al., 1996) at a spatial resolution of 2.5° every six hours for the years 1978-2008 from 30° N

to 70° N and 20° W to 20° E. Surface wind conditions were obtained from the same dataset, but the spatial extent was limited to the area most representative of the radar measurement site in the Netherlands (i.e. 50° N to 60° N and 0° E to 10° E). Wind data (ms^{-1}) were described by the U (east/west) component (east being positive) and V (north/south) component (north being positive); both indicated the direction into which the wind was blowing. These data were used to make a 30-year climatological assessment of wind conditions in western Europe and to calculate wind profit (see Section 4.4.1).

Gridded wind data from the analysis dataset of the European Centre for Medium Range Weather Forecasts (ECMWF) deterministic model were obtained from 2006-2008 for the 925 mb and 850 mb pressure levels at three hour intervals. These data, at a spatial resolution of 0.5° for 2006 and 0.25° thereafter, were used to calculate airspeeds (see Section 4.4.2).

4.3.2 Radar data

Groundspeeds and flight directions were measured every half hour using ten sequential rotations (in ten second intervals) from a long-range medium-power stacked-beam radar in Wier, the Netherlands (53° 15'25"N, 5° 37'12"E) operated by the Royal Netherlands Air Force (Buurma, 1995). Migration data were collected from 2006-2008, encompassing three spring and three autumn migration seasons. Groundspeeds and flight directions were derived from individual tracks across the entire Wier radar area from the two lowest altitude radar beams, covering approximately 100-6000m altitude. These data were used to calculate half-hourly mean groundspeeds (ms^{-1}) per radar beam. This study focused on nocturnal migration and thus only included measurements made between sunset and sunrise.

To ensure that only migratory movements were included in the analysis, a Rayleigh test (Batschelet, 1981) was applied at each time step. Only time steps with a distribution of flight directions sufficiently concentrated to reject the null hypothesis of a uniform distribution were retained ($\alpha < 0.001$).

4.4 Methods

In all comparisons, February, March, April, and May were considered spring. August, September, October, and November were considered autumn. Analyses were conducted and graphics produced using the statistical software package R (R Development Core Team, 2010). The R-code for wind analysis is available upon request and can easily be implemented for other geographical areas or time periods.

4.4.1 Wind profit analysis

Wind data from the NCEP/NCAR dataset were grouped into $10^\circ \times 10^\circ$ subsections (hereafter “wind subsections”) to calculate monthly and seasonal frequency distributions of wind speed and direction per wind subsection. Directions were divided into 360 groups (one for each angular degree). Speeds were classified into five ranges of 0-5, 5-10, 10-15, 15-20, and $> 20 \text{ ms}^{-1}$. Seasonal wind summary plots (wind roses) were created for each wind subsection for spring (Figure 4.2) and autumn (Figure 4.3). Monthly wind summary plots were also created for wind subsections in Europe and Africa (see Appendix C).

We then performed a quantitative assessment of the monthly and seasonal “profitability” of the wind at 850 mb and the surface for the wind subsection most representative of the radar measurement site in the Netherlands (i.e. 50°N to 60°N and 0°E to 10°E , hereafter “Netherlands wind subsection”), by considering the length of the wind vector along the preferred migratory direction (Equation 4.2).

$$WP = V_W \cos \theta \quad (4.2)$$

Where wind profit (WP , ms^{-1}) equals wind speed (V_W , ms^{-1}) times the cosine of the angle between wind direction and the preferred migratory direction (θ). This is equivalent to $\text{EQ}^{\text{Tailwind}}$ described in section 3.3.1 of Chapter 3.

The preferred autumn migratory direction used to calculate wind profit was 223° . This was the mean of two significant autumn migratory directions in the Netherlands (van Belle et al., 2007) and was similar to the main autumn migratory directions reported for many locations in western Europe – e.g. 220° at a coastal site in southern Spain (Bruderer and Liechti, 1998); 230° for southern Germany and Switzerland (Bruderer et al., 1989); and 225° at Falsterbo in southwestern Sweden (Zehnder et al., 2001). This preferred direction was reversed to 43° for spring.

Spring and autumn wind profit distributions from the 850 mb pressure level were also calculated for other wind subsections in Western Europe using the same methods described above (see Appendix C).

4.4.2 Flight analysis

Weighted probability distributions were calculated, for spring and autumn separately, based on the number of tracks in both beams used to calculate the mean groundspeed at each time step.

While species could not be identified directly from this radar, species groups could be inferred from measured airspeeds (Bruderer and Boldt, 2001).

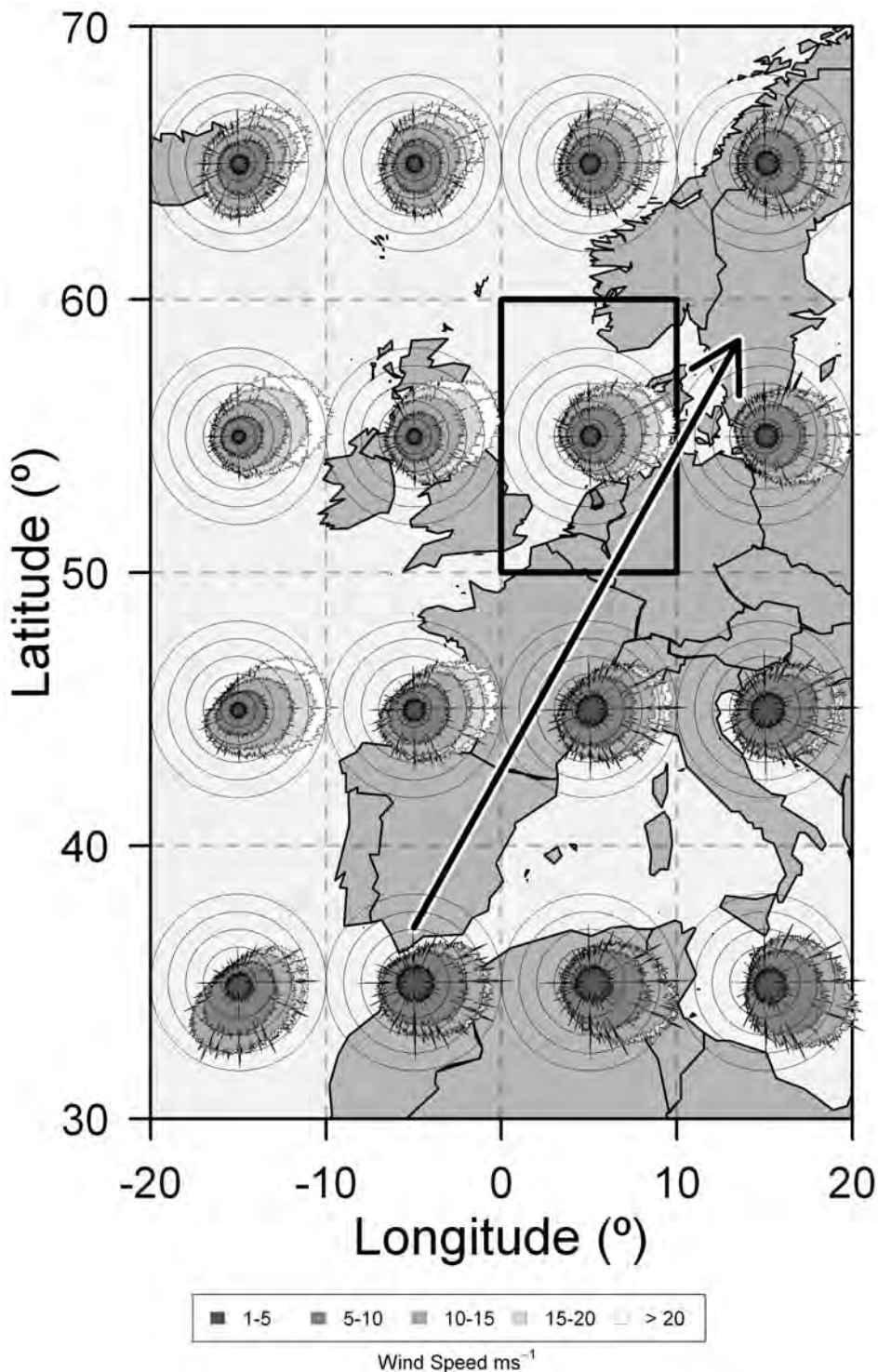


Figure 4.2 (previous page): Spring wind rose maps covering western Europe displaying 30 years (1978–2008) of wind data from the 850 mb pressure level. Wind roses indicate the direction into which the wind blows. Total distance from the center indicates the relative frequency of wind in a particular direction, while shades describe the relative frequencies of the different wind speed ranges (ms^{-1}) in that direction. Concentric circles indicate relative frequency in increments of 0.1%; with the outer circle indicating 0.5% relative frequency. Large arrows in the background indicate the general direction of migration for spring. The Netherlands wind subsection is heavily outlined.

We calculated airspeeds through the vector subtraction of the wind components in the ECMWF dataset from the radar-measured groundspeeds according to Shamoun-Baranes et al. (2007). These ECMWF wind data were linearly interpolated in space and time to match the center of the radar and the time of each measurement. Airspeeds were calculated in the upper beam using wind data from the 850 mb pressure level and in the lower beam using data from the 925 mb pressure level.

4.5 Results

4.5.1 Wind conditions

A qualitative examination of the seasonal wind rose maps showed that wind conditions were more supportive of the northeasterly movement of spring migration and frequently and forcefully opposed to the southwesterly movement of autumn migration (Figures 4.2 and 4.3). There appeared a great deal of intra-seasonal variability between adjacent wind subsections (particularly latitudinally). Wind speeds were consistently highest between 50° N and 60° N, although speeds at all latitudes decreased farther inland. Winds south of 40° N in both seasons were weaker in speed and more variable in directionality than winds north of 40° N.

A quantitative assessment of wind profit between the two seasons within the Netherlands wind subsection was performed for both the surface and 850 mb pressure level (Table 4.1). Winds were significantly more profitable ($P < 0.001$; one-sided Mann-Whitney test) in spring ($n=372,800$) than autumn ($n=378,200$) at both levels. The percentage of wind profit values greater than zero, describing the percentage of observations in which wind had some component in the direction of migration, showed that beneficial winds were also more frequent in spring compared to autumn. Furthermore, the mean of wind profit values greater than zero was higher in spring than in autumn; thus winds in the direction of migration were stronger in spring than autumn.

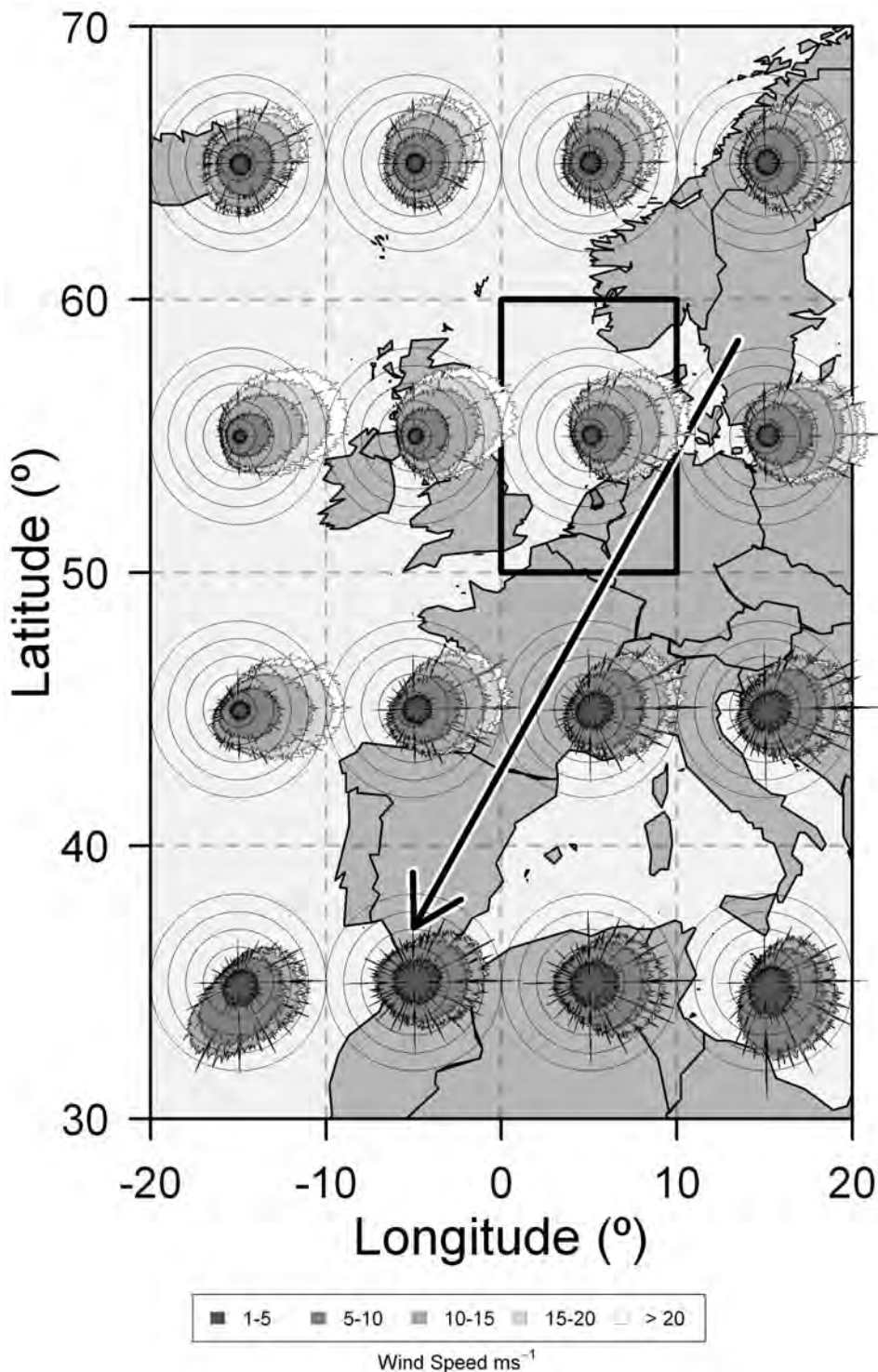


Figure 4.3 (previous page): Autumn wind rose maps covering western Europe displaying 30 years (1978-2008) of wind data from the 850 mb pressure level. Wind roses indicate the direction into which the wind blows. Total distance from the center indicates the relative frequency of wind in a particular direction, while shades describe the relative frequencies of the different wind speed ranges (ms^{-1}) in that direction. Concentric circles indicate relative frequency in increments of 0.1%; with the outer circle indicating 0.5% relative frequency. Large arrows in the background indicate the general direction of migration for autumn. The Netherlands wind subsection is heavily outlined.

Table 4.1: Seasonal and monthly mean and standard deviation (SD) of wind profit values (ms^{-1}), the percentage of wind profit values greater than zero ($\% > 0$), and the mean of wind profit values greater than zero (mean > 0) are shown using 30 years (1978-2008) of wind data from the surface and 850mb pressure level from the Netherlands wind subsection.

	Surface				850 mb			
	Mean	SD	%> 0	Mean > 0	Mean	SD	%> 0	Mean > 0
Spring	1.4	6.1	57.1	5.5	2.9	7.9	62.3	7.7
Autumn	-2.3	5.6	34.6	3.7	-4.4	7.4	28.5	4.3
February	2.5	6.9	63.0	6.7	3.7	9.3	62.7	9.3
March	2.5	6.3	64.2	6.2	4.1	8.2	67.5	8.5
April	0.4	5.5	52.2	4.6	1.8	7.2	58.4	6.6
May	0.1	5.1	49.4	4.3	2.2	6.5	60.3	6.3
August	-1.6	4.6	37.7	3.0	-3.5	5.8	28.1	3.2
September	-2.0	5.4	35.9	3.6	-4.0	7.0	29.2	4.3
October	-2.8	6.0	32.4	3.8	-5.5	7.9	25.4	4.3
November	-2.9	6.3	32.5	4.1	-4.6	8.7	31.3	5.3

Wind profit was greater at the surface than at 850 mb during autumn and at 850 mb, than at the surface, during spring. At the 850 mb pressure level, profitable winds were more than twice as frequent in spring than autumn. While there was considerable variation within a season, no autumn month displayed more beneficial winds than a spring month.

4.5.2 Flight speed

Observed groundspeeds were significantly faster during spring than autumn ($P < 0.001$; one-sided Mann-Whitney test). Airspeeds, however, were somewhat slower in spring than autumn ($P < 0.001$; one-sided Mann-Whitney test; Table 4.2). The measured airspeeds indicate that nocturnal migrants in both

Table 4.2: Mean and standard deviation (SD) of air- and groundspeeds (ms^{-1}), are shown for spring (n=3,511,778) and autumn (n=3,189,424)

	Spring		Autumn	
	Mean	SD	Mean	SD
Groundspeed	22.1	5.5	18.9	3.7
Airspeed	13.6	3.6	14.0	4.7

seasons include a broad range of passerines as well as faster flying migrants such as waders and waterfowl (Bruderer and Boldt, 2001).

4.6 Discussion

Our study has shown that, in spring compared to autumn: 1) wind conditions along the western migration route through Europe are more supportive of migration, 2) mean groundspeeds measured in Netherlands are 16.9% faster, and 3) mean airspeeds measured in Netherlands are 2.9% slower. Therefore, birds passing through this radar measurement site in spring have faster mean groundspeeds, with no more fuel expenditure, than birds passing through in autumn. All other things being equal, this suggests an increase of at least 16.9% in migration speed through the Netherlands in spring compared to autumn due to the effect of wind on groundspeeds.

Recent positive trends in the frequency of favorable winds in spring have been associated with earlier spring arrival of song thrushes in the southeast Baltic region (Sinelschikova et al., 2007) which may in turn reflect faster migration speeds. In recent years, the relationship between climate change and migration phenology has received a great deal of attention (Forchhammer et al., 2002; Cotton, 2003; Jonzén et al., 2006), yet the potential role of wind conditions has rarely been studied in this context.

Gauthreaux et al. (2005), showed that prevailing wind patterns also favor migratory movement in spring more than autumn in North America. The authors described a “go-with-the-prevailing-flow” strategy in spring compared to a “sit-and-wait-for-favorable-winds” strategy in autumn. As studies on the timing of migration in relation to weather suggest, birds tend to migrate more readily in profitable rather than prohibitive wind conditions in both seasons (Richardson, 1990a, and references therein). Thus, if birds employ the “sit-and-wait-for-favorable-winds” strategy in both seasons, in our study area they would migrate more frequently in spring (appearing to “go-with-the-prevailing-flow”), and less often in autumn.

Newton (2008) suggests that migration can be delayed for days or weeks

at a time due to unfavorable weather conditions. Weber and Hedenström (2000) theorize that, if wind conditions are correlated in time, it is optimal for a bird to wait for better wind conditions (even when they are energetically prepared to migrate) unless the probability that the unfavorable winds will persist is close to one. Our study shows that the frequency of beneficial winds (and therefore the time a bird may have to wait for beneficial winds) can differ dramatically by season, direction of migration, and geographic location. Therefore, in areas with frequently prohibitive winds, birds must either remain longer at a stopover waiting for conditions to improve or depart in suboptimal conditions resulting in greater energy expenditure, slower groundspeeds, or some combination of the two, and hence slower migration speeds.

Our study has shown that wind conditions exhibit consistent seasonal and geographic patterns. However, it is not clear whether birds are aware of these patterns and, if so, to what extent. Do birds have an idea of the frequency of favorable winds within a particular region, and is that foreknowledge applied in their stopover, refueling, and route-selection strategies (i.e. can areas with consistently unfavorable winds be considered a kind of ecological barrier)? More experienced migrants may even learn to anticipate the frequency of beneficial winds in a particular area and adjust the rigidity of their wind selection criteria and/or compensation strategy accordingly.

This raises interesting questions regarding detours from more direct migratory routes and the use of alternative migratory routes between spring and autumn (i.e. loop migration). Alerstam (2001) describes detours circumventing ecological barriers which are still energetically optimal and demonstrates that wind conditions influence the optimality of a particular route (Alerstam, 1979). Because of wind's influence on optimal routes and its persistent nature, areas with frequently prohibitive winds may be viewed as a type of ecological barrier.

In conclusion, consideration of the wind conditions relative to migration is important for a better interpretation of migration speed. We provide a simple methodology to quantify regional wind conditions for any geographic area and time period of interest. While wind is only one of several internal and external factors influencing migration speed, it may help explain part of the variability observed between and within regions, species, seasons, and years. For example, Fransson (1995) reported faster migration speeds in spring than in autumn. The lesser whitethroat, though migrating SE in autumn and expected to encounter more beneficial winds, still flew faster in spring. Yet, the seasonal difference in migration speed was smaller than in the other species, suggesting both seasonal and wind effects. Reanalysis of results such as these and new studies are needed to help clarify wind's importance relative to other

factors. Individual-based simulation models (Erni et al., 2005; Vrugt et al., 2007), in combination with advances in tracking technologies (Robinson et al., 2010), could improve our understanding of the interactions between influential variables, as they allow us to consider specific environmental and physiological details relating to a particular migratory individual.

Acknowledgments

Our migration studies are facilitated by the BiG Grid infrastructure for eScience (<http://www.bigggrid.nl>). NCEP Reanalysis data were provided by the NOAA/OAR/ESRL PSD, Boulder, Colorado, USA, via their website (<http://www.esrl.noaa.gov/psd/>). ECMWF data were provided through KNMI. We thank the scientific editor and two anonymous reviewers for their valuable comments and suggestions regarding an earlier version of this manuscript.

The influence of weather on altitude selection by nocturnal migrants in mid-latitudes

Kemp, M.U., Shamoun-Baranes, J., Dokter, A.M., van Loon, E.E., & Bouten, W. *Ibis submitted*

5.1 Abstract

By altering its flight altitude, a bird can change the atmospheric conditions it experiences during migration. Although many factors potentially influence a bird's decision to choose a particular altitude for migration, wind is generally accepted as being the most influential. Nonetheless, studies indicate that the influence of wind is not so clearly defined, particularly outside of the trade-wind zone, and that other factors may play a role. The aim of this study was to determine which factors influenced the altitude distribution of birds during nocturnal migration. We used operational weather radar to measure the flight altitudes of nocturnally migrating birds during spring and autumn in the Netherlands. We first determined if nightly altitude distributions of proportional bird density could be explained by vertical distributions of wind support using three different techniques from previous research. We then applied a stepwise regression analysis using Generalized Additive Models (GAMs) to determine which atmospheric variables, in addition to altitude, best explained variability in proportional bird density per altitude layer per night. We found that migrants generally remained at low altitudes in this area and that altitude alone explained 52 and 73% of the observed variability in proportional bird density in spring and autumn, respectively. Overall, we found weak correlations between altitudinal distributions of wind support and

proportional bird density; however, we found that improving tailwind support with height increased the probability of birds climbing to higher altitude, and, when birds did fly higher than normal, they generally concentrated around the lowest altitude with acceptable (but not necessarily optimal) wind conditions. The GAM analysis also indicated an influence of temperature on flight altitudes, suggesting that birds avoided colder temperatures. Our findings also suggested that birds increased flight altitudes to seek out more supportive winds when wind conditions near the surface were prohibitive. Thus, birds did not select flight altitudes to exclusively optimize wind support and seemed to prefer flying at relatively low altitudes unless wind conditions at the surface were unsupportive of migration but improved at higher altitude. Overall, flight altitudes of birds in relation to environmental conditions reflect a balance between different adaptive pressures.

5.2 Introduction

Avian migrants, many traveling thousands of kilometers twice each year between their breeding and wintering grounds, must interact with a range of atmospheric conditions. By influencing a bird's flight efficiency and ability to navigate, these atmospheric conditions can affect the bird's capacity to successfully maintain its desired course and schedule (Shamoun-Baranes et al., 2010). Therefore, one would expect birds to preferentially fly at altitudes where atmospheric conditions are most supportive of their migratory flight. For diurnal soaring migrants, flight range is maximized by utilizing thermal convection to gain altitude between bouts of gliding, and maximum flight altitudes increase with increasing thermal strength and convective boundary layer depth (Shannon et al., 2002; Shamoun-Baranes et al., 2003b). At night, however, in the absence of vertical mixing induced by convective thermals, the convective boundary layer collapses and the atmosphere becomes generally more stratified (Stull, 1988). Thus, nocturnal migrants have the option to select (often from within wide ranges) rather distinct atmospheric conditions (e.g. temperature, humidity, and wind condition) by adjusting their altitude.

The majority of quantitative empirical research has suggested that wind is the most influential atmospheric variable on the flight altitudes of nocturnally migrating birds and other atmospheric variables such as temperature and humidity exert only minor influence (Bruderer et al., 1995b; Liechti et al., 2000; Liechti and Schmaljohann, 2007; Schmaljohann et al., 2009). Specifically, these studies report a strong correlation between altitudinal distributions of avian migrants and altitudinal distributions of either wind profit (i.e. the support a bird obtains from a particular set of wind conditions) or some estimate of

flight range based largely on wind profit. However, these studies have been primarily conducted inside the trade-wind zone of North Africa and the Middle East.

Based on atmospheric general circulation patterns (Rohli and Vega, 2007), the northern and southern hemispheres on Earth can be subdivided into three latitudinal zones: the trade-wind zone (0° - 30°) in which Hadley cells dominate, the mid-latitudes (30° - 60°), and the polar region (60° - 90°). The wind scenario prevalent in the trade-wind zone, and in the polar region, is such that wind direction often changes by 180° with altitude. Thus, inside the (northern hemisphere) trade-wind zone beneficial winds are available on most nights either at high altitude (in spring as migrants move away from the equator) or at low altitude (in autumn as migrants move toward the equator). Accordingly, prohibitive winds are also present every night and at generally predictable altitudes. In the mid-latitudes, conversely, upper-level winds generally do not reverse direction from the surface. Therefore, beneficial winds are not always available and the altitudinal distribution of wind support is less predictable. Furthermore, inside the trade-wind zone cloud cover is infrequent (other than in the Intertropical Convergence Zone) and temperatures within the normal altitudes of bird migration are generally above freezing (cf. Bruderer et al., 1995b; Klaassen and Biebach, 2000; Liechti et al., 2000; Schmaljohann et al., 2009). Thus, it is unclear to what degree the relationships derived in these studies apply outside of areas exhibiting these specific atmospheric conditions.

Studies from outside the trade-wind zone also indicate an influence of wind on migratory altitudes; however, these reports do not necessarily suggest that birds always select altitudes to optimize wind support. From a visual and radar analysis conducted in the southern United States at the border between the trade-wind and mid-latitude zones, Gauthreaux (1991) found a strong correlation between the altitude of peak migration and the altitude of most supportive winds when migrants flew at higher altitudes than normal and suggested that these higher-than-normal flight altitudes occurred when winds at lower altitude were prohibitive and winds at higher altitude were supportive. Several studies suggest that migrants generally fly at higher altitudes with tailwinds than with headwinds (see Bruderer, 1971; Kerlinger and Moore, 1989; Richardson, 1990a, and references therein), and another study suggests that migrants remain at lower altitudes when wind speeds are high irrespective of wind direction (Able, 1970).

In any case, the influence of wind cannot be understood in isolation from other atmospheric components (Bruderer, 1971). For instance, Bruderer (1971) observed rain and clouds depressing migratory altitudes even when more supportive winds were available at higher altitude. Other observational reports

from outside of the trade-wind zone support this assessment, suggesting that atmospheric variables other than wind may influence the altitude of avian migration (see Eastwood, 1967; Kerlinger and Moore, 1989, and references therein). In particular, there are reports of cloud cover affecting migratory altitudes; though the specific influence is contentious with conflicting reports suggesting that birds tend to fly above (Bellrose and Graber, 1963), below (Nisbet, 1963; Able, 1970), and even within clouds (Bellrose and Graber, 1963; Eastwood and Rider, 1965; Griffin, 1973). Perhaps lending some clarification, Bruderer (1971) observed that birds flew above lower-altitude clouds (even into comparatively less supportive winds at higher altitude) but below higher-altitude clouds (particularly frontal clouds, unbroken clouds, and clouds producing precipitation). Deduced from an observed correlation between the 90% level of migration and the altitude at which freezing temperatures occurred, Bruderer (1971) also theorized that birds may choose altitudes to optimize thermoregulation; though some birds were observed flying in temperatures as low as -15°C. Elkins (2004) suggested that freezing temperatures may only be troublesome when the air is very saturated with moisture, as this could lead to ice accumulation on plumage; however, Bruderer (1971) reported birds flying in below-freezing temperatures even when the atmosphere was very humid and the formation of ice-crystals was to be expected. Theoretical work suggests that a migrant's flight range may be strongly limited by dehydration, particularly in dry areas, and that migrants should select altitudes that minimize water loss (Carmi et al., 1992; Gerson and Guglielmo, 2011; Klaassen, 1996). Finally, although avian physiology exhibits adaptations resulting in a more efficient exchange of oxygen from the pulmonary to the circulatory system, theory suggests that atmospheric properties highly correlated with altitude such as oxygen partial pressure (Altshuler and Dudley, 2006) and air density (Pennycuick, 2008), along with temperature and humidity, may influence a bird's flight efficiency.

Thus, the altitude distributions of birds observed during migration may reflect a trade-off between multiple objectives, such as optimizing energy expenditure, flight time, safety, and water balance. Therefore, further quantitative analyses, in different geographic areas and integrating multiple atmospheric variables, are desirable to 1) test relationships quantified or suggested in other regions between atmospheric variables and avian migratory altitudes for universal applicability, and 2) to improve our understanding of how birds potentially balance these different adaptive pressures when selecting flight altitudes during migration.

The main aim of this study is to determine how atmospheric conditions influence the nocturnal altitude distributions of migrating birds in our study

area. We examine altitude distributions of nocturnally migrating birds obtained using C-band Doppler weather radar in the Netherlands – a location where prevailing atmospheric conditions are quite different from those of the trade-wind zone (Rohli and Vega, 2007). Since most quantitative research has focused on the influence of wind, and for comparative purposes, we first explore possible relationships between wind conditions and migratory altitude by applying three approaches from previous research: 1) following Gauthreaux (1991), we consider a subset of nights in which birds fly higher than normal and test if the altitude of peak migration is correlated with the lowest altitude with acceptable wind support; 2) we quantify the nightly correlation between wind profit (i.e. the support a bird obtains from a particular set of wind conditions) and the proportion of birds at each altitude level, as done in some studies inside the trade-wind zone (e.g. Liechti et al., 2000; Schmaljohann et al., 2009), and 3) we apply a simulation model, following Bruderer et al. (1995b), in which the probability of a bird changing altitude is a function of the change in tailwind strength with altitude. Finally, rather than studying wind in isolation of other atmospheric conditions and in order to study flight altitude distributions in the context of multiple adaptive pressures, we perform a stepwise regression analysis to explore the potential influence of multiple atmospheric variables that, through observation, theory, or statistical inference, have been suggested to influence the altitude of avian migration. Because the specific influence of many of these atmospheric variables on avian altitude distributions is not known, particularly for this location, we employ Generalized Additive Models (GAMs) in which the relationship between predictor and response variable is not restricted to a predefined parametric form.

5.3 Materials and methods

5.3.1 Radar measurements of bird density

We used methods described by Dokter et al. (2011) to derive altitude profiles of bird density (Bd ; birds/km 3) and average groundspeed (ms $^{-1}$) every five minutes from a C-band Doppler weather-radar located in De Bilt, the Netherlands (52.11°N 5.18°E; Figure 5.1) during spring (1 February - 31 May) and autumn (1 August - 30 November) of 2008 and 2009. Each altitude profile described Bd and average groundspeed from 0.2 to 4 km above the ground in altitude bins of 200 m. Thus each profile consisted of 19 measurements, each calculated from within a circular measurement window extending 25 km laterally from the center of the radar (Figure 5.1).

As a means of additional quality control, we used HIRLAM wind data (see section 5.3.2) to calculate airspeeds from these groundspeeds by vector

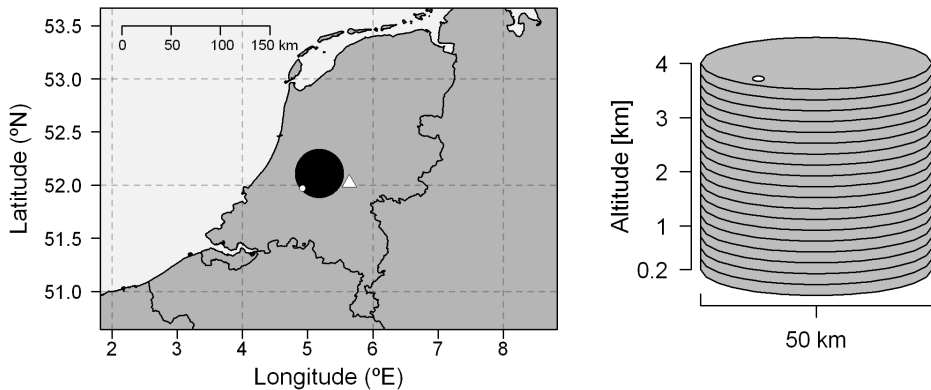


Figure 5.1: On the left, a map with a black circle indicating the range of the C-band Doppler weather radar in De Bilt, the Netherlands. A white triangle indicates the closest grid point in the HIRLAM dataset, from which weather data were obtained. On the right, a vertical profile of the radar’s measurement volume indicating the 19 altitude bins within which measurements of bird density (Bd) were calculated. In both images, a small white circle indicates the location of the cloud-measuring LIDAR ceilometer at the Cabauw experimental site for atmospheric research.

subtraction. We set Bd measurements to zero if the associated airspeed was not between 7 and 25 ms^{-1} , as this range captures the airspeeds of the majority of nocturnal migrants (Bloch and Bruderer, 1982; Bruderer and Boldt, 2001).

Bruderer et al. (1995b), and references therein, observed that nocturnal migrants can spend the first two hours after sunset probing the atmosphere and concentrate in preferred altitudinal strata thereafter. We therefore calculated a representative altitude profile of Bd for each night (hereafter “nightly Bd profile”) using the median Bd value per altitude bin occurring between two and three hours after sunset (i.e. after birds had presumably selected their altitudes in relation to the night’s atmospheric conditions). We only considered nights in which total migration (i.e. the sum of all Bd in the nightly Bd profile) was greater than $20 \text{ birds}/\text{km}^3$, because measurements were less reliable when Bd values were very small. Given this threshold, we retained 29% of the 238 available spring nights and 18% of the 236 available autumn nights.

We then translated these nightly Bd profiles into “proportional bird-density (pBd) profiles” by dividing Bd in each altitude bin by the sum of all Bd in the nightly profile. For our comparisons with previous research, we used these nightly pBd profiles. In Figure 5.2, we show for each season the weighted aver-

age altitude distribution of pBd (in which pBd is weighted by the total Bd in the associated profile), the range of deviations from that weighted average per altitude bin, and two example distributions (one similar to and one different from the weighted average).

The pBd values for any given altitude profile were constrained due to the fact that they necessarily summed to a value of one. To deal with this constraint, we applied the additive log-ratio (ALR) transformation (Aitchison, 1982) to these pBd values. For each of the 19 altitude bins (a) of a nightly profile (i), we calculated ALR-transformed pBd_a^i (hereafter tBd_a^i with respect to pBd^i in the first or lowest altitude bin, which was centered on 0.3 km, as

$$tBd_a^i = \log \left(\frac{pBd_a^i}{pBd_1^i} \right) \quad (5.1)$$

We did not use any tBd values calculated in a reference bin (i.e. where $a = 1$) to calibrate our models. This transformation produced an unreal solution for any observation in which pBd was equal to zero, so these observations were also excluded from our analysis. What remained were 322 and 286 tBd measurements in spring and autumn, respectively. tBd served as the response variable in our GAM regression analysis. We back-transformed tBd_a^i in all but the reference altitude bin as

$$pBd_a^i = \frac{\exp(tBd_a^i)}{1 + \sum_{a=2}^{19} \exp(tBd_a^i)} \quad (5.2)$$

and in the reference altitude bin as

$$pBd_1^i = 1 - \sum_{a=2}^{19} pBd_a^i \quad (5.3)$$

We present the results of our analysis after back-transforming GAM predictions to pBd wherever possible.

5.3.2 Meteorological data

We derived altitude profiles, to a height of 4 km, of wind condition (ms^{-1}), temperature (T ; K), atmospheric pressure (A_P ; mb), and relative humidity (RH ; %) using data from the gridded HIRLAM atmospheric model (Cats and Wolters, 1996; Undén et al., 2002). These data had a spatial resolution of $0.1^\circ \times 0.1^\circ$ on a rotated grid, temporal resolution of one hour, and were discretized vertically at fixed pressure levels separated by not more than 20 mb. Using data from the grid point nearest to the center of the De Bilt radar (~ 33 km east at 5.64°E 52.02°N ; see Figure 5.1), we linearly interpolated all variables to

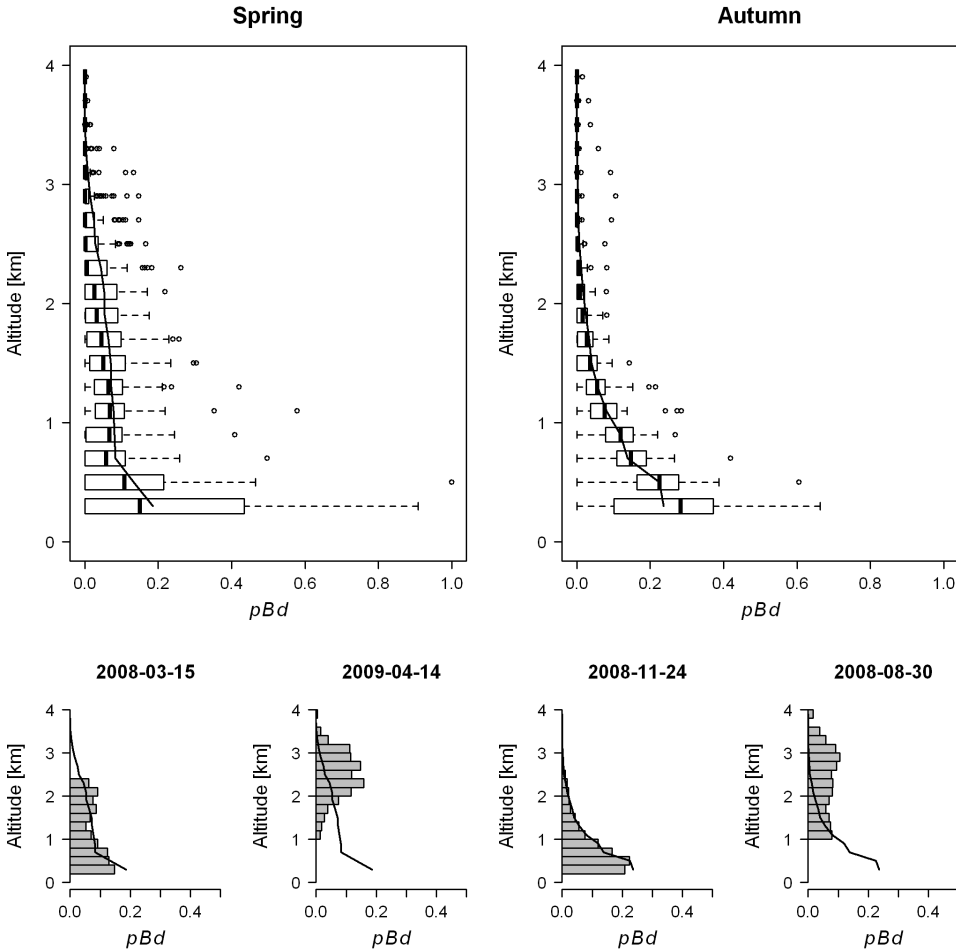


Figure 5.2: In all plots, a black line indicates the weighted average altitude distribution of proportional bird density (pBd) for the particular season (three plots of spring on left; three plots of autumn on right). In the top two plots, box-plots indicate the range of deviations from the weighted average pBd per altitude bin. Boxes indicate the upper and lower quartiles and median, “whiskers” indicate values < 1.5 times the inter-quartile range beyond the quartiles, and points indicate outliers. Along the bottom are two example distributions from each season: one that closely approximates the weighted average distribution for that season and one that is quite different from the weighted average distribution for that season. The title of each plot indicates the night (at sunset) during which the distribution occurred.

the center of each altitude bin. We then calculated “nightly weather profiles”, comparable to the nightly Bd profiles, by linearly interpolating these weather conditions in time along each altitude bin to 2.5 hours after sunset each night (determined using the R package `maptools` Lewin-Koh et al., 2011). For each observation, we then calculated specific humidity (SH ; g/kg), describing the mass of the water vapor present per kilogram of atmosphere, as

$$SH = \frac{w}{1+w} \quad (5.4)$$

where the mixing ratio (w) was defined as

$$w = \frac{0.622e}{A_P - e} \quad (5.5)$$

vapor pressure (e) was given by

$$e = e_s \cdot \frac{RH}{100} \quad (5.6)$$

and saturation vapor pressure (e_s), as given by Buck (1981), was

$$e_s = (1.0007 + 3.46 \cdot 10^{-6} \cdot A_p) \cdot 6.1121 \cdot \exp\left(17.502 \cdot \frac{T - 273}{240.97 + (T - 273)}\right) \quad (5.7)$$

for temperatures above freezing and

$$e_s = (1.0003 + 4.18 \cdot 10^{-6} \cdot A_p) \cdot 6.1115 \cdot \exp\left(22.452 \cdot \frac{T - 273}{272.55 + (T - 273)}\right) \quad (5.8)$$

for temperatures below.

Wind data were described by two components, U and V (ms^{-1}), indicating the speed and direction into which the wind was blowing. The U vector described the wind’s east/west component (toward east being positive) and V described the north/south (toward north being positive). Several variables were derived from the U and V wind components to represent wind conditions relative to a bird’s expected flight behavior. We calculated the tailwind (Tw ; ms^{-1}) component (Shamoun-Baranes et al., 2007), and a measure of wind profit (WP ; ms^{-1}). For both variables, a preferred migratory direction was required. We assumed an autumn migratory direction of 225° , consistent with the autumn migratory directions used in previous studies in the Netherlands (e.g. van Belle et al., 2007, and Chapter 4) and similar to migratory directions

observed by radar in several locations throughout Europe – e.g. 220° at a coastal site in southern Spain (Bruderer and Liechti, 1998); 230° for southern Germany and Switzerland (Bruderer et al., 1989); and 225° at Falsterbo in southwestern Sweden (Zehnder et al., 2001). We then reversed this preferred direction to 45° in spring, similar to the mean spring migratory direction of 41° observed by radar in western Europe (Dokter et al., 2011). According to our formulation of WP , birds were assumed to have a fixed airspeed and fully compensate for side-wind displacement by adjusting their groundspeed and heading (see EQ^{Airspeed} in section 3.3.2 of Chapter 3 for details).

$$WP = W_{spd} \cdot \cos \theta + \sqrt{z^2 - (W_{spd} \cdot \sin \theta)^2} - z \quad (5.9)$$

where WP was a function of wind speed (W_{spd}) and the angular difference between the wind direction and the bird's preferred migratory direction (θ). Because passerines dominate nocturnal migration over Europe (Hahn et al., 2009), we set the birds' airspeed (z) to 12 ms⁻¹, which is representative of the airspeeds calculated for many migrating passerine species (Bloch and Bruderer, 1982; Bruderer and Boldt, 2001). Since birds were assumed to have a fixed airspeed in this equation, conditions existed in which full compensation for side-wind displacement was not possible. Under such conditions (i.e. with a negative value occurring under the square root), this formulation did not have a real solution. In spring and autumn, respectively, 119 and 147 observations at individual altitude bins were removed from all analyses because WP had no real solution. In order to represent wind at a particular flight altitude in relation to the most supportive wind conditions in the vertical profile, we calculated relative wind profit (rWP), which we defined as WP at a given altitude minus the best WP in the associated nightly weather profile; thus, zero was the highest value possible for rWP . To reflect the observation by Gauthreaux (1991) that birds flew at higher altitude to avoid low-altitude headwinds, we calculated a measure of WP relative to the WP at the surface (WP_{sfc}), which we will refer to hereafter as rWP_{sfc} . To do so, we first defined WP_{sfc} in binary terms (bWP_{sfc}), with bWP_{sfc} being one if WP_{sfc} was negative and zero if WP_{sfc} was non-negative. We then defined $rWP_{sfc} = bWP_{sfc} \cdot (WP - WP_{sfc})$. We calculated relative tailwind (rTw) and tailwind relative to the surface (rTw_{sfc}) in a similar manner. We considered rWP , rTw , rTw_{sfc} , and rWP_{sfc} in our GAM analysis.

Cloud cover was measured by a Vaisala CT75K LIDAR ceilometer at the Cabauw experimental site for atmospheric research (abbreviated Cesar) located at 51.97°N 4.926°E (~25 km to the southwest of the center of the De Bilt radar; see Figure 5.1). We accessed these data via the online Cesar database (The Cesar Consortium, 2011). Cloud-base height (m) was calculated every

30 seconds with 15 m vertical resolution. Three nights in spring were removed from the analysis because cloud data were missing. For our stepwise GAM regression analyses, we defined nightly cloud persistence (Cp) per altitude bin. Cp was parameterized as the cumulative fraction of cloud-base observations between sunset and three hours after sunset from 200 m up to the respective altitude bin.

5.3.3 Wind and migratory altitudes: comparisons with previous research

Following the analysis of Gauthreaux (1991), we considered a specific subset of nights in which the altitude bin with the largest proportion of birds was above 400 m. Using only these nights (35 in spring and 18 in autumn), we quantified the correlation between the altitude bin with the largest pBd and the lowest altitude bin with acceptable wind support using Pearson's product moment correlation coefficient (hereafter "Pearson's r "). We defined the lowest altitude bin with the acceptable wind support, again following Gauthreaux (1991), as the lowest altitude bin in which the wind blew toward the N-NE in spring or the S-SW in autumn. If no altitude bins satisfied this requirement, we used instead the altitude bin with the lowest wind speed.

Following the approach taken in several studies from inside the trade-wind zone (e.g. Liechti et al., 2000; Schmaljohann et al., 2009), we quantified the nightly correlation between vertical distributions of pBd and wind support (Tw and WP) using Spearman's rank correlation coefficient (hereafter Spearman's ρ): a non-parametric measure of association in which a value of one indicates a perfect positive correlation, negative one a perfect negative correlation, and zero no correlation. We only ever calculated Spearman's ρ correlations for nights with a majority of their observations present.

Following the approach taken by Bruderer et al. (1995b), we applied a simulation model to predict nightly altitude distributions of pBd . According to this model, the probability of a bird changing altitudes was a function of the difference in Tw strength between adjacent altitude bins (hereafter ΔTw). We first calibrated a linear regression to quantify for our dataset the probability of a bird changing altitude as a function of ΔTw . To do so, we assumed that pBd in one altitude bin compared to pBd in an adjacent altitude bin indicated the birds' preference between the bins. Thus for each observation, we defined P as pBd in the altitude bin immediately above the current bin divided by the sum of pBd in both bins. As such, values of P greater than 0.5 indicated that more birds preferred conditions in the next highest altitude bin, while values of P less than 0.5 indicated that more birds preferred conditions in the current altitude bin. We then applied a logit transformation to P (hereafter P_L) to

serve as the response variable in the regression. Accordingly, we calculated ΔTw as Tw in the altitude bin immediately above minus Tw in the current altitude bin, such that positive values for ΔTw indicated increasing tailwind support in the next highest altitude bin. We then calibrated a linear regression (i.e. $P_L = a + b\Delta Tw$; where a and b were coefficients calibrated from the data) based on the normal distribution. Each observation was weighted by the square-root of the sum of Bd in the two altitude bins from which P was calculated. According to the regression relationship that resulted, we simulated a distribution of pBd for each night in our study. We began each night's simulation with a probability distribution in which all birds were expected to be in the lowest altitude bin, and we iteratively adjusted this distribution according to P predicted in each bin by ΔTw . We continued to iterate until the distribution achieved convergence, which we defined to occur when the root-mean-square error (RMSE) between the previous and current iterations was < 0.0001 . As did Bruderer et al. (1995b), we quantified the percentage of variability explained by this simulation model as

$$1 - \frac{\sum_{i=1}^n |x_i - y_i|}{\sum_{i=1}^n x_i + y_i} \quad (5.10)$$

where x_i are measured values and y_i are predicted.

5.3.4 GAM analysis

We applied a Generalized Additive Modeling (GAM) approach (Hastie and Tibshirani, 1990) based on a Gaussian distribution to explore potential relationships between atmospheric variables (from the nightly weather profiles) and tBd (i.e. ALR-transformed pBd at each altitude from the nightly bird-probability profiles). We applied penalized likelihood fitting to estimate the smoothness of terms in our GAMS. The computations were done in the R language (R Development Core Team, 2010) using the `gam()` function from the `mgcv` package (Wood, 2008).

We began with a base model that contained only altitude (Alt) as a predictor variable to account for any persistence in the altitude distributions of migrating birds that may be attributable to altitude itself, for example, arising from birds preferring lower altitudes to facilitate navigation using ground-based points of reference (Liechti et al., 2000). From this base model, we performed forward stepwise regression, using repeated random sampling as a means of cross-validation, to arrive at the best performing combination of predictor variables for each season. For each possible predictor variable, we tested a model containing that variable by repeatedly (50 times) selecting a random 80% of available nights for calibration – leaving 20% for testing. We

recorded the RMSE, Spearman's ρ , and percentage of variability explained – following the method of Bruderer et al. (1995b) described above – between our back-transformed model predictions and pBd from the 20% of nights left for testing. We retained the variable that produced the smallest average RMSE value. Using the same repeated random sampling procedure, we tested adding subsequent variables to the model. We added the variable that led to the lowest cross-validation RMSE, was significant ($\alpha < 0.05$) in the model, and did not cause previously selected variables to become non-significant. Further, we applied a chi-squared test to confirm that the inclusion of each variable resulted in a significant ($\alpha < 0.01$) improvement over the previous model. The variables we tested in this analysis are listed in Table 5.1 where we provide a short description of each variable and give a reference for our motivation to include it in our analysis.

Due to the effects of repeated random sampling and the flexibility allowed by GAMs, different final models may result from this stepwise procedure if it were run multiple times. Therefore, we performed the entire forward stepwise analysis 50 times for each season. We retained the set of predictor variables that occurred most often per season and described the performance of the models containing those variables. As well, we reported the number of times each individual variable was selected in a final model to indicate the stability of the selection procedure and the relative importance of each variable in predicting tBd .

5.4 Results

5.4.1 Weather conditions

The geographical area in which our study was conducted has a Cfb climate-type (i.e. temperate with no dry season and warm summers) according to the Köppen-Geiger climate classification system (Peel et al., 2007). Consistent with the results in Chapter 4, nightly weather profiles indicated that wind speeds generally increased with altitude, and, particularly in autumn, winds blew more frequently and forcefully from the west. Consequently, wind conditions were generally more supportive of the northeasterly movement of spring migration than the southwesterly movement of autumn migration (Figures 5.3 and 5.4). In both seasons, T , SH , and RH decreased with altitude. Autumn temperatures were somewhat higher than spring at all altitudes (Figures 5.3 and 5.4).

Table 5.1: Variables tested as predictors of proportional bird density (tBd) in a forward stepwise GAM regression analysis. Descriptions of variables are given in the last column along with a reference justifying the inclusion of the variable.

Variable	Units	Description and motivation
Alt	km	The height of the middle of an altitude bin above ground, which is included by default (Liechti et al., 2000)
rTw	ms^{-1}	Tailwind strength at a given altitude minus the strongest tailwind in the altitude profile (e.g. Bruderer et al., 1995b; Liechti et al., 2000)
rTw_{sfc}	ms^{-1}	Tailwind at a given altitude minus tailwind at the surface, if tailwind at the surface is negative, otherwise zero (Gauthreaux, 1991)
rWP	ms^{-1}	Wind profit at a given altitude minus the best wind profit in the altitude profile (e.g. Schmaljohann et al., 2009)
rWP_{sfc}	ms^{-1}	Wind profit at a given altitude minus wind profit at the surface, if wind profit at the surface is negative, otherwise zero (Gauthreaux, 1991)
T	K	Air temperature (e.g. Bruderer, 1971; Carmi et al., 1992)
RH	%	Relative humidity (e.g. Klaassen, 1996)
SH	g/kg	Mass of water vapor per kilogram of atmosphere (e.g. Gerson and Guglielmo, 2011)
Cp	%	Percentage of time that clouds were present (cf. Eastwood, 1967; Bruderer, 1971)

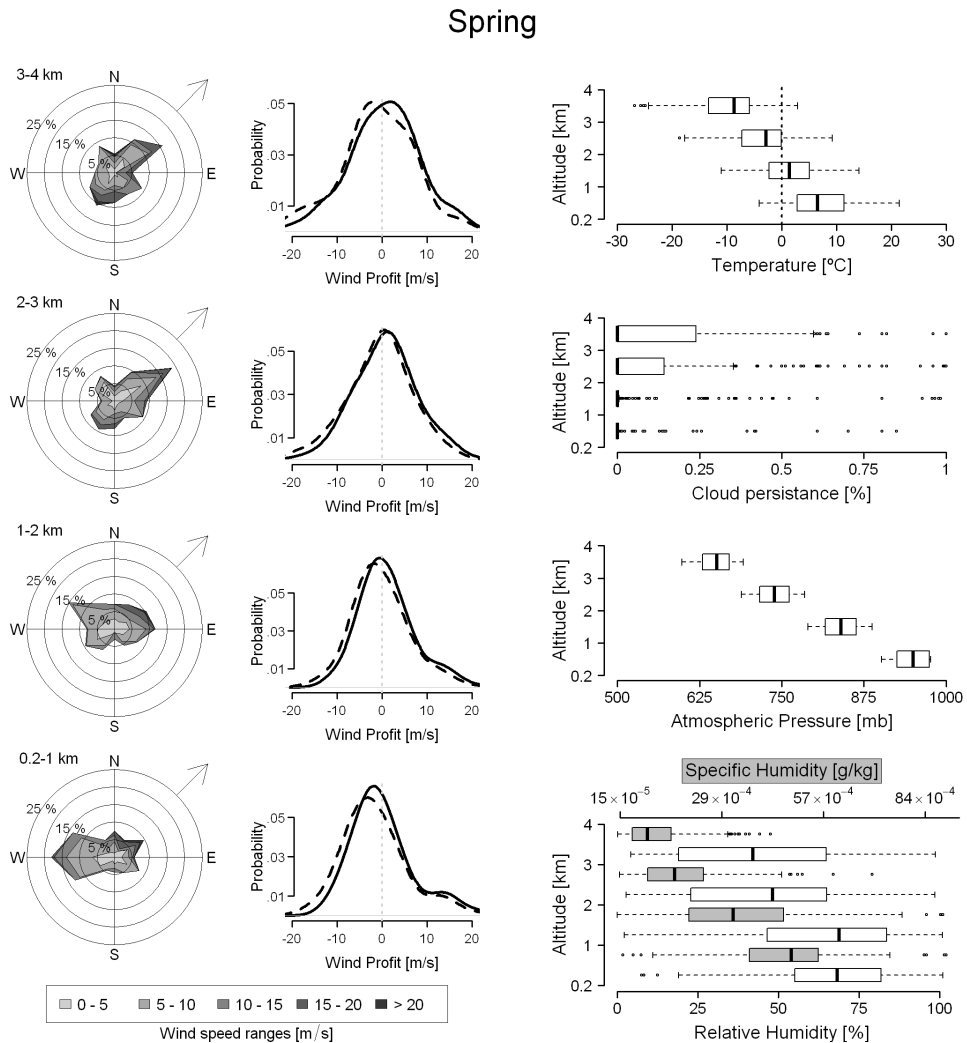


Figure 5.3: Graphical summaries of the weather conditions for spring from the nightly weather profiles used in our study. Wind condition, described in one kilometer altitude intervals, is shown on the left by wind rose plots and probability distributions of tailwind (T_w ; solid line) and wind profit (WP ; dashed line). Distance from the center of a wind rose indicates the relative frequency of the wind blowing into a particular direction, and shades of gray indicate the individual relative frequencies of the different wind speed ranges for a particular direction. Concentric circles indicate relative frequencies in increments of 5%, with the outer circle indicating 25% relative frequency. Continued on next page...

Figure 5.3 (continued): On the right, box-plots indicate distributions of temperature (T), cloud persistence (Cp), atmospheric pressure (A_P), and relative (RH) and specific humidity (SH) per 1 km altitude interval. Boxes in these box-plots indicate the upper and lower quartiles and median, “whiskers” indicate values < 1.5 times the inter-quartile range beyond the quartiles, and points indicate outliers. A dashed vertical line in the temperature plot indicates the freezing point.

5.4.2 Wind and migratory altitudes: comparisons with previous research

Pearson’s r correlations between the lowest altitude with acceptable wind support, as defined by Gauthreaux (1991), and the altitude with the largest proportion of birds on nights when the highest bird density was in an altitude bin above 0.4 km (see Figure 5.5) were significantly positive in spring ($r = 0.59$; $n = 35$; $P < 0.001$). In autumn, this correlation was also significantly positive ($r = 0.68$; $n = 18$; $P < 0.01$); however, this significant correlation would not exist without the leverage of a single point exhibiting a Cook’s distance of 2.3 (see Figure 5.5).

Nightly Spearman’s ρ correlations between wind support (considering either Tw or WP) and pBd (see Figure 5.4.2; and compare to Liechti et al., 2000; Schmaljohann et al., 2009) were rather weak in both spring (means of 0.15 and 0.17, respectively) and autumn (means of 0.12 and 0.30, respectively). Correlations were more positive when considering WP (i.e. when accounting for side winds) than Tw , though the difference was only significant in autumn (paired two-sided Mann-Whitney test; $n_{spring} = 62$, $n_{autumn} = 36$; $P \leq 0.001$).

In reproducing the analysis by Bruderer et al. (1995b), our linear regression model suggested a statistically significant but very weak relationship between ΔTw (i.e. the change in tailwind strength between altitude bins) and P_L (i.e. the logit of the proportional difference in pBd between altitude bins). The resulting equation for autumn ($P_L = -0.34 + 0.06\Delta Tw$, $n = 361$, $r^2 = 0.01$, $P \leq 0.05$) suggested a weaker and less-significant relationship between ΔTw and P_L than in spring ($P_L = -0.29 + 0.13\Delta Tw$, $n = 559$, $r^2 = 0.05$, $P \leq 0.001$). In both seasons, and contrary to the results of Bruderer et al. (1995b), we found that the intercept in the equations was highly significant.

The simulations resulting from the regression relationships between ΔTw and P_L explained 56% and 73% of the variability in nightly distributions of pBd in spring and autumn, respectively. These values were somewhat higher than those reported by (Bruderer et al., 1995b, ; i.e. 56% for spring and 63% for autumn). For comparison with other results in this paper, the average Spearman’s ρ correlation between the measured and simulated distributions

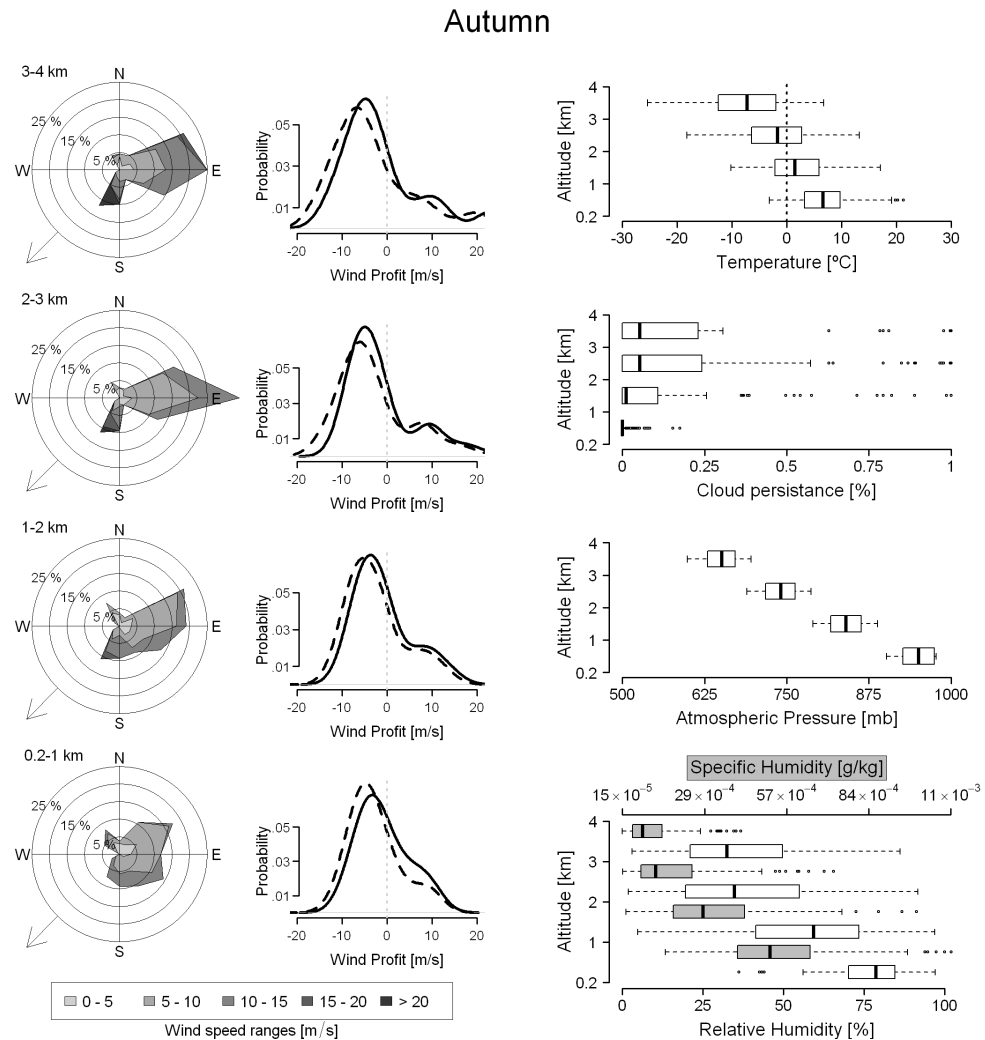


Figure 5.4: Graphical summaries of the weather conditions for autumn from the nightly weather profiles used in our study. Wind condition, described in one kilometer altitude intervals, is shown on the left by wind rose plots and probability distributions of tailwind (T_W ; solid line) and wind profit (WP ; dashed line). Distance from the center of a wind rose indicates the relative frequency of the wind blowing into a particular direction, and shades of gray indicate the individual relative frequencies of the different wind speed ranges for a particular direction. Concentric circles indicate relative frequencies in increments of 5%, with the outer circle indicating 25% relative frequency. Continued on next page...

Figure 5.4 (continued): On the right, box-plots indicate distributions of temperature (T), cloud persistence (Cp), atmospheric pressure (A_P), and relative (RH) and specific humidity (SH) per 1 km altitude interval. Boxes in these box-plots indicate the upper and lower quartiles and median, “whiskers” indicate values < 1.5 times the inter-quartile range beyond the quartiles, and points indicate outliers. A dashed vertical line in the temperature plot indicates the freezing point.

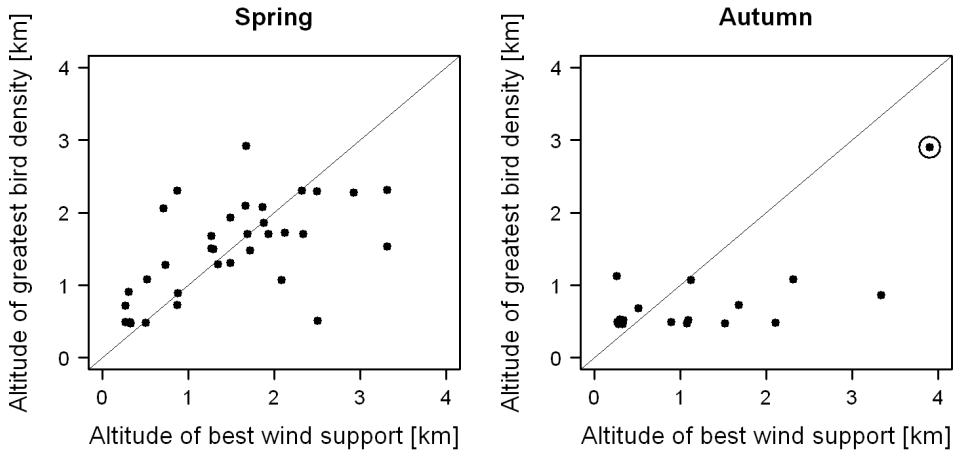
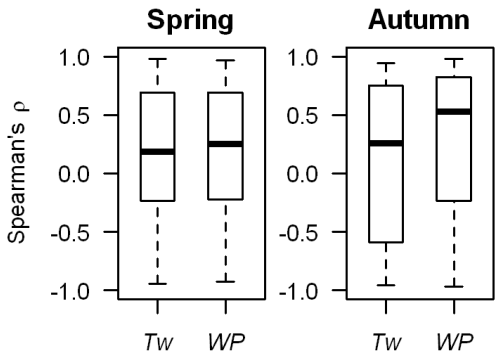


Figure 5.5: Scatter plots indicating the correlation between the altitude with best wind support (as calculated by Gauthreaux (1991)) and the altitude with most intense migration for those nights in spring (left; $n = 35$; $r = 0.59$; $P \leq 0.001$) and autumn (right; $n = 18$; $r = 0.68$; $P \leq 0.01$) when the altitude bin with most intense migration was > 0.4 km. In autumn, the correlation and its significance are critically dependent on the leverage of a single observation (circled). A diagonal line indicates a theoretical perfect positive correlation.

Figure 5.6: Box-plots indicating the distributions of nightly Spearman’s ρ correlations between pBd and wind support, considering either the tail-wind component (Tw) or wind profit (WP), for spring (left) and autumn (right). Boxes indicate the upper and lower quartiles and median, “whiskers” indicate values < 1.5 times the inter-quartile range beyond the quartiles.



was 0.54 in spring and 0.76 in autumn. Appendix D shows, for each night considered in this study, distributions of pBd resulting from these simulations alongside measured distributions of pBd and Tw . The simulated distributions of pBd do not vary a great deal from night to night, and most exhibit a rather exponential decrease with altitude.

5.4.3 GAM analysis

We performed a forward stepwise regression analysis 50 times per season to arrive at a robust combination of predictor variables that best explained the observed variability in the altitude distributions of avian migrants. While these models were selected and calibrated with tBd (i.e. pBd after an additive log-ratio transformation) serving as the response variable, we back-transformed our predictions and will therefore discuss model performance on the scale of pBd wherever possible. In Table 5.2, we report the number of times each potential predictor variable was selected in one of these 50 final models. Altitude (Alt) was included in these models by default and explained a large proportion of the variability in pBd by itself (52% and 73% in spring and autumn, respectively). This was roughly the same amount of variability explained by our simulation approach following Bruderer et al. (1995b). Measures of wind assistance relative to surface wind conditions (i.e. rWP_{sfc} and rTw_{sfc}) were selected more often than measures of wind assistance relative to all wind conditions in the nightly profile (i.e. rWP and rTw), and rTw_{sfc} was selected more often than rWP_{sfc} . Temperature (T) and measures of humidity (RH and particularly SH) were often selected in a final model.

In Table 5.3, we present the model that resulted most often per season for each level of complexity (i.e. number of predictor variables). The most frequently selected or ‘best’ model was the same in both seasons, with rTw_{sfc} having been selected first and T having been selected thereafter. The functional relationship of Alt , rTw_{sfc} , and T to tBd in these models is illustrated in Figure 5.7. As well, Appendix E shows, for each night considered in this study, measured distributions of pBd , with their associated T , Tw , SH , and Cp distributions, alongside the weighted average seasonal distribution of pBd and the distribution of pBd predicted by the best GAM model for that season. The predicted distributions from these GAM models vary more than those from the simulation and do a better job of capturing “peaks” in pBd at higher altitude.

In the best model for both seasons, a rather linear decrease in tBd occurred with increasing Alt (Figure 5.7), and Alt explained more variability in tBd than any other variable (Table 5.3). The functional form of rTw_{sfc} in the best model for both seasons indicated that, when Tw was negative at the

Table 5.2: The number of times each potential predictor variable was selected in a final GAM model during the 50 stepwise model selection iterations for spring and autumn is shown. Altitude was included in each model by default.

Abbreviation	Variable	Times selected	
		Spring	Autumn
<i>Alt</i>	Altitude	50	50
<i>rTw</i>	Relative <i>Tw</i>	11	3
<i>rTw_{sfc}</i>	<i>Tw</i> relative to surface	45	50
<i>rWP</i>	Relative <i>WP</i>	14	1
<i>rWP_{sfc}</i>	<i>WP</i> relative to surface	16	6
<i>T</i>	Temperature	19	32
<i>RH</i>	Relative humidity	0	13
<i>SH</i>	Specific humidity	7	15
<i>Cp</i>	Cloud persistence	2	0

Table 5.3: The most frequently selected models from the 50 stepwise model-selection iterations are shown for spring and autumn. Predictor variables other than altitude were selected according to repeated random sampling cross-validation. For each season, we indicate the most frequently occurring model for each level of complexity (i.e. number of predictor variables). From those model-selection iterations that produced the most frequently occurring models at the highest complexity (8 in spring and 24 in autumn), we report the average of the mean RMSE (on the scale of *pBd*), Spearman's ρ , and variance explained – as defined by Bruderer et al. (1995b) – at each level of complexity.

Season	Number of variables	Final GAM model	RMSE	Spearman's ρ	Variance explained
Spring	1	<i>Alt</i>	0.096	0.32	52.2
	2	<i>Alt</i> + <i>rTw_{sfc}</i>	0.087	0.38	55.0
	3	<i>Alt</i> + <i>rTw_{sfc}</i> + <i>T</i>	0.084	0.44	57.1
Autumn	1	<i>Alt</i>	0.064	0.74	73.1
	2	<i>Alt</i> + <i>rTw_{sfc}</i>	0.059	0.79	73.8
	3	<i>Alt</i> + <i>rTw_{sfc}</i> + <i>T</i>	0.058	0.77	75.4

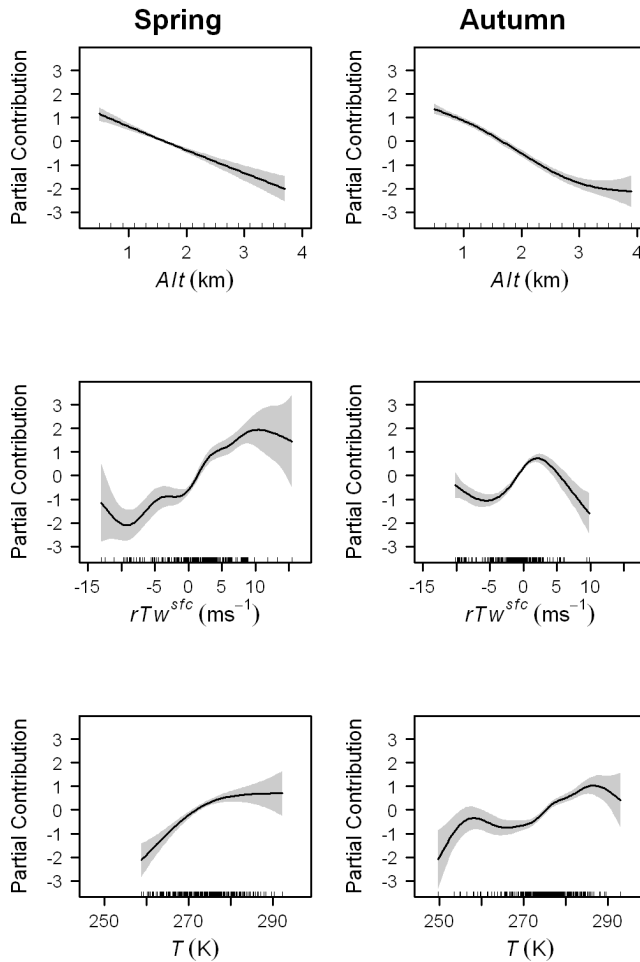


Figure 5.7: Plots indicating the partial contributions of the variables comprising the most frequently selected models resulting from the 50 forward stepwise model-selection iterations for spring (left column) and autumn (right column). Variables are given from top to bottom in the order they were (most often) selected. In each plot, the x-axis indicates the range of the predictor variable, and rug plots along the bottom indicate the occurrence of a particular value of that predictor variable. The y-axis indicates the partial contribution of each predictor variable on the scale of tBd (i.e. pBd or proportional bird density after the additive log-ratio transformation). Shaded areas indicate two standard errors from the estimate. Model predictions (on the scale of tBd) are obtained by summing the partial contributions of each predictor variable.

surface, larger proportions of birds occurred at altitudes at which Tw was stronger than at the surface (Figure 5.7); conversely, smaller proportions of birds occurred at altitudes at which Tw was weaker than at the surface. The functional form of T in both seasons suggested that birds generally avoided colder temperatures. In both seasons, the functional forms of rTw_{sf} and T nearer their extremes exhibited sinuosity and changes in direction that may be driven by relatively few data points. Rug plots in Figure 5.7 show a sparseness of data points at these extremes, with confidence intervals (areas shaded gray in Figure 5.7) around predictions made in this part of the domain being higher as a result.

5.5 Discussion

Often, the paradigm used to understand bird migration is one of optimization (Alerstam, 2011), where behavior is described in the context of optimizing one or more predefined criteria. The criteria often considered in the context of bird migration are time, energy, water balance, and predation risk. When studying flight altitude selection in the context of optimality, energy and water balance have been the primary criteria considered (e.g. Klaassen and Biebach, 2000; Liechti et al., 2000; Schmaljohann et al., 2009); however, time and safety, for example the risk of becoming disoriented or not efficiently finding a suitable stopover site, may also be important adaptive constraints on altitude selection. In general, (and particularly in the absence of complicating factors such as those outlined below), nocturnal migrants should select altitudes with greater wind support when minimizing travel time or energy expenditure to reach the migration target, and empirical studies of avian altitude distributions have often reached this conclusion (e.g. Bruderer et al., 1995b; Liechti et al., 2000; Schmaljohann et al., 2009).

Our study also suggests that birds prefer altitudes with more supportive winds (see Figure 5.5 and the partial contributions of rTw_{sf} in Figure 5.7), and specific examples in our study suggest that birds are quite capable of identifying and selecting profitable winds (e.g. 4-9 May 2008; see Appendix E). We also find that increasing tailwind strength with altitude (ΔTw) increases the probability of birds climbing to higher altitude. However, while our results suggest that birds prefer supportive winds, we find little or no correlation between the nightly vertical profiles of either WP or Tw and the altitude distributions of pBd (Figure 5.4.2), and wind support explains a relatively small amount of the variability we observed in migratory altitudes (see Table 5.3). Recall as well the significant negative intercepts in the regression equations describing the relationships between ΔTw and P_L in the approach following

Bruderer et al. (1995b). These intercepts mean that in spring and autumn ΔTw has to be greater than 2.23 and 5.67 ms⁻¹, respectively, before a majority of birds prefer the next highest altitude bin. Thus, the simulations from these regression relationships are heavily influenced by these intercepts, and the intercepts are likely a reflection of the average distribution of pBd . It is reasonable then that Alt itself in our GAM models explains roughly the same about of variability in pBd as our simulation approach following Bruderer et al. (1995b). Apparently, birds are not exclusively selecting flight altitudes based on wind conditions that would optimize time or energy expenditure. As has been shown in other areas (Bruderer, 1971), the effects of wind on migratory altitude cannot be considered in isolation from other atmospheric factors. This is likely due to birds considering multiple objectives (and trade-offs between these objectives) during migratory flight.

From an aerodynamic perspective, migrating at higher altitudes should be beneficial since the decrease in air density associated with higher altitudes reduces frictional resistance (i.e. parasite drag) thereby increasing the distance a bird is able to fly with a given amount of energy and reducing the time it will take to do so (Pennycuick, 2008). Despite this potential benefit, both Gauthreaux (1991) and Bruderer (1971) observed birds flying at lower altitudes even when winds were somewhat better aloft, suggesting that lower altitudes may be favored over higher ones. Our results corroborate this assessment: the average altitude distribution of pBd (Figure 5.2), the significant negative intercepts in our comparison with the analysis of Bruderer et al. (1995b), and the functional relationship between Alt and tBd revealed in our GAM analysis (Figure 5.7) suggest a preference for lower altitudes. As well, our comparison with the analysis by Gauthreaux (1991) shows that, even when birds do fly higher than normal, they concentrate around the lowest altitude with acceptable, though note not necessarily optimal, wind conditions (Figure 5.5). In aggregate, our results suggest that climbing to high altitude in this region may be a risky and/or costly endeavor or that there are additional benefits associated with migrating at lower altitude.

In addition to the fact that it takes time and energy simply to reach higher altitudes (Hedenström and Alerstam, 1992; Liechti et al., 2000), there are several atmospheric variables correlated with altitude that, particularly through their potential influence on a bird's rate of water-loss, could curb the potential benefits of high-altitude migratory flight, resulting in a general tendency to remain at low altitudes (Carmi et al., 1992; Klaassen, 1995, 1996, 2004). Atmospheric pressure necessarily decreases with altitude, which forces a corresponding decrease in oxygen partial-pressure and, along with the aforementioned decrease in frictional resistance, a decrease in lift (i.e. induced drag

Pennycuick, 2008). As well, temperature in the troposphere generally decreases with altitude, unless a low-level temperature inversion is present, and decreasing temperature reduces the amount of moisture the air is able to hold. Therefore when birds inhale the colder (and likely drier) air at higher altitude, they warm that air (increasing the amount of water the air is able to hold), saturate the air with water from their own body, and then lose the water through exhalation (Klaassen, 1996). The decrease in lift with altitude is not such a problem from a aerodynamic perspective, since there is often more benefit from the reduction in friction than detriment from the reduction in lift; however, slightly more aerobic power is required, and thus more oxygen, yet available oxygen decreases with altitude. This necessitates an increase in pulmonary ventilation which forces a further increase in the rate of water-loss (Carmi et al., 1992). So while the rate of water-loss increases in higher temperatures (see Schmaljohann, 2008, and references therein) as birds attempt to reduce heat-stress by evaporative cooling (Klaassen, 1996), potentially more water is lost in colder temperatures due to the difference in temperature between cooler ambient air and warmer exhaled breath (Klaassen, 1996). Our GAM analysis suggests that birds avoid very cold temperatures (see Figure 5.7). Avoidance of very warm temperatures in these models, however, is not apparent. Perhaps temperatures in the Netherlands did not reach the threshold for “very warm” often enough during the migration seasons we examined to be well-represented in our models (see distributions of T in Figures 5.3 & 5.4 and the rug plots along the bottom of plots illustrating the functional relationship of T to tBd in Figure 5.7).

Despite studies suggesting that flight range may be limited by dehydration, previous empirical studies have shown birds selecting altitudes based largely on wind conditions (e.g. Bruderer et al., 1995b; Liechti et al., 2000), and specifically selecting altitudes to minimize energy costs rather than water-loss (Schmaljohann et al., 2009). Recall, however, that these studies were primarily conducted in the trade-wind zone where the influence of Hadley cell rotation, and the associated shift of wind direction with altitude, can result in winds near the surface being persistently prohibitive, while wind conditions at higher altitude are less-prohibitive or even supportive. Our GAM results suggest that birds are more likely to seek out supportive winds at higher altitude if winds near the surface are prohibitive (see the partial contribution of rTW_{sfc} in Figure 5.7), and many of the cases in our study in which birds flew at higher altitude are associated with prohibitive winds near the surface and less-prohibitive or even supportive winds at higher altitude (see e.g. 9 October 2008 and 27 October 2009 & 4-25 May 2008 among many others in Appendix E). In contrast, we do not generally see migrants climbing to

higher altitude when wind conditions at the surface are already supportive (see e.g. 24-25 November 2008 and 15 October 2009 & 7 April 2008 and 2-3 March 2009 in Appendix E). Perhaps high-altitude migration is due primarily to avoidance of prohibitive winds near the surface rather than selection of optimal winds at higher altitude, which would be in accordance with findings in this and previous studies. An interesting avenue for future research would be to study if migrants fly at higher altitudes only when wind conditions are sufficiently prohibitive near the surface and more supportive at higher altitude, and perhaps to identify thresholds for ‘sufficiently prohibitive’ and ‘more supportive’. From an evolutionary perspective, it would be interesting to see if these thresholds were adjusted along the migration route according to the general atmospheric circulation patterns of a region and season.

Another possible difference between the migratory behavior we observed in the Netherlands and what has been observed in some previous studies is that birds in the Netherlands are not in the process of crossing an ecological barrier. Several systematic examinations of avian altitude distributions in relation to weather have been conducted in the proximity of an ecological barrier such as the Sahara desert (e.g. Klaassen and Biebach, 2000; Liechti and Schmaljohann, 2007; Schmaljohann et al., 2009) or the Gulf of Mexico (Gauthreaux, 1991). Crossing such an ecological barrier may significantly alter behavior as it may be beneficial to cross the barrier as quickly as possible. In cases where minimizing time is essential, finding and utilizing the most beneficial winds may be of paramount importance. Alternatively, when not crossing an ecological barrier, a bird may be willing to accept sub-optimal winds at lower altitudes in order to conserve moisture, reduce the risk of being blown off course by high-speed winds at higher altitude, search for suitable stopover habitat, or navigate more easily. If birds navigate using ground-based visual cues (Bruderer, 1982; Fortin et al., 1999), increasing atmospheric turbidity (being unavoidable as light travels greater distances through the atmosphere) and increasingly shallow angles between a bird and its ground-based points of reference with altitude likely inhibit navigation.

That C_p was not selected often in our models should not lead necessarily to the conclusion that clouds had no influence on altitude selection. It is possible, for instance, that we introduced a bias in our dataset by only considering nights with relatively intense migration. As well, clouds can be difficult to quantify, particularly per altitude bin, as they can be discontinuous and heterogeneously distributed in space and time. Bruderer (1971) observed that the type and quality of cloud cover determined its influence on migratory altitudes, yet many aspects of cloud cover cannot be measured or modeled yet systematically. Thus, relevant features of a particular cloud formation may not have been

captured in our formulation of C_p .

A shortcoming of the methods we, and others, have applied to model the altitude distributions of avian migrants arises from the tendency to assume uniformity in avian decision making over time and space. For example, we necessarily use a single preferred direction in the calculation of WP and T_w when it is quite possible that migrants with different endogenous directions were considered in our analyses. Furthermore, species migrating at different times of the season may prioritize adaptive pressures, and therefore atmospheric variables, differently. Nonetheless, our GAM models explain a rather large percentage of the variability in migratory altitudes, and the variables selected in our GAM analysis are likely representative of the general behavior of migrants in this area. This is particularly likely since the same predictor variables, indicating similar relationships with migratory altitude, were selected in both seasons.

Our GAM results show that birds predominantly remain at low flight altitudes in this region. Since this behavior is not consistent with time or energy minimization when wind conditions improve with altitude, the behavior may indicate birds balancing the optimization of time and/or energy with considerations of their safety, water balance, and perhaps other criteria. When wind conditions are supportive already at low altitude, and birds can make acceptable forward progress, negative impacts on their safety and water balance associated with high-altitude flight may offset potential gains in time and energy from more supportive winds at higher altitude. When wind conditions are unsupportive at low altitude, however, birds may be willing to climb to higher altitude, accepting an increase in their rate of water-loss and a decrease in safety, so that they can find supportive winds and maintain an acceptable travel speed. Even so, birds stop climbing once they reach an altitude with acceptable wind conditions rather than continuing to climb and incurring increasingly negative effects on their safety and water balance.

5.6 Conclusion

In general, we may expect that birds can and should adapt their flight altitudes in such a way as to account for flight time, energy expenditure, water balance, and safety, yet the relative importance of these pressures may change between species, regions, seasons, and phases of migration. In some situations, traveling as fast as possible in a desired direction may take precedence, making the influence of wind paramount. In our study area, where freezing temperatures, cloud cover, and frequent frontal systems exist, birds seem to balance considerations of time, energy, water, and safety and do not appear to

select altitudes for migration based solely on wind condition. This result supports a recent trend in literature suggesting that passerine migrants may not be as selective of tailwind support as previously suspected (Alerstam et al., 2011; Karlsson et al., 2011). Thus, while birds exhibit some general behavioral adaptations to atmospheric conditions on a large scale (e.g. avoidance of headwinds), individuals may be flexible in their responses to conditions en route – perhaps even depending on the persistent atmospheric (or geographic) conditions in an area.

This study highlights the potential gains to be made using existing weather radar to study migratory movements with high temporal and altitudinal resolution. With an existing network of similar radars already covering so much of Europe, the potential exists for a great deal of informative analyses allowing specifically the types of comparisons between different locations needed to separate the individual influences of and quantify trade-offs between different atmospheric (and non-atmospheric) variables; quantify the priority or precedence birds give these variables; and determine if this priority or precedence depends on the condition of other variables, geographical location, and time of year. Ultimately, we may determine that altitude selection in birds is based on just a few general rules and is otherwise quite flexible; alternatively, we may realize that there are a great many endogenous and interdependent rules that we were previously unable to disentangle. Likely, the situation is, as described by Alerstam (1981), “a harmonious mixture of rigid and flexible behavior adapted to a bewildering number of factors affecting the safety and economics of the migratory journey”. An integrative combination of analytical tools, measurements across multiple spatial and temporal scales, and experiments that enable researchers to consider multiple objectives and trade-offs simultaneously are likely to bring us much further in our understanding of migratory behavior (Bowlin et al., 2010).

Acknowledgments

We would like to thank the Royal Netherlands Meteorological Institute (KNMI) for data from the De Bilt weather radar, Toon Moene and KNMI for providing and assisting with HIRLAM weather data, and Henk Klein Baltink and KNMI for assisting with cloud data. We also thank Hidde Leijnse and Hans van Gasteren for their valuable contributions and discussion as well as Prof. Bruno Bruderer, one anonymous reviewer, and the editors of the journal *Ibis* for their thoughtful critiques and suggestions on a previous manuscript. Our studies are facilitated by the NLeSC (<http://www.esciencecenter.com/>) and BiG Grid (<http://www.biggrid.nl>) infrastructures for e-Science and supported

financially by the Ministry of Defense (Flysafe2).

6

Predicting migration intensity at multiple sites using operational weather radar

6.1 Introduction

The first reported bird strike to a powered aircraft was recorded in the journal of the first pilot on record: Orville Wright (Thorpe, 2003). It should not be surprising then that bird strikes remain a significant threat to aviation still today (Allan, 2002; Dolbeer et al., 2000). Between 1950 and 1999, at least 190 European military aircraft were lost due to birds (Richardson and West, 2000). In the United States alone, the Federal Aviation Administration (FAA) reports that over 100,000 bird strikes to general and civil aircraft were reported (voluntarily) between 1990 and 2010 (Dolbeer et al., 2012).

In civil aviation, flights often cannot be canceled or even significantly delayed without incurring large financial consequences. It is often impractical, therefore, to avoid bird strikes by restricting these types of flights for any considerable length of time. Rather, these industries have focused their efforts on tactics such as land management (i.e. habitat modification), harassment or scaring techniques, and species removal. More than 70% of the bird strikes in the FAA's report occurred below 500 ft. (~ 152 m) above ground level and decreased exponentially thereafter, suggesting that the risk of a bird strike in civil and general aviation is concentrated primarily around aerodromes during take-off and landing. While these are critical phases of flight, they comprise a relatively small percentage of the total flight time. Military training flights, on the other hand, frequently occur at lower altitudes where the risk of a bird strike can be high for the entirety of the flight; however, for military training flights, adjusting flight trajectories, delaying take-off, or even cancelling flights is both practical and feasible (Shamoun-Baranes et al., 2008; van Belle et al.,

2007).

Because military aviation has the option to adjust, delay, or cancel training flights at times of intense migratory activity, countries have developed systems to monitor (near) real-time migratory activity to make these determinations (Shamoun-Baranes et al., 2008) and to predict the intensity of migration from environmental variables including forecasted weather conditions (e.g. van Belle et al., 2007; Rabøl, 1974; Blokpoel, 1969; Bouten et al., 2005, 2003). Predictive models of bird migration intensity have primarily been calibrated using localized measurements of migration intensity obtained from direct observation, infrared devices, military surveillance radar, or dedicated bird-detection radar; however, models calibrated for one location do not necessarily perform well at other locations far away (van Belle et al., 2007), so the predictions from these models may have a limited spatial range in which they are valid.

In this study, we aim to develop an ensemble of models to forecast migration intensity that is calibrated using measurements of migration intensity obtained from existing operational weather radar at two locations in the Netherlands. Because models calibrated for one location do not necessarily perform well far away from that location, the use of operational weather radar in the development of these models is particularly attractive. Vast networks of operational weather radars are already in place – e.g. the radar systems involved in the Operational Programme for the Exchange of weather RAdar information or OPERA network in Europe (Holleman et al., 2008), the Baltic Sea Experiment radar network (BALTRAD; Alestalo, 2002), and the Next-Generation Radar or NEXRAD network in the United States (Chilson et al., 2012) – creating the potential for standardized locally-calibrated predictive models covering enormous geographic areas. Thus, a second aim of this study is to outline a model-development procedure that can be easily applied to new locations. The models developed in this study, and the model-development procedure described, are intended to produce the most accurate predictions of migration intensity possible, which requires a different approach from the development of models to better understand the relationship between migratory dynamics and environmental conditions. Because we intend for this model-development procedure to be robust and generally applicable, we employ generalized additive models (GAMs; Hastie and Tibshirani, 1990) in development and testing. GAMs are particularly useful in this context because they are not constrained to predefined parametric relationships between predictor and response variables.

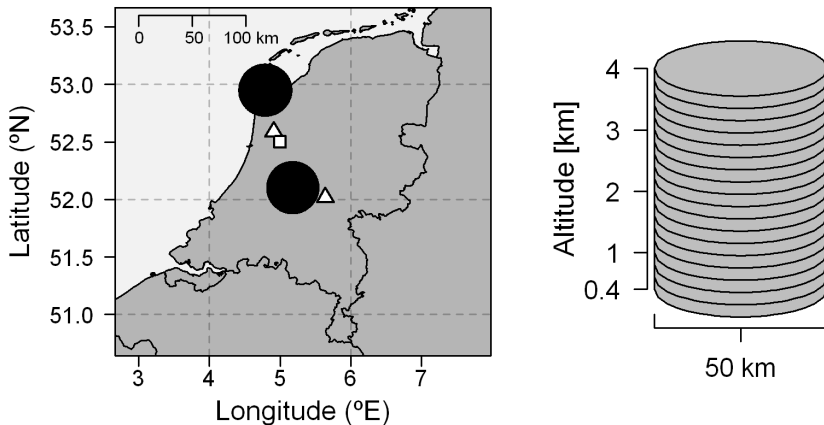


Figure 6.1: At left, a map of the Netherlands with large black circles indicating the ranges of the C-band Doppler weather radar sites in De Bilt (52.11°N 5.18°E) and Den Helder (52.95°N 4.79°E). White triangles indicate the closest grid point in the HIRLAM dataset to each radar, from which most weather data were obtained. A white square indicates the location of the NCEP grid point from which temperature data were obtained to calculate climatological normals. At right, a vertical profile of the radar measurement volume indicating the 18 altitude bins within which measurements of bird density (Bd) were calculated.

6.2 Materials

6.2.1 Radar measurements of migration intensity

From the spring (1 February - 31 May) and autumn (1 August - 30 November) of 2008 and 2009, we used methods described by Dokter et al. (2011) to derive altitude profiles of bird density (Bd ; birds/km³) and average speed ($Bspd$; ms⁻¹) and direction ($Bdir$; ° clockwise from north) relative to the ground every five minutes from two C-band Doppler weather-radars located in the Netherlands (De Bilt 52.11°N 5.18°E and Den Helder 52.95°N 4.79°E ; see Figure 6.1). Each altitude profile described Bd , $Bspd$, and $Bdir$ from 0.4 to 4 km above the ground in altitude bins of 200 m. Thus each profile consisted of 18 measurements, each calculated from within a circular measurement window extending from 5 to 25 km laterally from the center of the radar (Figure 6.1).

As a means of additional quality control, we used HIRLAM wind data (see section 6.2.2) to calculate airspeeds from $Bspd$ and $Bdir$ by vector subtraction. We set Bd measurements to zero if the associated airspeed was not between

7 and 25 ms⁻¹, as this range captures the airspeeds of the majority of avian migrants (Bloch and Bruderer, 1982; Bruderer and Boldt, 2001) and largely excludes the airspeeds of migrating insects (Alerstam et al., 2011; Aralimarad et al., 2011; Chapman et al., 2008).

We calculated height-integrated bird density (iBd ; birds/km²) from each 5-minute interval altitude profile as

$$iBd = \sum_{h=1}^{18} Bd_h \cdot \Delta h \quad (6.1)$$

where Bd was integrated over the 18 altitude bins (h). We then aggregated these 5-minute interval iBd measurements into one-hour averages to serve as the response variable in our models.

6.2.2 Variables used to predict hourly migration density

Baseline intensity

Migratory activity is known to exhibit seasonal and diel dynamics that should be represented in models to predict migration intensity. One option is for researchers to calculate baseline intensity explicitly as the average bird density in their dataset having occurred at a particular time of the day and year (e.g. van Belle et al., 2007). In linear and generalized linear models, this method has the advantage of being able to capture a potentially non-linear process over time using a variable that can be treated linearly in these models. Through the use of smoothing terms, GAMs are able to capture non-linear processes directly in a model. This allows for the use of time directly in our models, permitting the GAM fitting procedure to determine the optimal (possibly non-linear) representation of the influence of time on migration intensity. Thus, we use the day of the year (DOY) and the proportion of the day (P_{day}) or night (P_{night}) directly in our models to reflect any temporal patterns in migration intensity. P_{day} and P_{night} were calculated relative to sunrise and sunset such that $P_{day} = 0$ at sunrise and 1 at sunset and, conversely, $P_{night} = 0$ at sunset and 1 at sunrise.

The use of GAMs also allowed for the incorporation of interaction terms: that is, terms which account for the fact that the influence of one predictor variable on the response is dependent upon the value of the other predictor variable. Thus, the two predictor variables ‘interact’ with one another regarding their influence on the response variable. We expected that DOY and P_{day} or P_{night} would likely exhibit such a dynamic relationship, because, for example, the times of sunrise and sunset – and therefore the lengths of day and night – were variable through a migration season. We therefore included these

time-related variables as interaction terms in our models. Because the units of *DOY* and either P_{day} or P_{night} were quite different from one another, we used non-isotropic tensor splines (Wood, 2006) to fit their functional relationship to iBd in our models. Hereafter, we refer to this smoothed interaction term between *DOY* and either P_{day} or P_{night} as a single variable called *sTime*. This baseline intensity variable *sTime* was included in all models by default.

Autocorrelation

Erni et al. (2002b) suggested that migration intensity was autocorrelated on successive nights; however, Erni et al. (2002b) did not include a parameter to explicitly account for this autocorrelation in their analysis because for their analysis they desired that “predictions for migration should depend only on weather conditions and the date and not on previous observations, which may not exist”. Our aim in this study was to develop forecast models of migration intensity for flight safety, so incorporating previous measurements of bird density to improve the accuracy of our predictions was desirable. We therefore measured the autocorrelation between successive iBd measurements in our dataset, and included two variables meant to capture temporal autocorrelation in our models: 1) the mean iBd value over the previous hour (hereafter iBd_h) and 2) the mean iBd value on the previous day or night (hereafter iBd_d).

Atmospheric variables

To aid in the development of future models, we relied exclusively on atmospheric data available in the High Resolution Limited Area Model (i.e. HIRLAM; Cats and Wolters, 1996; Undén et al., 2002) or the freely-available National Centers for Environmental Prediction (NCEP)/ Department of Energy (DOE) Reanalysis II dataset (Kanamitsu et al., 2002) (see Chapter 2 for more details). HIRLAM, from which the majority of variables were obtained, is a high-resolution gridded atmospheric model that reflects the combined initiatives of the meteorological offices of multiple European countries to develop and maintain a numerical short-range weather forecasting system for operational use (Cats and Wolters, 1996; Undén et al., 2002). Our use of data from this model has several likely benefits: 1) for practicality, the model-development procedure we apply will be directly exportable to new locations in Europe and elsewhere that HIRLAM data are available – importantly, the organizations developing and implementing the HIRLAM model are often the same organizations operating and maintaining the weather radar systems being used to quantify bird migration; 2) because HIRLAM is a forecasting

system, models resulting from this development procedure may be applied toward the prediction of migration intensity to serve in flight safety and other contexts such as mitigating bird-strikes with wind turbines (Desholm et al., 2006); 3) predictions of migration intensity can potentially be made for locations without a weather radar using local weather conditions obtained from HIRLAM as input into models of migration intensity calibrated for nearby locations.

Using data from the gridded HIRLAM atmospheric model, we derived altitude profiles, to a height of 1 km, of wind condition (ms^{-1}), temperature (T ; K), atmospheric pressure (AP ; mb), and relative humidity (RH ; %). These data had a spatial resolution of $0.1^\circ \times 0.1^\circ$ on a rotated grid, temporal resolution of one hour, and were discretized vertically at fixed pressure levels separated by not more than 12 mb. Using data from the HIRLAM grid point nearest the center of the De Bilt radar (~ 33 km east at 52.02°N 5.64°E ; see Figure 6.1) or the Den Helder radar (~ 41 km south at 52.59°N 4.91°E ; see Figure 6.1), we calculated averages of each variable from these vertical profiles. We then calculated the 24-hour change in T , AP , and RH , hereafter denoted ΔT , ΔAP , and ΔRH , respectively. We also derived estimates of the accumulation of precipitation (R ; mm) over each hour from the HIRLAM model.

Wind data were described by two components, U and V (ms^{-1}), indicating the speed and direction into which the wind was blowing. The U vector described the wind's east/west component (toward east being positive) and V described the north/south component (toward north being positive). Calculating flow-assistance is a useful way to reduce the complex and non-linear effects of the two components of a flow (e.g. U and V) into a single value that facilitates quantitative comparisons between different flow conditions and incorporation of wind support into linear models (see Chapter 3); however, GAMs allow for the inclusion of interaction terms in which the influence of each variable is dependent on the value of the other. Thus, we can include U and V wind components in our models directly as interaction terms and avoid any potential loss of information associated with calculating flow-assistance (e.g. arising from the assumption of a single preferred direction of migration). Hereafter, we refer to this smoothed interaction term composed of U and V wind components as *sWind*. Note that we tested several of the representations of wind profit described in Chapter 3 and found that *sWind* always resulted in more accurate predictions.

Following Erni et al. (2002b), we calculated rain duration (R_{dur}) in thirds for each day and night, describing the proportion of hours of the day or night that R was > 0 , and applied that value to all observations during the asso-

ciated day or night. Migration can be particularly intense following successive days/nights with unsupportive weather conditions (Richardson, 1990a). Therefore, again following Erni et al. (2002b), we calculated the potential accumulation of migrants due to previous days/nights with precipitation as $Racc_i = \frac{1}{3}Racc_{i-1} + \frac{2}{3}rain_{i-1}$ where $rain$ was set to zero for days/nights without rain ($Rdur = 0$) and one for days/nights with rain ($Rdur > 0$). Similarly, we calculated an accumulation effect due to successive days/nights with unsupportive wind conditions as $Wacc_i = \frac{1}{3}Wacc_{i-1} + \frac{2}{3}wind_{i-1}$ where $wind$ was set to zero for days/nights with supportive winds and one for days/nights with unsupportive winds. To define supportive and unsupportive winds, we used $EQ^{Tailwind}$ (see Section 3.3.1) with the preferred direction of migration set to the circular mean (Batschelet, 1981) of the measured tracks (i.e. $Bdir$) and calculated headings for the particular season, location, and time (i.e. diurnal or nocturnal). We considered wind conditions supportive if $EQ^{Tailwind} > -7$ during the first hour of the day or night and unsupportive if $EQ^{Tailwind} \leq -7$ during the first hour of the day or night. The threshold of -7 for acceptable winds was also taken from Erni et al. (2002b). We then calculated a combined cumulative effect of successive days/nights with rain or unsupportive winds as $RWacc_i = \frac{1}{3}RWacc_{i-1} + \frac{2}{3}wx_{i-1}$ where wx was set to zero for days/nights without rain and with supportive winds and one for days/nights with rain or unsupportive winds.

Richardson (1990a) noted that, in order to separate the effect of temperature from seasonal and diel effects on migration intensity, deviations from the average temperature for the time of day and year should be used rather than absolute temperatures. We therefore used the RNCEP package (see Chapter 2) to calculate climatological temperature normals using data from the National Centers for Environmental Prediction (NCEP)/ Department of Energy (DOE) Reanalysis II dataset (hereafter referred to as R-2; Kanamitsu et al., 2002). We obtained temperature data (K) from the R-2 grid point closest to the De Bilt and Den Helder radar sites (located at 52.5°N 5°E; see Figure 6.1) for the 1000 and 925 mb pressure levels in six-hour intervals from 1980-2010. Using the mean of the temperatures in the two pressure levels at each time step, we calculated temperature normals ($Tnorm$) per day of year and time of day using tensor product smooths (Wood, 2006). We calculated deviations from these normals as $T - Tnorm$ and refer to these deviations hereafter as $Tdev$.

6.3 Methods

Based on a quasi-Poisson distribution, we applied penalized likelihood fitting to estimate the smoothness of smoothed terms in our GAMs. Computations

were done in the R language (R Development Core Team, 2010) using the `gam()` function from the `mgcv` package (Wood, 2008). In all cases, we calibrated models for diurnal and nocturnal migration independently for each radar and season. Table 6.1 gives an overview of the predictor variables considered in these analyses.

Throughout these analyses, we refer to model ‘performance’, which was determined by 50-times repeated random-sampling cross-validation using 70% of data for calibration, leaving 30% for testing. A model’s performance was the mean absolute deviation (*MAD*) between the model predictions and the 30% of data set aside for testing averaged over all 50 cross-validation iterations.

6.3.1 Model development

Benchmark models

We developed four benchmark models and determined the performance of each. Benchmark models only contained variables to account for the time of day and year and autocorrelation and did not contain variables to account for atmospheric dynamics. One benchmark model contained only *sTime*; a second was composed of *sTime*+*iBd_h*; a third was composed of *sTime*+*iBd_d*; a fourth was composed of *sTime* + *iBd_h* + *iBd_d*.

Ensemble model development

From a base model containing only the variable *sTime*, we developed an ensemble of models in which one model was calibrated for each possible combination of predictor variables, considering up to five predictor variables (plus *sTime*) in any one model. Ultimately, these models were calibrated using all available data; however, we first determined the performance of each model according to our cross-validation procedure. Models with better performance (i.e. lower *MAD*) were given more weight in the resulting ensemble. The weight (*WGT*) of a prediction (*Pred*) for the *ith* model in the ensemble was defined as

$$WGT_i = \frac{MAD_{max} - MAD_i}{MAD_{max} - MAD_{min}}, \quad (6.2)$$

where *MAD_{max}* was the largest and *MAD_{min}* the smallest *MAD* value of any of the *n* models in the ensemble. An ensemble prediction (*Pred_E*) was then calculated as the weighted mean of the individual predictions of the *n* models in the ensemble as

$$Pred_E = \frac{\sum_{i=1}^n WGT_i \cdot Pred_i}{n}. \quad (6.3)$$

Table 6.1: Variables used to predict hourly migration intensity (iBd). The first column provides the abbreviated form of the variable used in the text; the second column indicates the units of the variable; and the third column provides a brief description of the variable.

Abbreviation	Units	Description
$sTime$	–	Smoothed interaction term composed of the day of the year (DOY) and the proportion of the day (P_{day}) or night (P_{night})
iBd_h	$\ln\left(\frac{\text{birds}}{\text{km}^2}\right)$	Mean iBd the previous hour
iBd_d	$\ln\left(\frac{\text{birds}}{\text{km}^2}\right)$	Mean iBd the previous day or night
$sWind$	ms^{-1}	Smoothed interaction term composed of U (east/west) and V (north/south) wind components
$Tdev$	K	Deviation from normal of the average temperature between 0.4 to 1 km
AP	mb	Average atmospheric pressure between 0.4 to 1 km
RH	%	Average relative humidity between 0.4 to 1 km
ΔT	K	24-hour change in temperature
ΔAP	mb	24-hour change in AP
ΔRH	%	24-hour change in RH
R	mm	Precipitation amount
$Rdur$	thirds	Duration of precipitation over a day or night
$Racc$	–	Accumulation of migrants due to precipitation
$Wacc$	–	Accumulation of migrants due to unsupportive winds
$RWacc$	–	Accumulation due to precipitation or unsupportive winds

We indicated the performance of the baseline models, the weighted ensemble, and the range of performances of the individual models in the ensemble. As well, we indicated the performance of the ensemble after removing models containing iBd_h and the performance of the ensemble after removing models containing iBd_h and/or iBd_d . This was done to show the performance of the ensemble at forecast distances greater than one hour (but less than one day) and greater than one day, respectively.

6.3.2 Models for one location applied to the other

As mentioned, van Belle et al. (2007) found that models for one location did not predict well at a different location; however, the comparisons made in that study considered locations quite removed from one another (i.e. predictions for the Netherlands were made using models developed for southern Germany, Denmark, and southern Sweden). As well, the predictor and response variables were not necessarily consistent between the sites. Migration intensity was measured according to different methods using different devices (e.g. infrared device, pencil-beam radar, military surveillance radar), and meteorological variables were obtained from different sources. We have made bird density measurements in a consistent manner using two radars that are very similar to one another and not so far removed from one another in space (~ 98 km). As well, we have obtained meteorological predictor variables for each site from the same data set. Because our study differed in these aspects from the study of van Belle et al. (2007), it was informative to apply our baseline and ensemble models, calibrated using data from one radar site, toward the prediction of migration intensity at the other radar site. We indicated all permutations of model performance (i.e. baseline, individual models, ensemble, ensemble without models containing iBd_h , and ensemble without models containing iBd_h and/or iBd_d) for models calibrated to one location and used to predict intensity at the alternative location.

6.4 Results

6.4.1 Migratory dynamics and predictor variables

Time series of migration intensity, temperature (T), tailwind assistance according to EQ^{Tailwind}, and precipitation (R) are shown in Figure 6.2 for De Bilt and Den Helder. Migration was generally more intense at De Bilt than Den Helder, but at both locations intense migration was the exception rather than the norm. Temperatures were slightly cooler in spring compared to autumn but were rarely below freezing at either site. Winds were more frequently

supportive in spring than autumn. Note also that tailwind support oscillated strongly at Den Helder in autumn.

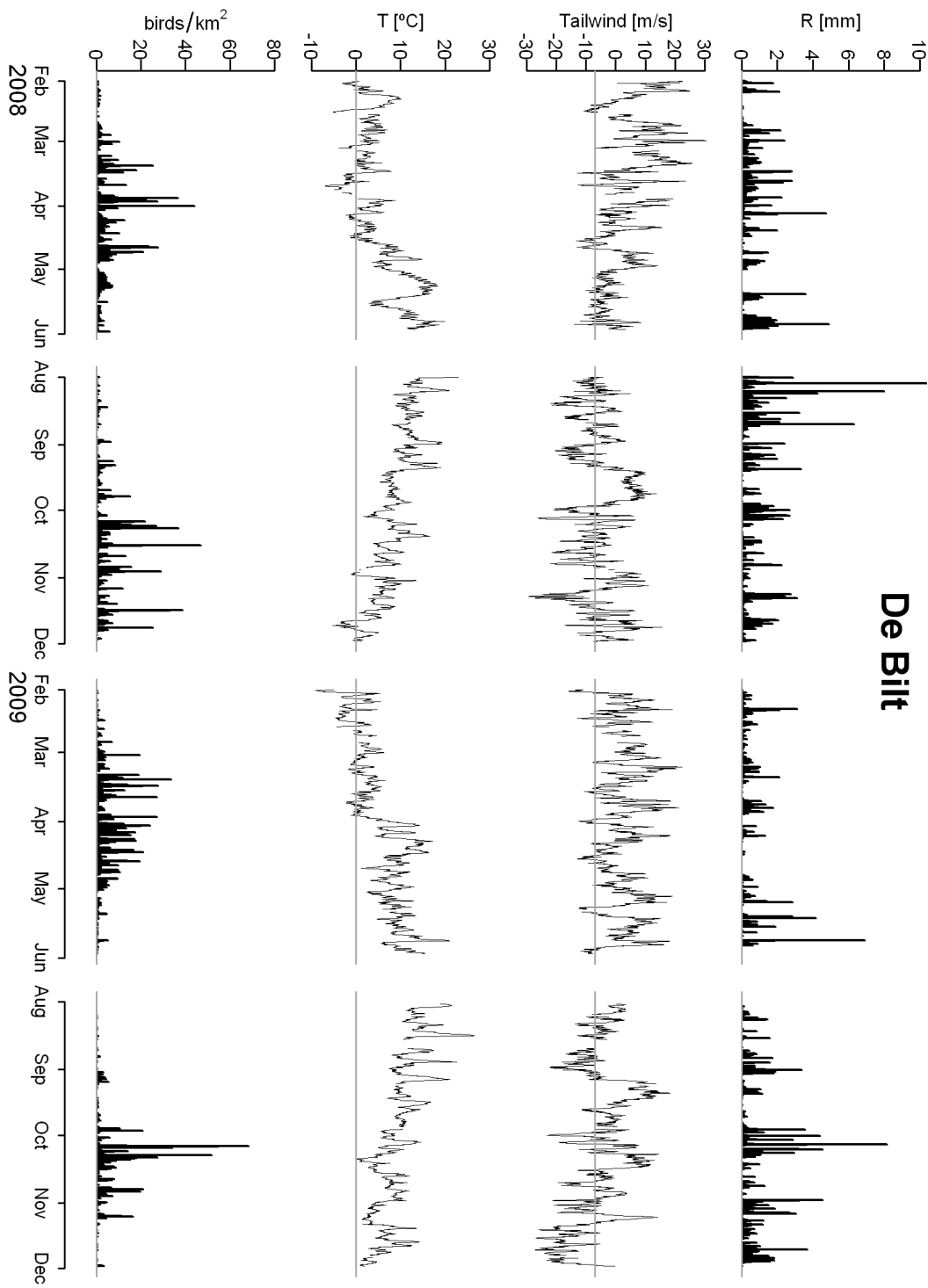
Circular frequency distributions of the measured tracks and calculated headings from De Bilt and Den Helder are shown in Figure 6.3. The circular mean of these tracks and headings, also indicated in Figure 6.3, was used to classify winds as either supportive or unsupportive according to $EQ^{Tailwind}$. This circular mean is quite representative in most cases; however, in Den Helder during spring diurnal and autumn nocturnal migration there are two rather distinct groups of track directions (apparent from the bimodal distributions in Figure 6.3) with the circular mean falling between the two. This may somewhat confound the calculation of $Wacc$ and $RWacc$ in these cases. Recall that tailwind support oscillated strongly at Den Helder in autumn (see Figure 6.2). This was probably not due to rapid changes in wind condition but to the different preferred directions used to calculate tailwind support between day and night (see Figure 6.3).

6.4.2 Baseline intensity

The functional relationship of the baseline intensity variable (*sTime*) to migration intensity is shown in Figures 6.4 and 6.5 for De Bilt and Den Helder, respectively. *sTime* was included in all models by default. The performance of all models (including models containing only the variable *sTime*) are indicated in Figures 6.7 and 6.8 and plots of measured against predicted migration intensity are shown in Figures 6.9 and 6.10 for De Bilt and Den Helder, respectively. Although models were calibrated independently for diurnal/nocturnal and spring/autumn migration, the baseline intensity rather smoothly transitioned from one model to the next (apparent from the general seamlessness of the contours between the plots in Figures 6.4 and 6.5). Nocturnal migration in spring was generally most intense during April at both locations, and nocturnal migration in autumn was most intense around mid-October in De Bilt but closer to the first of November at Den Helder. At both locations, nocturnal migration was more concentrated to a particular part of the season during autumn compared to spring. The most intense diurnal migration tended to occur near sunrise; however, this may very well reflect the end of nocturnal migration rather than the beginning of diurnal migration.

6.4.3 Autocorrelation in migration intensity

Plots indicating autocorrelation in *iBd* measurements to a lag of one week are shown in Figure 6.6 for both radar sites. The *iBd* measurements were positively autocorrelated at lags of one hour and one day in all cases, so our



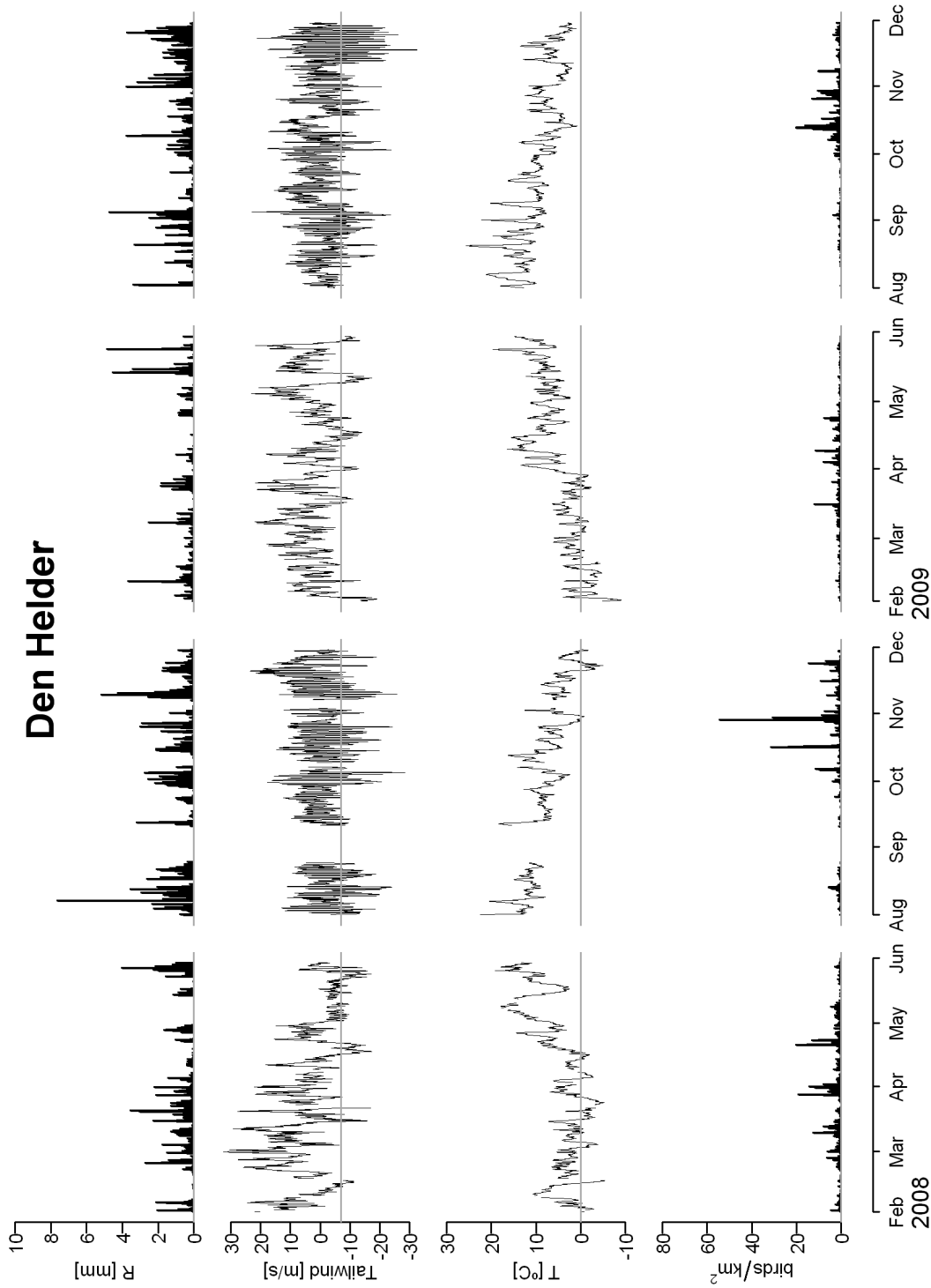


Figure 6.2 (previous two pages): Time series plots for De Bilt (first) and Den Helder (second) indicating (from top to bottom) precipitation (R), tailwind assistance, temperature (T), and migration intensity. For plots of tailwind assistance, a horizontal gray line at -7 indicates the transition between winds considered supportive and unsupportive. In all other plots, this horizontal gray line indicates a value of zero.

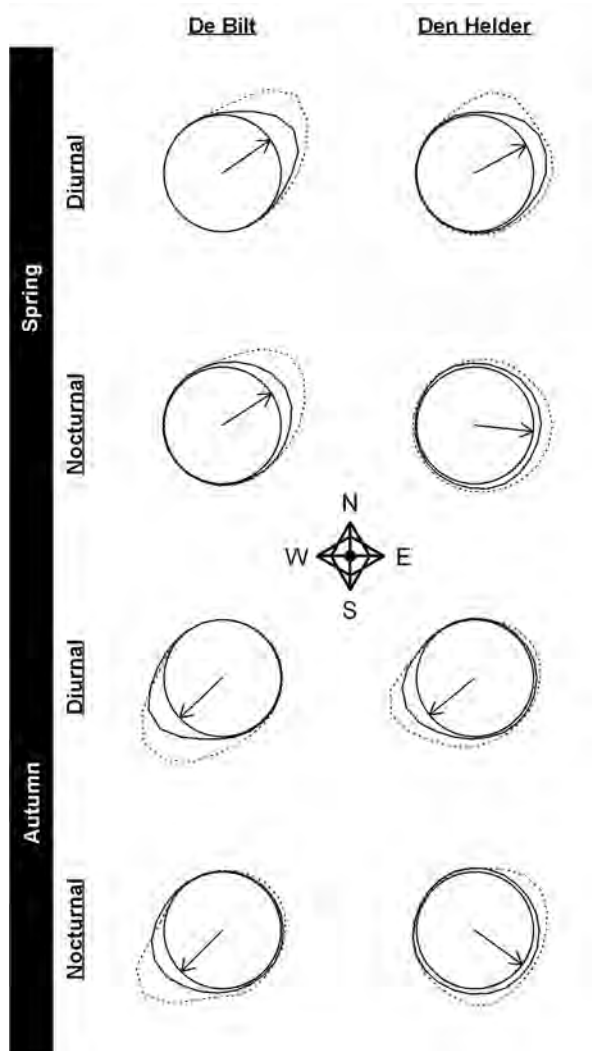


Figure 6.3: Circular frequency distributions of measured track directions (dashed lines) and calculated headings (solid lines) that were associated with airspeeds determined to be between 7 and 25 ms^{-1} . An arrow in each plot indicates the circular mean of the tracks and headings, which was used to calculate $\text{EQ}^{\text{Tailwind}}$ and determine whether wind conditions were supportive or unsupportive. A compass in the center of the figure indicates direction.

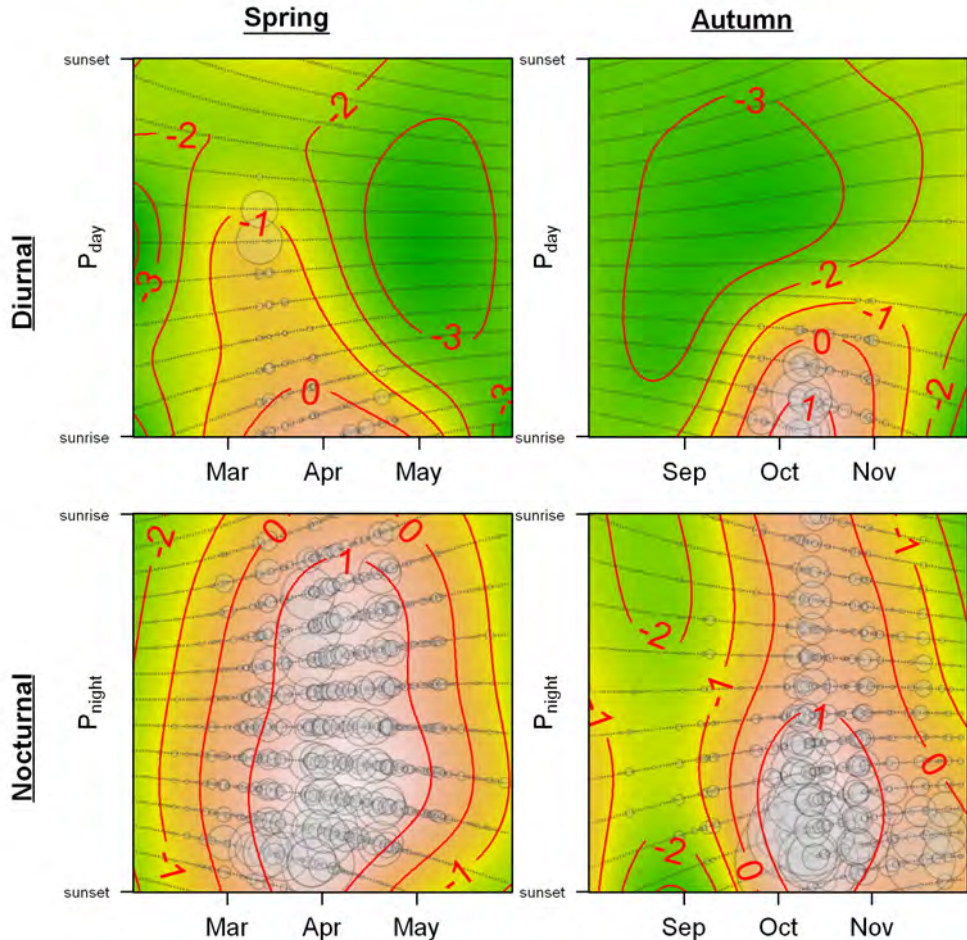


Figure 6.4: Plots illustrating the functional form (i.e. partial contribution) of the baseline intensity variable ($sTime$) in models of migration intensity in De Bilt. Spring conditions are shown in the left column, and autumn conditions are shown on the right. Diurnal migration is shown in the top row and nocturnal migration in the bottom. $sTime$ is represented as a smoothed interaction between the day of the year (DOY) along the x-axis and the fraction of the day (P_{day}) or night (P_{night}) relative to sunrise and sunset along the y-axis. Colors and contours indicate predicted migration intensity on the scale of the linear predictor. Predictions on the scale of the response variable (i.e. iBd) can be obtained by summing the partial contributions of all predictor variables in a model (in this case only $sTime$) and then applying the exponential function. Semi-transparent circles indicate iBd measurements and their size reflects the value of iBd .

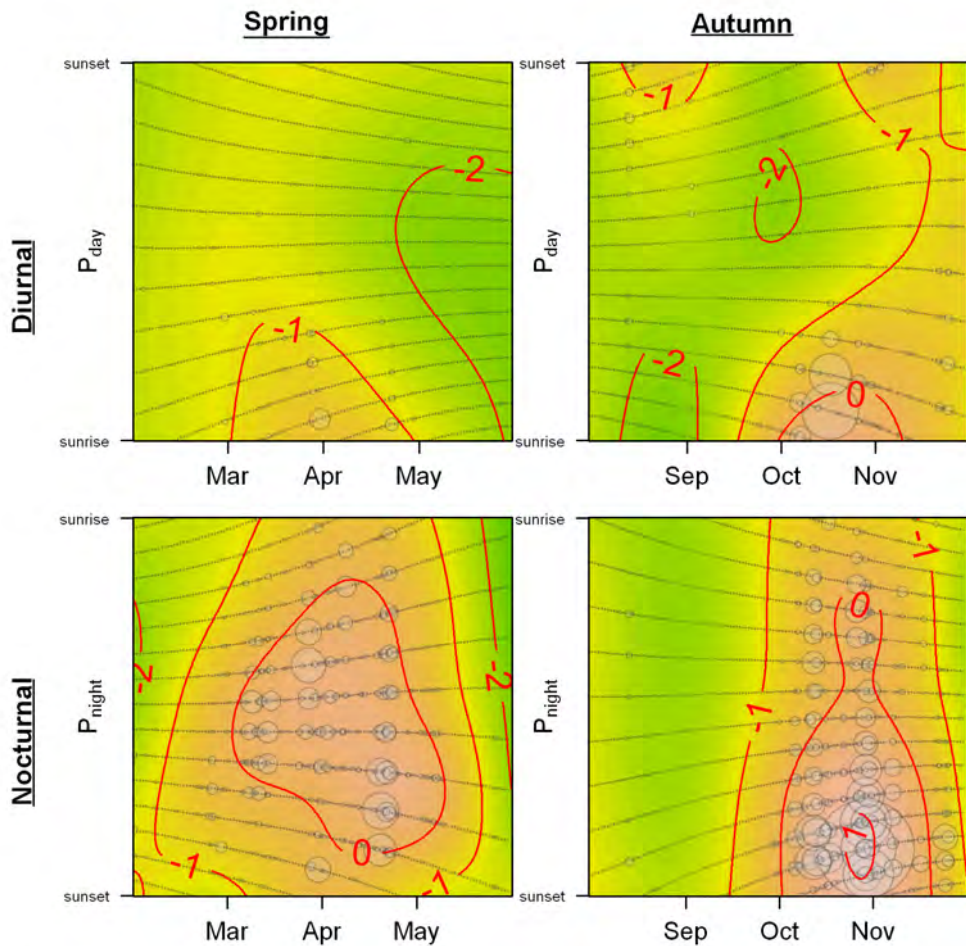


Figure 6.5: Plots illustrating the functional form (i.e. partial contribution) of the baseline intensity variable $sTime$ in models of migration intensity in Den Helder. Spring conditions are shown in the left column, and autumn conditions are shown on the right. Diurnal migration is shown in the top row and nocturnal migration in the bottom. $sTime$ is represented as a smoothed interaction between the day of the year (DOY) along the x-axis and the fraction of the day (P_{day}) or night (P_{night}) relative to sunrise and sunset along the y-axis. Colors and contours indicate predicted migration intensity on the scale of the linear predictor. Predictions on the scale of the response variable (i.e. iBd) can be obtained by summing the partial contributions of all predictor variables in a model (in this case only $sTime$) and then applying the exponential function. Semi-transparent circles indicate iBd measurements and their size reflects the value of iBd .

variables meant to capture autocorrelation (i.e. iBd_h and iBd_d) should be useful predictors of future migration intensity. In spring, migration intensity oscillated between being autocorrelated and not being autocorrelated through the one-day lag; whereas in autumn, migration intensity was positively autocorrelated (to greater and lesser degree) throughout the one-day lag. At De Bilt in fact, there was a peak in autocorrelation at a lag of 12-hours suggesting that migration intensity 12-hours previous was just as indicative of current migration intensity as migration intensity 24-hours previous. Thus, when migration was intense in autumn, it was intense during both the day and the night. In spring, however, diurnal and nocturnal migration occurred independently. The performance of all models (including models containing the variables iBd_h and iBd_d) are indicated in Figures 6.7 and 6.8 and plots of measured against predicted migration intensity are shown in Figures 6.9 and 6.10 for De Bilt and Den Helder, respectively.

6.4.4 Model performance

In Figure 6.7, the performance of our benchmark and ensemble models for De Bilt are shown alongside the performance of models applied to De Bilt that were calibrated for Den Helder. Similarly in Figure 6.8, the performance of our benchmark and ensemble models for Den Helder are shown alongside the performance of models applied to Den Helder that were calibrated for De Bilt. In both cases, we have indicated the range of performances of the individual models making up the ensemble and the weighted mean performance of the ensemble as a whole. The ensemble system was composed in total of 3473 unique models; however, 1093 models contained the variable iBd_h and were therefore only available to make forecasts one hour in advance. An additional 794 models contained iBd_d and were only available to make forecasts one day in advance. Therefore, we have also indicated the weighted mean performance of the ensemble at forecast distances greater than one hour (but less than one day) and at forecast distances greater than one day. The ensembles (at all forecast distances) generally performed better than the benchmarks composed of either $sTime$ alone or $sTime + iBd_d$, and these two benchmark models performed similarly to one another. The best model in the ensemble was generally the benchmark model composed of $sTime + iBd_h$; however, in some cases other individual models in the ensemble performed slightly better (e.g. during autumn nocturnal migration at De Bilt, see Figure 6.7). The benchmark model composed of $sTime + iBd_d + iBd_h$ also performed quite well, but it seemed that including iBd_d did little, if anything, to improve the performance of the $sTime + iBd_h$ model. Note that for nocturnal migration in spring at De Bilt (see Figure 6.7), the weighted mean performances of the

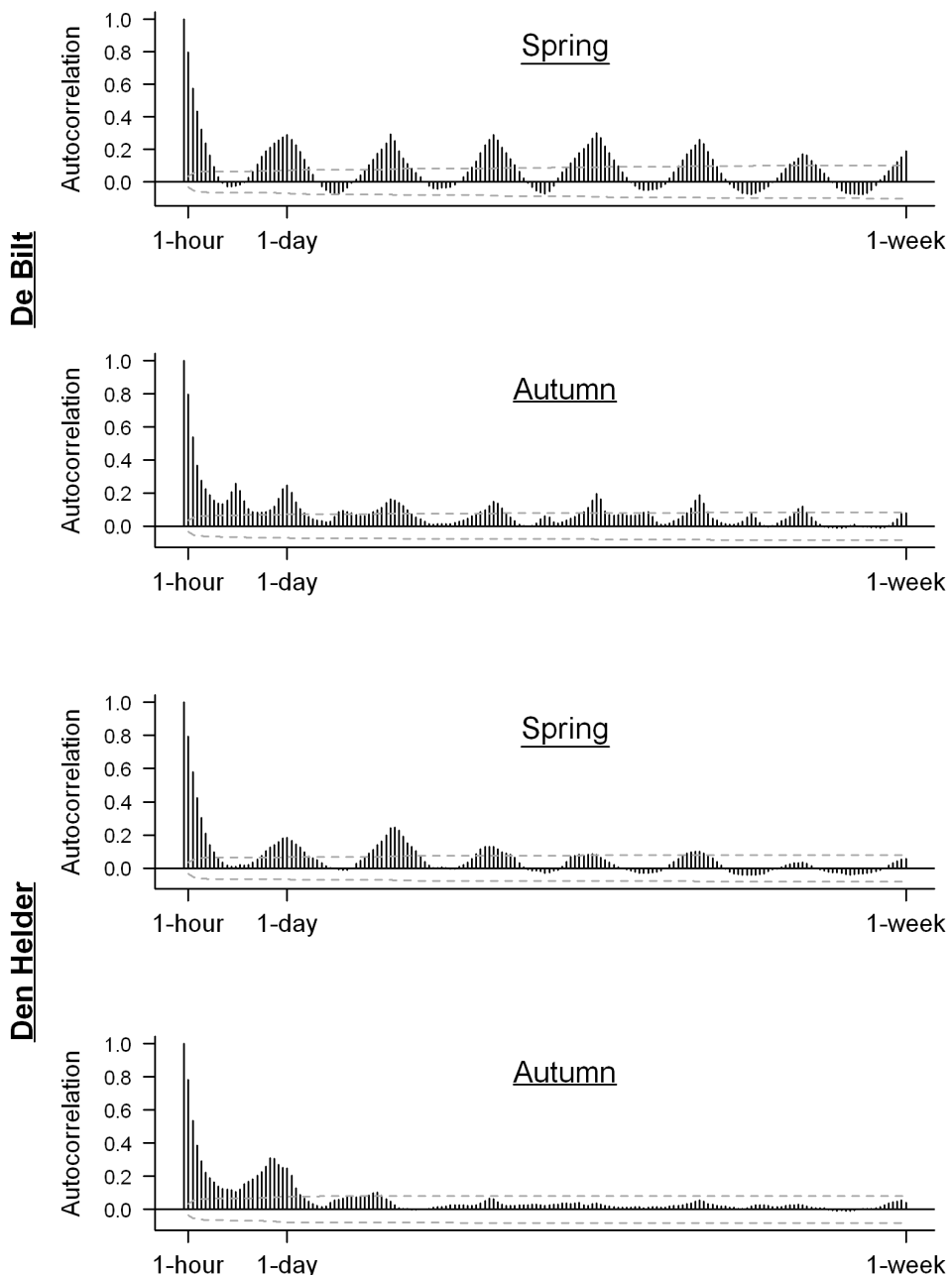


Figure 6.6 (previous page): Plots indicating autocorrelation in iBd measurements to a lag of one week at De Bilt (top two) and Den Helder (bottom two). Spring and autumn are shown separately for each radar. Dashed gray horizontal lines indicate the 99% confidence interval.

ensemble at all forecast distances were not visible. In this case, there were a few models that performed extremely poorly, which drove the weighted average performances beyond the range of values we showed in the plot. See the Discussion in Section 6.5 for more details.

Models calibrated to data from the alternative radar site performed worse than models calibrated for the actual site; however, in several cases these “alternative-site” models performed rather well. At De Bilt the alternative-site models performed only slightly worse than the actual-site models, but at Den Helder the alternative-site models were quite a bit worse than the actual-site models.

The magnitude of the MAD values appeared to show a strong dependence on the range of measured values, so absolute comparisons of the MAD values between sites and times should be made with caution. For example, one should not necessarily make the conclusion from Figures 6.7 and 6.8 that models of diurnal migration were better than models of autumnal migration even though MAD values were lower during the day compared to the night, because measured bird densities were also much smaller during the day compared to the night.

In Figures 6.9 and 6.10, we have plotted measured against predicted bird densities for De Bilt and Den Helder, respectively. In these plots, we show the predictions of two benchmark models, the full ensemble, the ensemble at a forecast distance greater than one hour (but less than one day), and the ensemble at a forecast distance greater than one day. All model permutations had a better fit to the data than the benchmark model containing the baseline intensity (i.e. $sTime$) only. In all cases, these models predicted the low intensity migration quite well but had difficulty predicting the few very intense migration events. Specifically, the models tended to underpredict the most intense migration events, and this occurred particularly when models did not contain iBd_h .

Figure 6.7: The performance (i.e. mean absolute deviation or *MAD*) of models of hourly migration intensity for De Bilt are shown. The performance of these “actual-site” models was determined by 50-times repeated random sampling cross-validation. The performance of models calibrated for Den Helder and then used to predict at De Bilt (i.e. “alternative-site” models) is also shown. In both cases, the units of *MAD* are *birds/km³*. White box plots and symbols indicate the performance of the actual-site models, gray box plots and symbols indicate the performance of the alternative-site models, and a dashed line separates the two. The ranges of performance of the individual models in an ensemble are shown as box plots distinguishing the median, inter-quartile range, one and a half-times the inter-quartile range beyond the quartiles, and outliers. Superimposed atop these box plots are the weighted mean performances of the full ensemble, the ensemble at forecast distances greater than one hour, and the ensemble at forecast distances greater than one day. Along the bottom of each box plot are the individual performances of the four benchmark models. A legend indicates the model that is represented by each symbol.

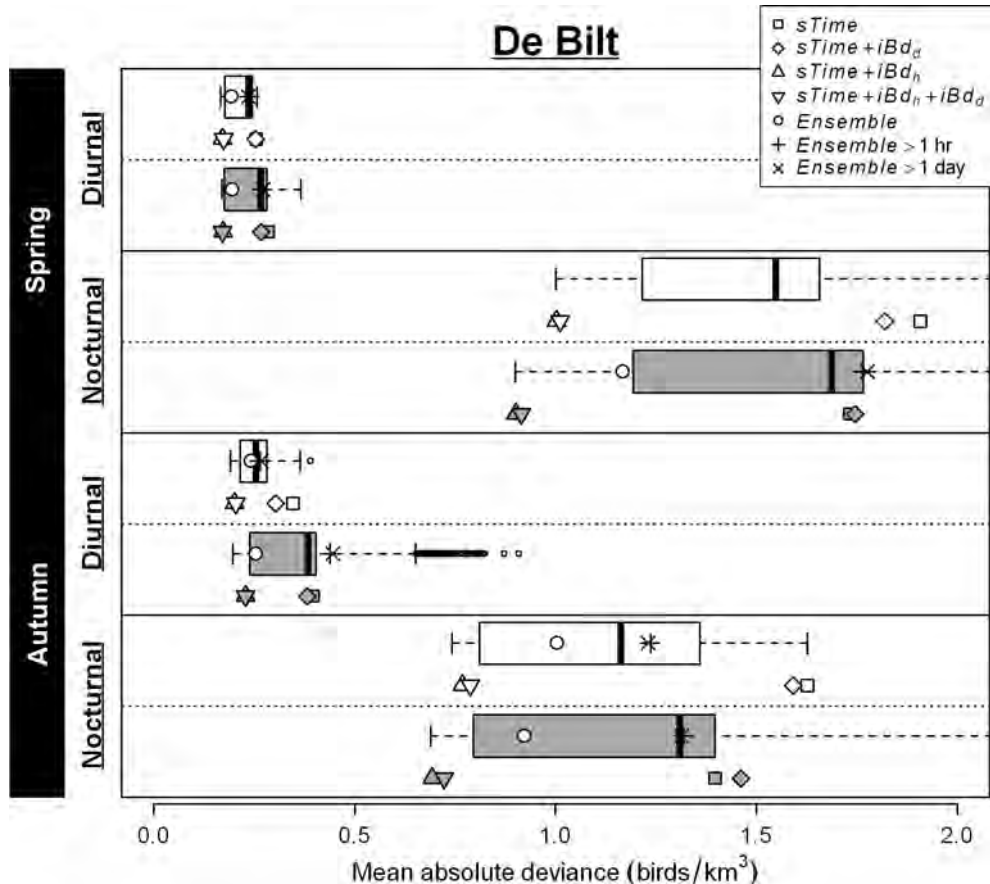
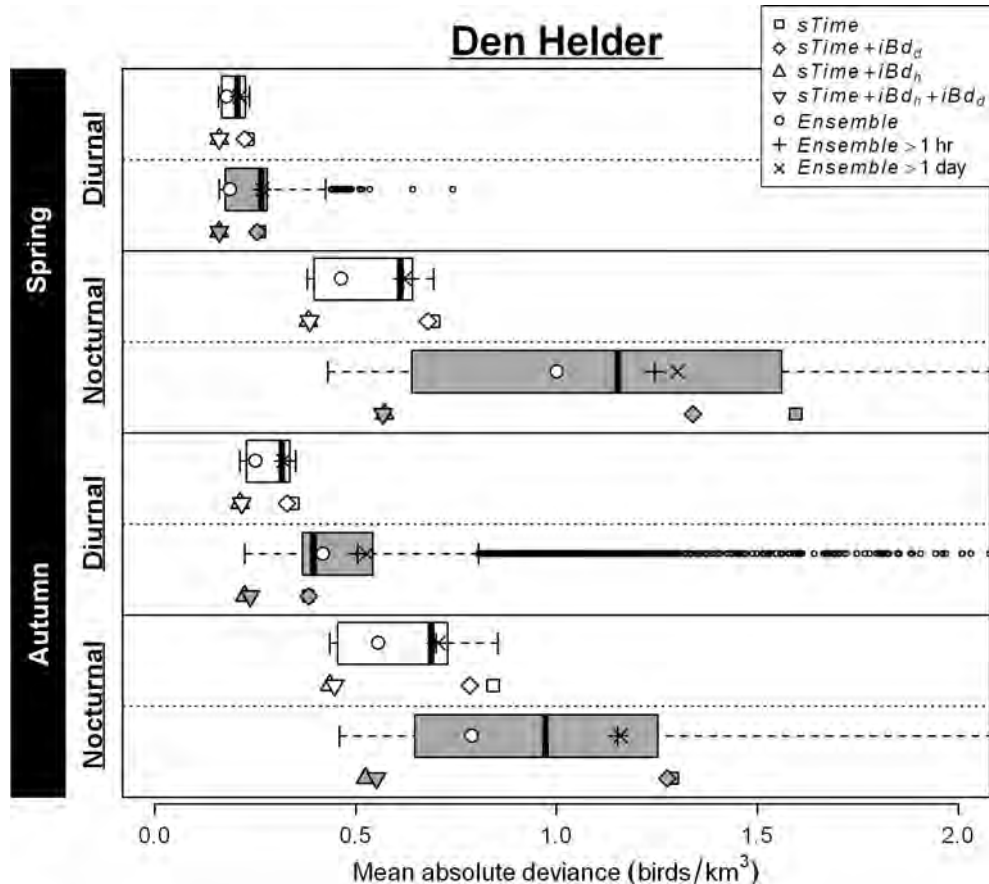


Figure 6.8: The performance (i.e. mean absolute deviation or *MAD*) of models of hourly migration intensity for Den Helder are shown. The performance of these “actual-site” models was determined by 50-times repeated random sampling cross-validation. The performance of models calibrated for De Bilt and then used to predict at Den Helder (i.e. “alternative-site” models) is also shown. In both cases, the units of *MAD* are *birds/km³*. White box plots and symbols indicate the performance of the actual-site models, gray box plots and symbols indicate the performance of the alternative-site models, and a dashed line separates the two. The ranges of performance of the individual models in an ensemble are shown as box plots distinguishing the median, inter-quartile range, one and a half-times the inter-quartile range beyond the quartiles, and outliers. Superimposed atop these box plots are the weighted mean performances of the full ensemble, the ensemble at forecast distances greater than one hour, and the ensemble at forecast distances greater than one day. Along the bottom of each box plot are the individual performances of the four benchmark models. A legend indicates the model that is represented by each symbol.



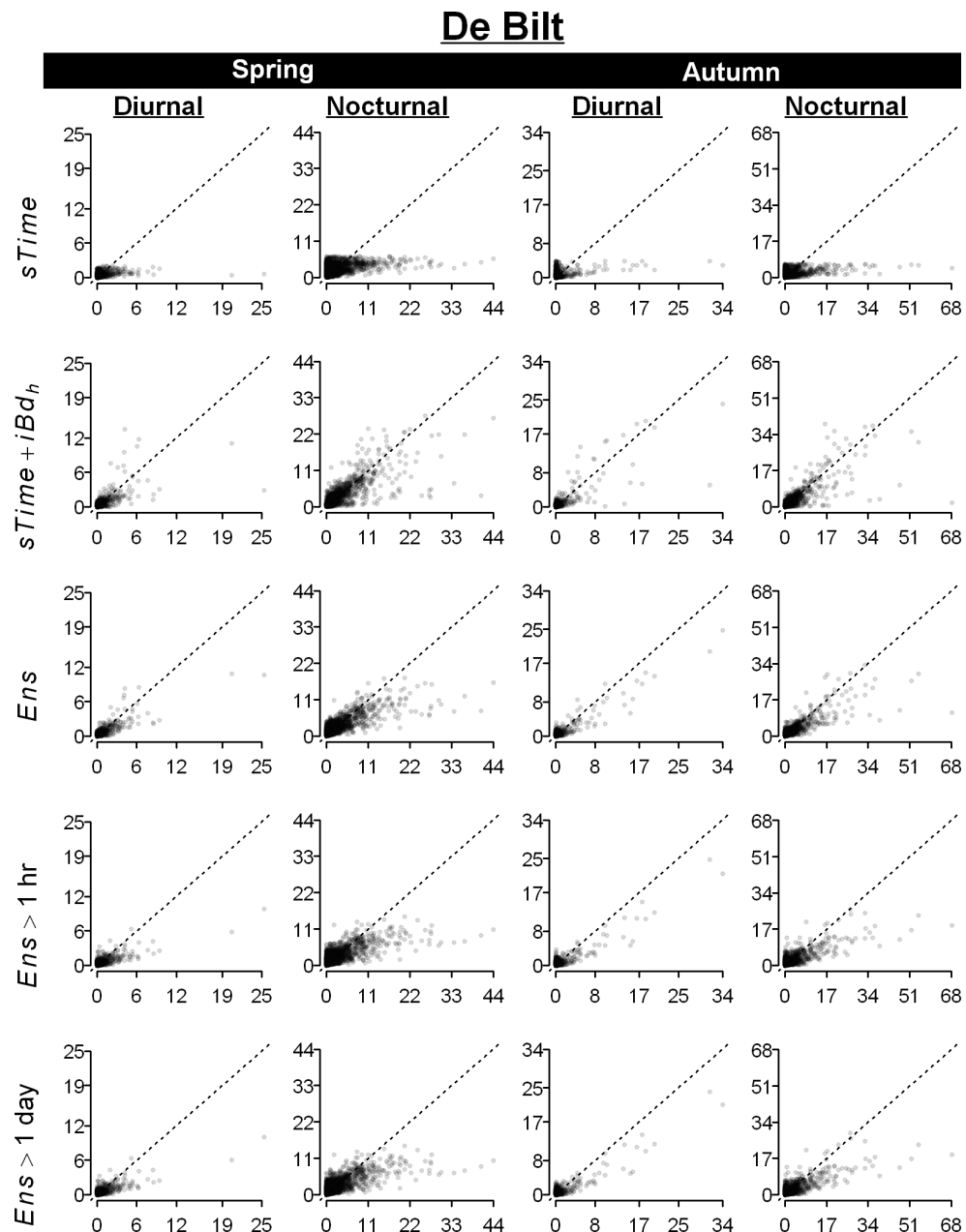


Figure 6.9 (previous page): Scatter plots of predicted and measured bird densities for De Bilt are shown. Measured bird densities are always indicated along the x-axis and predicted densities along the y-axis, both in units of birds/km^3 . Points are semi-transparent, so darkness indicates point density. A dashed diagonal line indicates a theoretical perfect positive relationship. Plots in the same column of the figure are from the same season and time (i.e. diurnal or nocturnal) and their axes are scaled similarly. Plots in the same row of the figure indicate a particular model. From top to bottom, the models are the benchmark model containing the baseline variable $sTime$, the benchmark model composed of $sTime$ and iBd_h , the full ensemble, the ensemble at a forecast distance greater than one hour, and the ensemble at a forecast distance greater than one day.

6.5 Discussion

6.5.1 Model development

General considerations

A model containing only the baseline intensity variable ($sTime$) was able to explain a large amount of variability in iBd and performed better than some of the other models in the ensemble that contained more variables. If weather data and measurements of bird density were unavailable for some reason, the $sTime$ model could be used to give a general indication of the intensity of migration based only on the day of the year and the time of the day. Models that incorporated weather conditions generally performed better than the $sTime$ model, however, and also performed better than the benchmark model containing $sTime + iBd_d$, suggesting that migration intensity on a given day was better predicted by forecasted weather conditions than by migration intensity measured the previous day. Nonetheless, models that incorporated iBd_h performed better still. This is perhaps to be expected, since iBd_h reflects explicitly the migratory decisions birds in the area have already made. The relationships we uncover between migration intensity and environmental variables are informative, but we may never be able to account for all of the processes that have influence on migratory decisions at a given time and location. Currently, for instance, we cannot account for environmental conditions encountered earlier in the migratory journey that may have influenced current migratory decisions.

Clearly, using previous measurements of migration intensity can improve predictive models of future migration intensity; however, very recent measurements (i.e. iBd_h) improved predictions much more than older measurements (i.e. iBd_d). Regardless, an advantage of the use of weather radar (as opposed to military radar or dedicated bird-tracking radar, for example) is that data from weather radar are needed and valuable in many contexts, so a great deal

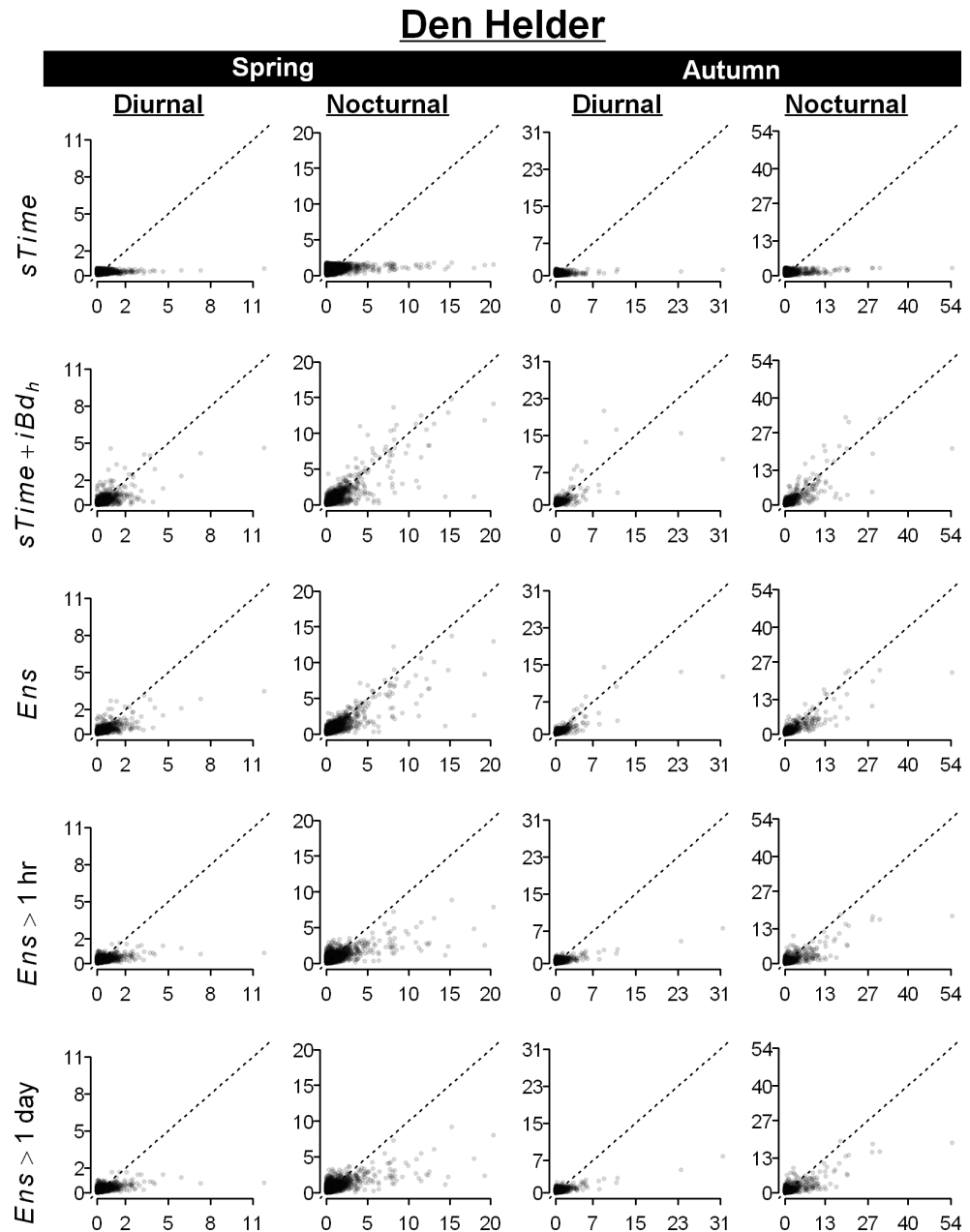


Figure 6.10 (previous page): Scatter plots of predicted and measured bird densities for Den Helder are shown. Measured bird densities are always indicated along the x-axis and predicted densities along the y-axis, both in units of birds/km³. Points are semi-transparent, so darkness indicates point density. A dashed diagonal line indicates a theoretical perfect positive relationship. Plots in the same column of the figure are from the same season and time (i.e. diurnal or nocturnal) and their axes are scaled similarly. Plots in the same row of the figure indicate a particular model. From top to bottom, the models are the benchmark model containing the baseline variable *sTime*, the benchmark model composed of *sTime* and *iBd_h*, the full ensemble, the ensemble at a forecast distance greater than one hour, and the ensemble at a forecast distance greater than one day.

of effort is put toward having these radars continuously operational. Thus, we can be relatively certain that previous measurements of migration intensity will be available for input into these models. Unfortunately, *iBd_h* is only available for forecast distances of one hour, which limits the operational applicability of models in the ensemble that contain this variable. Perhaps the two-hours-previous *iBd* measurement, which would be available for forecast distances of two hours, would also improve model performance. This seems plausible, since the autocorrelation plot in Figure 6.6 suggests a strong correlation still at a lag of two-hours.

In accordance with the findings of van Belle et al. (2007), models in our study calibrated for a particular location performed better at that location than models applied to that location that were calibrated elsewhere. The distance between our two radar sites was not that great (~ 98 km), but the different positions of these two sites (perhaps relative to the coast) seemed to result in different migratory dynamics (see e.g. Figures 6.2 and 6.2 as well as Figure 6.3). Nonetheless, the performance in this study of models used in one location that were calibrated for an alternative location is encouraging, as in many cases these models still performed rather well (particularly when the variable *iBd_h* was included in the models). Naturally, areas covered by a weather radar should have ensemble models calibrated explicitly for their location; however, there are (and will likely continue to be) spatial gaps in radar coverage within which models cannot be explicitly calibrated. Our results suggest that models from nearby locations may be useful in filling these spatial gaps. Predictions for these gaps could be made using local environmental conditions as input into an ensemble prediction system calibrated for a nearby location. Alternatively, the predictions from models for several nearby locations could be spatially interpolated to fill these gaps. In either case, the more sensors with individual predictive models that are available, the more accurate information we will have to fill these gaps. For instance,

a large network of sensors will be useful in determining the spatial range in which measurements (and similarly predictions) are valid by allowing for the calculation of spatial autocorrelation. As well, such a network would allow for the use of modern spatial interpolation techniques such as kriging (cf. Hengl et al., 2007). Kriging would not only allow us to create a contiguous predictive surface over the spatial range of available sensors, potentially incorporating underlying landscape types as explanatory variables, it would enable the identification of particular geographic areas where the interpolation was less reliable. These aspects of kriging may be particularly beneficial since the distances over which measurements (and therefore predictions) are valid likely depend on particular features in an area such as the sizes and positions of large water bodies and/or mountains (cf. Åkesson et al., 1996; Bruderer and Liechti, 1998; Fortin et al., 1999). A further possibility to consider in filling gaps between sensors may be to use simulation models such as the FLAT model introduced in Chapter 3 to propagate birds measured in one location through space to other locations. When birds are observed by radar leaving the southern tip of Norway, for example, the FLAT model could simulate the birds' continued movement through space to indicate when and where they will likely arrive on Great Britain or the European mainland. This approach has shown promise in previous research (Shamoun-Baranes and van Gasteren, 2011).

Our analyses were conducted using two autumn and two spring migration seasons. van Belle et al. (2007) determined that the longer the time series used to calibrate predictive models of bird migration, the more robust and accurate are the resulting models. The time series used in this study likely represent the minimum amount of data upon which the calibration of models is feasible. Models will certainly be more robust when calibrated in areas with longer time series of data. Furthermore, as more data become available for a particular location, the ensemble modeling system can (and likely should) be re-calibrated incorporating all available data. The model-development framework we have outlined can be used to ensure that the recalibration of these models is done efficiently and consistently.

Unique considerations

The model development procedure we have described is flexible enough to incorporate more predictor variables. Therefore, when developing models of migration intensity, predictor variables other than the ones mentioned here may be incorporated that reflect location-specific relationships between environmental conditions and migration intensity uncovered in previous research in the area. Regardless of whether more variables are included or not, how-

ever, issues are likely to arise during model development that are unique to the time period, location, and/or data set considered. These issues may require unique considerations or adjustments to the general modeling procedure outlined thus far. In this section, we discuss some of the issues that arose as we developed models for De Bilt and Den Helder and suggest potential approaches for dealing with these issues.

For nocturnal migration in spring at De Bilt, there were a few models that performed exceptionally poorly. While the median *MAD* value of the models in the ensemble was 1.55, a few models had *MAD* values in the hundreds, and the worst of these models had an *MAD* value of 2703. These poorly performing models resulted in the weighted average performance of the entire ensemble being 2.44, therefore just outside the viewing area of the plot in Figure 6.7. GAMs can produce biased estimates near the edges of a domain or “edge effects” that are associated with higher-dimensional smoothing (see Webster et al., 2006, citing Hastie and Tibshirani, 1990), which can result in large errors when predictions are made from the edges of these domains. There are several options for dealing with a subset of the ensemble that performs much worse than the rest. One option is to allow the models to remain in the ensemble. The models are weighted in the ensemble according to their performance, so poorly performing models carry less weight in the overall predictions. However, when some models perform very poorly, models that perform moderately poorly will perhaps carry more weight in the ensemble than is desirable. Another straight-forward option is to remove all models from the ensemble with performances that are considered to be outliers from the performance of the rest of the models in the ensemble. In our case, for example, we could remove all models from the ensemble with *MAD* values that were larger than one-and-a-half times the inter-quartile range beyond the upper-quartile, which is an approach that could be automated and kept consistent. For nocturnal migration in spring at De Bilt, applying this procedure would have resulted in the removal of 262 models with *MAD* values greater than 2.32. Still another option is to identify the variable that is causing the problems and limit the amount of smoothing that the GAM fitting procedure is allowed to apply to the variable. We found, for instance, that all of the models exhibiting this abysmal performance contained the variable *prcp*. After identifying the troublesome variable and restricting the amount of smoothing allowed, the performance of all models containing that variable must be recalculated in order to determine their new weight in the ensemble. This approach would likely require manual intervention into the model-development procedure.

Variables that need to be set per site can be problematic and require sufficient data and perhaps also knowledge of the migratory dynamics in an

area. Therefore, a potential limitation on the exportability of the model-development procedure we have outlined is in the calculation of the accumulation variables, particularly $Wacc$ and $RWacc$. While the methods we have applied to calculate these accumulations is exportable, the settings of particular parameters may be more or less applicable depending on the migratory dynamics of a particular time and location. In our analysis, the preferred direction of migration we determined was representative of the distributions of tracks and headings in most cases; however, at Den Helder during spring diurnal and autumn nocturnal migration there appeared to be two distinct groups or ‘cohorts’ exhibiting different track directions (see Figure 6.3). The circular mean of the tracks and headings at these times fell between the two cohorts, and, therefore, the preferred migratory direction assumed in these cases was not explicitly representative of either cohort. While the two cohorts were not separated by 180° such that all supportive winds for one cohort were prohibitive for the other and vice versa, some wind conditions supportive of one cohort were probably prohibitive for the other and vice versa. In locations where this is an issue, it may be beneficial to calculate an accumulation due to wind for each cohort individually, each based on a preferred direction of migration calculated according to the circular mean of the tracks and headings of a particular cohort. Another potential issue is the threshold at which winds are considered supportive or unsupportive, which was set to $EQ^{Tailwind} = -7$ in our analyses. We observed a step-change in iBd values when they were plotted against wind support according to $EQ^{Tailwind}$ (not shown), and this step-change occurred near a value of -7, but this value may not be representative in other locations. It is therefore advisable to plot iBd against wind support for a location to determine an appropriate threshold. Regardless, accumulation due to successive days of bad weather remains difficult to capture in models and is likely influenced by conditions encountered earlier in the migratory journey and ‘upstream’ of the measurement location. An integrated network of sensors should be beneficial in this context as information from upstream radars can be incorporated into downstream models.

6.5.2 Flight safety

A primary use of the models developed in these analyses was to forecast migration intensity for flight safety. In the models that resulted from this procedure, small and medium intensity migration (which comprise the majority of measurements) are predicted quite well (see Figures 6.9 and 6.10); however, the very infrequent instances of intense migration are not well-predicted. Specifically in the context of flight safety, where the peak migration events are quite important, it may be beneficial to add additional weight during model calibra-

tion to observations exhibiting more intense migration, and we explored the possibility of doing so in our analyses. We found that the peaks were better represented in the resulting models, since the weighting procedure resulted in response variables that were parameterized to fit the peaks of the calibration data set very well; however, it is questionable whether or not these peaks will occur under similar conditions in subsequent years. For example, in order to compensate for the few intense (but very influential, due to the weighting) bird density measurements, the functional form of the baseline intensity variable (*sTime*; shown in Figures 6.4 and 6.5) becomes very distorted. It is unlikely that migration will be intense on precisely the same day and time the following year because (among other things) the atmospheric conditions will likely be quite different. The functional forms of the other variables in the models are likely to be similarly distorted in ways that are not representative of their actual influence on migration intensity. This method of weighting more intense migration events in the calibration of models may become more feasible as more data become available and intense migration can be observed to occur (and not occur) through a more representative range of the domains of each predictor variable.

Until more data are available, a temporary solution may be to merge the weighted and unweighted models into a single ensemble system. The models developed without weighting perform well and accurately reflect the majority of the data. The models developed with weighting applied in proportion to the intensity of migration better capture the peak migration events. Thus, an optimal solution may be a hybrid of the weighted and unweighted model ensembles. A potential method to merge the two ensembles would be to make a prediction by each individually, determine the average of those predictions, and use this average to determine how much influence the weighted and unweighted ensembles should be given in the final prediction. The lower the average, the more influence given to the unweighted models; the higher the average, the more influence given to the weighted models. Figure 6.11 illustrates this concept. The influence of the predictions from the weighted model ensemble can be calculated as

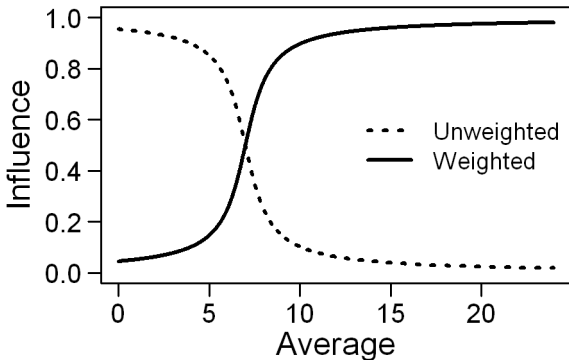
$$\frac{\tan^{-1}(a \cdot x - a \cdot b)}{\pi} + 0.5, \quad (6.4)$$

and the influence of the predictions from the unweighted model ensemble can be calculated as

$$1 - \frac{\tan^{-1}(a \cdot x - a \cdot b)}{\pi} + 0.5 \quad (6.5)$$

where x indicates the average of the predictions of the weighted and un-

Figure 6.11: This figure illustrates the concept of predictions being based on the influence of two ensemble systems: one with weighting applied in the calibration process to better represent very intense migration and one without weighting applied in the calibration process to better represent the smaller (and more frequently occurring) bird densities. When the average of the predictions of the two ensembles is small, the final prediction is based on the unweighted model ensemble. As the average prediction of the two ensemble systems increases, the final prediction is based more and more on the weighted model ensemble.



weighted ensembles, a indicates how fast the transition between the two model-types occurs, and b indicates the inflection point or the value of x at which the influence of the weighted and unweighted ensembles is equal.

The appropriate amount by which to weigh measurements of bird density in the calibration of models may depend on the particulars of the data set. We found that weighing each iBd measurement by $iBd^{1.25}$ produced decent results. The parameters a and b , controlling the influence of the weighted and unweighted ensembles should be calibrated to produce the most accurate predictions for a given time and location.

6.6 Conclusion

With the model-development framework outlined in this chapter, models of migration intensity can be systematically developed for new locations. The models that result from this procedure can be used to forecast migration intensity up to several days in advance, which is generally the valid range of the numerical weather forecasts upon which most of the models in the ensemble depend. As well, our results suggest that the models of migration intensity can provide useful information on migratory dynamics in nearby locations, particularly for short-term forecasts. This is particularly useful for locations that are not covered by a weather radar and therefore have no measurements of

bird density with which to calibrate unique models. The study also shows that incorporating (particularly recent) measurements of bird density into forecast models improves their performance.

This study highlights the potential benefits of extracting bird density information from operational weather radar and provides a system to develop predictive models of bird density in new locations as data from these radars become available. Ultimately, the measurements of bird density from individual weather radars (and the models developed from them) should be integrated into unified large-scale monitoring and prediction systems that will dramatically improve flight safety (for both military and civil aviation) and likely revolutionize the field of ornithology.

Acknowledgments

We would like to thank the Royal Netherlands Meteorological Institute (KNMI) for providing data from the De Bilt and Den Helder weather radars and Toon Moene, Hidde Leijnse, Adriaan Dokter, and KNMI for providing and assisting with HIRLAM weather data. We also thank Hidde Leijnse, Hans van Gasteren, James McLaren, and Adriaan Dokter for invaluable discussion and contributions throughout. NCEP/DOE Reanalysis II data were provided by the NOAA/OAR/ESRL PSD, Boulder, Colorado, USA (<http://www.esrl.noaa.gov/psd/>). Our studies are facilitated by the NLeSC (<http://www.esciencecenter.com/>) and BiG Grid (<http://www.bigggrid.nl>) infrastructures for e-Science and supported financially by the Ministry of Defense (Flysafe2).

General discussion and synthesis

7.1 Weather or climate?

Tinbergen (1963) posited that, for a complete understanding of any animal behavior, four fundamental questions concerning said behavior should be addressed: mechanism (called ‘causation’ by Tinbergen), adaptation (called ‘survival value’ by Tinbergen), ontogeny, and phylogeny (called ‘evolution’ by Tinbergen).

Mechanistic questions concern the behavior itself: what exactly is the behavior, what processes are involved, and how is the behavior carried out? Questions of adaptation are concerned with why a particular behavior is advantageous to the animal in terms of its survival (or, perhaps ultimately, the survival of its offspring). Ontogenetic questions deal with the developmental stages in an animal’s life-cycle that have resulted in a particular behavior; questions of ontogeny often attempt to distinguish between innate and environmentally-induced behavior. Phylogenetic questions concern the progression of ancestry, selected by nature, that has resulted in a particular animal exhibiting a particular behavior. Mechanistic and ontogenetic questions are generally concerned with ‘how’ a behavior occurs, whereas adaptive and phylogenetic questions are concerned with ‘why’. Questions of ontogeny and phylogeny are considered ‘dynamic’ in that they address a sequence of events that has resulted in a particular behavior, whereas questions of mechanism and adaptation are considered ‘static’ in that they are concerned with the behavior itself.

The analyses herein have been devoted primarily to understanding bird behavior in response to atmospheric conditions. Atmospheric dynamics can have an impact on the answers to each of Tinbergen’s four questions; however

some questions are better addressed through considerations of ‘weather’ while others are best addressed with considerations of ‘climate’. Weather describes short-term atmospheric conditions and fluctuations, while climate describes long-term averages and trends of atmospheric conditions. Perhaps more succinctly, “climate is what you expect, weather is what you get”. Thus, questions regarding the influence of atmospheric processes on avian behavior in terms of phylogeny and (perhaps to a slightly lesser degree) ontogeny correspond with climatic conditions. Conversely, questions regarding the influence of atmospheric processes on avian behavior in terms of causation and function (i.e. mechanism and adaptation) correspond with weather conditions.

In Chapter 3, we considered different behaviors that birds can adopt to deal with various wind conditions. These behaviors differed largely with respect to the bird’s degree of compensation for side-wind displacement. We then illustrated how these behaviors can impact travel speeds, routes, and the probability of successful arrival. Thus, we examined the mechanism of compensation and the potential adaptive or survival value of the different behaviors. In that context, we considered behavioral responses to instantaneous wind conditions (i.e. weather); however in Chapter 4, we examined persistent wind patterns over 30 years to determine if these persistent (i.e. climatic) dynamics could affect differences in avian migration speed between spring and autumn. These wind patterns may not only influence an individual bird’s migration duration over a particular season, persistence in these conditions may influence many aspects of avian behavior. Birds may learn to anticipate particular wind conditions at different times and locations and adapt their wind selection and compensation and navigation strategies in response (i.e. ontogeny see e.g. Klaassen et al., 2011; Thorup et al., 2003; GagHardo et al., 2001). As well, these persistent wind patterns have shaped ancestral dispersal, influencing current migration routes (i.e. phylogeny Alerstam, 2001). On an evolutionary scale, adaptation to persistent patterns in wind conditions is a potential explanation for some ‘loop’ migrations (cf. Berthold, 2001; Alerstam et al., 2003) in which a bird’s outbound and return journeys follow different paths.

Because atmospheric conditions, expressed as both weather and climate, can influence many aspects of avian behavior, we introduced the RNCEP package of functions in Chapter 2 that can be used to quickly retrieve weather data for any location on Earth and subsequently calculate climatic variables from those data. Similarly, the flight simulator function in the RNCEP package can be used to consider individual migratory flights at particular times and locations, or it can be used to consider the same migratory flight over a sequence of many days, months, or years. Thus, this suite of functions is useful

when addressing questions of a mechanistic, adaptive, ontogenetic, or phylogenetic nature.

7.2 Optimal migration

Optimal migration theory defines a framework around which questions concerning the adaptive or survival value of behaviors may be examined (Alerstam, 2011); however, the application of optimal migration concepts depends on our having a correct understanding of what criteria determine optimality, particularly when multiple objectives are being optimized simultaneously. The ultimate measure of the optimality of a particular behavior is its effect on an animal's fitness (i.e. the animal's ability to produce viable offspring). We often consider, as proxies for fitness, more immediate optimality criteria including energy consumption, time expenditure, predation risk, and survival probability, and we often assume that for a behavior to persist it should be optimal. This is probably a good assumption in practice, since nature does not indefinitely tolerate inefficiency; however, behaviors can be optimal only in relation to the particulars of the environment, which are constantly changing. Thus, it is probably unavoidable that suboptimal behaviors exist as environments are dynamic and heterogeneous. An optimal behavior today in one location may be suboptimal tomorrow in a different location. As well, behavior that is globally optimal (i.e. optimal in the widest range of circumstances) may appear decidedly suboptimal for any one time and location. Furthermore, what is optimal behavior for a particular species may not be optimal for all individuals of the species, though individual variability by the members of a species likely makes the species as a whole more robust against the uncertainties of a dynamic environment. Regardless, no species or individual can exhibit optimal behavior in all regards, since to optimize one criterion often necessitates a sacrifice of another. This situation, thankfully, leads to conditions in which no single species dominates all niches and multiple species can coexist.

While natural systems are deterministic, i.e. they are determined explicitly by prior events, they are also chaotic. Small variations in any of an infinite number of determining factors can accumulate through the system and produce wildly different outcomes. Weather is a prototypical chaotic system described metaphorically by the ‘butterfly effect’ (Abraham and Ueda, 2000), which has become synonymous with chaos theory. Owing to this chaos, an ‘optimal’ behavior in some cases may be to remain flexible in response to particular stimuli. For instance, it is often beneficial for a bird to delay migration until wind conditions are supportive; however, it is probably not beneficial for this behavior to be hard-coded such that a bird will not migrate

without supportive winds, particularly if supportive winds are very infrequent (Weber and Hedenström, 2000). Unsurprisingly, research suggests that birds often do migrate without tailwind assistance, particularly in locations where tailwind support is infrequent, but that the birds still preferentially select less-prohibitive wind conditions from those available (see e.g. Karlsson et al., 2011; Erni et al., 2002b). We found complimentary results in Chapter 5 in which birds showed a preference for altitudes with better wind conditions, but were not blindly driven to seek out the most supportive winds available. Rather, birds were balancing trade-offs between different immediate optimization criteria in order to maximize the most important optimization criterion: successfully passing their genes onto the next generation. It seems that in altitude selection as in the timing of migration, bird's behavioral responses to wind (at least) are flexible and somewhat opportunistic.

7.3 Robust decision-making

Behavioral responses should probably be based on multiple stimuli rather than on a single factor whenever possible. The Three Mile Island nuclear disaster in the United States in 1979 illustrates this point, as the meltdown was due in large part to operators relying on a single sensor. Unbeknownst to the operators who had come to rely on the sensor, it was only indirectly related to the state of the system (Rogovin and Frampton Jr., 1980). Consulting other sensors would have indicated the true situation, or at least suggested a disagreement between sensors. When multiple cues are consulted, decision making is more robust against potential errors between a particular cue and the outcome it suggests. Unsurprisingly, we find that birds do utilize multiple sources of input to make decisions. In navigation, for example, birds consult the sun and stars, as well as geomagnetic references, landmarks, and perhaps even scent to determine their location in relation to their goal (Able, 2001; Wallraff, 2004; Åkesson and Hedenström, 2007; Wiltschko and Wiltschko, 2003). Debate remains regarding how birds prioritize between these cues and codify them into a single indication of direction, but Liu and Chernetsov (2012) reviewed studies with conflicting results on this point and have suggested that the conflicts may be due to genuine differences between species.

In navigation, issues such as the sizes and locations of ecological barriers can affect the optimality of a bird selecting a particular route; however, navigational cues (e.g. celestial, geomagnetic, and landmark indicators) should all theoretically agree on a bird's location in relation to its goal. If there is disagreement, one or more of the cues are incorrect and the bird must decide which to believe. Atmospheric variables, on the other hand, may often

give conflicting cues that are each correct (e.g. wind conditions are supportive, indicating to the bird that it should migrate, but at the same time a change in atmospheric pressure is indicating an approaching storm). When different atmospheric cues give conflicting signals, birds should consider the impacts suggested by each cue individually because of the independent influences of the different atmospheric components. Certain atmospheric variables may take precedence in particular situations, but only when other variables are determined to be within acceptable limits. The dynamics and thresholds of acceptability and optimality remain in flux because the optimal decision with regard to one variable is determined by the states of all other variables.

Naturally, optimal decision-making depends as well on an individual's tolerances and capabilities with respect to different atmospheric conditions. The influence of decreasing air pressure with altitude, for instance, affects the flight dynamics of birds differently depending on their morphology (Pennycuick, 2008). Differences in flight capacity can determine in which wind conditions birds can make forward progress or in which wind conditions a bird can fully compensate for sidewind displacement. Swanson and Liknes (2006) showed that bird species exhibit differences in their ability to tolerate cold temperatures. Although that study considered birds at rest, differences in the thermoregulatory capacities of birds likely persist in flight. Thus, different bird species may prioritize atmospheric variables differently and therefore base their decisions more heavily on particular atmospheric cues, similar to the intra-specific differences in the prioritization of navigational stimuli suggested by Liu and Chernetsov (2012).

7.4 Assessing wind drift

What is made clear throughout these analyses is that weather has a strong impact on the decisions made by migrating birds. We have examined what birds do in response to particular atmospheric conditions, and we have postulated as to why birds might react in the ways we observe. Thus, we have primarily focused on the 'why' questions of phylogeny and adaptation. We have not considered in great detail, however, how birds are capable of reacting in the ways we observe. For instance, we have seen that birds adjust their timing and altitude selection during migration at least partly in response to weather conditions. In particular, birds seem to avoid wind conditions that prohibit their movement in seasonally appropriate directions. In order to choose between wind conditions, particularly with regard to altitude selection, a bird must have some way to determine the influence of different wind conditions.

Being primarily Earth-bound, it may be difficult for humans to comprehend

hend a bird not being able to perceive the influence of wind. When we ride a bike, for instance, we can see the progress we are making, and we can feel the wind pushing us in a particular direction. The reason we are able to judge the influence of the wind while cycling is because we are bound to the “stationary” Earth and can use it as a frame of reference. We know that we want to proceed along a particular direction relative to the Earth and by visually assessing our speed in that direction (and accounting for the effort we are exerting), we get an indication of how much the wind is assisting or prohibiting our movement. As well, we are able to feel the speed and direction of the wind because we are not generally moving along with the wind and are instead, for all intents and purposes, bound to the Earth. We therefore feel pressure in the direction from which the wind is blowing, and the intensity of this pressure indicates the wind’s speed.

A bird in flight should also be able to utilize the fixed Earth as a visual point of reference and determine how the wind is effecting its progress; however, there are complicating factors to consider. Many species, particularly passineres which were the focus of much of this thesis, migrate at night; so on moonless nights, particularly in areas with sparse human populations, Earth-bound objects may be difficult to see. Cloud, haze, or fog may obscure a bird’s view of the Earth as well. Even under the best atmospheric conditions, the higher a bird flies, the shallower the angles become between it and its ground-based points of reference. The shallower these angles become, the more difficult it is to visually assess movement in relation to the reference object, which is why the stars (while helpful in determining direction) are useless in assessing wind drift – they are simply too far away.

We may be tempted to evaluate a bird’s perception of its environment in terms of our own senses. After all, ours are the only senses we have to experience the world. Even things that we can “sense” using instrumentation, we must translate to a medium that we can sense unaided in order for us to process the information; consider, for example, our use of “false color” to view parts of the electromagnetic spectrum outside of our visible range or high-speed photography to view actions that are too fast for our eyes to perceive. Because we view the world through our own senses, it is difficult for us to imagine, for example, what it means to “sense” the Earth’s magnetic field as birds do. We understand, however, that this is a sense quite different from any of our own and therefore requires scrutinization. We may be less discerning of senses that we share with birds (such as vision), expecting that these senses function similarly to our own, but we would be remiss in doing so. Birds are much more visually acute than humans and have significantly larger eyes relative to their body size than other vertebrates. Consider that approximately

50% of the volume of a bird's cranium is dedicated to housing its eyes, while human eyes occupy only about 5% of the volume of their skull (Waldvogel, 1990). The relatively large size of bird's eyes is not only indicative of the importance of vision in the life of birds, larger eyes allow for larger images to be projected onto the retina increasing visual acuity (Jones et al., 2007). Bird's large lateral viewing area (Martin, 2011) allows them to simultaneously consider their movement relative to several reference objects on both sides of their head, which should aid in their ability to quickly and accurately assess wind drift by visual means Liechti (2006). Another important aspect of avian vision is their 'flicker-fusion frequency' or the frequency at which they can visually resolve images. Humans perceive continuous motion in images flickering at rates above 50 to 60 Hz, and images flickering at even higher rates become blurred, unstable, and erratic in human vision. Birds have a much higher flicker-fusion frequency than humans and can resolve individual flickers at rates upwards of 100 Hz (Jones et al., 2007). As well as helping birds to avoid obstacles by allowing them to resolve the very fast movements associated with high-speed flight, this high flicker-fusion frequency also enables birds to better detect very slow movement. For instance, unlike humans, birds are able to visually detect the movement of the sun and stars (Jones et al., 2007). It is reasonable to suspect, therefore, that birds are more capable of assessing wind drift by considering the relative motion of reference objects on Earth than humans would be at equivalent altitude. So with a visual point of reference, birds are well-adapted to assess the influence of different wind conditions on their movement.

Research has suggested that some migrants can assess wind conditions even without having a visual point of reference on the Earth (see Richardson, 1990b, and references therein); however, a cogent theory to describe how birds can assess wind drift without a visual point of reference has been elusive. Nonetheless, birds have been observed with radar maintaining constant flight trajectories even when their view of the Earth was totally obscured. Without evidence suggesting otherwise, we may assume that a bird in flight is unable to feel the wind the way we do on Earth. Pressure, which we said is what we feel from the wind on Earth, describes a force defined as mass x acceleration. The wind exerts a force on us and we exert an equal and opposite force so as to maintain our position. It is the acceleration of the wind that we feel, not the movement. A bird in the air, without a visual point of reference, will be moved along with the wind and, therefore, will not feel any acceleration. Consider that when cycling at the same speed and in the same direction as the wind, we are unable to feel the wind directly; however, because we are on the Earth, we are able to determine that we are moving faster than we should

be for the effort we are exerting. Thus, a bird moving along with the wind without a visual point of reference would likely be unable to feel the wind itself; nonetheless, the bird may be able to feel changes in wind condition, because changes denote an acceleration. The problem, however, is that while the bird may be able to feel the way in which the wind is changing, it won't know the state from which the wind is changing. In other words, a bird without a visual point of reference can feel the fluctuations around the mean wind conditions but never knows what those mean conditions actually are. That is, unless there is anisotropy in these fluctuations that provides information on the mean airflow. Reynolds et al. (2010) have suggested that there is in fact asymmetry in these fluctuations and have theorized that insects can use this information to orient in relation to the wind. The ability to detect these fine-scale fluctuations has not been convincingly demonstrated in birds, though the potential for birds to utilize this information has been theorized for some time (Larkin, 1980).

Birds may also be able to assess wind drift without a visual point of reference by calibrating an alternative reference system while visual points of reference are available. For example, a bird could determine the pressure field it experiences when it is compensating for displacement using visual points of reference. Once the visual points of reference are unavailable (e.g. after the sun has set or when the bird has climbed to higher altitude or flown over a dense cloud layer), the bird may be able to maintain its degree of compensation by maintaining the pressure field it determined was appropriate. A bird that assessed drift in this way would continue to compensate for the wind conditions it experienced when it calibrated the reference pressure field and would not be able to account for changes in wind condition that occurred thereafter. Liechti (1993) found that birds at high altitude appeared to compensate for displacement according to the wind conditions at lower altitude, which is in accordance with birds assessing drift in the manner just described.

Many of the theories developed concerning avian migration inherently assume that birds are able to assess the effect of the wind on their progress. For instance, those of the flow-assistance models we introduced in Chapter 3 that assume compensation implicitly assume that birds can assess the effect of the wind in order to compensate for it. The accompanying trajectory simulator (i.e. the FLAT model) then applies these assumptions to move a simulated bird through space, even in locations where the means by which birds determine the effects of wind are uncertain (such as at sea). We observe birds behaving in ways that suggest they are able to determine the effects of wind. For instance in Chapter 5, we found that wind was important in altitude selection, implying that birds are able to distinguish between the effects of wind at dif-

ferent altitudes. Nonetheless, we should consider when and where this ability to assess the influence of wind is feasible (and at what level of accuracy). Also in Chapter 5, we found that wind support relative to support at the surface was better able to describe altitude distributions than wind support relative to all altitudes. Perhaps birds consider wind conditions with respect to conditions at the surface because conditions assessed near the surface are easier to determine and more reliable.

Clearly, gaps remain in our knowledge of the sensory abilities of birds to judge the atmosphere, particularly when they are in motion. Future research utilizing high-resolution GPS tracking data, perhaps in combination with simulation models such as the FLAT model described in Chapter 3, may indicate when and where birds are (un)able to assess the influence of wind, potentially providing insight into the mechanisms involved.

7.5 Quantifying model performance

Many of the analyses in this thesis rely on models of one sort or another to either capture relationships contained in data (e.g. Chapters 5 and 6) or conceptually reduce a system to some manageable core components (e.g. Chapter 3). Models can be quite useful tools both for increasing our understanding of a system and for generating predictions of future conditions; however, the measure according to which a particular model's performance should be assessed is not always so clear.

In theory, the measure used to assess a model's performance should depend only on the goals one hopes to achieve with the model. In reality, however, there are limitations on what is quantifiable, and researchers must often aggregate (i.e. summarize) measurements and/or predictions and describe model performance based on those aggregates. In studies of altitude selection by avian migrants, for instance, researchers have often extracted a single attribute of an altitude distribution of migrants for examination – for example, the altitude with the greatest number of birds (e.g. Gauthreaux, 1991) or the altitude above or below which some proportion of the birds occurred (e.g. Shamoun-Baranes et al., 2003b). Particularly if the aim of the research is to better understand variability in these specific attributes, using these aggregated descriptors is beneficial (or at least not limiting). We began examining altitude distributions by applying just such a method in Chapter 5; however, the decision to use these aggregates may also be based on the fact that it is more difficult (both technically and conceptually) to consider altitude profiles in their entirety. In particular, there is a statistical challenge to quantitatively compare modeled and predicted distributions of any kind.

We applied several measures in Chapter 5 to compare predicted and measured altitude distributions of avian migrants. We compared these distributions by ranking the altitude bins and determining the correlation between the ranks. This measure, called Spearman's ρ , is an ordinal-level measure of association that has been applied in several previous studies for the purpose of comparing predicted and measured altitude distributions of avian migrants (e.g. Liechti et al., 2000; Schmaljohann et al., 2009) and has the benefit of being easy to apply and interpret. As well, Spearman's ρ can be used to compare measurements and predictions that are on different scales. For instance, measured altitude distributions of avian migrants can be compared directly with altitude distributions of wind support or estimates of flight range. This method has its weaknesses as well: e.g. absolute comparisons are not possible, and the influence of each altitude bin is equivalent regardless of how many birds are or are not present. Consider a situation in which 90% of birds are observed in only one altitude bin and the other 10% of birds are scattered throughout the remaining altitudes. A model then predicts that 90% of birds will occur in the correct altitude bin and the other 10% of birds are scattered throughout the remaining altitudes. Even though 90% of birds were correctly predicted in the one altitude bin, the Spearman's ρ correlation between the predicted and measured distributions will be dominated by the influence of the 10% of birds scattered throughout the remaining altitude bins of the measured and predicted distributions. Consider another situation in which predicted and measured distributions over 20 altitude bins are compared. Suppose that birds are only ever present in the lowest 10 altitude bins. A model that predicts all birds occurring in the lowest 10 altitude bins, but predicts the distribution of those birds in the lowest 10 bins completely at random, will on average have a Spearman's ρ correlation of 0.86 with the measured distribution. This suggests quite a strong correlation, but all that is truly known about the system is that birds always fly in the lowest 10 altitude bins. Therefore, another weakness of Spearman's ρ is its dependence on particular features of a dataset (e.g. the number of altitude bins), often disallowing meaningful comparisons between the results of different studies.

In an effort to arrive at more quantitative comparisons between predicted and measured altitude distributions of birds, we applied two other measures: root-mean-squared-error ($RMSE$) and the proportion of variance explained (Var_{exp}). $RMSE$ is defined as

$$RMSE = \sqrt{\frac{\sum_{i=1}^n (x_i - y_i)^2}{n}}, \quad (7.1)$$

and we calculate Var_{exp} following Bruderer et al. (1995b) as

$$Var_{exp} = 1 - \frac{\sum_{i=1}^n |x_i - y_i|}{\sum_{i=1}^n x_i + y_i}. \quad (7.2)$$

In both cases, x_i are measured values and y_i are predicted. These two measures require predictions to be on the same scale as measurements, so comparing altitude distributions of wind support and altitude distributions of proportional bird density are not possible. These are both ratio-level measures of the accuracy of predictions, which can be used to quantify error per altitude bin; Spearman's ρ , on the other hand, summarizes all altitude bins in a profile with one value. There is one potential aspect to consider, however, when comparing predicted and measured altitude distributions, that $RMSE$ and Var_{exp} cannot capture. These altitude distributions are determined over space, vertically, but neither $RMSE$ nor Var_{exp} considers how close the predictions were to the measurements in terms of distance over vertical space. As a simple example, suppose that all birds were measured in one altitude bin centered on 0.3 km. According to either $RMSE$ or Var_{exp} , predictions are considered equally incorrect if all birds are predicted in one altitude bin centered on 4 km or one altitude bin centered on 0.5 km. Clearly, a prediction that places birds in a bin 3700 m away from the proper bin is less correct than a prediction that places birds in a bin 200 m away, but $RMSE$ and Var_{exp} do not reflect this.

For examining avian altitude distributions in future research, and developing models to predict avian altitude distributions, we suggest that another measure of model performance be considered, perhaps alongside those previously mentioned. This measure, called the earth movers' distance (EMD ; Haibin and Okada, 2007; Urbanek and Rubner, 2011), is commonly used in image analysis and retrieval to quantify differences between images. Informally, EMD determines the minimum amount of work required to turn one distribution into another, thereby reducing the comparison of two distributions to a transport problem. Because the distance between altitude bins is a true distance (in the case of our altitude analyses in Chapter 5, the distance between the centers of the bins was 200 m), EMD can describe the conversion of one distribution to another in units of distance (e.g. meters). The resulting metric indicates the average distance that the birds in the predicted distribution would need to be moved (vertically) in order to reproduce the measured distribution. Thus, altitude bins in one study being of different resolution than altitude bins in another study does not prevent explicit comparisons between the results of the two studies. While EMD can be calculated on absolute distributions (e.g. using the actual number of migrants per altitude bin), there will be variability in the EMD measurements that is due only to differences in these absolute numbers disallowing meaningful comparisons between EMD

from one time or location to the next. By considering proportional distributions, the results of all comparisons will be equivalent.

The earth movers' distance, which is most often utilized in fields as seemingly-unrelated to bird migration as computer science and image retrieval, can help us better understand variability in avian altitude selection and highlights the benefit to be gained from incorporating concepts, methods, and tools from other disciplines into ecological and biological research.

7.6 Migration research

As with many ecological topics, exploring the patterns and dynamics involved in bird migration is benefited by the efficient integration of data from multiple fields. Not only must we integrate data, we must combine entire systems, procedures, methods, and the expertise necessary to fully utilize each. In fact, much of this thesis is predicated on integrating tools and methods from different disciplines to better understand migratory dynamics. The radars we have used, for example, provide incredible information on bird movements but were developed (and, indeed, continue) to serve entirely different purposes. To effectively handle, process, and utilize data from numerical weather models, which we used extensively in these analyses, requires knowledge of the underlying atmospheric systems they describe and the often unique formats in which they are stored. Many of the methods we employed require knowledge of statistical analysis and programming and can be computationally demanding. As well, the large amounts of data involved necessitate effective data management, storage, and access techniques. In short, being open to and receptive of technologies and techniques used in other fields will continue to benefit biological and ecological research, which necessarily considers interactions between many different systems.

Tools and workflows that facilitate the integration of information from different systems are therefore of the utmost importance, and they will become increasingly so as data sets become larger and more complex. As mentioned elsewhere in this thesis, the recently-developed capacity to automatically extract bird migration information from Doppler weather radar is an exciting and potentially revolutionary step. The spatial and temporal coverage of these radar systems is unprecedented in ornithology, allowing for research on a scale that has been hitherto impossible. Nonetheless, efficiently processing, organizing, and maintaining these data will be a substantial task. An individual radar can generate gigabytes of data per hour, and associated environmental data sets can be similarly cumbersome. In Europe, each radar is maintained by the country in which it resides, which can lead to issues regarding data

conversion, transmission, and consistency between sites.

Utilization of these radar systems in meteorology is not immune to these challenges, and the meteorological offices of many European countries have taken steps toward addressing these issues through the organization of the The Operational Programme for the Exchange of weather RAdar information (OPERA). The OPERA network is intended to provide a platform wherein “expertise on operationally-oriented weather radar issues is exchanged and holistic management procedures are optimized... [with the intent to] harmonize data and product exchange at the European level.” Utilizing these data for bird migration studies will require a similar level of organization. An optimal situation may be to have data relevant to bird migration studies organized under the umbrella of the OPERA network such that bird migration information becomes a typical product of OPERA output. Opportunities to similarly utilize the NEXRAD radar network in the United States are also being explored (Chilson et al., 2012). Occasionally, partnerships of this sort can be confounded by a divergent set of goals; however, this specific partnership has the potential to be mutually beneficial for both the biological and meteorological communities. Since each group often considers radar echos relevant to the other as “clutter”, improvements in identification advance the research potential of both groups. Furthermore, the timing and spatial distribution of migrating birds have shown strong relationships with climatic variability (see e.g. Sinelschikova et al., 2007; Jonzén et al., 2006; Jenni and Kéry, 2003; Hüppop and Hüppop, 2003; Crick, 2004) such that knowledge of one system may provide insight into the other.

The potential benefits of a network of radar sensors such as OPERA or NEXRAD in bird migration studies far outweigh the challenges associated with developing and implementing the required systems and workflows to obtain and organize the relevant data. Simply being able to quantitatively map the seasonal flow of avian biomass over such a large area will represent a considerable leap forward and result in data sets that benefit conservation and management efforts. Beyond that, with coverage over large geographical areas and measurements made from standardized systems, there is enormous potential to conduct comparative analyses. Behavioral differences due to the time of the year, the altitude of flight, and the type of underlying landscape can be examined at a scale and resolution previously unattainable. We may determine which behaviors are unchanged over time and space and which behaviors are dependent on environmental conditions and in what ways. For instance, in Chapter 4, we examined the effect of persistent wind patterns on migration speed. With an extensive and contiguous radar network, we can determine whether these patterns persist outside of our study area and con-

sider the cumulative effects of these persistent patterns over entire migration routes. As well, we can determine if the atmospheric influences on avian altitude selection we uncovered in Chapter 5 persist in other areas with different atmospheric conditions and landscapes. Predictive models of migration intensity such as those we developed in Chapter 6, and indeed flight safety in general, will surely benefit from a unified network of sensors that will allow us to implement geostatistics in our analyses, incorporate the element of space in our models, and make predictions that account for upstream and downstream flows of birds between sensors. These types of models will likely utilize not only the measurements from the individual radar systems in the network, they will incorporate simulation models such as the FLAT model described in Chapter 3 to propagate birds measured at a particular radar site through space and time. In all these cases, tools such as those contained in the RNCEP package from Chapter 2 will be useful as they facilitate the handling and integration of environmental data in bird migration studies, specifically allowing for the rapid adjustment of the spatial and temporal domains considered. Utilizing radar measurements across large geographic areas and integrating knowledge from multiple disciplines, we may more fully address all four of Tinbergen's questions when considering how birds weather the weather.

Bibliography

- Able, K. P. 1970. A radar study of the altitude of nocturnal passerine migration. *Bird-Banding* **41**:282–290.
- Able, K. P. 2001. The concepts and terminology of bird navigation. *Journal of Avian Biology* **32**:174.
- Abraham, R., and Y. Ueda, 2000. The chaos avant-garde: memories of the early days of chaos theory. World Scientific series on nonlinear science: Monographs and treatises, World Scientific. URL <http://books.google.nl/books?id=0E667XpBq1UC>.
- Aitchison, J. 1982. The statistical analysis of compositional data. *Journal of the Royal Statistical Society. Series B (Methodological)* **44**:139–177.
- Åkesson, S., and A. Hedenstrom. 2000. Wind selectivity of migratory flight departures in birds. *Behavioral Ecology and Sociobiology* **47**:140–144.
- Åkesson, S., and A. Hedenstrom. 2007. How migrants get there: migratory performance and orientation. *Bioscience* **57**:123–133.
- Åkesson, S., L. Karlsson, G. Walinder, and T. Alerstam. 1996. Bimodal orientation and the occurrence of temporary reverse bird migration during autumn in south Scandinavia. *Behavioral Ecology and Sociobiology* **38**:293–302.
- Åkesson, S., and R. Sandberg. 1994. Migratory orientation of passerines at dusk, night and dawn. *Ethology* **98**:177–191.

- Åkesson, S., G. Walinder, L. Karlsson, and S. Ehnbom. 2002. Nocturnal migratory flight initiation in reed warblers *Acrocephalus scirpaceus*: effect of wind on orientation and timing of migration. *Journal of Avian Biology* **33**:349–357.
- Alerstam, T. 1979. Wind as selective agent in bird migration. *Ornis Scandinavica* **10**:76–93.
- Alerstam, T., 1981. The course and timing of bird migration. Pages 9–54 in D. Aidley, editor. *Animal Migration*. Cambridge University Press, Cambridge, UK.
- Alerstam, T. 2001. Detours in bird migration. *Journal of Theoretical Biology* **209**:319–331.
- Alerstam, T., 2003. Bird migration speed. in P. Berthold, E. Gwinner, and E. Sonnenschein, editors. *Avian Migration*. Springer, Berlin, Heidelberg.
- Alerstam, T. 2011. Optimal bird migration revisited. *Journal of Ornithology* **152**:5–23.
- Alerstam, T., J. W. Chapman, J. Bäckman, A. D. Smith, H. Karlsson, C. Nilsson, D. R. Reynolds, R. H. G. Klaassen, and J. K. Hill. 2011. Convergent patterns of long-distance nocturnal migration in noctuid moths and passerine birds. *Proceedings of the Royal Society B: Biological Sciences* doi:[10.1098/rspb.2011.0058](https://doi.org/10.1098/rspb.2011.0058).
- Alerstam, T., A. Hedenstrom, and S. Åkesson. 2003. Long-distance migration: evolution and determinants. *Oikos* **103**:247–260.
- Alerstam, T., and r. Lindström, 1990. Optimal bird migration: the relative importance of time, energy, and safety. Pages 331–351 in E. Gwinner, editor. *Bird Migration: Physiology and Ecophysiology*. Springer, Berlin Heidelberg New York.
- Alestalo, M. 2002. Preface [of Special Issue]. *Boreal Environmental Research* **7**:305.
- Allan, J. R., 2002. The costs of bird strikes and bird strike prevention. in L. Clark, editor. *Human conflicts with wildlife: economic considerations*. National Wildlife Research Council, Fort Collins, Colorado, USA.
- Altshuler, D. L., and R. Dudley. 2006. The physiology and biomechanics of avian flight at high altitude. *Integrative and Comparative Biology* **46**:62–71.

- Aralimarad, P., A. M. Reynolds, K. S. Lim, D. R. Reynolds, and J. W. Chapman. 2011. Flight altitude selection increases orientation performance in high-flying nocturnal insect migrants. *Animal Behaviour* **82**:1221–1225.
- Batschelet, E. 1981. Circular statistics in biology. Academic Press, London.
- Bauchinger, U., and M. Klaassen. 2005. Longer days in spring than in autumn accelerate migration speed of passerine birds. *Journal of Avian Biology* **36**:3–5.
- Becker, R. A., A. R. Wilks, R. Brownrigg, and T. P. Minka, 2010. maps: draw geographical maps. R package version 2.1-4. URL <http://cran.r-project.org/web/packages/maps/>.
- Bellrose, F. C., and R. R. Graber, 1963. A radar study of the flight direction of nocturnal migrants. Pages 362–389 in International Ornithological Congress, volume 13.
- Berthold, P. 2001. Bird Migration: A General Survey. 2nd edition. Oxford University Press, Oxford.
- Bloch, R., and B. Bruderer. 1982. The air speed of migrating birds and its relationship to the wind. *Behavioral Ecology and Sociobiology* **11**:19–24.
- Blokpoel, H., 1969. An attempt to forecast the intensity of nocturnal fall migration. Pages 285–298 in M. S. Kuhring, editor. Proceedings of the World Conference on Bird Hazards to Aircraft. National Research Council of Canada, Kingston, Canada.
- Bouten, W., J. van Belle, A. Benabdelkader, L. Buurma, H. van Gasteren, A. Hoon, G. Heuvelink, R. Foppen, G. van Reenen, H. Seijmonsbergen, J. Shamoun, and H. Sierdsema, 2003. Towards an operational bird avoidance system: combining models and measurements. in Proceedings of the 26th International Bird Strike Committee, volume 2. Warsaw.
- Bouten, W., J. van Belle, H. van Gasteren, J. A. Vrugt, J. Shamoun-Baranes, and L. Buurma, 2005. Predicting bird migration: data-driven versus concept-driven models. Pages 231–240 in M. S. Kuhring, editor. Proceedings of the 27th International Bird Strike Committee, volume 2. Athens, Greece.
- Bowlin, M. S., I.-A. Bisson, J. Shamoun-Baranes, J. D. Reichard, N. Sapir, P. P. Marra, T. H. Kunz, D. S. Wilcove, A. Hedenstrom, C. G. Guglielmo, S. Åkesson, M. Ramenofsky, and M. Wikelski. 2010. Grand challenges in migration biology. *Integrative and Comparative Biology* **50**:261–279.

- Brandes, D., and D. Ombalski. 2004. Modeling raptor migration pathways using a fluid-flow analogy. *The Journal of Raptor Research* **38**:195–207.
- Bridge, E. S., K. Thorup, M. S. Bowlin, P. B. Chilson, R. H. Diehl, R. W. Fléron, P. Hartl, K. Roland, J. F. Kelly, W. D. Robinson, and M. Wikelski. 2011. Technology on the move: recent and forthcoming innovations for tracking migratory birds. *Bioscience* **61**:689–698.
- Brodersen, J., P. A. Nilsson, J. Ammitzbøll, L.-A. Hansson, C. Skov, and C. Brönmark. 2008. Optimal swimming speed in head currents and effects on distance movement of winter-migrating fish. *PLoS ONE* **3**:e2156.
- Bruderer, B. 1971. Radarbeobachtungen über den Frühlingszug im schweizerischen Mitteland (Ein Beitrag zum Problem der Witterungsabhängigkeit des Vogelzuges). *Ornithologische Beobachtungen* **68**:89–158.
- Bruderer, B., 1982. Do migrating birds fly along straight lines? Pages 3–14 in F. Papi and H. Wallraff, editors. *Avian navigation*. Springer, Berlin.
- Bruderer, B. 1997. The study of bird migration by radar part 1: the technical basis. *Naturwissenschaften* **84**:1–8.
- Bruderer, B., and A. Boldt. 2001. Flight characteristics of birds. *Ibis* **143**:178–204.
- Bruderer, B., and F. Liechti. 1998. Flight behaviour of nocturnally migrating birds in coastal areas: crossing or coasting. *Journal of Avian Biology* **29**:499–507.
- Bruderer, B., F. Liechti, and D. Erich. 1989. Radarbeobachtungen über den herbstlichen Vogelzug in Süddeutschland. *Vogel und Luftverkehr* **9**:174–194.
- Bruderer, B., T. Steuri, and M. Baumgartner. 1995a. Short-range high-precision surveillance of nocturnal migration and tracking of single targets. *Israel Journal of Zoology* **41**:207–220.
- Bruderer, B., L. G. Underhill, and F. Liechti. 1995b. Altitude choice by night migrants in a desert area predicted by meteorological factors. *Ibis* **137**:44–55.
- Buck, A. L. 1981. New equations for computing vapor pressure and enhancement factor. *Journal of Applied Meteorology* **20**:1527–1532.
- Buurma, L. S. 1995. Long-range surveillance radars as indicators of bird numbers aloft. *Israel Journal of Zoology* **41**:221–236.

- Calenge, C. 2006. The package "adehabitat" for the R software: A tool for the analysis of space and habitat use by animals. *Ecological Modelling* **197**:516–519.
- Carmi, N., B. Pinshow, W. P. Porter, and J. Jaeger. 1992. Water and energy limitations on flight duration in small migrating birds. *The Auk* **109**:268–276.
- Castro-Santos, T. 2005. Optimal swim speeds for traversing velocity barriers: an analysis of volitional high-speed swimming behavior of migratory fishes. *Journal of Experimental Biology* **208**:421–432.
- Cats, G., and L. Wolters. 1996. The Hirlam project. *Computational Science and Engineering, IEEE* **3**:4–7.
- Chapman, J. W., R. H. G. Klaassen, V. A. Drake, S. Fossette, G. C. Hays, J. D. Metcalfe, A. M. Reynolds, D. R. Reynolds, and T. Alerstam. 2011. Animal orientation strategies for movement in flows. *Current Biology* **21**:R861–R870.
- Chapman, J. W., R. L. Nesbit, L. E. Burgin, D. R. Reynolds, A. D. Smith, D. R. Middleton, and J. K. Hill. 2010. Flight orientation behaviors promote optimal migration trajectories in high-flying insects. *Science* **327**:682–685.
- Chapman, J. W., D. R. Reynolds, H. Mouritsen, J. K. Hill, J. R. Riley, D. Sivell, A. D. Smith, and I. P. Woiwod. 2008. Wind selection and drift compensation optimize migratory pathways in a high-flying moth. *Current Biology* **18**:514–518.
- Chilson, P. B., E. Bridge, W. F. Frick, J. W. Chapman, and J. F. Kelly. 2012. Radar aeroecology: exploring the movements of aerial fauna through radio-wave remote sensing. *Biology Letters* doi: [10.1098/rsbl.2012.0384](https://doi.org/10.1098/rsbl.2012.0384).
- Chmielewski, F.-M., and T. Rötzer. 2002. Annual and spatial variability of the beginning of growing season in Europe in relation to air temperature changes. *Climate Research* **19**:257–264.
- Conard, N. J. 2003. Palaeolithic ivory sculptures from southwestern Germany and the origins of figurative art. *Nature* **426**:830–832.
- Cook, B. I., T. M. Smith, and M. E. Mann. 2005. The North Atlantic Oscillation and regional phenology prediction over Europe. *Global Change Biology* **11**:919–926.

- Cotté, C., Y.-H. Park, C. Guinet, and C.-A. Bost. 2007. Movements of foraging king penguins through marine mesoscale eddies. *Proceedings of the Royal Society B: Biological Sciences* **274**:2385–2391.
- Cotton, P. A. 2003. Avian migration phenology and global climate change. *Proceedings of the National Academy of Sciences of the United States of America* **100**:12219–12222.
- Crick, H. Q. P. 2004. The impact of climate change on birds. *Ibis* **146**:48–56.
- Delingat, J., F. Bairlein, and A. Hedenstrom. 2008. Obligatory barrier crossing and adaptive fuel management in migratory birds: the case of the Atlantic crossing in Northern Wheatears (*Oenanthe oenanthe*). *Behavioral Ecology and Sociobiology* **62**:1069–1078.
- Desholm, M., A. D. Fox, P. D. L. Beasley, and J. Kahlert. 2006. Remote techniques for counting and estimating the number of bird-wind turbine collisions at sea: a review. *Ibis* **148**:76–89.
- Dingle, H. 1996. Migration: the biology of life on the move. Oxford University Press, New York.
- Dokter, A. M., F. Liechti, H. Stark, L. Delobbe, P. Tabary, and I. Holleman. 2011. Bird migration flight altitudes studied by a network of operational weather radars. *Journal of the Royal Society Interface* **8**:30–43.
- Dolbeer, R. A., S. E. Wright, and E. C. Cleary. 2000. Ranking the Hazard Level of Wildlife Species to Aviation. *Wildlife Society Bulletin* **28**:372–378.
- Dolbeer, R. A., S. E. Wright, J. Weller, and M. J. Begier, 2012. Wildlife strikes to civil aircraft in the United States 1990–2010. National wildlife strike database serial report 17, Federal Aviation Administration.
- Doty, B., T. Holt, and M. Fiorino, 1995. The Grid Analysis and Display System (GrADS). Technical report, Institute of Global Environment and Society (IGES).
- Drake, V. A., and R. A. Farrow. 1988. The influence of atmospheric structure and motions on insect migration. *Annual Review of Entomology* **33**:183–210.
- Eastwood, E. 1967. Radar Ornithology. The Chaucer Press, Bungay, Suffolk.
- Eastwood, E., and G. C. Rider. 1965. Some radar measurements of the altitude of bird flight. *British Birds* **58**:393–426.

- Elkins, N. 2004. Weather and bird behaviour. 3rd edition. T. and A. D. Poyser, London.
- Ellegren, H. 1993. Speed of migration and migratory flight lengths of passerine birds ringed during autumn migration in Sweden. *Ornis Scandinavica* **24**:220–228.
- Ellis, H. I., and J. R. J. Jr. 1991. Total Body Water and Body Composition in Phalaropes and Other Birds. *Physiological Zoology* **64**:973–984.
- Emlen, S. T. 1967. Migratory orientation in the Indigo Bunting, *Passerina cyanea*: part I: evidence for use of celestial cues. *The Auk* **84**:pp. 309–342.
- Emlen, S. T., and J. T. Emlen. 1966. A technique for recording migratory orientation of captive birds. *The Auk* **83**:361–367.
- Erni, B., F. Liechti, and B. Bruderer. 2002a. Stopover strategies in passerine bird migration: a simulation study. *Journal of Theoretical Biology* **219**:479–493.
- Erni, B., F. Liechti, and B. Bruderer. 2005. The role of wind in passerine autumn migration between Europe and Africa. *Behavioral Ecology* **16**:732–740.
- Erni, B., F. Liechti, L. G. Underhill, and B. Bruderer. 2002b. Wind and rain govern the intensity of nocturnal bird migration in central Europe - a log-linear regression analysis. *Ardea* **90**:155–166.
- Foken, T., and C. Nappo. 2008. Micrometeorology. Springer. URL <http://books.google.nl/books?id=2y0yHjsevvMC>.
- Forchhammer, M. C., E. Post, and N. C. Stenseth. 2002. North Atlantic Oscillation timing of long- and short-distance migration. *Journal of Animal Ecology* **71**:1002–1014.
- Fortin, D., F. Liechti, and B. Bruderer. 1999. Variation in the nocturnal flight behaviour of migratory birds along the northwest coast of the Mediterranean Sea. *Ibis* **141**:480–488.
- Fransson, T. 1995. Timing and speed of migration in north and west European populations of Sylvia Warblers. *Journal of Avian Biology* **26**:39–48.
- Furrer, R., D. Nychka, and S. Sain, 2010. fields: tools for spatial data. R package version 6.3. URL <http://cran.r-project.org/web/packages/fields/>.

- GagHardo, A., P. Ioalé, F. Odetti, and V. P. Bingman. 2001. The ontogeny of the homing pigeon navigational map: evidence for a sensitive learning period. *Proceedings of the Royal Society of London. Series B: Biological Sciences* **268**:197–202.
- Gaspar, P., J.-Y. Georges, S. Fossette, A. Lenoble, S. Ferraroli, and Y. Le Maho. 2006. Marine animal behaviour: neglecting ocean currents can lead us up the wrong track. *Proceedings of the Royal Society B: Biological Sciences* **273**:2697–2702.
- Gates, W. H. 1933. Hailstone damage to birds. *Science* **78**:263–264.
- Gauthreaux, J., Sidney A. 1991. The flight behavior of migrating birds in changing wind fields: radar and visual analyses. *American Zoologist* **31**:187–204.
- Gauthreaux, S. A., J. E. Michi, and C. G. Belser, 2005. The temporal and spatial structure of the atmosphere and its influence on bird migration strategies. Pages 182–193 in R. Greenberg and P. P. Marra, editors. *Birds of Two Worlds: The Ecology and Evolution of Migration*. The Johns Hopkins University Press, Baltimore.
- Gerson, A. R., and C. G. Guglielmo. 2011. Flight at low ambient humidity increases protein catabolism in migratory birds. *Science* **333**:1434–1436.
- Gibson, R. N. 2003. Go with the flow: tidal migration in marine animals. *Hydrobiologia* **503**:153–161.
- Githeko, A., and W. Ndegwa. 2001. Predicting malaria epidemics in the Kenyan Highlands using climate data: a tool for decision makers. *Global Change and Human Health* **2**:54–63.
- Gramacy, R. B., and M. Taddy. 2010. Categorical inputs, sensitivity analysis, optimization and importance tempering with tgp version 2, an R package for treed Gaussian process models. *Journal of Statistical Software* **33**:1 – 48.
- Green, M., and T. Alerstam. 2002. The problem of estimating wind drift in migrating birds. *Journal of Theoretical Biology* **218**:485–496.
- Griffin, D. R. 1973. Oriented bird migration in or between opaque cloud layers. *Proceedings of the American Philosophical Society* **117**:117–141.
- Griffin, D. R., and C. D. Hopkins. 1974. Sounds audible to migrating birds. *Animal Behaviour* **22**:672–678.

- Guisan, A., and N. E. Zimmermann. 2000. Predictive habitat distribution models in ecology. *Ecological Modelling* **135**:147–186.
- Gwinner, E. 2003. Circannual rhythms in birds. *Current Opinion in Neurobiology* **13**:770–778.
- Gwinner, E., and B. Helm, 2003. Circannual and circadian contributions to the timing of avian migration. *in* P. Berthold, E. Gwinner, and E. Sonnenschein, editors. *Avian Migration*. Springer.
- Hahn, S., S. Bauer, and F. Liechti. 2009. The natural link between Europe and Africa – 2.1 billion birds on migration. *Oikos* **118**:624–626.
- Haibin, L., and K. Okada. 2007. An efficient earth mover's distance algorithm for robust histogram comparison. *Pattern Analysis and Machine Intelligence, IEEE Transactions on* **29**:840–853.
- Hastie, T., and R. Tibshirani. 1990. Generalized additive models. Chapman and Hall, London; New York.
- Hays, G. C., S. Fossette, K. A. Katselidis, P. Mariani, and G. Schofield. 2010. Ontogenetic development of migration: Lagrangian drift trajectories suggest a new paradigm for sea turtles. *Journal of the Royal Society Interface* **7**:1319–1327.
- Hedenström, A., and T. Alerstam. 1992. Climbing performance of migrating birds as a basis for estimating limits for fuel-carrying capacity and muscle work. *Journal of Experimental Biology* **164**:19–38.
- Hedenström, A., and T. Alerstam. 1995. Optimal flight speed of birds. *Philosophical Transactions: Biological Sciences* **348**:471–487.
- Hedenström, A., and T. Alerstam. 1998. How fast can birds migrate? *Journal of Avian Biology* **29**:424–432.
- Hengl, T., G. B. Heuvelink, and D. G. Rossiter. 2007. About regression-kriging: from equations to case studies. *Computers & Geosciences* **33**:1301–1315.
- Hey, T., and A. E. Trefethen. 2005. Cyberinfrastructure for e-Science. *Science* **308**:817–821.
- Hijmans, R. J., S. E. Cameron, J. L. Parra, P. G. Jones, and A. Jarvis. 2005. Very high resolution interpolated climate surfaces for global land areas. *International Journal of Climatology* **25**:1965–1978.

- Holleman, I., L. Delobbe, and A. Zgonc. 2008. Update on the European weather radar network (OPERA). *in* Proc. 5th Eur. Conf. on Radar in Meteorology and Hydrology, *Helsinki, Finland*. Finnish Meteorological Institute.
- Horton, T. W., R. N. Holdaway, A. N. Zerbini, N. Hauser, C. Garrigue, A. Andriolo, and P. J. Clapham. 2011. Straight as an arrow: humpback whales swim constant course tracks during long-distance migration. *Biology Letters* **doi:10.1098/rsbl.2011.0279**.
- Hughes, L. 2000. Biological consequences of global warming: is the signal already apparent? *Trends in Ecology and Evolution* **15**:56–61.
- Hüppop, O., and K. Hüppop. 2003. North Atlantic Oscillation and timing of spring migration in birds. *Proceedings of the Royal Society of London. Series B: Biological Sciences* **270**:233–240.
- James, M. C., R. A. Myers, and C. A. Ottensmeyer. 2005. Behaviour of leatherback sea turtles, *Dermochelys coriacea*, during the migratory cycle. *Proceedings of the Royal Society B: Biological Sciences* **272**:1547–1555.
- Janzen, F. J. 1994. Climate change and temperature-dependent sex determination in reptiles. *Proceedings of the National Academy of Sciences* **91**:7487–7490.
- Jenni, L., and M. Kéry. 2003. Timing of autumn bird migration under climate change: advances in long-distance migrants, delays in short-distance migrants. *Proceedings of the Royal Society of London. Series B: Biological Sciences* **270**:1467–1471.
- Jenni, L., and M. Schaub, 2003. Behavioural and physiological reactions to environmental variation in bird migration. Pages 155–171 *in* P. Berthold, E. Gwinner, and E. Sonnenschein, editors. *Avian Migration*. Springer-Verlag, Berlin Heidelberg.
- Jones, M. P., K. E. Pierce Jr., and D. Ward. 2007. Avian vision: a review of form and function with special consideration to birds of prey. *Journal of Exotic Pet Medicine* **16**:69 – 87.
- Jonzén, N., A. Lindén, T. Ergon, E. Knudsen, J. O. Vik, D. Rubolini, D. Piacentini, C. Brinch, F. Spina, L. Karlsson, M. Stervander, A. Andersson, J. Waldenström, A. Lehikoinen, E. Edvardsen, R. Solvang, and N. C. Stenseth. 2006. Rapid advance of spring arrival dates in long-distance migratory birds. *Science* **312**:1959–1961.

- Kalnay, E., M. Kanamitsu, R. Kistler, W. Collins, D. Deaven, L. Gandin, M. Iredell, S. Saha, G. White, J. Woollen, Y. Zhu, A. Leetmaa, R. Reynolds, M. Chelliah, W. Ebisuzaki, W. Higgins, J. Janowiak, K. C. Mo, C. Ropelewski, J. Wang, R. Jenne, and D. Joseph. 1996. The NCEP/NCAR 40-year reanalysis project. *Bulletin of the American Meteorological Society* **77**:437–471.
- Kanamitsu, M., W. Ebisuzaki, J. Woollen, S.-K. Yang, J. J. Hnilo, M. Fiorino, and G. L. Potter. 2002. NCEP/DOE AMIP-II Reanalysis (R-2). *Bulletin of the American Meteorological Society* **83**:1631–1643.
- Karlsson, H., C. Nilsson, J. Bäckman, and T. Alerstam. 2011. Nocturnal passerine migration without tailwind assistance. *Ibis* **153**:485–493.
- Karlsson, H., C. Nilsson, J. Bäckman, and T. Alerstam. 2012. Nocturnal passerine migrants fly faster in spring than in autumn: a test of the time minimization hypothesis. *Animal Behaviour* **83**:87–93.
- Kerlinger, P., and F. R. Moore. 1989. Atmospheric structure and avian migration. *Current Ornithology* **6**:109–142.
- Klaassen, M. 1995. Water and energy limitations on flight range. *The Auk* **112**:260–262.
- Klaassen, M. 1996. Metabolic constraints on long-distance migration in birds. *Journal of Experimental Biology* **199**:57–64.
- Klaassen, M. 2004. May dehydration risk govern long-distance migratory behaviour? *Journal of Avian Biology* **35**:4–6.
- Klaassen, M., and H. Biebach. 2000. Flight altitude of trans-Saharan migrants in autumn: a comparison of radar observations with predictions from meteorological conditions and water and energy balance models. *Journal of Avian Biology* **31**:47–55.
- Klaassen, R. H. G., M. Hake, R. Strandberg, and T. Alerstam. 2011. Geographical and temporal flexibility in the response to crosswinds by migrating raptors. *Proceedings of the Royal Society B: Biological Sciences* **278**:1339–1346.
- Kneib, T., and T. Petzoldt. 2007. Introduction to the special volume on “Ecology and Ecological Modeling in R”. *Journal of Statistical Software* **22**:1–7.

- Kokko, H. 1999. Competition for early arrival in migratory birds. *Journal of Animal Ecology* **68**:940–950.
- Kunz, T. H., S. A. Gauthreaux, N. I. Hristov, J. W. Horn, G. Jones, E. K. V. Kalko, R. P. Larkin, G. F. McCracken, S. M. Swartz, R. B. Srygley, R. Dudley, J. K. Westbrook, and M. Wikelski. 2008. Aeroecology: probing and modeling the aerosphere. *Integrative and Comparative Biology* **48**:1–11.
- Larkin, R. P. 1980. Transoceanic bird migration: evidence for detection of wind direction. *Behavioral Ecology and Sociobiology* **6**:229–232.
- Lawton, R. O., U. S. Nair, S. Pielke, R. A., and R. M. Welch. 2001. Climatic impact of tropical lowland deforestation on nearby montane cloud forests. *Science* **294**:584–587.
- Leshem, Y., and Y. YomTov. 1996. The use of thermals by soaring migrants. *Ibis* **138**:667–674.
- Lewin-Koh, N. J., R. Bivand, contributions by Edzer J. Pebesma, E. Archer, A. Baddeley, H.-J. Bibiko, S. Dray, D. Forrest, M. Friendly, P. Giraudoux, D. Golicher, V. G. Rubio, P. Hausmann, K. O. Hufthammer, T. Jagger, S. P. Luque, D. MacQueen, A. Niccolai, T. Short, B. Stabler, and R. Turner, 2011. maptools: Tools for reading and handling spatial objects. R package version 0.8-12. URL <http://CRAN.R-project.org/package=maptools>.
- Liechti, F. 1993. Nächtlicher Vogelzug im Herbst über Süddeutschland: Winddrift und Kompensation. *Journal für Ornithologie* **134**:373–404.
- Liechti, F. 1995. Modelling optimal heading and airspeed of migrating birds in relation to energy expenditure and wind influence. *Journal of Avian Biology* **26**:330–336.
- Liechti, F. 2006. Birds: blowin' by the wind? *Journal of Ornithology* **147**:202–211.
- Liechti, F., and B. Bruderer. 1995. Direction, speed, and composition of nocturnal bird migration in the south of israel. *Israel Journal of Zoology* **41**:501–515.
- Liechti, F., and B. Bruderer. 1998. The relevance of wind for optimal migration theory. *Journal of Avian Biology* **29**:561–568.
- Liechti, F., M. Klaassen, and B. Bruderer. 2000. Predicting migratory flight altitudes by physiological migration models. *Auk* **117**:205–214.

- Liechti, F., S. Komenda-Zehnder, and B. Bruderer. 2012. Orientation of passerine trans-Saharan migrants: the directional shift ('Zugknick') reconsidered for free-flying birds. *Animal Behaviour* **83**:63–68.
- Liechti, F., and H. Schmaljohann. 2007. Wind-governed flight altitudes of nocturnal spring migrants over the Sahara. *Ostrich* **78**:337–341.
- Liu, X., and N. Chernetsov. 2012. Avian orientation: multi-cue integration and calibration of compass systems. *Chinese Birds* **3**:1–8.
- Lohmann, K. J., and C. M. F. Lohmann. 1992. Orientation to oceanic waves by green turtle hatchlings. *Journal of Experimental Biology* **171**:1–13.
- Luschi, P., G. C. Hays, and F. Papi. 2003. A review of long-distance movements by marine turtles, and the possible role of ocean currents. *Oikos* **103**:293–302.
- MacArthur, R. H. 1972. *Geographical Ecology*. Harper and Row, New York.
- Mandel, J. T., K. L. Bildstein, G. Bohrer, and D. W. Winkler. 2008. Movement ecology of migration in turkey vultures. *Proceedings of the National Academy of Sciences of the United States of America* **105**:19102–19107.
- Marengo, J., C. Nobre, J. Tomasella, M. Cardoso, and M. Oyama. 2008. Hydro-climatic and ecological behaviour of the drought of Amazonia in 2005. *Philosophical Transactions of the Royal Society of London B Biological Sciences* **363**:1773–1778.
- Martin, G. R. 2011. Understanding bird collisions with man-made objects: a sensory ecology approach. *Ibis* **153**:239–254. URL <http://dx.doi.org/10.1111/j.1474-919X.2011.01117.x>.
- McLaren, J. D., J. Shamoun-Baranes, and W. Bouten. 2012. Wind selectivity and partial compensation for wind drift among nocturnally migrating passerines. *Behavioral Ecology* **In press**.
- Murray, D., J. McWhirter, S. Wier, and S. Emmerson, 2003. The Integrated Data Viewer: a Web-enabled application for scientific analysis and visualization. *in* 19th Intl. Conf. on IIPS for Meteorology, Oceanography and Hydrology. URL <http://ams.confex.com/ams/pdfpapers/57870.pdf>.
- Nathan, R. 2005. Long-distance dispersal research: building a network of yellow brick roads. *Diversity and Distributions* **11**:125–130.

- Nathan, R., N. Sapir, A. Trakhtenbrot, G. G. Katul, G. Bohrer, M. Otte, R. Avissar, M. B. Soons, H. S. Horn, M. Wikelski, and S. A. Levin. 2005. Long-distance biological transport processes through the air: can nature's complexity be unfolded in silico? *Diversity and Distributions* **11**:131–137.
- Newton, I. 2008. *The Migration Ecology of Birds*. 1 edition. Academic Press/Elsevier, Amsterdam.
- Nievergelt, F., F. Liechti, and B. Bruderer. 1999. Migratory directions of free-flying birds versus orientation in registration cages. *Journal of Experimental Biology* **202**:2225–2231.
- Nisbet, I. C. T. 1963. Measurements with radar of the height of nocturnal migration over Cape Cod, Massachusetts. *Bird-Banding* **34**:57–67.
- Ottersen, G., B. Planque, A. Belgrano, E. Post, P. Reid, and N. Stenseth. 2001. Ecological effects of the North Atlantic Oscillation. *Oecologia* **128**:1–14.
- Parmesan, C. 2006. Ecological and evolutionary responses to recent climate change. *Annual Review of Ecology, Evolution, and Systematics* **37**:637–669.
- Parmesan, C., and G. Yohe. 2003. A globally coherent fingerprint of climate change impacts across natural systems. *Nature* **421**:37–42.
- Peel, M. C., B. L. Finlayson, and T. A. McMahon. 2007. Updated world map of the Köppen-Geiger climate classification. *Hydrology and Earth System Sciences* **11**:1633–1644.
- Pennycuick, C. 2008. *Modelling the Flying Bird*. Academic Press/Elsevier, Amsterdam.
- Persson, A., 2011. User guide to ECMWF forecast products. European Centre for Medium-Range Weather Forecasts. URL http://www.ecmwf.int/products/forecasts/guide/user_guide.pdf.
- Piersma, T., and J. Jukema. 1990. Budgeting the flight of a long-distance migrant - changes in nutrient reserve levels of bar-tailed godwits at successive spring staging sites. *Ardea* **78**:315–337.
- Plate, T., and R. Heiberger, 2004. abind: combine multi-dimensional arrays. R package version 1.1-0. URL <http://cran.r-project.org/web/packages/abind/>.

- Pounds, J. A., M. P. L. Fogden, and J. H. Campbell. 1999. Biological response to climate change on a tropical mountain. *Nature* **398**:611–615.
- Prange, H. D. 1976. Energetics of swimming of a sea turtle. *Journal of Experimental Biology* **64**:1–12.
- Pyle, P., N. Nur, R. P. Henderson, and D. F. DeSante. 1993. The effects of weather and lunar cycle on nocturnal migration of landbirds at southeast Farallon Island, California. *The Condor* **95**:343–361.
- R Development Core Team, 2010. R: a language and environment for statistical computing. URL <http://cran.r-project.org/>.
- Rabøl, J., 1974. Forecast models for bird-migration intensities in Denmark. in Proceedings of the 9th International Bird Strike Committee. Frankfurt.
- Raess, M. 2008. Continental efforts: migration speed in spring and autumn in an inner-Asian migrant. *Journal of Avian Biology* **39**:13–18.
- Rew, R., G. Davis, S. Emmerson, H. Davies, E. Hartnett, and D. Heimbigner, 2010. The NetCDF users guide version 4.1.1. University Corporation for Atmospheric Research. URL <http://www.unidata.ucar.edu/software/netcdf/docs/netcdf/>.
- Reynolds, A. M., D. R. Reynolds, A. D. Smith, and J. W. Chapman. 2010. A single wind-mediated mechanism explains high-altitude ‘non-goal oriented’ headings and layering of nocturnally migrating insects. *Proceedings of the Royal Society B: Biological Sciences* **277**:765–772.
- Richardson, W. J. 1978. Timing and amount of bird migration in relation to weather: a review. *Oikos* **30**:224–272.
- Richardson, W. J., 1990a. Timing of bird migration in relation to weather: updated review. Pages 78–101 in E. Gwinner, editor. *Bird Migration: Physiology and Ecophysiology*. Springer, Berlin.
- Richardson, W. J. 1990b. Wind and orientation of migrating birds: A review. *Cellular and Molecular Life Sciences* **46**:416–425.
- Richardson, W. J., and T. West, 2000. Serious birdstrike accidents to military aircraft: updated list and summary. Pages 67–97 in Proceedings of the 25th International Bird Strike Committee, volume 1. Amsterdam.
- Rio, M. H., and F. Hernandez. 2004. A mean dynamic topography computed over the world ocean from altimetry, in situ measurements, and a geoid model. *Journal of Geophysical Research* **109**:C12032.

- Robinson, W. D., M. S. Bowlin, I. Bisson, J. Shamoun-Baranes, K. Thorup, R. H. Diehl, S. M. Kunz, and D. W. Winkler. 2010. Integrating concepts and technologies to advance the study of bird migration. *Frontiers in Ecology and the Environment* **8**:354–361.
- Rogovin, M., and G. T. Frampton Jr., 1980. Three Mile Island: a report to the commissioners and to the public. Technical Report Volume I, Nuclear Regulatory Commission. URL <http://www.threemileisland.org/downloads/354.pdf>.
- Rohli, R. V., and A. J. Vega. 2007. Climatology. Illustrated edition. Jones and Bartlett Publishers, Boston.
- Root, T. L., J. T. Price, K. R. Hall, S. H. Schneider, C. Rosenzweig, and J. A. Pounds. 2003. Fingerprints of global warming on wild animals and plants. *Nature* **421**:57–60.
- Sakai, M., K. Aoki, K. Sato, M. Amano, R. W. Baird, D. L. Webster, G. S. Schorr, and N. Miyazaki. 2011. Swim speed and acceleration measurements of short-finned pilot whales (*Globicephala macrorhynchus*) in Hawai'i. *Mammal Study* **36**:55–59.
- Salmon, M., and K. J. Lohmann. 1989. Orientation cues used by hatchling loggerhead sea turtles (*Caretta caretta* L.) during their offshore migration. *Ethology* **83**:215–228.
- Salmon, M., and J. Wyneken. 1987. Orientation and swimming behavior of hatchling loggerhead turtles *Caretta caretta* L. during their offshore migration. *Journal of Experimental Marine Biology and Ecology* **109**:137–153.
- Schaub, M., F. Liechti, and L. Jenni. 2004. Departure of migrating European robins, *Erithacus rubecula*, from a stopover site in relation to wind and rain. *Animal Behaviour* **67**:229–237.
- Schmaljohann, H. 2008. Sustained bird flights occur at temperatures far beyond expected limits. *Animal Behaviour* **76**:1133.
- Schmaljohann, H., F. Liechti, and B. Bruderer. 2009. Trans-Saharan migrants select flight altitudes to minimize energy costs rather than water loss. *Behavioral Ecology Sociobiology* **63**:1609–1619.
- Schmaljohann, H., and B. Naef-Daenzer. 2011. Body condition and wind support initiate the shift of migratory direction and timing of nocturnal departure in a songbird. *Journal of Animal Ecology* **80**:1115–1122.

- Sedda, L., H. E. Brown, B. V. Purse, L. Burgin, J. Gloster, and D. J. Rogers. 2012. A new algorithm quantifies the roles of wind and midge flight activity in the bluetongue epizootic in northwest Europe. *Proceedings of the Royal Society B: Biological Sciences* doi:10.1098/rspb.2011.2555.
- Sgouros, T., 2004. OPeNDAP user guide version 1.14. The University of Rhode Island and The Massachusetts Institute of Technology. URL www.opendap.org/pdf/guide.pdf.
- Shamoun-Baranes, J., A. Bahrad, P. Alpert, P. Berthold, Y. Yom-Tov, Y. Dvir, and Y. Leshem. 2003a. The effect of wind, season and latitude on the migration speed of white storks *Ciconia ciconia*, along the eastern migration route. *Journal of Avian Biology* 34:97–104.
- Shamoun-Baranes, J., W. Bouten, L. Buurma, R. DeFusco, A. Dekker, H. Sierdsema, F. Sluiter, J. van Belle, H. van Gasteren, and E. E. van Loon. 2008. Avian information systems: developing web-based bird avoidance models. *Ecology and Society* 13:38.
- Shamoun-Baranes, J., W. Bouten, and E. E. van Loon. 2010. Integrating meteorology into research on migration. *Integrative and Comparative Biology* 50:280–292.
- Shamoun-Baranes, J., Y. Leshem, Y. Yom-Tov, and O. Liechti. 2003b. Differential use of thermal convection by soaring birds over central Israel. *Condor* 105:208–218.
- Shamoun-Baranes, J., and H. van Gasteren. 2011. Atmospheric conditions facilitate mass migration events across the North Sea. *Animal Behaviour* 81:691–704.
- Shamoun-Baranes, J., E. van Loon, F. Liechti, and W. Bouten. 2007. Analyzing the effect of wind on flight: pitfalls and solutions. *Journal of Experimental Biology* 210:82–90.
- Shannon, H. D., G. Young, M. Yates, M. Fuller, and W. Seegar. 2002. American White Pelican soaring flight times and altitudes relative to changes in thermal depth and intensity. *Condor* 104:679–683.
- Shepard, D., 1968. A two-dimensional interpolation function for irregularly-spaced data. Pages 517–524 in *Proceedings of the 1968 23rd ACM national conference*. ACM '68, ACM, New York, NY, USA. URL <http://doi.acm.org/10.1145/800186.810616>.

- Shoemaker, V., and K. A. Nagy. 1977. Osmoregulation in amphibians and reptiles. *Annual Review of Physiology* **39**:449–471.
- Sinelschikova, A., V. Kosarev, I. Panov, and A. Baushev. 2007. The influence of wind conditions in Europe on the advance in timing of the spring migration of the song thrush (*Turdus philomelos*) in the south-east Baltic region. *International Journal of Biometeorology* **51**:431–440.
- Smith, A. G., and H. R. Webster. 1955. Effects of hail storms on waterfowl populations in Alberta, Canada: 1953. *The Journal of Wildlife Management* **19**:368–374.
- Stout, I. J., and G. W. Cornwell. 1976. Nonhunting mortality of fledged North American waterfowl. *The Journal of Wildlife Management* **40**:681–693.
- Stull, R. B. 1988. *An Introduction to Boundary Layer Meteorology*. 1st edition. Kluwer Academic Publishers, Dordrecht.
- Swanson, D. L., and E. T. Liknes. 2006. A comparative analysis of thermogenic capacity and cold tolerance in small birds. *Journal of Experimental Biology* **209**:466–474.
- Tarroso, P., and H. Rebelo. 2010. E-Clic – easy climate data converter. *Ecography* **33**:617–620.
- The Cesar Consortium, 2011. Cesar: Cabauw experimental site for atmospheric research. URL <http://www.cesar-database.nl/>.
- Thorpe, J. 2003. Fatalities and destroyed civil aircraft due to bird strikes. 1912 - 2002. International Bird Strike Committee **IBSC26**.
- Thorup, K., T. Alerstam, M. Hake, and N. Kjellen. 2003. Bird orientation: compensation for wind drift in migrating raptors is age dependent. *The Royal Society Biology Letters* **270**:8–11.
- Thorup, K., and J. Rabøl. 2001. The orientation system and migration pattern of long-distance migrants: conflict between model predictions and observed patterns. *Journal of Avian Biology* **32**:111–119.
- Tinbergen, N. 1963. On aims and methods in Ethology. *Zeitschrift für Tierpsychologie* **20**:410–443.
- Tucker, V. A. 1968. Respiratory physiology of house sparrows in relation to high-altitude flight. *Journal of Experimental Biology* **48**:55–66.

- Undén, P., L. Rontu, H. Järvinen, P. Lynch, J. Calvo, G. Cats, J. Cuxart, K. Eerola, C. Fortelius, J. A. Garcia-Moya, C. Jones, G. Lenderlink, A. McDonald, R. McGrath, B. Navascues, N. W. Nielsen, V. Ødegaard, E. Rodriguez, M. Rummukainen, R. Rööm, K. Sattler, B. H. Sass, H. Savijärvi, B. W. Schreur, R. Sigg, H. The, and A. Tijm. 2002. HIRLAM-5 Scientific Documentation. Swedish Meteorological and Hydrological Institute (SMHI).
- Urbanek, S., and Y. Rubner. 2011. emdist: Earth Mover's Distance. R package version 0.2-1. URL <http://CRAN.R-project.org/package=emdist>.
- van Belle, J., J. Shamoun-Baranes, E. E. van Loon, and W. Bouten. 2007. An operational model predicting autumn bird migration intensities for flight safety. *Journal of Applied Ecology* **44**:864–874.
- Vavrek, M. J. 2011. fossil: palaeoecological and palaeogeographical analysis tools. *Palaeontologia Electronica* **14**.
- Vrugt, J. A., J. v. Belle, and W. Bouten. 2007. Pareto front analysis of flight time and energy use in long-distance bird migration. *Journal of Avian Biology* **38**:432–442.
- Waldvogel, J. A. 1990. The Bird's Eye View. *American Scientist* **78**:342–353.
- Wallraff, H. G. 2004. Avian olfactory navigation: its empirical foundation and conceptual state. *Animal Behaviour* **67**:189–204.
- Walther, G. R., E. Post, P. Convey, A. Menzel, C. Parmesan, T. J. C. Beebee, J. M. Fromentin, O. Hoegh-Guldberg, and F. Bairlein. 2002. Ecological responses to recent climate change. *Nature* **416**:389–395.
- Wang, J. Y. 1960. A critique of the heat unit approach to plant response studies. *Ecology* **41**:785–790.
- Weber, T. P., T. Alerstam, and A. Hedenstrom. 1998. Stopover decisions under wind influence. *Journal of Avian Biology* **29**:552–560.
- Weber, T. P., and A. Hedenstrom. 2000. Optimal stopover decisions under wind influence: the effects of correlated winds. *Journal of Theoretical Biology* **205**:95–104.
- Webster, T., V. Vieira, J. Weinberg, and A. Aschengrau. 2006. Method for mapping population-based case-control studies: an application using generalized additive models. *International Journal of Health Geographics* **5**:26.

- Wikelski, M., R. W. Kays, N. J. Kasdin, K. Thorup, J. A. Smith, and G. W. Swenson. 2007. Going wild: what a global small-animal tracking system could do for experimental biologists. *Journal of Experimental Biology* **210**:181–186.
- Wikelski, M., E. M. Tarlow, A. Raim, R. H. Diehl, R. P. Larkin, and G. H. Visser. 2003. Avian metabolism: costs of migration in free-flying songbirds. *Nature* **423**:704–704.
- Wilson, R., E. Shepard, and N. Liebsch. 2008. Prying into the intimate details of animal lives: use of a daily diary on animals. *Endangered Species Research* **4**:123–137.
- Wiltschko, R., and W. Wiltschko. 2003. Avian navigation: from historical to modern concepts. *Animal Behaviour* **65**:257–272.
- Wiltschko, W., and R. Wiltschko. 2005. Magnetic orientation and magnetoreception in birds and other animals. *Journal of Comparative Physiology A: Neuroethology, Sensory, Neural, and Behavioral Physiology* **191**:675–693.
- Wingfield, J. C. 1984. Influence of weather on reproduction. *Journal of Experimental Zoology* **232**:589–594.
- Wood, S. N. 2006. Low-rank scale-invariant tensor product smooths for generalized additive mixed models. *Biometrics* **62**:1025–1036.
- Wood, S. N. 2008. Fast stable direct fitting and smoothness selection for generalized additive models. *Journal of the Royal Statistical Society: Series B (Statistical Methodology)* **70**:495–518.
- Wu, L.-Q., and J. D. Dickman. 2012. Neural correlates of a magnetic sense. *Science* doi: **10.1126/science.1216567**.
- Yaukey, P. H., and S. C. Powell. 2008. Numbers of migratory birds stopping over in New Orleans, Louisiana, USA in relation to weather. *The Wilson Journal of Ornithology* **120**:286–295.
- Yohannes, E., H. Biebach, G. Nikolaus, and D. J. Pearson. 2009. Migration speeds among eleven species of long-distance migrating passerines across Europe, the desert and eastern Africa. *Journal of Avian Biology* **40**:126–134.
- Zehnder, S., S. Åkesson, F. Liechti, and B. Bruderer. 2001. Nocturnal autumn bird migration at Falsterbo, South Sweden. *Journal of Avian Biology* **32**:239.

Summary

The life cycle of many bird species involves the twice-annual movement between a breeding ground and a wintering ground that we refer to as ‘migration’. To complete these journeys, birds must successfully navigate many obstacles including a dynamic atmosphere. To make optimal use of this ever-fluctuating milieu requires not only an uncanny sense of timing but an intuitive sense of the environment and its proclivities.

The subject of this thesis is the relationship between bird migration and the atmosphere, though we perhaps give the most consideration to the role of wind. Often the concepts addressed lean toward migrants engaged in flapping flight, however, many of the theoretical discussions apply to birds in general; where appropriate, we distinguish between weather effects on different flight strategies. All measurements of bird migration dynamics were made in the Netherlands using either Medium-Power Military Surveillance Radar (MPR) or Doppler weather radar. Atmospheric data were obtained almost exclusively from gridded datasets derived from analysis/forecast models in combination with data assimilation systems.

The thesis is roughly divided into three parts: tools and methods, biological analyses, and applications.

Tools and methods

There are many ways in which the atmosphere can influence migration. Components of the atmosphere (e.g. wind condition, temperature, humidity) can each exert independent influence on migratory efficiency, yet the specific influence of each component must often be considered in the context of the others.

A significant obstacle in these types of analyses is therefore the efficient management of (often large amounts of) data. A wide range of variables must be collected from often disparate data sources stored in various formats and often at different spatio-temporal resolution. These data must be appropriately merged, and, in order to be useful, tools must be in place to visualize and analyze these data. Having these tools and systems in place is often the first step toward conducting efficient and productive analyses. We therefore began by introducing in Chapter 2 the RNCEP package containing functions to obtain atmospheric data from two high-quality, and freely-available, gridded global data sets, potentially process those data into various longer-term climatic indices, and visualize the data on a map. In order to benefit a diverse research community, the package was written in the open-source R language.

Wind is a particularly challenging variable to consider in bird migration studies. Whereas variables such as temperature and humidity can be described with a single value, two values (often speed and direction or zonal and meridional components) are generally necessary to properly quantify wind condition. The fact that wind is composed of two interdependent components complicates quantitative comparisons of wind condition in relation to migration, for example in linear models. It is possible to reduce the two components of the wind to a single value, which is often termed ‘wind profit’ in bird migration studies, but doing so requires making specific assumptions about a bird’s goals (and perhaps abilities). In Chapter 3, we described methods that have been previously applied to determine wind profit and developed some new methods as well. We determined the sensitivity of these various methods to uncertainty in their assumptions, and we quantified differences between the methods for specific wind conditions. To illustrate the cumulative effects of these methods, we simulated bird flight according to the different assumed behaviors using real wind conditions. We identified differences in ground- and airspeed, route, and arrival probability that arose when selecting one method or another. Because of the differences we identified, and because the magnitude of these differences depended heavily on the specific wind conditions encountered, researchers should consider the assumptions that are made in the application of a particular wind profit equation in the context of their specific migratory system. To facilitate these considerations, we have incorporated into the RNCEP package a dynamic flight-simulation model in which the specific assumptions of a wind profit equation can be applied to a particular migratory system to determine the real-world consequences of the assumptions that are made.

Biological analyses

With tools and methods in place, it was possible to derive biological insight by analyzing bird migration dynamics in relation to atmospheric conditions. In Chapter 4, we considered seasonal differences in avian migration speed. The speed and direction of the wind can have a dramatic impact on the ground-speed of a migrating bird, which in turn affects a migrant's overall migration speed. Wind conditions, while variable, also exhibit persistent dynamics described by the general circulation of the atmosphere. We hypothesized that wind conditions in Western Europe were more supportive of northeasterly-directed spring migration than southwesterly-directed autumn migration. We further proposed that these seasonal differences in wind support may lead to seasonal differences in the groundspeed of migrants, resulting in equivalent differences in overall migration speed. Using a simple wind profit equation, we first quantified any differences in the frequency of supportive winds between spring and autumn throughout Europe. We found that winds in the Netherlands were much more supportive of spring migration than autumn migration. Similarly, we found that migrants in the Netherlands had a significantly higher groundspeed in spring compared to autumn. Since these seasonal differences in groundspeed were not caused by seasonal differences in airspeed, our results suggested significantly higher migration speeds through the Netherlands in spring compared to autumn due to prevailing winds. The frequency of beneficial winds may also affect migration speed by impacting the time birds must remain at a stopover site waiting for wind conditions in which they can make acceptable progress. We proposed that areas with frequently prohibitive winds may be considered as a kind of ecological barrier and that birds may be able to optimize time and energy expenditure by circumventing some of these areas.

Birds have the opportunity to select often quite different atmospheric conditions simply by adjusting their altitude. By considering the altitudes birds select during migration, we may derive a better understanding of the influence of different atmospheric components on migration and also determine the priority birds place on different atmospheric properties. The majority of quantitative empirical research has suggested that birds select migratory altitudes based primarily on considerations of wind condition. In Chapter 5, following the approaches presented in several previous studies, we considered whether and to what degree wind could explain altitude distributions of nocturnally migrating birds in the Netherlands. We then performed forward stepwise variable selection using Generalized Additive Models to determine the specific influence of various atmospheric variables on, and the precedence these variables take in determining, altitude distributions of avian migrants. Overall,

we found weak correlations between altitude distributions of wind support and altitude distributions of migrating birds; however, we did find wind to be influential: increasing tailwind support with height increased the probability of birds climbing to higher altitude; birds sought out supportive winds at higher altitude when winds near the surface were prohibitive; and birds seemed to assess wind support at a given altitude in relation to conditions at the surface rather than in relation to best wind conditions available. We also found that birds avoided lower temperatures. Nonetheless, altitude itself explained the largest amount of variability in avian altitude distributions and suggested that migrants generally preferred lower altitudes. While birds can minimize the time and energy spent on migration by selecting altitudes with more profitable wind conditions, high altitude flight may entail risks that birds deem unnecessary when they can make acceptable progress at lower altitude. This suggested that birds balanced trade-offs between multiple objectives and optimized their travel based on multiple criteria.

Applications

As our understanding of migratory dynamics in relation to atmospheric conditions improves, we can move toward developing applications that benefit both birds and society. In this context, we developed an ensemble prediction system in Chapter 6 to forecast migration intensity at two locations in the Netherlands using measurements obtained from Doppler weather radar. This ensemble system can be applied, for example, in flight safety to help prevent collisions between birds and aircraft. Natural systems tend to be chaotic in that subtle variations in any of a number of initial conditions can accumulate and propagate through the system to produce dramatically different outcomes. Ensembles tend to dampen chaotic influences on predictions by averaging the outcomes suggested by many different models, making ensemble predictions generally more robust. Also, the agreement among the individual models in an ensemble implicitly indicates the probability of a particular outcome. Our use of an ensemble also enabled us to account for the effects of many different atmospheric variables on bird migration despite the complicated correlations that often exist between these variables. We determined the performance of our ensemble system in reference to some benchmarks, and we determined how well models developed for each location predicted conditions at the other location. The ensemble development procedure we implemented was robust and exportable such that it could be used to quickly develop predictive models of migration intensity in new locations. Since networks of weather radar already exist, the procedure we outlined can potentially be used to develop

standardized predictive models over vast geographical areas.

Samenvatting

Veel vogelsoorten migreren ieder jaar van hun overwinteringsgebied naar hun broedgebied en terug. Onderweg hebben de vogels te maken met wisselende weersomstandigheden en andere obstakels. Het succesvol volbrengen van de migratie vereist een haast bovennatuurlijk goed gevoel voor timing en een goede intuïtie met betrekking tot de grillen der natuur.

Het onderwerp van deze dissertatie is de relatie tussen de weersomstandigheden en vogelmigratie, waarbij de nadruk ligt op de invloed van wind op de klapwiekende vlucht van zangvogels; echter, de theoretische discussies zijn veelal van toepassing op vogelsoorten in het algemeen. Waar relevant maken we onderscheid tussen weerseffecten op verschillende vluchtstrategieën. De vogelmigratiegegevens voor dit onderzoek zijn afkomstig van militaire observatieradar (Medium-Power Radar; MPR) en Doppler weerradar; gegevens over de weersomstandigheden zijn vooral afkomstig van externe bronnen. Deze bronnen gebruiken modellen en allerlei typen metingen om ruimtelijk verdeelde schattingen te maken van de toestand van de atmosfeer.

De dissertatie is onderverdeeld in 3 delen, te weten: methodes, biologische analyses, en toepassingen.

Methodes

Weersomstandigheden zoals wind, temperatuur en luchtvuchtigheid kunnen de efficiëntie van migratie op veel manieren beïnvloeden. Het effect van een gegeven factor kan echter meestal niet losgekoppeld worden van andere factoren—de analyse krijgt daardoor dus een multidimensinaal karakter. Omdat er veel gegevens gemoeid zijn met elke factor, en er meerdere factoren

onderzocht worden, is efficiënt gegevensbeheer van groot belang. De gegevens kunnen tevens uit verschillende bronnen afkomstig zijn, en hebben ook niet altijd dezelfde indeling of ruimtelijke resolutie. Voordat ze gebruikt kunnen worden, moeten de gegevens dus geconverteerd en geïnterpoleerd worden door middel van software. De RNCEP software (Hoofdstuk 2) is ontwikkeld om de toegang tot twee kwalitatief goede en online gratis beschikbare gegevensbronnen te vergemakkelijken. De functionaliteit van de software omvat het on-demand downloaden, bewerken, aggregeren en visualiseren van atmosferische variabelen. De software is geschreven in de open-source taal R, zodat andere onderzoekers er makkelijk toegang toe hebben.

Met betrekking tot de statistische analyse is met name wind een lastige variabele. Dit komt omdat de windconditie op een gegeven punt in de ruimte en tijd niet in één getal samen te vatten is—wind is een vector met twee componenten: snelheid en richting. Hierin onderscheidt wind zich van andere variabelen zoals luchtvuchtigheid en temperatuur. Omdat de twee componenten van de windvector niet onafhankelijk zijn, wordt kwantitatieve analyse zoals bijvoorbeeld lineaire regressie bemoeilijkt. De windvector wordt in vogelmigratiestudies daarom vaak gereduceerd tot één getal, de zogenaamde ‘wind profit’, maar dit vereist een aantal aannames met betrekking tot de doelen die vogels nastreven, en wellicht ook met betrekking tot hun fysiologische grenzen.

In Hoofdstuk 3 behandelen we de bestaande methodes om de wind profit te berekenen en introduceren we een aantal nieuwe, door ons ontwikkelde methodes. We hebben onderzocht in welke mate de aannames van elke methode van invloed zijn op het gesimuleerde vlieggedrag van vogels, gegeven de gemeten windcondities. We hebben daarbij in het bijzonder gelet op verschillen in snelheid ten opzichte van de grond, snelheid ten opzichte van de lucht, route, en de waarschijnlijkheid van aankomst. We concluderen dat verschillende methodes kunnen leiden tot grote verschillen in gesimuleerd gedrag, en dat de magnitude van de onderlinge verschillen vooral afhangt van de specifieke weersomstandigheden. In toekomstige onderzoeken moet daarom rekening gehouden worden met de mogelijke effecten van de aannames die ten grondslag liggen aan het berekenen van de wind profit. Om dit te vergemakkelijken, hebben we de RNCEP software uitgebreid met een generiek toepasbaar, dynamisch model voor het simuleren van vlieggedrag gegeven zulke aannames.

Biologische analyses

De door ons ontwikkelde methodes hebben het mogelijk gemaakt om vogelmigratie in relatie tot de weersomstandigheden te analyseren. In Hoofdstuk 4 behandelen we de seizoenale verschillen in migratiesnelheid, waarbij de snel-

heid en richting van de wind een dramatische invloed heeft op de snelheid waarmee een vogel zich ten opzichte van de grond verplaatst, en daarmee dus ook op de totale migratiesnelheid. Hoewel windcondities kunnen variëren op korte termijn, is er tevens sprake van meer aanhoudende dynamiek die gedreven wordt door de wereldwijde luchtcirculatie. Wij hebben verondersteld dat de windcondities in West-Europa beter geschikt zijn voor de lentemigratie, die in noordoostelijke richting plaatsvindt, dan voor de herfstmigratie, die in zuidwestelijke richting plaatsvindt. We hebben verder verondersteld dat de verschillen in windcondities tussen deze seizoenen van invloed kunnen zijn op de snelheid waarmee migranten zich verplaatsen ten opzichte van de grond, en dus ook op de totale migratiesnelheid.

Met behulp van een simpele wind profit formule hebben we vergeleken hoe vaak de windcondities in Europa gedurende de lente en de herfst gunstig zijn voor vogelmigratie. Hieruit blijkt dat windcondities in Nederland veel gunstiger zijn voor de lentemigratie dan voor de herfstmigratie. Gedurende de lentemigratie hadden migranten in Nederland een significant hogere snelheid ten opzichte van de grond dan gedurende de herfstmigratie. De seizoенale verschillen in snelheid ten opzichte van de grond waren het gevolg van de heersende windrichting. De windcondities kunnen de migratiesnelheid ook nog op een andere manier beïnvloeden, namelijk doordat vogels langer op zogenoemde ‘stopover sites’ moet blijven in afwachting van windcondities waarbij ze acceptabele voortgang kunnen boeken. Gebieden waar zulke condities relatief zeldzaam zijn, kunnen beschouwd worden als ecologische barièrres. Door zulke barièrres te vermijden kunnen migranten wellicht zuiniger omgaan met hun beschikbare energie en tijd.

Afhankelijk van de vlieghoogte kunnen de weersomstandigheden vaak relatief sterk variëren; vogels kunnen daarvan gebruik maken door hoger of juist lager te gaan vliegen. Door te onderzoeken welke hoogtes de vogels prefereren, zouden we een beter begrip kunnen ontwikkelen van het effect van weersomstandigheden op migratie, en van het belang dat vogels toekennen aan bepaalde weersomstandigheden. Kwantitatief empirisch onderzoek dat tot nu toe gedaan is, suggereert veelal dat de vlieghoogte vooral beïnvloed wordt door de heersende windcondities. In Hoofdstuk 5 hebben wij voor Nederland onderzocht in welke mate de dichtheidsverdeling van vogels met hoogte verklaard kan worden door de heersende windcondities. We hebben daartoe een voorwaartse, stapsgewijze variabele-selectie uitgevoerd in combinatie met ‘Generalized Additive Models’, zodat bepaald kon worden wat de specifieke invloed is van individuele atmosferische variabelen, en welke variabelen belangrijker zijn dan andere. Wij hebben aangetoond dat de dichtheidsverdeling met de hoogte slechts zwak gecorreleerd is aan de verdeling van windcondities

met de hoogte. Wind is echter wel degelijk van invloed: vogels waren meer geneigd om op grotere hoogte te gaan vliegen als er daar een sterker positief effect van rugwind was; wanneer de windcondities aan het oppervlak ongunstig waren en op grotere hoogte gunstig, gingen vogels hoger vliegen; vogels leken de wind profit verdeling met de hoogte te evalueren in verhouding tot de wind profit aan het oppervlak, en niet zozeer in verhouding tot de meest gunstige wind profit in het verticale profiel. Behalve wind is ook de temperatuur van invloed. We hebben gevonden dat vogels liever niet op hoogtes vliegen waar de lucht koud is. Echter, de belangrijkste verklarende factor in de selectie van de vlieghoogte door vogels was simpelweg de hoogte zelf—vogels vliegen het liefst vrij laag boven het oppervlak als ze de keuze hebben. Vogels zouden weliswaar zuiniger met hun beschikbare energie en tijd kunnen omgaan door op een grotere hoogte te gaan vliegen als er daar gunstiger windcondities heersen, maar het vliegen op grotere hoogte kan verhoogde risico's met zich meebrengen, die de vogels wellicht onnodig achten zolang de windcondities op lagere hoogte een acceptabele voortgang toelaten. Dit gedrag suggereerde dat vogels een optimale balans zoeken in het compromis tussen verschillende doelstellingen.

Toepassingen

Wanneer we beter begrijpen hoe migratie gedreven wordt door de weersomstandigheden, kunnen we toepassingen beter implementeren, wat ten gunste zal komen van zowel vogels als de maatschappij. Binnen dit kader hebben wij een systeem ontwikkeld dat metingen afkomstig van Doppler weerradars in Nederland gebruikt om de migratie-intensiteit van vogels te voorspellen op twee plaatsen, zodat vliegtuigen daar rekening mee kunnen houden en er minder kans is op botsingen met vogels (Hoofdstuk 6). Het systeem is gebaseerd op een ensemble van verschillende modellen. Natuurlijke systemen kunnen namelijk chaotisch gedrag vertonen, waarbij aanvankelijk kleine verschillen in korte tijd kunnen leiden tot zeer uiteenlopend gedrag. Ensemblevoorspellingen worden gemaakt op basis van meerdere modellen, waardoor chaotische effecten uitmiddelen en de voorspelling als geheel meestal meer robuust is dan een voorspelling op basis van slechts één model. Een ander voordeel van ensemblevoorspellingen is dat de mate van overeenstemming tussen de verschillende ensembles een maat vormt voor de onzekerheid van de voorspelling als geheel. Door gebruik te maken van een ensemble was het mogelijk om het effect van de weersomstandigheden op vogelmigratie statistisch te analyseren, onderwijl rekening houdend met de complexe correlatie tussen verschillende variabelen. We hebben het voorspellende vermogen van ons systeem getest aan de hand

van een aantal criteria, en we hebben bepaald of een ensemblesysteem dat voor de ene locatie ontwikkeld is, ook goede voorspellingen kan doen voor de andere locatie. De procedure voor het ontwikkelen van het model was robuust en overdraagbaar, zodat het systeem gebruikt kan worden om binnen korte tijd voorspellende modellen te maken van migratie-intensiteit op nieuwe locaties. Deze procedure is in principe geschikt om gestandaardiseerde voorspellende modellen te construeren voor zeer grote gebieden, waarbij gebruik gemaakt zou kunnen worden van bestaande netwerken van Doppler-radars.

Acknowledgments

The analyses described herein are the result of a combined effort among scientists with backgrounds in biology, meteorology, physical geography, statistics, computer science, visualization, engineering, and others. Many of these scientists' expertise overlaps several of these fields. It is their shared fascination with the world of birds and pervasive love of knowledge and science that has made this thesis possible. I have been privileged to know and benefit from this exciting and diverse group.

I am indebted to my promoter, Prof. dr. ir. Willem Bouten, and co-promoters, Dr. Judy Shamoun-Baranes and Dr. ir. Emiel van Loon, for giving me the opportunity to be involved in this cutting-edge research group. Whereas PhD students are often mentored by an individual supervisor with particular expertise, I was fortunate enough to benefit from this collection of mentors with a broad range of skills and knowledge. I learned from each of them, and their different backgrounds and styles resulted in my having a more multifaceted education. Our dialog was very open, and they were forthright with both criticism and praise. They valued my opinion and trusted my judgment, allowing me to travel much of Europe serving as a proud ambassador of the Computational Geo-Ecology (CGE) group. Beyond being helpful supervisors, with characteristics complimentary of one another, they are genuinely wonderful and interesting people, and I have enjoyed knowing them both in and out of the workplace.

I have grown quite close to many of my colleagues, and will remember particularly fondly the entertaining (and often nonsensical) lunchtime banter we shared. It will be difficult to now part ways, but hopefully many of our paths will at some point cross again. My fellow PhD researchers: Niels Anders,

Ehsan Forootan, Jamie McLaren, Dang Thu Ha Phan, Héctor Serna-Chavez, Ivan Soenario, Jurriaan Spaaks, Wouter Vansteelant, and Laurens Veen, with whom I have shared so much of this experience, were instrumental in the pleasurable transition between continents and cultures I experienced. Besides being an excellent friend, colleague, and officemate, Laurens is a wizard with all things technical and provided invaluable support and insight on many occasions. I owe a particular thanks to Jurriaan for kindly providing a Dutch translation of the summary of this thesis and for initiating (and perpetuating) the CGE writers' club. To those who attended these writers' club meetings and provided insightful (and not too painful) critiques of my work, I am most grateful. I cannot thank Jamie McLaren enough for always taking the time to discuss concepts and answer my questions concerning mathematics, biology, birds, Dutch culture, etc., etc. His friendship and comradery have had a tremendous, positive impact on my experience. I was fortunate as well to have shared time at the UvA with Adriaan Dokter, Diana Gorea, Tomislav Hengl, and Stacy Shinneman. I particularly enjoyed, and will remember fondly, organizing and conducting summer courses with Wouter and Stacy. From Adriaan, I learned a great deal, particularly concerning birds and mathematics, and the discussions between he, Jamie, and I were a constant source of inspiration. Tomislav felt like family almost immediately; more specifically, he felt like a domineering older brother... but family nonetheless. He not only helped further my understanding of spatial analysis and the R programming language, he constantly reminded me to savor all aspects of this experience. The staff of the IBED Secretariat, and in particular Mijke Heldens, provided assistance (and, in the case of Mijke, well-needed distractions) throughout... by the way, Mijke, I have a letter from the IND for you to translate.

I would also like to thank the members of my PhD defense committee for taking the time to review and consider my thesis and for their stimulating and thoughtful questions during the defense. Similarly, I would like to thank Jamie and Adriaan, again, for serving as paronyms during my defense ceremony.

The primary source of funding for my research was the European Space Agency (ESA) and the Ministry of Defence, in particular the Royal Netherlands Air Force (RNLAf). The RNLAf, as well as the Belgian Air Force (BAF), also shared bird migration data obtained from their surveillance radars, facilitating my research. I was privileged to meet and work with Serge Sorbi from the BAF and Inge Both, Arie Dekker, and Hans van Gasteren from the RNLAf. In particular, Hans provided invaluable support and direction concerning not only my work for the RNLAf but also my research and progress in general.

The Royal Netherlands Meteorological Institute (KNMI) provided a great

deal of the data that I used in my research. Not only did they provide and assist with atmospheric data from numerical weather models and measurements from the Cabauw experimental site for atmospheric research, it was from weather radars operated by KNMI that measurements of bird movement were obtained for several of the analyses herein. In particular, I would like to thank Henk Klein Baltink, Martin de Graaf, and Toon Moen for providing their expertise and assisting with these data. Hidde Leijnse, as well, not only provided assistance with data but served as a point of contact with KNMI and was a constant, beneficial source of advice and guidance.

My work was facilitated by the BiG Grid infrastructure for e-Science and was assisted greatly by the ICT infrastructure, services, and expertise provided by SARA. In particular, Bart Heupers, Tijs de Kler, Coen Schrivers, and Lykle Voort developed and maintained data base facilities and visualization tools that were invaluable to my work. As a representative of the LifeWatch program, I was privileged to be given the opportunity on several occasions to demonstrate these tools at international conferences using the Virtual Lab for Bird Migration Modelling.

During the course of my PhD studies, I was fortunate to be involved in the development of a research collaborative entitled the “European Network for the Radar surveillance of Animal Movement” (ENRAM). The members of ENRAM, representing research institutes in over a dozen European nations, are too numerous to name individually; nonetheless, I would like to mention Judy Shamoun-Baranes with the University of Amsterdam, Jason Chapman with Rothamsted Research, Ommo Hüppop with Vogelwarste Helgoland, and Felix Liechti with Vogelwarste Sempach for having organized and graciously hosted ENRAM meetings.

I am still indebted to my instructors at Louisiana State University (and, in fact, all of my previous educators) who helped set me on this path. In particular, I would like to thank Dr. Robert Rohli for his supervision, advice, guidance, and friendship. I would also like to thank Dr. Kevin Robbins who introduced me to the R language, providing me with skills that have served me so well during the course of my research.

My family deserves the lion’s share of my thanks, as anything good that I am or will be is due in no small part to the sacrifices they have made on my behalf; many of those sacrifices I may never fully appreciate. My mother, in particular, has been the single greatest influence in my life and has shown me endless love and support. Though her presence and personality are powerful, her guidance is light-handed. She has allowed (and indeed encouraged) me to grow and learn independently and has placed in me a great deal of trust and responsibility from a very early age. She has always maintained that I

am perfect, and while I know better, her belief has kept me moving in the right direction. My father is responsible for instilling in me a penchant for skepticism, beneficial for scientific pursuits. My grandfather, around whom has developed a large, wonderfully-supportive, and loving family, is an inspiration for me, and I am continually impressed by his worldliness and vitality. My brother Reese, with whom I am most at ease, has always been my best friend. Being away from him has perhaps been the most challenging aspect of my time here. I have been proud to watch (though from afar) as he begins to cultivate his own beautiful family... welcome Marcelle! I have been fortunate to have positive figures in my life who, though not related by blood, I surely count among family. In particular, I am grateful for the guidance and support I received from Bill Carville and Butch Kerr.

My wife Callie, with whom I have shared this experience most intimately, is extraordinary. I have been so fortunate to find her (and even more fortunate in convincing her to marry me!), and I feel privileged to have been welcomed so unreservedly into her wonderful, loving family. It has been incredible for me to spend our first several years as man and wife together on this adventure. The two of us are a team, even when we disagree, and I can imagine no substitute for her partnership. She is strong when I need support, gentle when I am vulnerable, and firm when I need direction. She is loving, reliable, and positive... not to mention beautiful! With her, I want for nothing, and I look forward with excitement to our adventures yet to come.

Callie and I have had such wonderful experiences and made such good friends here in the Netherlands; so many memorable BBQ's, boat rides, holidays, cycling trips, and parties... even a thwarted burglary (thanks to Maarten and Bullit) and a couple of fabulous weddings! We have made life-long friendships here with wonderful people from all over the world, and while I could not possibly list them all, many of them will hopefully make their way to the U.S. to visit Callie and I (and make room on their sofa for us when we return to visit them!).

I could continue these acknowledgments until they eclipsed the length of the thesis itself and still not mention everyone who deserves my thanks, which in my opinion is quite a fortunate position in which to find oneself.

Appendix A: Explicit descriptions of flow-assistance equations

Each of the nine figures below (A.1 - A.9) contains a complete and explicit overview of a particular flow-assistance equation. Along the left column of each figure, from top to bottom, is the flow-assistance equation itself, a graphical representation of the equation's components, a text summary describing the equation's components and assumptions, and a circular plot indicating the resulting flow-assistance values for different combinations of flow speed ($0 - 20 \text{ ms}^{-1}$) and direction ($0 - 360^\circ$). In these circular plots, flow speed is indicated by the distance from the center of the circle with the edges corresponding to flow speeds of 20 ms^{-1} . In both the circular plots and the graphical representation of the equation's components, a gray arrow indicates the preferred direction of movement (pdm). Note that in the graphic indicating the components of the model, the pdm is equivalent to 90° ; whereas in the circular plot representing the resulting flow-assistance values, the pdm is equal to 225° . For the circular plots, the preferred air- or ground speed, whenever required by an equation, was set to 12 ms^{-1} , and, for Fig. A.9, the proportion of compensation (f) was set to 0.5. Along the right column of these figures are the partial derivatives (i.e. sensitivities) of the flow-assistance equation to each of its respective assumptions. For each of an equation's assumptions, we provide the partial derivative equation and a circular plot indicating the sensitivity of the equation to that assumption for particular combinations of flow speed ($0 - 20 \text{ ms}^{-1}$) and direction ($0 - 360^\circ$). Some equations do not have assumptions that allow calculation of partial derivatives, so their sensitivity (i.e. the right column) contains only 'NA'. As with the other circular plots, flow speed is indicated by the distance from the center of the circle with the

edges corresponding to flow speeds of 20 ms^{-1} . The contoured surface of these plots indicates the change in flow-assistance (ms^{-1}) that would result from a one-unit change in the specified assumption for the particular combination of flow speed and direction. In these plots, the pdm was set to 225° ; any speed-related assumption was set to 12 ms^{-1} ; and, for Fig. A.9, the proportion of compensation (f) was set to 0.5. We show the sensitivity of each equation to specific amounts of uncertainty in Figure 3.3 of the main text.

Fig. A.1 Equation FlowSpeed

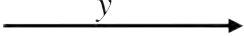
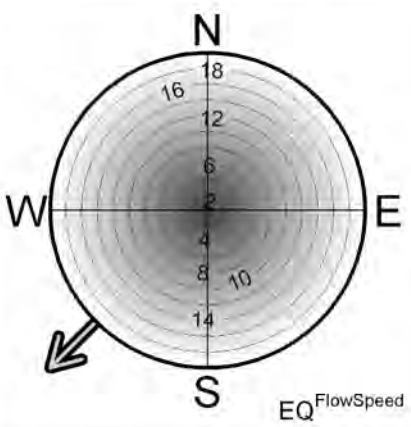
Flow-assistance	Sensitivity
$FA = y$	NA
	
Where: y = flow speed Explicit assumptions: - Movement with the flow	
	

Fig. A.2 Equation NegFlowSpeed

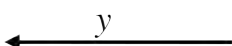
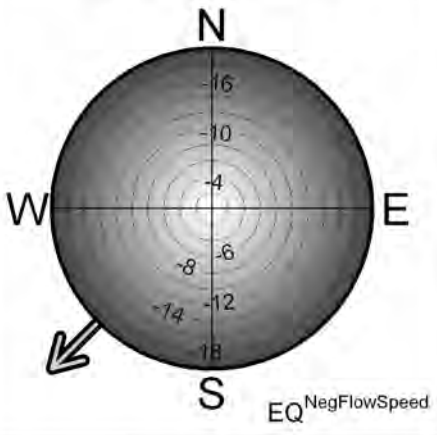
Flow-assistance	Sensitivity
$FA = -I * y$	<i>NA</i>
	
Where: y = flow speed Explicit assumptions: - Movement against the flow	
	

Fig. A.3 Equation Binary

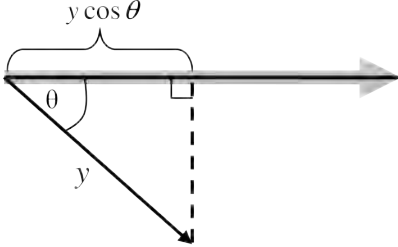
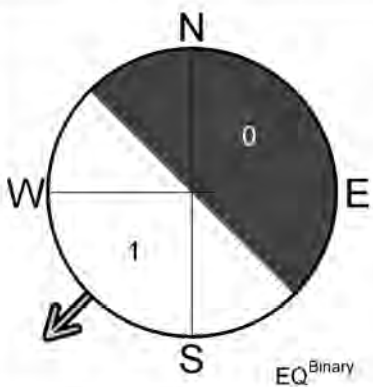
Flow-assistance	Sensitivity
$FA = \begin{cases} 0, & y \cos \theta \leq 0 \\ 1, & y \cos \theta > 0 \end{cases}$	NA
	
<p>Where:</p> <p>y = flow speed θ = flow direction – pdm</p> <p>Explicit assumptions:</p> <ul style="list-style-type: none"> - A preferred direction of movement (pdm) <p>Implicit assumptions:</p> <ul style="list-style-type: none"> - Full drift 	
	

Fig. A.4 Equation Tailwind

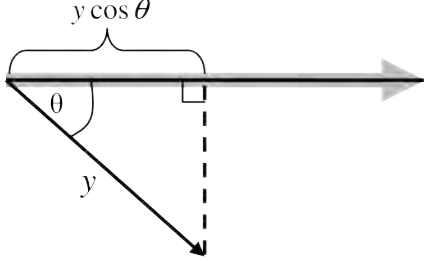
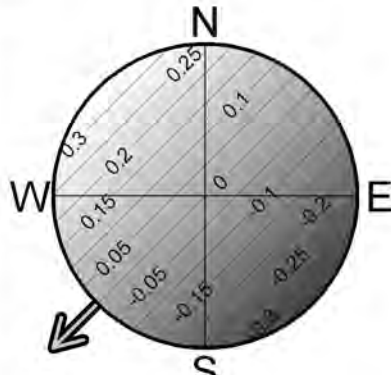
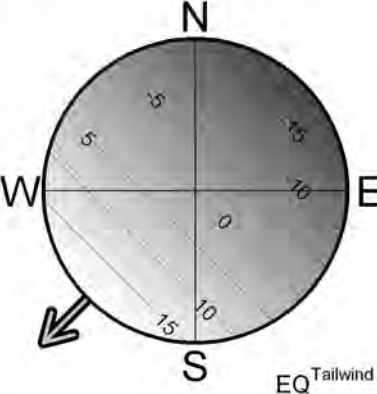
Flow-assistance	Sensitivity
$FA = y \cos \theta$	$\frac{\partial FA}{\partial \theta} = -y \sin \theta$
	
<p>Where:</p> <p>y = flow speed θ = flow direction – pdm</p> <p>Explicit assumptions:</p> <ul style="list-style-type: none"> - A preferred direction of movement (pdm) <p>Implicit assumptions:</p> <ul style="list-style-type: none"> - Full drift 	
	

Fig. A.5 Equation Airspeed

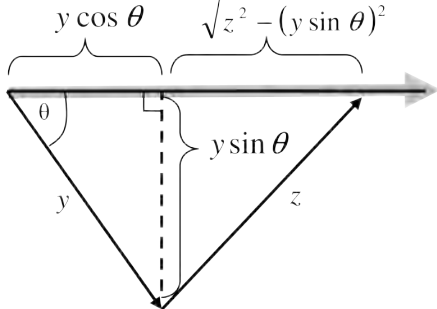
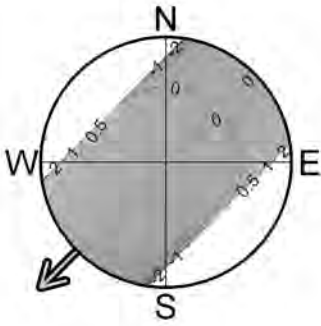
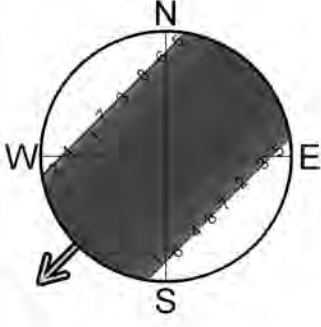
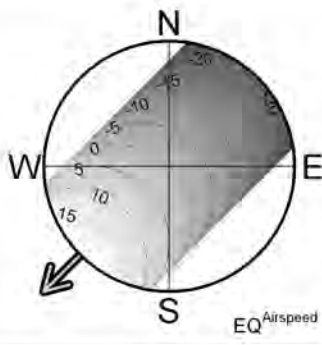
Flow-assistance	Sensitivity
$FA = y \cos \theta + \sqrt{z^2 - (y \sin \theta)^2} - z$ 	$\frac{\partial FA}{\partial \theta} = -y \sin \theta - \left(y^2 \sin \theta \cos \theta * (z^2 - (y \sin \theta)^2)^{-\frac{1}{2}} \right)$ 
<p>Where:</p> <ul style="list-style-type: none"> - y = flow speed - z = airspeed - θ = flow direction – pdm 	
<p>Explicit assumptions:</p> <ul style="list-style-type: none"> - A preferred direction of movement (pdm) - A constant airspeed - Complete compensation by adjusting heading and groundspeed 	
<p>Implicit assumptions:</p> <ul style="list-style-type: none"> - If airspeed is insufficient to maintain pdm, equation returns no real solution. 	$\frac{\partial FA}{\partial z} = z(z^2 - (y \sin \theta)^2)^{-\frac{1}{2}} - 1$ 
	

Fig. A.6 Equation Groundspeed

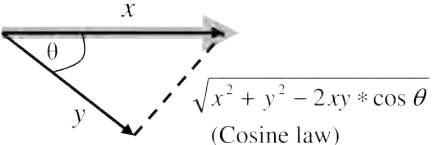
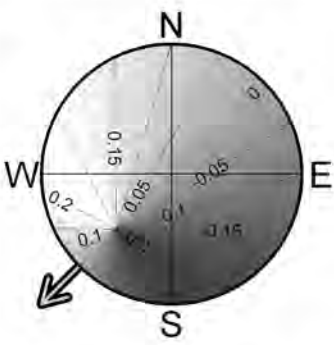
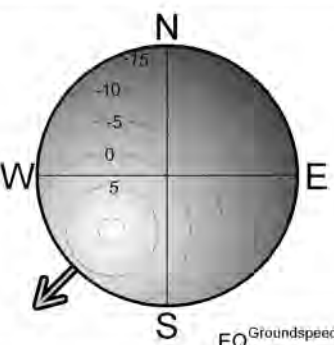
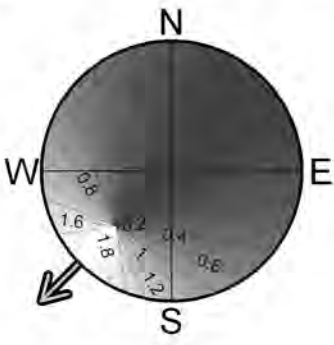
Flow-assistance	Sensitivity
$FA = x - \sqrt{x^2 + y^2 - 2xy * \cos \theta}$	$\frac{\partial FA}{\partial \theta} = -xy \sin \theta * (x^2 + y^2 - 2xy \cos \theta)^{-\frac{1}{2}}$
 <p>(Cosine law)</p>	
<p>Where:</p> <ul style="list-style-type: none"> - y = flow speed - x = groundspeed - θ = flow direction – pdm <p>Explicit assumptions:</p> <ul style="list-style-type: none"> - A preferred direction of movement (pdm) - A constant groundspeed <p>Implicit assumptions:</p> <ul style="list-style-type: none"> - Complete compensation by adjusting airspeed and heading - Tailwinds faster than the specified ground-speed are suboptimal 	$\frac{\partial FA}{\partial x} = 1 - (x - y \cos \theta) * (x^2 + y^2 - 2xy \cos \theta)^{-\frac{1}{2}}$
 <p>EQ^{Groundspeed}</p>	

Fig. A.7 Equation C.Groundspeed

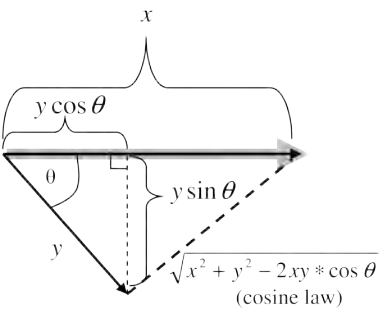
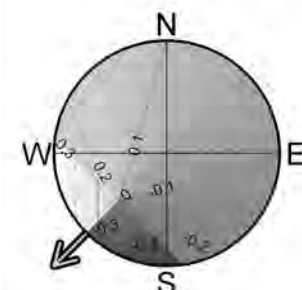
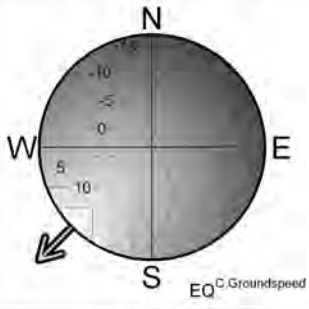
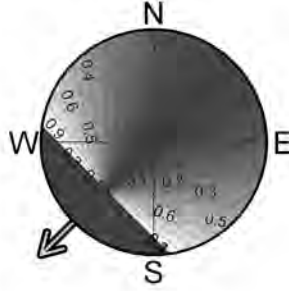
Flow-assistance	Sensitivity
$FA = \begin{cases} x - \sqrt{x^2 + y^2 - 2xy * \cos \theta}, & y \cos \theta \leq x \\ y \cos \theta - y \sin \theta , & y \cos \theta > x \end{cases}$ 	$\frac{\partial FA}{\partial \theta} = \begin{cases} -xy \sin \theta * (x^2 + y^2 - 2xy \cos \theta)^{-\frac{1}{2}}, & y \cos \theta \leq x \\ -y \sin \theta - y \cos \theta, & y \sin \theta > 0 \\ \text{Undefined,} & y \sin \theta = 0 \\ -y \sin \theta + y \cos \theta, & y \sin \theta < 0 \end{cases}$ 
<p>Where:</p> <ul style="list-style-type: none"> - y = flow speed - x = groundspeed - θ = flow direction – pdm <p>Explicit assumptions:</p> <ul style="list-style-type: none"> - A preferred direction of movement (pdm) - A constant groundspeed <p>Implicit assumptions:</p> <ul style="list-style-type: none"> - Complete compensation <ul style="list-style-type: none"> o Unless supportive axial flow is faster than specified groundspeed (in which case, no specific behavior is assumed) - Supportive axial flow faster than the specified groundspeed is increasingly beneficial. 	$\frac{\partial FA}{\partial x} = \begin{cases} 1 - (x - y \cos \theta) * (x^2 + y^2 - 2xy \cos \theta)^{-\frac{1}{2}}, & y \cos \theta \leq x \\ 0, & y \sin \theta > 0 \\ \text{Undefined,} & \theta = 0, \\ 0, & y \sin \theta < 0 \end{cases}$ 

Fig. A.8 Equation M.Groundspeed

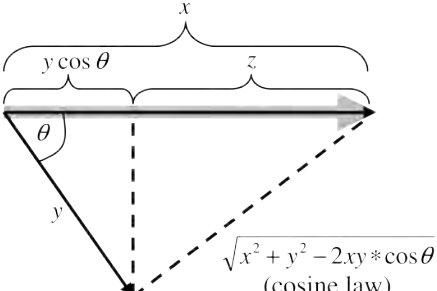
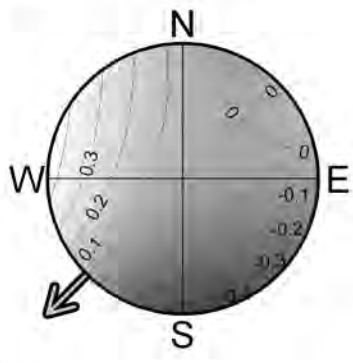
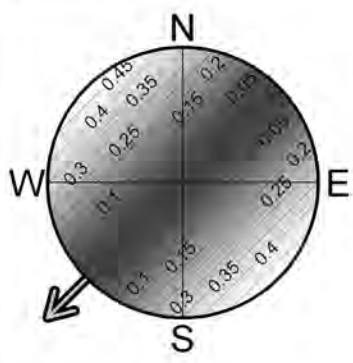
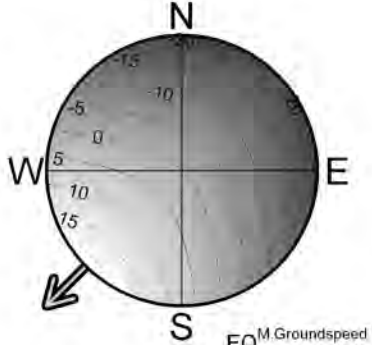
Flow-assistance	Sensitivity
$x = z + y \cos \theta$ $FA = x - \sqrt{x^2 + y^2 - 2xy * \cos \theta}$  $\sqrt{x^2 + y^2 - 2xy * \cos \theta} \quad (\text{cosine law})$	$\frac{\partial WP}{\partial \theta} = 0.5y \sin \theta \cdot$ $(-2yz \sin \theta - 2y^2 \sin \theta \cos \theta + 2xy \sin \theta) \cdot$ $((z \cos \theta)^2 + y^2 - 2xy \cos \theta)^{-\frac{1}{2}}$ 
<p>Where:</p> <ul style="list-style-type: none"> - y = flow speed - z = groundspeed in still conditions - x = groundspeed - θ = flow direction – pdm 	
<p>Explicit assumptions:</p> <ul style="list-style-type: none"> - A preferred direction of movement (pdm) - Groundspeed equal to groundspeed in still conditions plus flow component along the pdm. 	$\frac{\partial WP}{\partial z} = 1 - (z + y \cos \theta) \cdot$ $((z + y \cos \theta)^2 + y^2 - 2xy \cos \theta)^{-\frac{1}{2}}$ 
	

Fig. A.9 Equation PartialSpeed

Flow-assistance	Sensitivity
$FA = y \cos \theta + \sqrt{z^2 - (f * y \sin \theta)^2} - z$	$\frac{\partial FA}{\partial \theta} = -y \sin \theta - f^2 y^2 \sin \theta \cos \theta \cdot \left(z^2 - (f y \sin \theta)^2 \right)^{-\frac{1}{2}}$
Where: y = flow speed z = airspeed θ = flow direction – pdm f = proportion of compensation	$\frac{\partial FA}{\partial z} = z \left(z^2 - (f y \sin \theta)^2 \right)^{-\frac{1}{2}} - 1$
Explicit assumptions: <ul style="list-style-type: none"> - A preferred direction of movement (pdm) - A constant airspeed - Partial compensation by adjusting heading and groundspeed - The animal will compensate for a proportion of the flow lateral to the pdm as described by f 	$\frac{\partial FA}{\partial f} = -f y^2 \sin^2 \theta \left(z^2 - (f y \sin \theta)^2 \right)^{-\frac{1}{2}}$
Implicit assumptions: <ul style="list-style-type: none"> - If airspeed is insufficient to compensate the specified amount, equation returns no real solution. - $f = 1$ is complete compensation - $f = 0$ is full drift 	

Appendix B: FLAT model description

The FLow-Assistance Trajectory model (i.e. FLAT model) comprises a set of coupled differential equations which describe displacement of an individual animal over the surface of the Earth. Here we present the solutions of the discretized form of the equations. All angles and directions are considered in radians, locations in latitude and longitude, distances in meters, and speeds in meters per second.

We start by describing the forward ($M_{F,t}$) and sideways movement ($M_{S,t}$) of an animal in relation to its preferred direction of movement (α_t). In general, $M_{F,t}$ and $M_{S,t}$ are functions of α_t , north/south (v_t) and east/west (u_t) flow components describing the direction into which the flow is moving (north and east being positive, respectively), and possible other variables that describe aspects of the animal's strategy, behavior, or capabilities. Hence, $M_{F,t} = f(u_t, v_t, \alpha_t, \dots)$ and $M_{S,t} = g(u_t, v_t, \alpha_t, \dots)$. The specific form of the function for $M_{F,t}$ and $M_{S,t}$ depend on (known or assumed) prior assumptions about the animal's behavior. In FLAT these assumptions are cast in various flow-assistance equations. The following equations are distinguished.

EQ^{FlowSpeed}

$$M_{S,t} = (y_t + z_t) \cdot \sin(\theta_t)$$
$$M_{F,t} = (y_t + z_t) \cdot \cos(\theta_t)$$

EQ^{NegFlowSpeed}

$$M_{S,t} = (y_t - z_t) \cdot \sin(\theta_t)$$

$$M_{F,t} = (y_t - z_t) \cdot \cos(\theta_t)$$

EQ^{Tailwind}

$$M_{S,t} = y_t \sin(\theta_t)$$

$$M_{F,t} = z_t + y_t \cos(\theta_t)$$

EQ^{Groundspeed}

$$M_{S,t} = 0$$

$$M_{F,t} = x_t$$

EQ^{M.Groundspeed}

$$M_{S,t} = 0$$

$$M_{F,t} = z_{p,t} + y_t \cos(\theta_t)$$

EQ^{Airspeed}

$$M_{S,t} = 0$$

$$M_{F,t} = y_t \cos(\theta_t) + \sqrt{z_t^2 - (y_t \sin(\theta_t))^2}$$

EQ^{PartialSpeed}

$$M_{S,t} = (1 - f) \cdot y_t \sin(\theta_t)$$

$$M_{F,t} = y_t \sin(\theta_t) + \sqrt{z_t^2 - (f \cdot y_t \sin(\theta_t))^2}$$

where the components of these equations use the following naming conventions

- y_t = the flow speed of the fluid medium
- ϕ_t = the direction into which the flow is moving, hence ...

$$\phi_t = \begin{cases} \tan^{-1} \left(\frac{u_t}{v_t} \right); & v_t \geq 0 \text{ \& } u_t \neq 0 \text{ or } v_t > 0 \text{ \& } u_t = 0 \\ \pi + \tan^{-1} \left(\frac{u_t}{v_t} \right); & v_t < 0 \\ \alpha_t; & v_t = 0 \text{ \& } u_t = 0 \end{cases}$$

- $\theta_t = \phi_t - \alpha_t$ or the angular difference between flow direction and preferred direction of movement
- x_t = the animal's speed relative to the fixed earth (i.e. its groundspeed)
- z_t = the animal's speed relative to the flow (i.e. its relative speed)
- $z_{p,t}$ = the animal's *preferred* relative speed, possibly different from z_t

- f = the proportion of compensation for displacement from α_t

At minimum, each flow-assistance equation requires specification of v_t , u_t , α_t , and one of either x_t , z_t , or $z_{p,t}$.

After calculating forward and sideways movement relative to α_t , we calculate – over a small time interval (Δt) – the actual direction of movement or ‘bearing’ (γ_t) from $M_{S,t}$, $M_{F,t}$, and α_t as follows.

$$\gamma_t = \begin{cases} \alpha_t + \tan^{-1} \left(\frac{M_{S,t}}{M_{F,t}} \right); & M_{F,t} \geq 0 \text{ \& } M_{S,t} \neq 0 \text{ or } M_{F,t} > 0 \text{ \& } M_{S,t} = 0 \\ \alpha_t + \pi \tan^{-1} \left(\frac{M_{S,t}}{M_{F,t}} \right); & M_{F,t} < 0 \\ \alpha_t + 0; & M_{F,t} = 0 \text{ \& } M_{S,t} = 0 \end{cases}$$

Also, the distance traveled along γ_t over the time increment Δt (d_t) is

$$d_t = \sqrt{M_{S,t}^2 + M_{F,t}^2}$$

The values of the direction of movement (γ_t) and the distance traveled (d_t) can be combined in the Haversine formula to calculate displacement over the Earth’s surface (Vavrek, 2011).

The latitude coordinate (lat) of the animal at time $t + \Delta t$ is calculated as

$$lon_{t+\Delta t} = ((lon_t + dlon_{\Delta t} + \pi) \bmod 2\pi) - \pi$$

where ‘mod’ indicates a modulo operation to find the remainder of a division of the value on the left by the value on the right, and the change in longitude ($dlon_{\Delta t}$) is given by

$$dlon_{\Delta t} = \begin{cases} \tan^{-1} \left(\frac{Y_t}{X_t} \right); & X_t \geq 0 \text{ \& } Y_t \neq 0 \text{ or } X_t > 0 \text{ \& } Y_t = 0 \\ \pi + \tan^{-1} \left(\frac{Y_t}{X_t} \right); & X_t < 0 \\ 0; & X_t = 0 \text{ \& } Y_t = 0 \end{cases}$$

where

$$Y_t = \sin(\gamma_t) \cdot \sin \left(\frac{d_t}{R} \right) \cdot \cos(lat_t)$$

$$X_t = \cos \left(\frac{d_t}{R} \right) - \sin(lat_t) \cdot \sin(lat_{t+\Delta t})$$

At this stage, location ($lon_{t+\Delta t}, lat_{t+\Delta t}$) becomes the current location (lon_t , lat_t), and the iterative calculation starts over. At each (new) location (lon_t , lat_t), the flow field (v_t , u_t) may differ from the previous values. As well, the behavior of the animal, for example its preferred direction of movement (α_t)

and/or preferred relative speed ($z_{p,t}$), may change over time (i.e. during the course of the migration path) and may be updated.

The FLAT model is implemented in the RNCEP package (see Chapter 2). This package contains functions to access and manipulate global weather data from the National Centers for Environmental Prediction (NCEP) / National Center for Atmospheric Research (NCAR) Reanalysis dataset (Kalnay et al., 1996) and the NCEP / Department of Energy (DOE) Reanalysis II dataset (Kanamitsu et al., 2002).

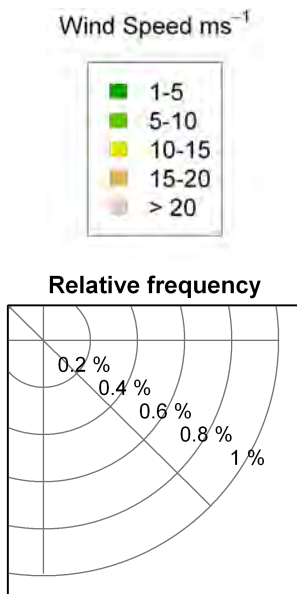
Appendix C: Wind maps and wind summaries for Europe

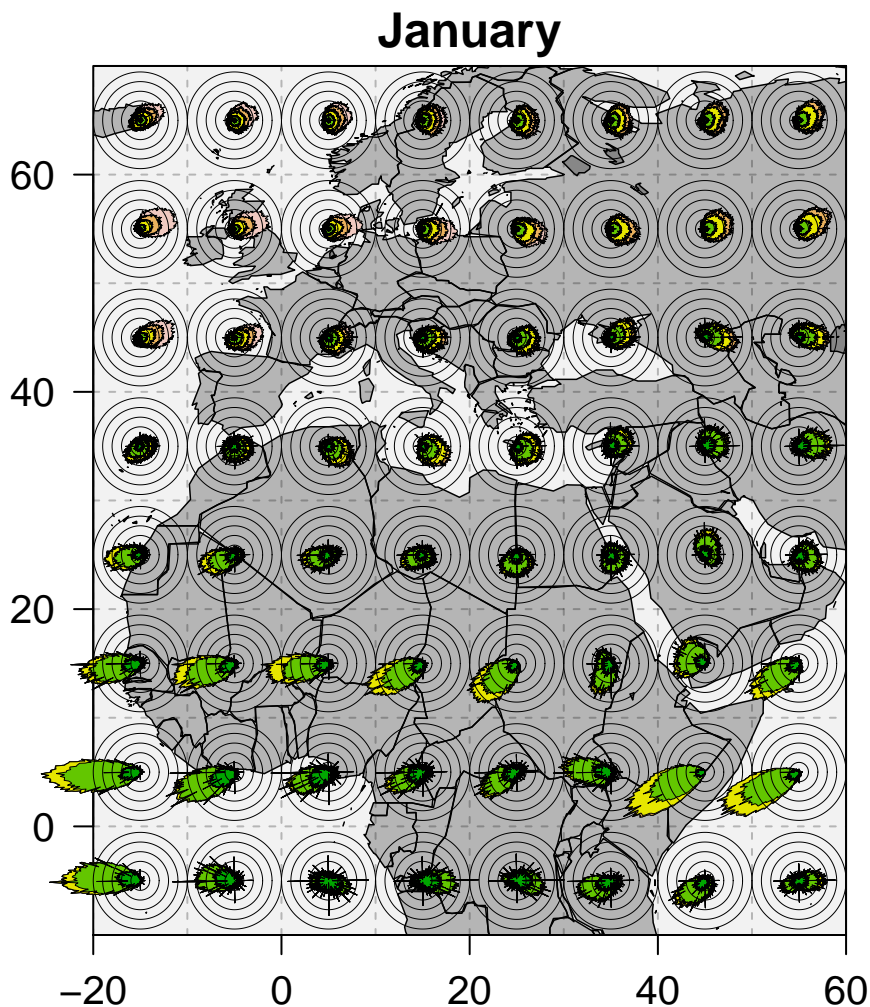
In Table C, we show summary statistics of wind profit for wind subsections in Europe. Wind profit was calculated following the same procedure described in Section 4.4.1. Thus, the preferred direction of migration was assumed to be 223° in autumn and 43° in spring.

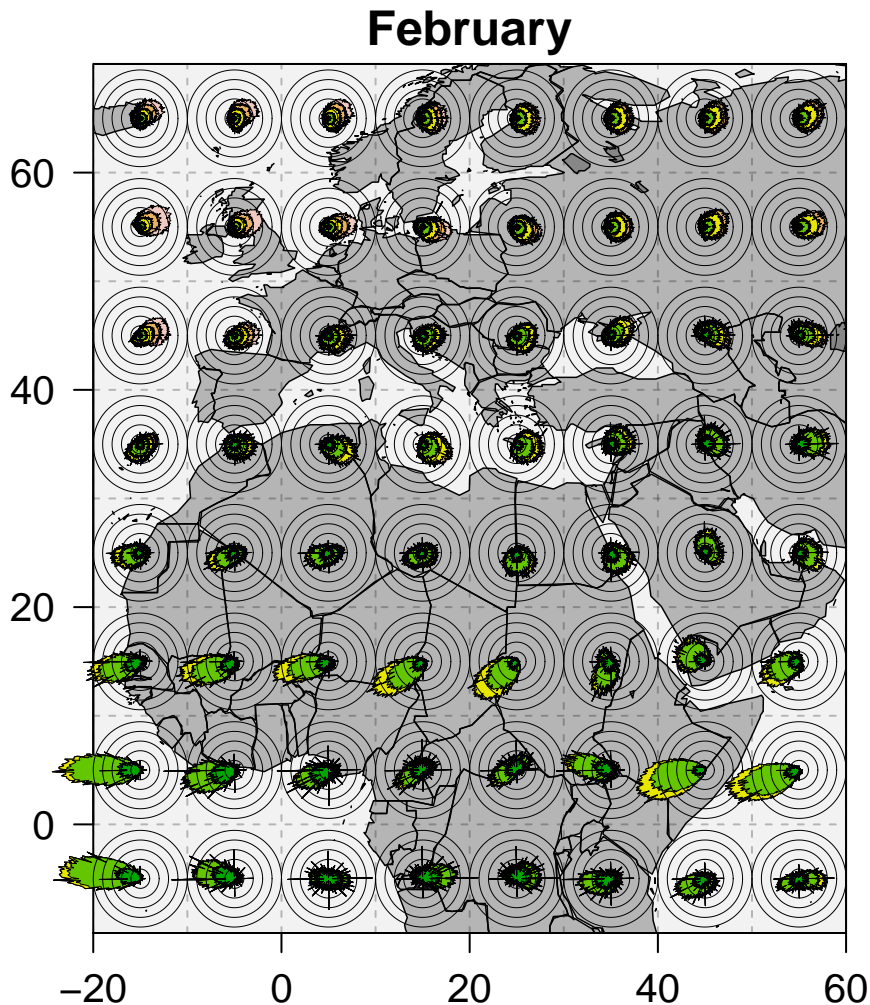
Table C: Summary statistics of wind profit including the mean, median, and standard deviation (SD) as well as the percentage of observations greater than or equal to zero ($\% \geq 0$) are shown for spring and autumn for wind subsections through Europe including those representing southern Sweden (50°N 10°E to 60°N 20°E), France (40°N 0°E to 50°N 10°E), and Northern Spain (40°N 10°W to 50°N 0°W).

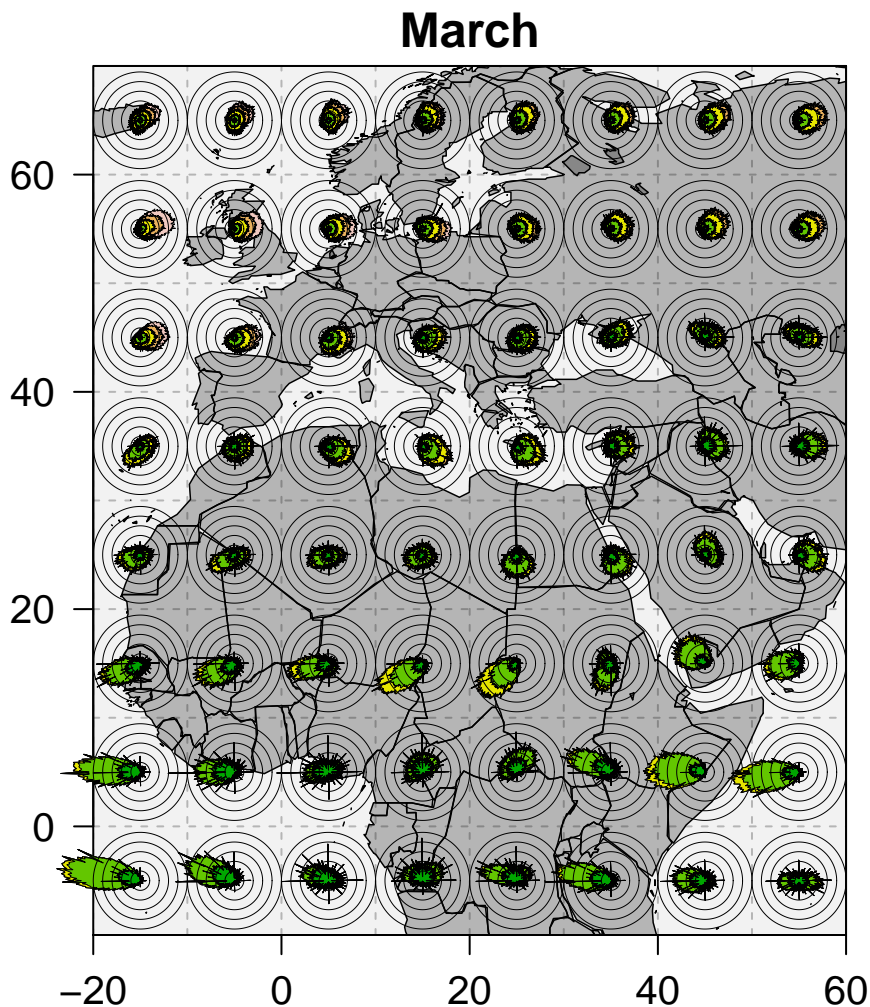
Wind Subsection	Spring				Autumn			
	Mean	Median	SD	% ≥ 0	Mean	Median	SD	% ≥ 0
Southern Sweden	2.2	1.9	6.8	61.7	-3.5	-3.4	6.6	30.1
France	1.2	0.9	6.5	56.0	-2.0	-1.5	6.1	38.4
Northern Spain	2.0	1.3	8.0	56.7	-2.7	-2.1	7.1	36.6

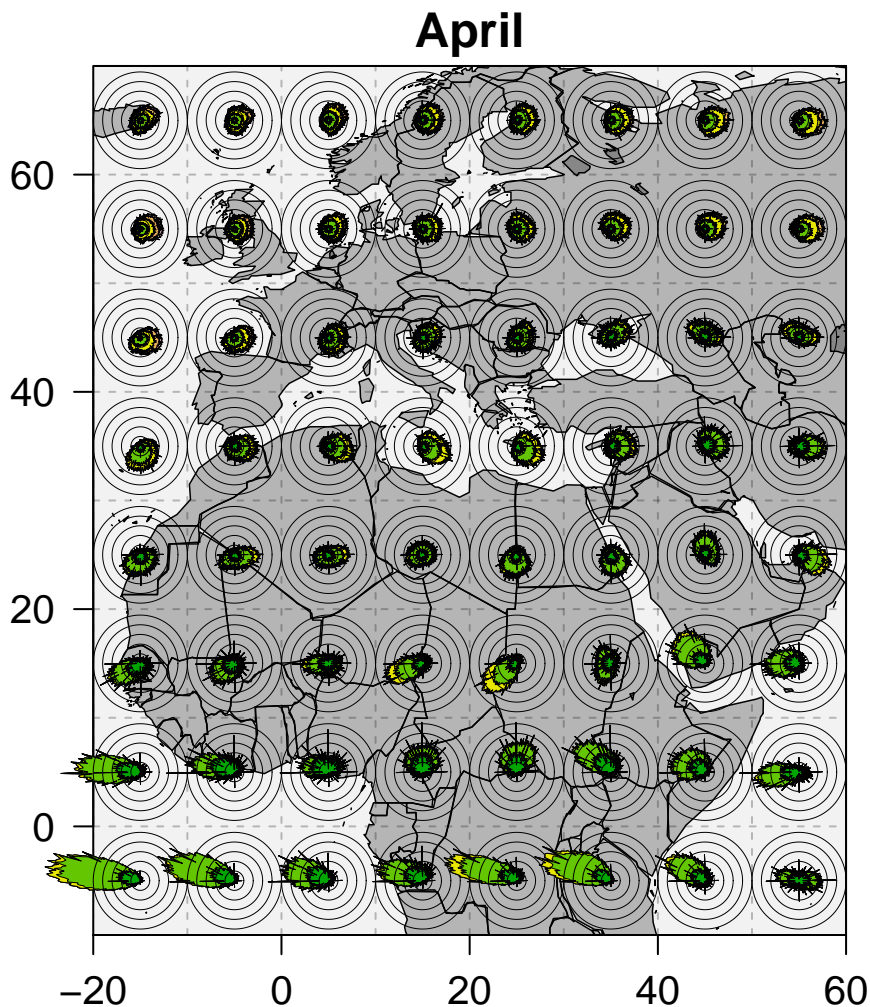
On the following pages are monthly wind rose maps covering Europe and Africa displaying 30 years (1978-2008) of wind data from the 850 mb pressure level from the NCEP/NCAR Reanalysis dataset. Wind roses indicate the direction into which the wind is blowing. Total distance from the center indicates the relative frequency of wind in a particular direction, while colors describe the individual relative frequencies of the different wind speed ranges (ms^{-1}) in that direction. Concentric circles indicate relative frequency in increments of 0.2%; with the outer circle indicating 1% relative frequency. See also the key indicating relative frequencies and wind speed ranges. These maps are also available from <http://dare.uva.nl/record/421932>.

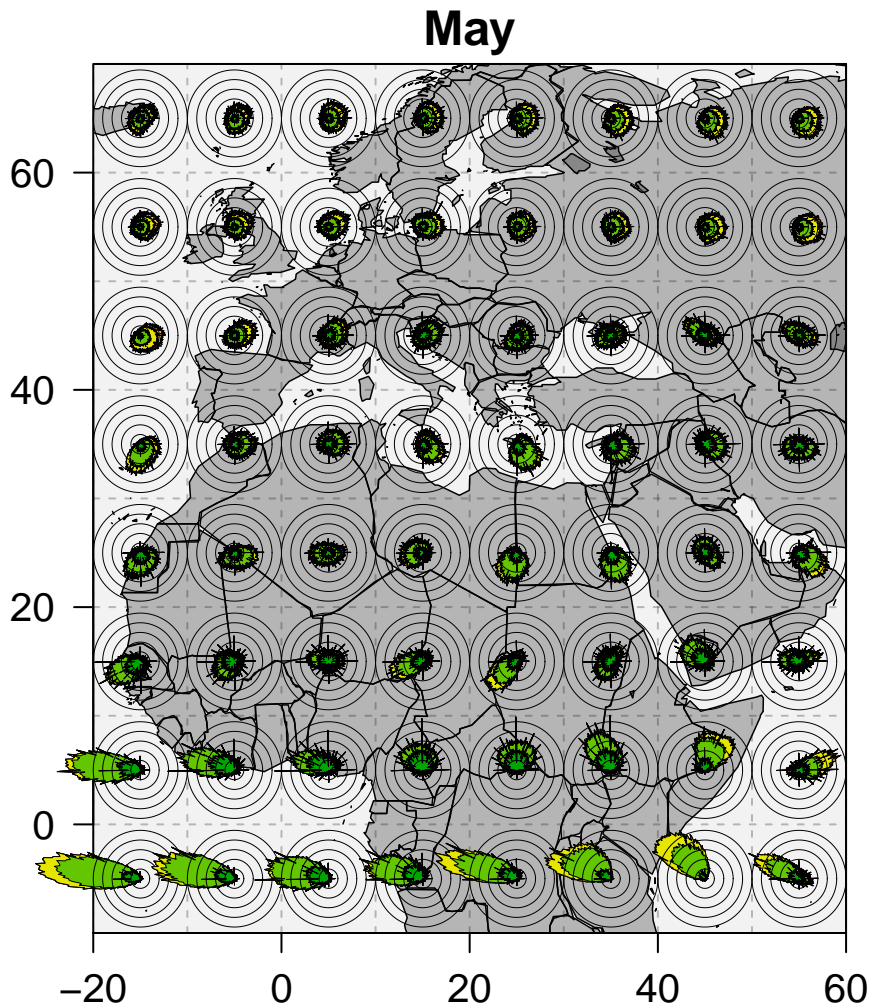


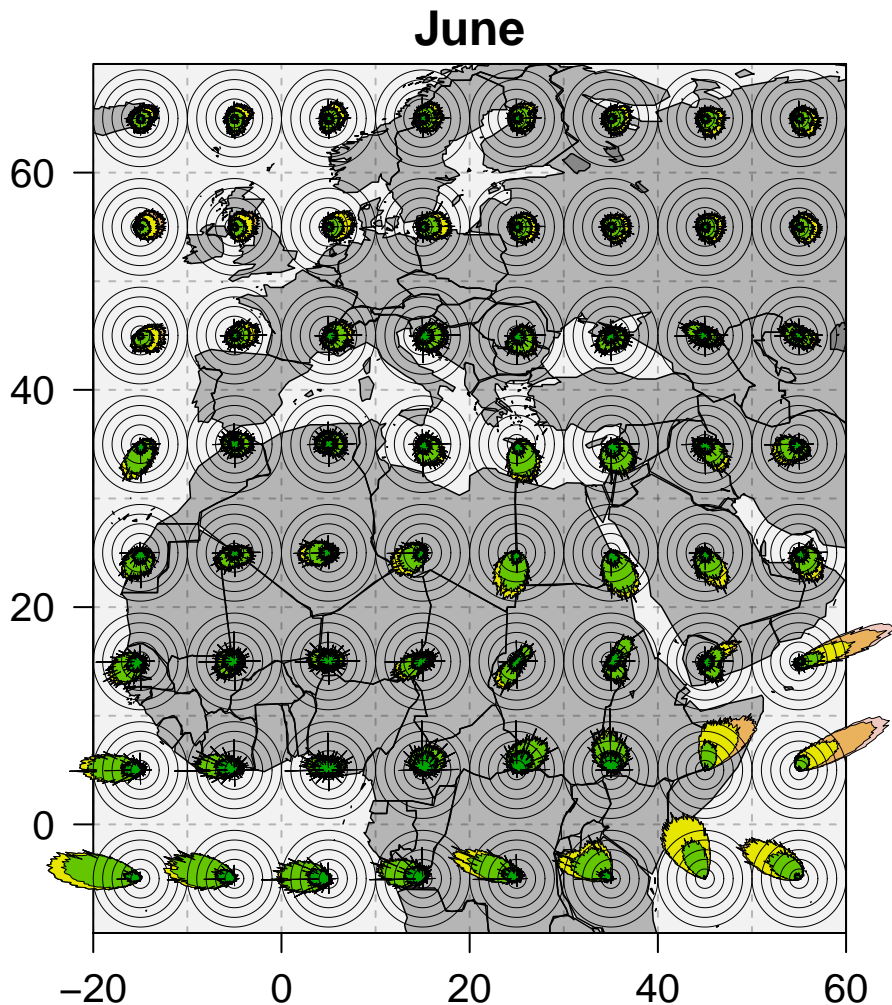


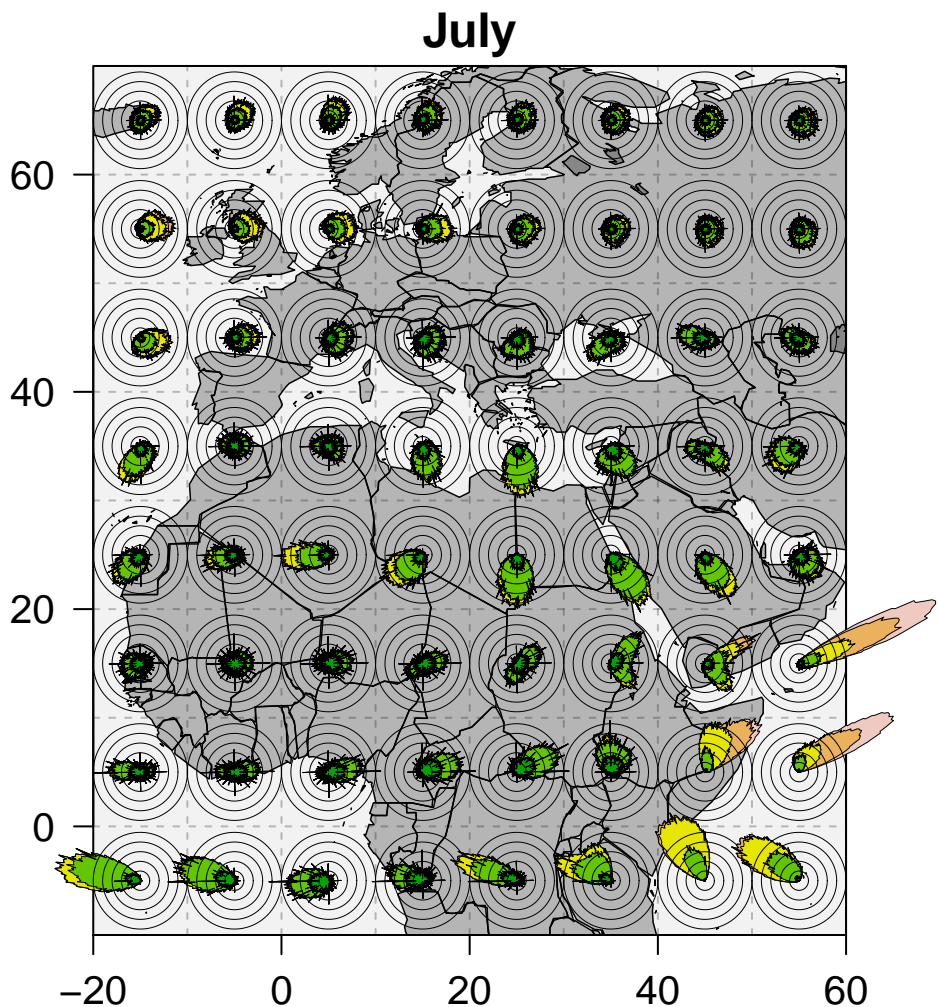




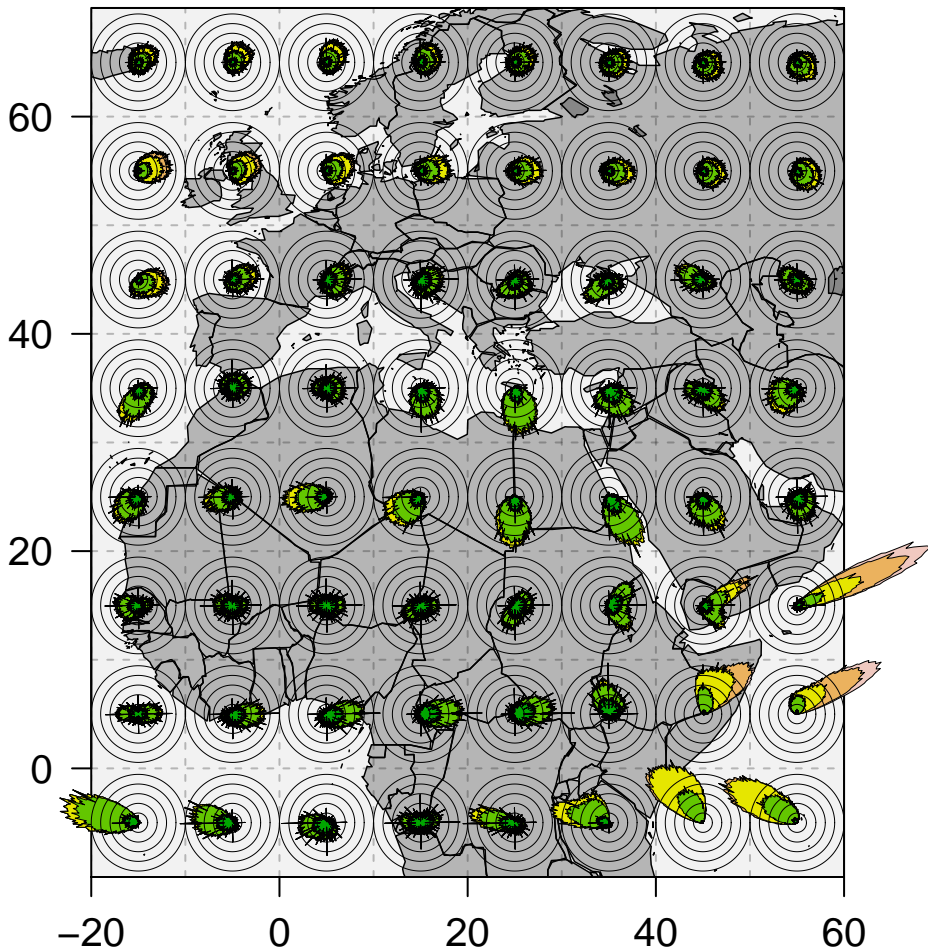


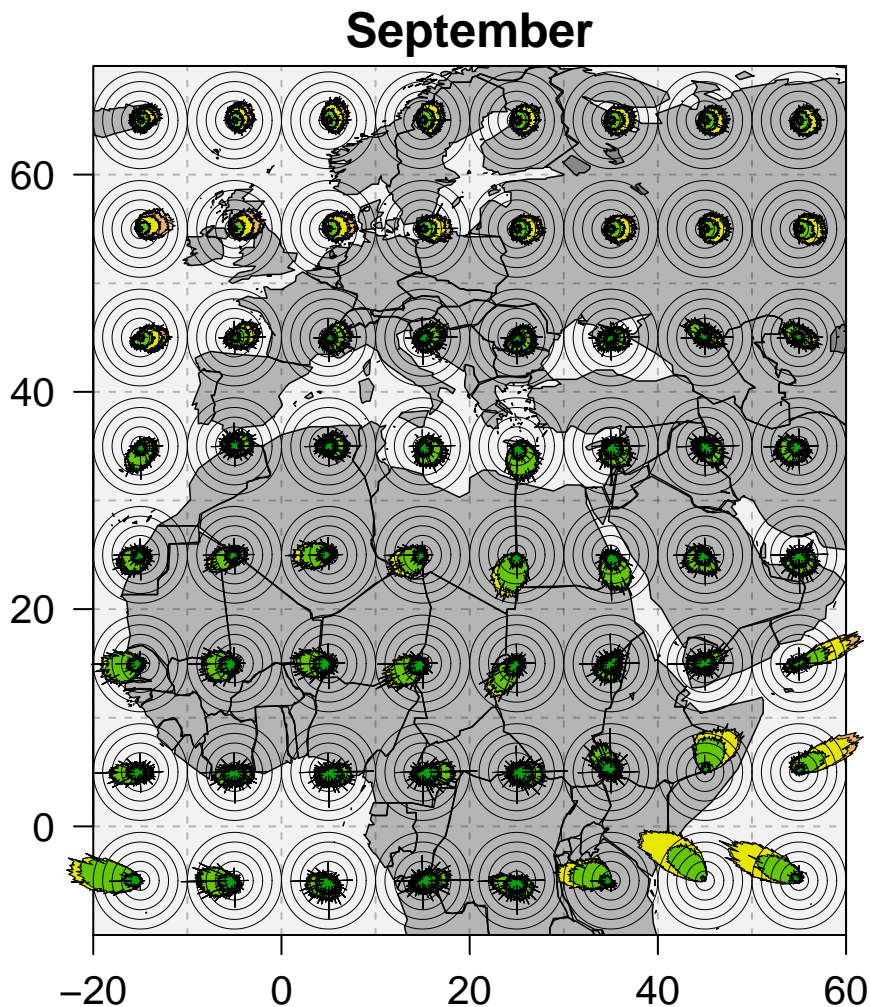


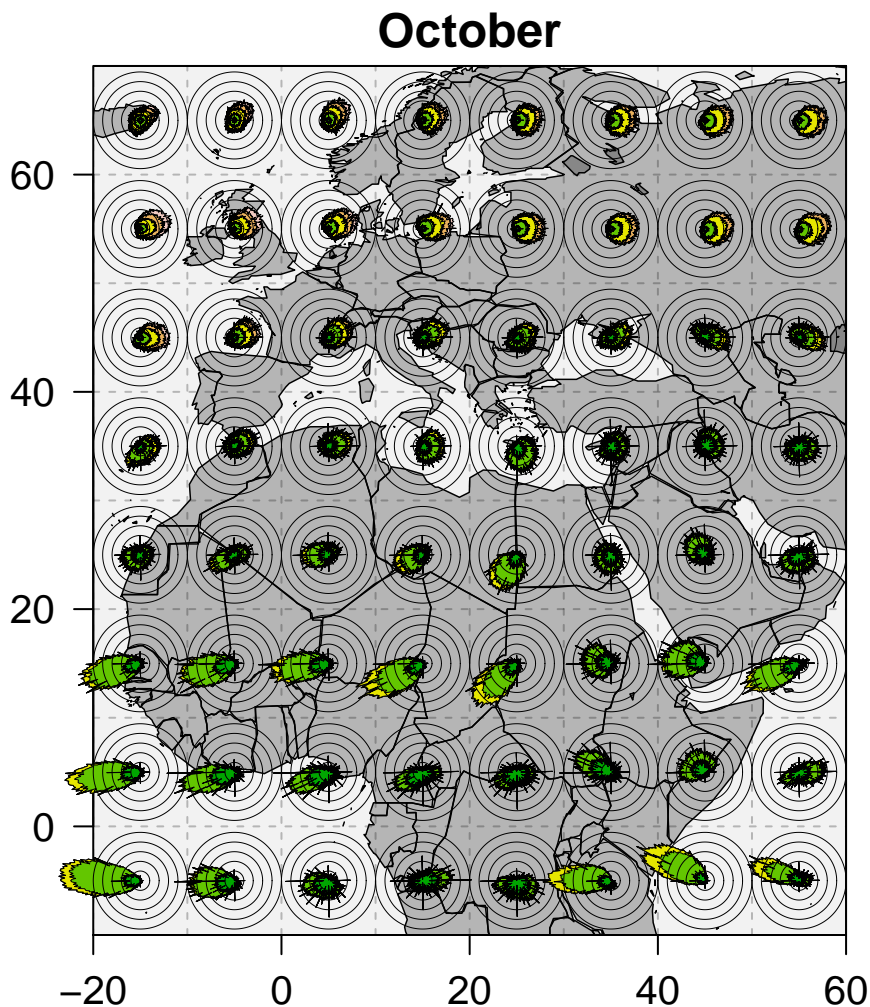


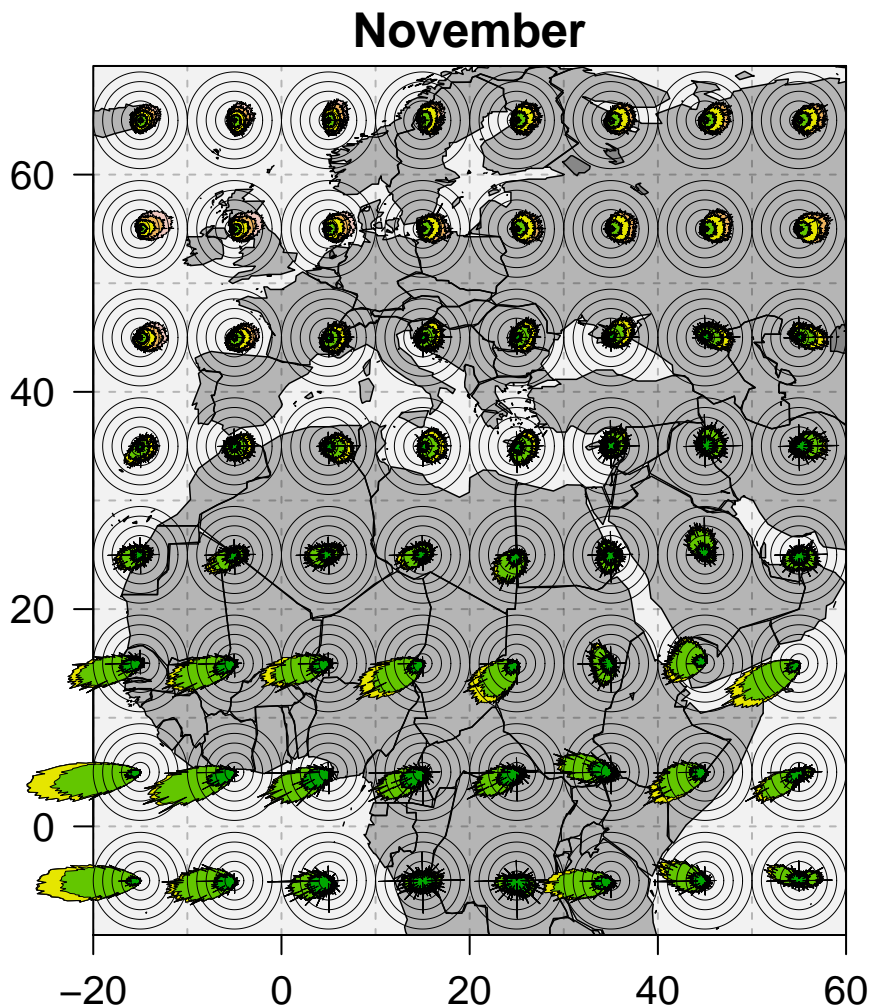


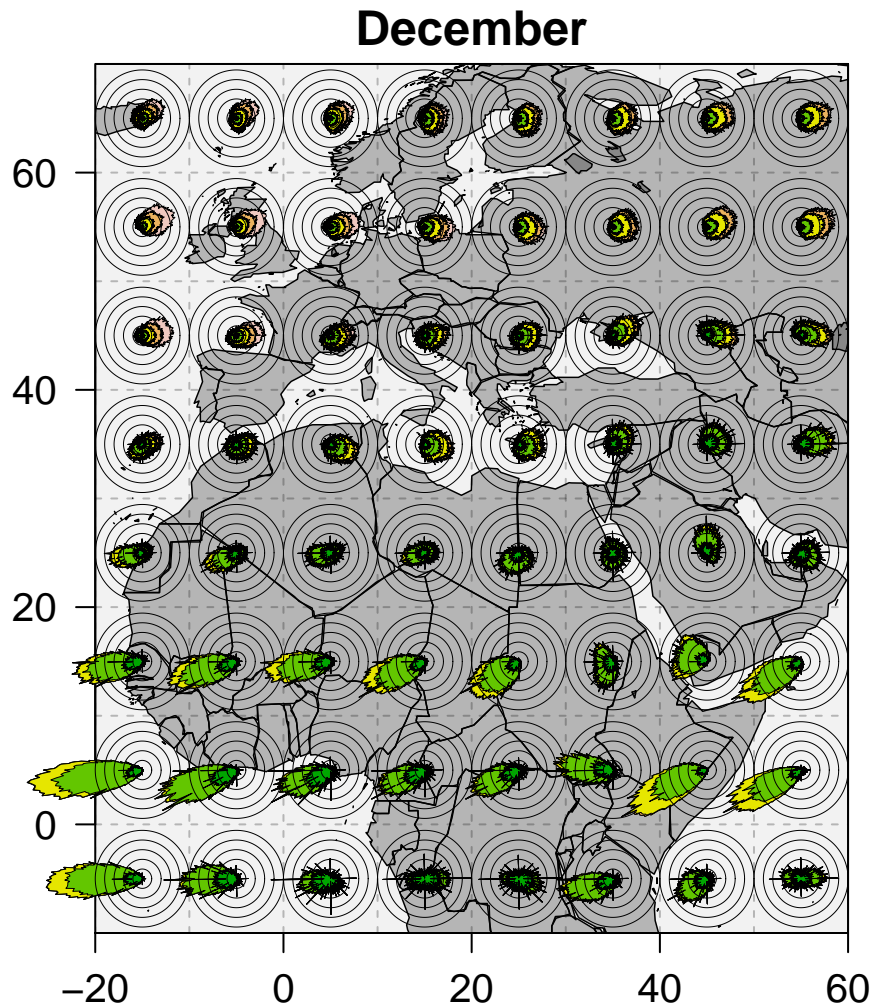
August





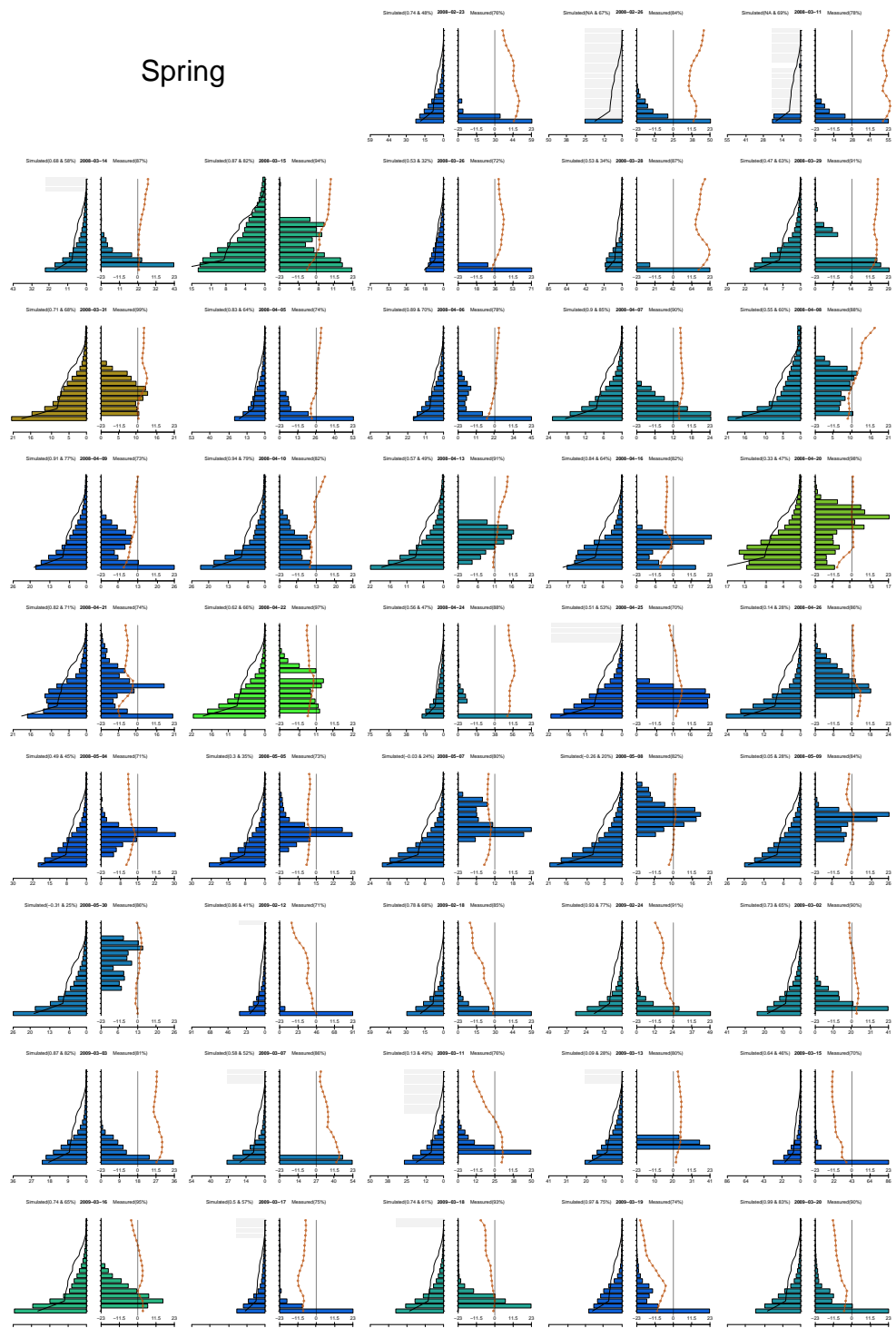




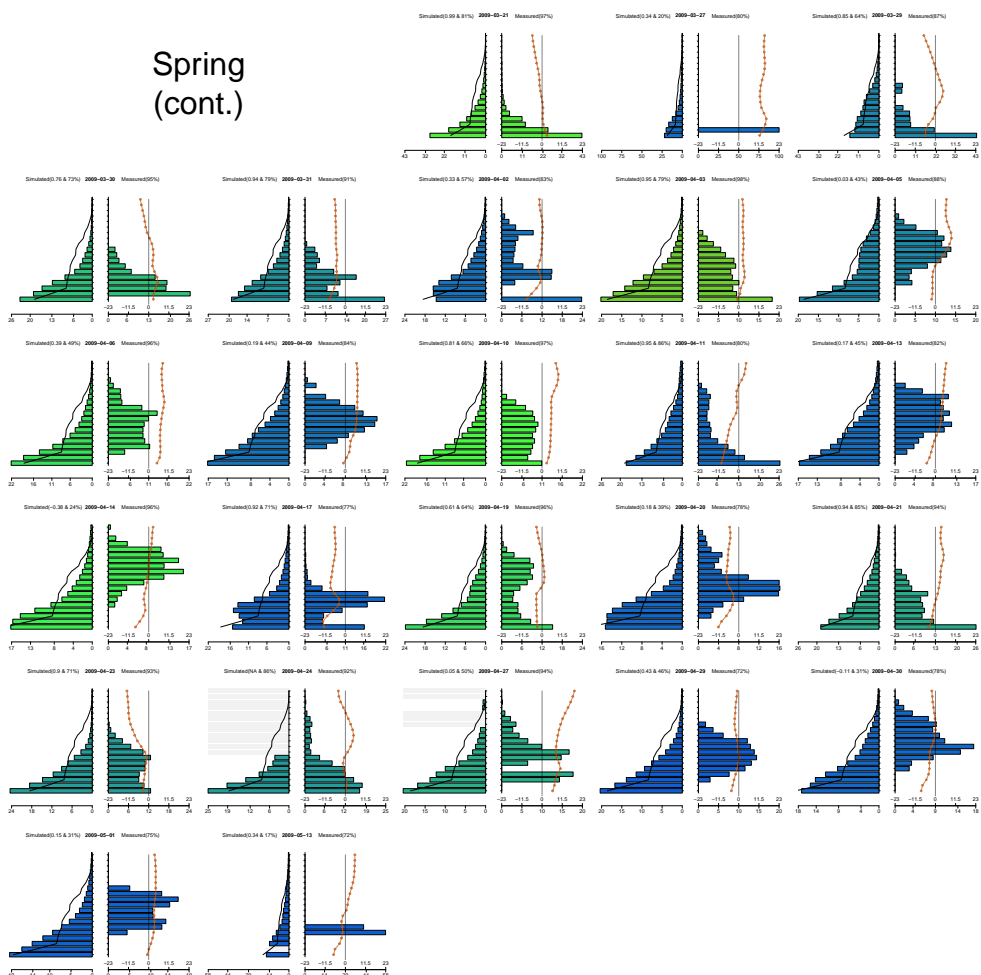


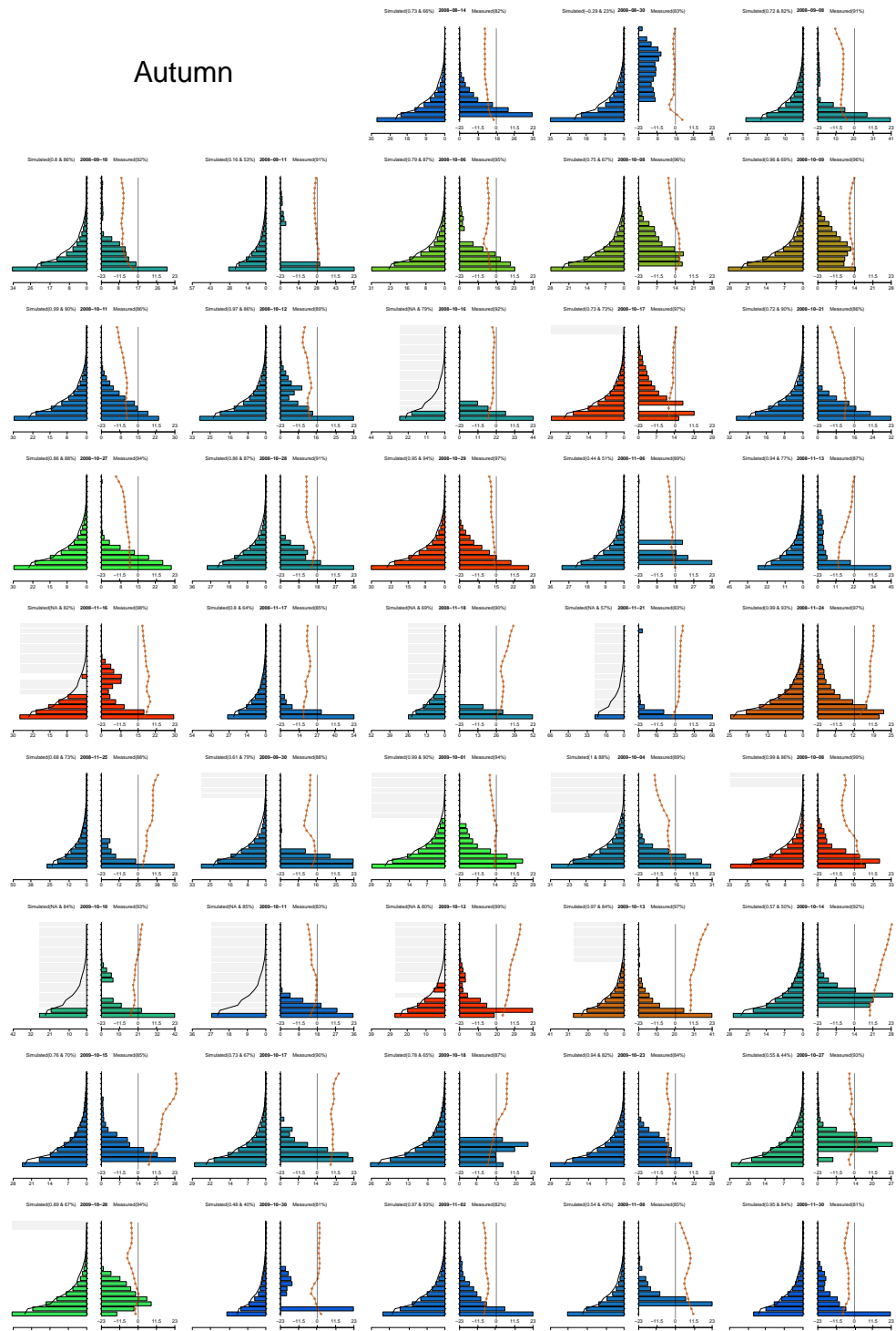
Appendix D: Results of simulation model predicting avian altitude distributions

Simulated nightly altitude distributions of pBd , from our comparison with the analysis of Bruderer et al. (1995), are shown with associated measured distributions of pBd and Tw for spring and autumn for altitudes between 0.2 and 4 km in bins of 200 m. On the right of each pair are measured distributions of pBd . Altitude distributions of Tw (orange line; ms^{-1}) are shown superimposed on top of the measured pBd distributions. The range of Tw values are indicated along the top of the x-axis and a vertical gray line indicates the transition point from negative to positive Tw values. Simulated distributions of pBd are shown on the left, with a black line indicating the weighted average distribution of pBd for that season. The color of the measured and predicted distributions of pBd indicate the measured intensity of migration on a given night from blue (least intense) through green to red (most intense). Altitude bins in the simulated distribution shown in transparent gray do not have a predicted value due to missing predictor variables. The numeric value given in parentheses next to the label “Measured” indicates the percentage of nights from that season with less-intense migration. The first value next to the label “Simulated” indicates the Spearman’s ρ correlation between the measured and simulated distributions of pBd and the second value indicates the proportion of variability in the measured distribution of pBd explained by the simulated distribution of pBd . The title of each plot indicates the night (at sunset) during which the conditions were measured. Note that Appendix D is only available in digital version of this thesis at <http://dare.uva.nl/record/421932>.



**Spring
(cont.)**

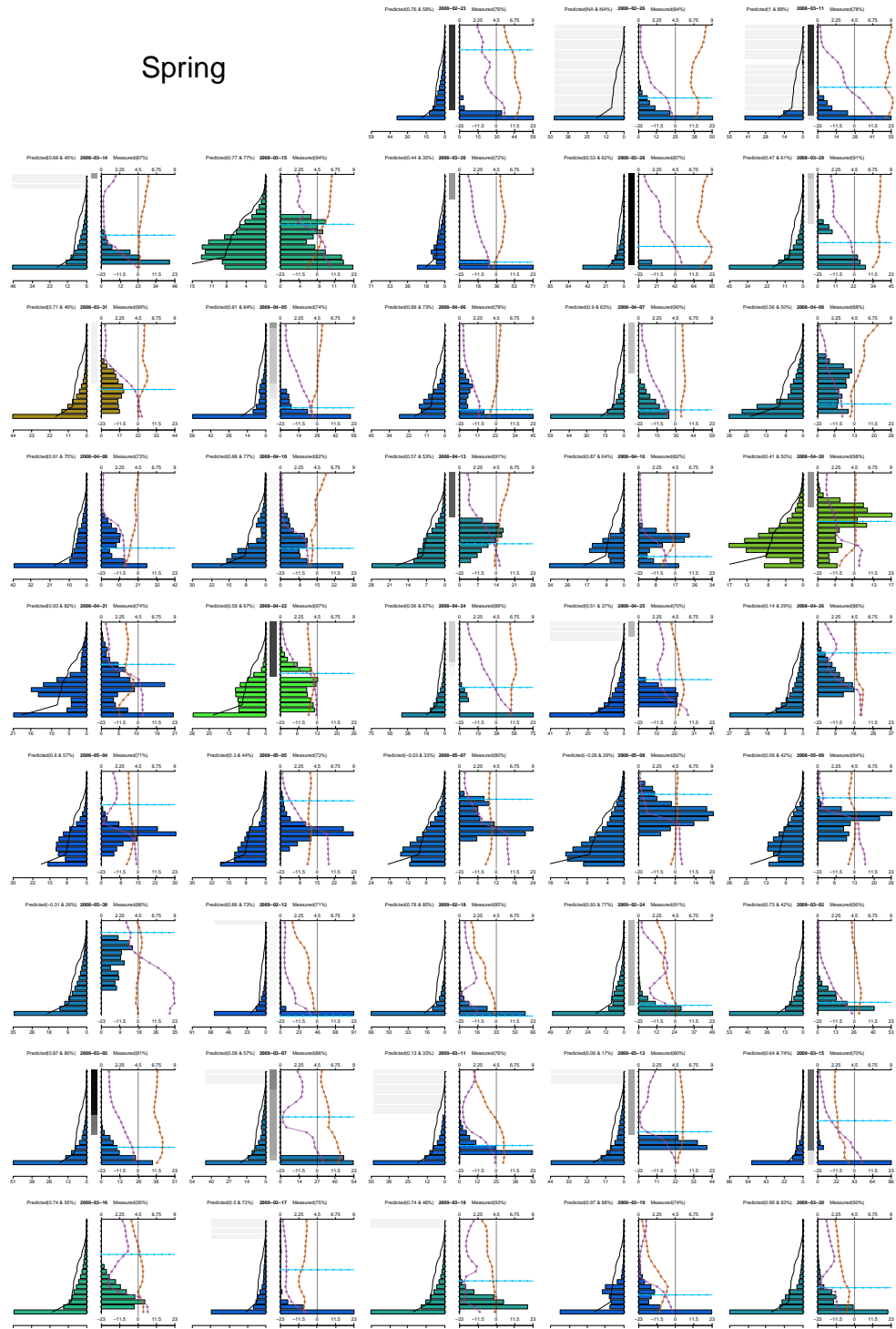




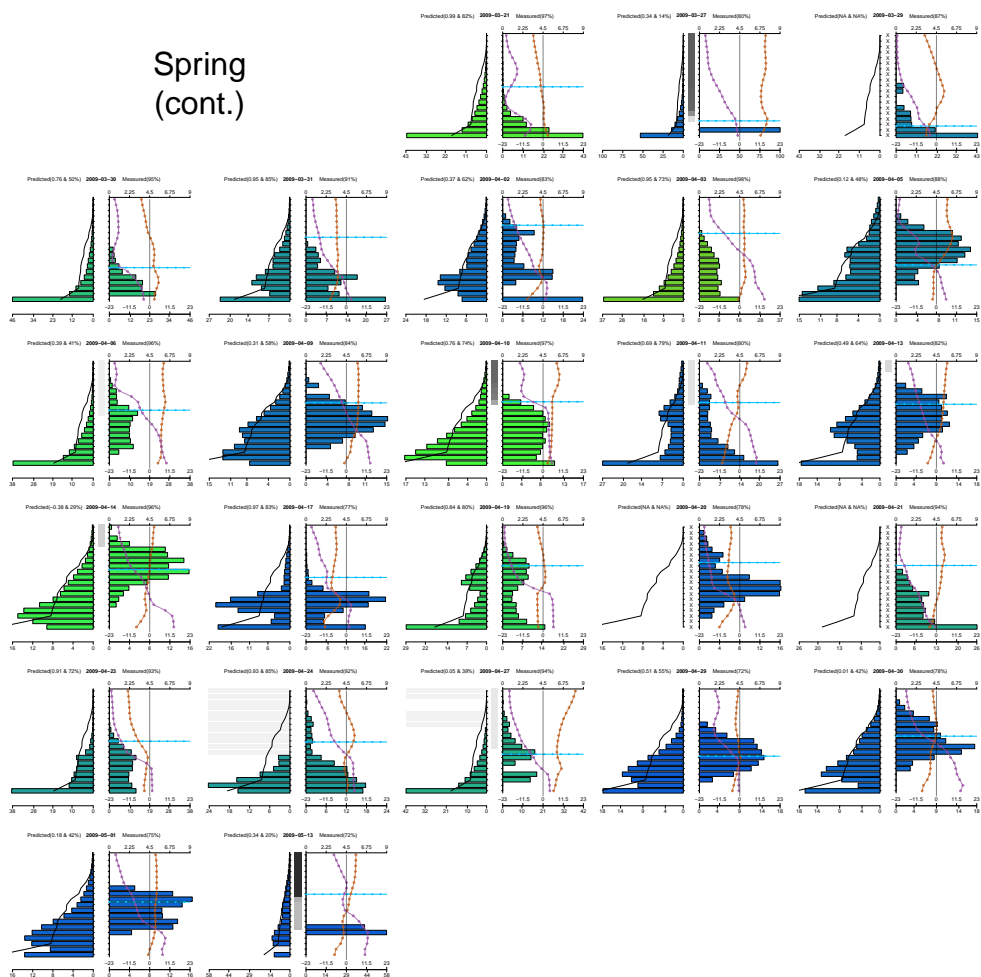
Appendix E: Results of GAM model predicting avian altitude distributions

Measured nightly altitude distributions of pBd , Tw , SH , Cp , and T (only the freezing point) along with associated altitude distributions of pBd predicted by our final GAM models for spring and autumn are shown for altitudes between 0.2 and 4 km in bins of 200 m. On the right of each pair are measured distributions of pBd . Altitude distributions of Tw (orange line; ms^{-1}) and RH (purple line; %) are shown superimposed on top of the measured pBd distributions along with a light blue horizontal line at the altitude at which freezing temperatures occurred. The range of Tw and RH values are indicated along the top of the lower x-axis and along the upper x-axis, respectively, and a vertical gray line indicates the transition point from negative to positive Tw values. Predicted distributions of pBd are shown on the left, with a black line indicating the weighted average distribution of pBd for that season. The color of the measured and predicted distributions of pBd indicates the measured intensity of migration on a given night from blue (least intense) through green to red (most intense). In between the predicted and measured distributions of pBd is a graphical representation of the value of Cp (%) for each altitude bin, with white indicating no Cp and black indicating 100% Cp . Altitude bins in the predicted distribution shown in transparent gray do not have a predicted value due to missing predictor variables, and missing values of Cp are indicated by an ‘X’. The numeric value given in parentheses next to the label “Measured” indicates the percentage of nights from that season with less-intense migration. The first value next to the label “Predicted” indicates the Spearman’s ρ correlation between the measured and predicted distributions of pBd and the second value indicates the proportion of variability in the measured distribution of

pBd explained by the predicted distribution of *pBd*. The title of each plot indicates the night (at sunset) during which the conditions were measured. Note that Appendix E is not available in the print version of this thesis; however, it is available in its entirety at <http://dare.uva.nl/record/421932>.



Spring
(cont.)



Autumn

